Order Number 9312179

Bis[pentamethyl(cyclopentadienyl)]uranium(IV) complexes of S,S diphenylsulfilimine

Ariyaratne, Kanahara A. N. S., Ph.D.

University of Hawaii, 1992

U·M·I
300 N. Zeeb Rd.
Ann Arbor, MI 48106

BIS[PENTAMETHYL(CYCLOPENTADIENYL)]URANIUM(IV) COMPLEXES OF S,S DIPHENYLSULFILIMINE

A DISSERTATION SUBMITTED TO THE GRADUATE DIVISION OF THE UNIVERSITY OF HAWAII IN PARTIAL FULFILLMENT OF THE REQUIREMENTS FOR THE DEGREE OF

DOCTOR OF PHILOSOPHY

IN CHEMISTRY

DECEMBER 1992

BY

KANAHARA A.N.S. ARIYARATNE

DISSERTATION COMMITTEE:

John W. Gilje, Chairperson

Roger E. Cramer

Craig M. Jensen

Ray L. McDonald

Jane S. Tribble

DEDICATION

I dedicate this work to my loving mother without whose support none of this could have been possible.

Amma, you are the best mother in the world. I love you.

ACKNOWLEDGEMENTS

I am thankful to Prof. John W. Gilje and Prof. Roger E. Cramer for their continued help and support throughout the past several years.

I would also like to thank Kathryn A. Mitchell for her friendship and the ability to keep a little brightness even in the darkest moments.

A special thanks goes to my loving wife Kalyani for her support, understanding and encouragement.

I also thank my parents, my brother, Kalyana and my two sisters, Champa and Wasantha for always believing in me and providing me with love, support and encouragement.

ABSTRACT

In toluene, the reaction of $Cp^*_2UCl_2$ with anhydrous $HNSPh_2$ yields the neutral N-donor adduct $Cp^*_2UCl_2(HNSPh_2)$, 1, that crystallizes in the monoclinic space group C2/c with unit cell parameters a = 23.83(3) A, b = 9.92(1) A, c = 27.29(3) A, β = 94.36(4)°, V = 6430(12) A^3, Z = 8, R = 6.77% and R_g = 7.17%. The structure was determined with 1310 unique reflections of I > 3σ.

Attempts to induce the dehydrochlorination of 1 to $Cp^*_2UCl(NSPh_2)$, 2, were not successful. However, 2 can be prepared by the reaction of $Cp^*_2UCl_2$ with one equivalent of $LiNSPh_2$. 2 reacts with another equivalent of $LiNSPh_2$ to give $Cp^*_2U(NSPh_2)_2$, 3. 2 and 3 can also be prepared by the reaction of $Cp^*_2UCl(CH_2)_2PR_2$ with one and two equivalents of $HNSPh_2$, respectively. 2 crystallizes in the monoclinic space group P21/n with unit cell parameters a = 12.120(5) A, b = 13.249(6) A, c = 21.644(8) A, β = 95.57(3)°, V = 3445(2) A^3, Z = 4, R = 6.55%, R_g = 8.00% for 2530 unique reflections with I > 2σ. The structure of 3 has been determined to be in the monoclinic space group C2/c with unit cell parameters a = 15.70(1) A, b = 13.00(1) A, c = 19.13(1) A, β = 92.98(6)°, V = 3898(5) A^3, Z = 4, R = 4.54%,

R_g = 6.56% for 6345 unique reflections with I > 2σ.

The reaction of 1 with $HNSPh_2 \cdot H_2O$ yields $Cp^*_2UCl(OH)(HNSPh_2)$, 4, that crystallizes in the monoclinic space group, P21/c with unit cell parameters a = 14.503(5) A, b = 30.10(1) A, c = 17.048(9) A, β = 102.20(3)°, V = 7273(5) A^3, Z = 8, R = 6.53%, R_g = 9.33% for 6280 unique reflections with I > 2σ. Further reaction of 4 with $HNSPh_2 \cdot H_2O$ forms the complex, 5. The structure of 5 has been determined to be in the triclinic space group P 1 bar with unit cell parameters a = 14.093(7) A, b = 15.36(1) A, c = 16.153(5) A, α = 88.9(1)°, β = 64.56(6)°, γ = 71.88(8)°, V = 3018(3) A^3, Z = 1, R = 5.64%, R_g = 7.91% for 5008 unique reflections with I > 3σ. Based on the crystallographic data, compound 5 has been formulated as $[Cp^*(Cl)(HNSPh_2)U-(\mu_3-OH)(\mu_2-O)_2-U(Cl)(HNSPh_2)_2]_2$.

TABLE OF CONTENTS

LIST OF TABLES

LIST OF FIGURES

Chapter 1

INTRODUCTION

Organouranium Complexes Containing Phosphorous Ylides and Nitrogen-Donor Ligands

1.1 Phosphorous Ylide Complexes of Uranium

Phosphorus ylides, $CH_2=PR_3$, play an important role in organic synthesis as Wittig reagents which convert carbonyl functionalities into alkenes.[1-3] They also behave as valuable ligands for many metals.[4-6] The nature of the P-C bond of the phosphorus ylide can be described in terms of the following resonance forms.

$$R_3P^+-CH^-_2 \quad <-------> \quad R_3P=CH_2$$

ylide ylene

The ylide form contains a highly polarized P-C bond between a positively charged phosphonium center and a carbanion. The ylene form contains a double bond between the P and the C atoms. Theoretical and experimental studies support the ylide formulation as predominant in the bonding of these molecules.[7] When one of the R

groups on the phosphorus is CH_3, deprotonation with alkyllithium reagents can produce lithiated dimethylide anions.

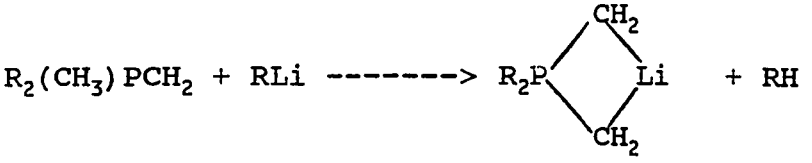

These ligands can display several different coordination modes in their metal complexes.

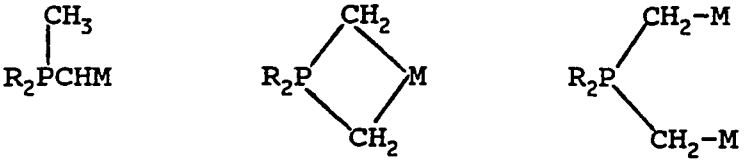

During the mid 1970's Maynard prepared the first phosphoylide complexes of actinide elements by reacting Cp_3UCl with lithiated phosphoylide reagents.[8-13]

$$Cp_3UCl + 1\ Li[(CH_2)(CH_2)PR_2] \text{ -----> } Cp_3U{=}CHPMeRR'$$

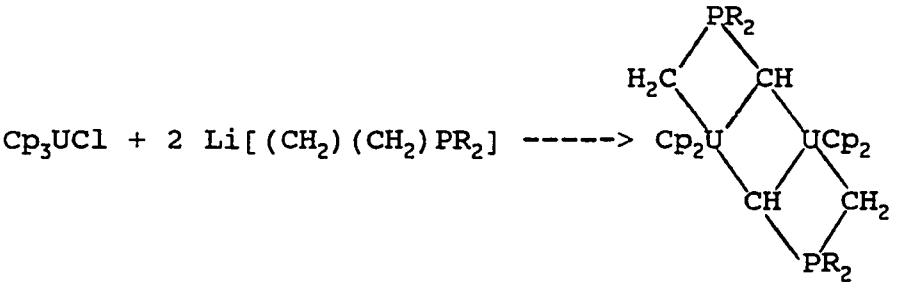

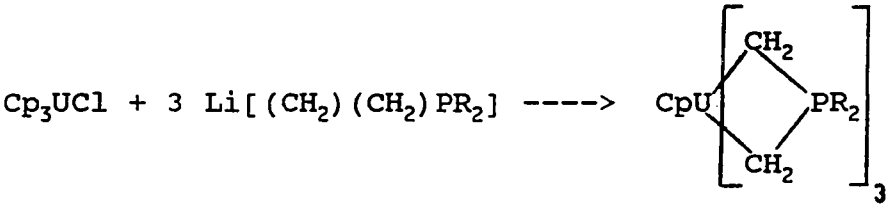

The U=C bond distances in $Cp_3U=CHPMeRR'$, (1a; R = R' = Me, 1b; R = R' = Ph, 1c; R = Me, R' = Ph), 2.287(9) A for 1a and 2.29(3) A for 1c, are significantly shorter than U-C single bonds, 2.40(2) A.[14-18] Structural, spectroscopic and theoretical data indicate multiple U-C bonding which can be described by the following resonance forms.[19]

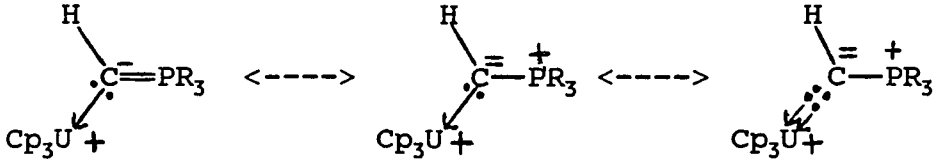

A hybrid of this structure is;

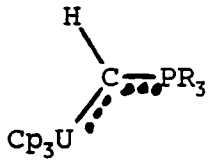

Reactivity of Metal Phosphoylide complexes

The following reactions demonstrate that the α carbon atom in the phosphoylide complex is nucleophilic.[20-22]

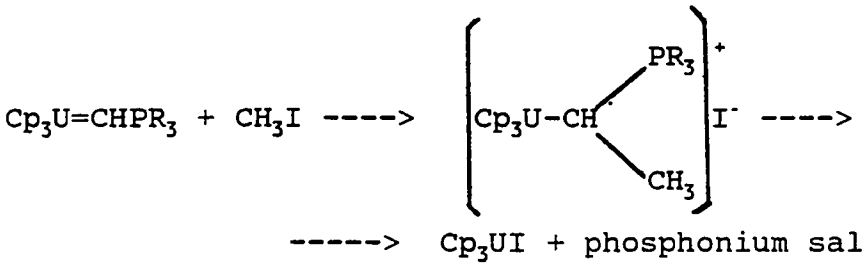

-----> Cp_3UI + phosphonium salts

$Cp_3U{=}CHPR_3 + HC{\equiv}CPh \text{ -----> } Cp_3U{-}C{\equiv}C{-}Ph + CH_2{=}CPR_3$

$Cp_3U{=}CHPMePh_2 + HNPh_2 \text{ -----> } Cp_3UNPh_2 + CH_2{=}PMePh_2$

While alkenes and alkynes do not react with $Cp_3U{=}CHPR_3$, polar unsaturated molecules insert into the U-C bond to form new unsaturated compounds.[23-25]

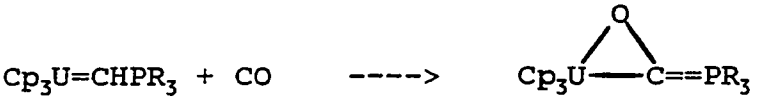

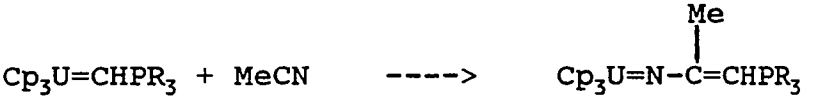

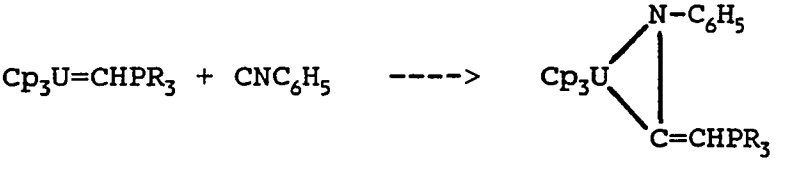

In addition to small polar molecules, more complex molecules such as transition metal carbonyls insert into the U-C double bond. The reactions of $M(CO)_6$ (M = W, Mo, Cr),[26,27] $CpMn(CO)_3$,[28] $[CpFe(CO)_2]_2$,[29] $CpCo(CO)_2$,[30] $Re_2(CO)_{10}$,[27] and $Ru_3(CO)_{12}$,[31] with $Cp_3U{=}CHPR_3$ have been studied. In all of these reactions a terminal carbonyl inserts into a uranium-carbon multiple bond according to following general equation.

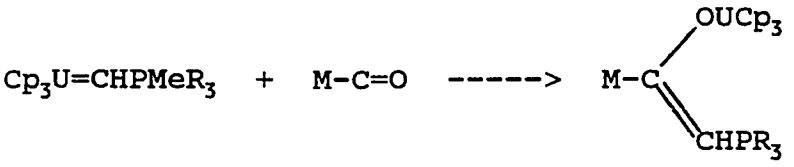

$Cp_3U=CHPMePh_2$ reacts with phenylisocyanate to form an insertion product.[32]

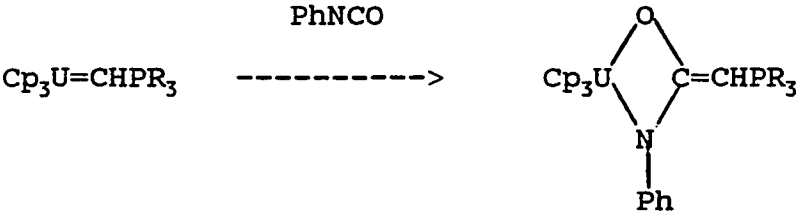

This insertion product catalyzes the cyclodimerization of phenylisocyanate.[27]

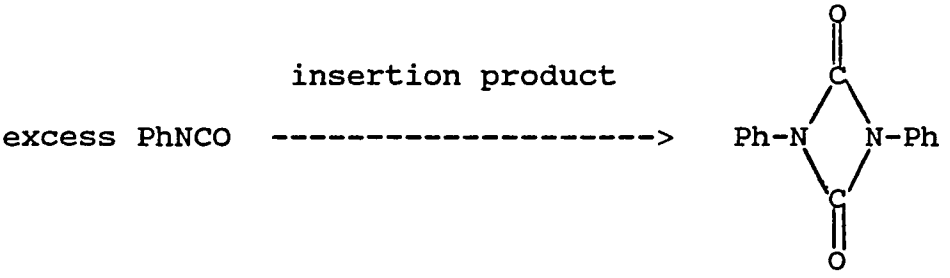

In addition to the Cp_3U-ylide synthesis described above, other actinide ylide systems have been

investigated. Two types of transition metal Cp_2MX ylide complexes (M = Ti, Zr, Hf) have been reported. In the complexes, $Cp_2Zr(X)[CHP(CH_3)_3]$, (X= Cl,[33,34] CH_3, $CH_2C(CH_3)_3$), $Cp_2Zr(R)[CHP(C_6H_5)_3]$, (R= C_6H_5,[35,36] C_2H_5[37]), $Cp_2M(Cl)[CHP(C_6H_5)_3]$ (M= Zr,Hf)[33,34] and $Cp_2M(Cl)[CHP(NR_2)_2R']$[38,39] (M= Ti, Zr, Hf; R= C_2H_5 or CH_3; R'= $N(C_2H_5)$ or CH_3) the ylide acts as a monodentate ligand. In the second type the ylide is chelating: $Cp_2Zr(H)[(CH_2)(CH_2)P(CH_3)_2]$[34], $Cp_2Zr(Cl)[(CH_2)(CH_2)P(CH_3)_2]$[34] and $Cp_2Zr(Cl)[(CH_2)(CH_2)P(N(C_2H_5)_2)_2]]$.[39-41] It has also been observed that some second type complexes convert spontaneously into the first type upon heating.[34]

The structural and the chemical similarities between the group IV Cp_2MCl_2 systems [M= Ti, Zr, Hf] and $Cp^*_2AnCl_2$ [Cp^*= $C_5(Me_5)$; An = U, Th], suggested that the phosphoylide coordination might be stabilized by the $Cp^*_2AnX_2$ system.[38]

$Cp^*_2AnCl_2$ reacts with $Li(CH_2)_2PR_2$ to form the phosphoylide complexes, shown below.[42]

$$Cp^*_2AnCl_2 + Li[(CH_2)(CH_2)PRR'] \xrightarrow{-LiCl} Cp^*_2AnCl(CH_2)_2PRR'$$

An = U(IV); R = Me, R'= Ph

An = Th(IV); R = R'= Ph, R = R' = Me

These complexes are thermally stable. They react with MeLi to produce $Cp^*_2An(Me)(CH_2)_2PRR'$ (An = U, Th; R = Me, R'=Ph; R =R'=Ph).[43] Analogous lanthanide complexes, $Cp^*_2Ln[(CH_2)_2PR_2]$ (Ln = Sm, Nd) have also been reported.[44]

1.2 Organoactinide Complexes with N-donor Ligands.

It has been observed that phosphine imides $[NPR_3]^-$, which are isoelectronic to phosphoylide ligands also coordinate to uranium and thorium.[45] Cp_3AnCl (An = U, Th) reacts with $LiNPPh_3$ to form $Cp_3AnNPPh_3$ according to the following equation.

$$Cp_3AnCl + LiNPPh_3 \longrightarrow Cp_3AnNPPh_3 + LiCl$$

Phosphine imide complexes of the transition elements, Ti, V, Nb, Ta, Mo, Re, Ru and Os are also reported.[46]

Molecular orbital calculations and bond length data indicate that Cp_3UNPPh_3 contains a U-N multiple bond.[45] In contrast to the large number of d-metal organoimides only a few f-metal organoimides are known. Only $[(Me_3Si)_2N]_3U(NSiMe_3)$,[47] $[(Me_3Si)_3N]_3U(NR)F$ (R = $SiMe_3$, Ph),[48] Cp_3UNPPh_3,[45] Cp_3UNPh[49] and $Cp_3UNC(Me)CHPMePh_2$[24] of this category have been structurally characterized.

They are prepared by;

$$[(Me_3Si)_2N]_3U + Me_3SiN_3 \text{ -----> } [(Me_3Si)_2N]_3U(NSiMe_3) + N_2$$

$$[(Me_3Si)_2N]_2U(NR) + AgPF_6 \text{ -----> } [(Me_3Si)_3N]_3U(NR)F + Ag^\circ + PF_5$$

$$Cp_3UCl + LiNPPh_3 \text{ -------> } Cp_3UNPPh_3 + LiCl$$

$$(C_5H_4Me)_3U(THF) + PhN_3 \text{ ------> } U(C_5H_4Me)_3NPh + N_2$$

$$Cp_3U{=}CHPMePh_2 + MeCN \text{ ------> } Cp_3U{=}N(Me)C{=}CHPMePh_2$$

The U-N distance, 1.90(3) A, in $[(Me_3Si)_2N]_3U(NSiMe_3)$, is the shortest U-N distance ever reported. According to Andersen and co-workers, the linear U-N-Si angle implies that both lone pairs of electrons on the nitrogen atoms are involved in bonding to uranium and the U-N bond is best viewed as a triple bond. Even though U-N triple bonds are known among Cp_3U complexes no U-N multiple bonds have so far been observed among Cp^*_2U compounds.

In addition to these examples where the N-ligand acts as a three electron pair donor, organoactinide complexes containing N-ligands that behave as one/two electron pair donors are also known. The U-N bond distance can be used to describe the nature of the U-N bond which ranges from 2.019(6) in Cp_3UNPh to 2.68(2) in $Cp_3U(NCS)(NCMe)$.[49,50] The U-N(NCMe) distance of 2.68(2) indicates a U-N single bond where the N behaves as a neutral single electron pair donor.

The first f-element complex containing a neutral phosphinimine ligand, $HNPPh_3$, $Cp^*_2UCl_2(HNPPh_3)$, was prepared according to following equation.[51]

$$Cp^*_2UCl_2 + HNPPh_3 \text{ -------> } Cp^*_2UCl_2(HNPPh_3)$$

Figure 3 shows the perspective view of this molecule. The U-N bond length of this complex, 2.43(1) A, is the shortest found to date in a uranium complex of a neutral nitrogen donor ligand.

Structure, energies and electronic properties of the ylide, $HNPH_3$, have been studied by K. Lammerstma and co-workers.[52] According to them, the P-N bond is highly polar with a short length of 1.543 A. The large Coulombic interaction between the phosphorous and the nitrogen makes the P-N bond very short. The difference in electronegativities between the two atoms enables the maximization of this polarity.

Based on the above information, the following resonance forms can be written for $HNPPh_3$, with the resonance form A being more important than B.

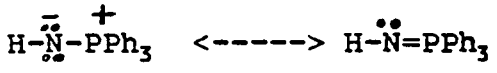

A B

According to these resonance forms, the nitrogen could act as a two electron pair donor which would potentially shorten the U-N bond of $Cp^*_2UCl_2(HNPPh_3)$.

The following resonance forms can be written for the $Cp^*_2UCl_2(HNPPh_3)$ where M = $Cp^*_2UCl_2$.

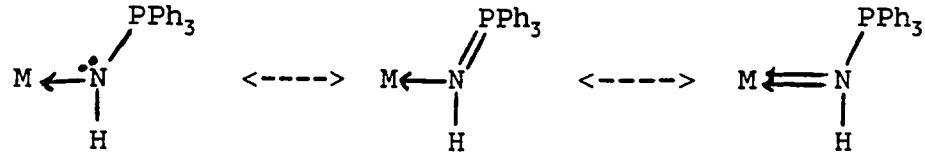

1.3 Sulfilimide Complexes of Transition Metals

The sulfilimide ion, $[NSR_2]^-$, which is a derivative of sulfilimine, $RNSR_2$, has been used as a stabilizing ligand in certain transition metal compounds.[53,54] However, very little is known about the coordination chemistry of sulfilimines and no organometallic sulfilimide complexes have been reported so far. The compounds, $F_5W(NSPh_2)$,[53] $F_4W(NSPh)_2$,[53] $Cl_4Mo(NSPh_2).CH_3CN$,[53] $(Cl_2FeNSPh_2)_2$,[54] $Cl_4Nb(NSPh_2).CH_3CN$,[54] $F_2VO(NSPh_2)$,[54] $Cl_2VO(NSPh_2)$,[54] containing the $[NSPh_2]^-$ ligand are known, but the x-ray crystal structures of only $F_4W(NSPh_2)_2$,[53] $Cl_2VO(NSPh_2)$[54] and $Cl_2Fe(NSPh_2)_2$[54] have been reported to date.

For example, $Cl_2VO(NSPh_2)$, whose perspective view is shown in Figure 1, is synthesized according to the following reaction.

$$VOCl_3 + Ph_2S{=}NSiMe_3 \text{ -----> } Ph_2S{=}N{-}V(O)Cl_2 + Me_3SiCl$$

The $RNSR_2$ ligand is very similar to $[CHPR_3]^{\cdot}$ and $RNPPh_3$. In a similar manner to $HNPPh_3$, the following resonance forms could be written for $HNSPh_2$.

According to the resonance form B, $HNSPh_2$ could also behave as a two electron pair donor in coordinating to a high valent metal center.

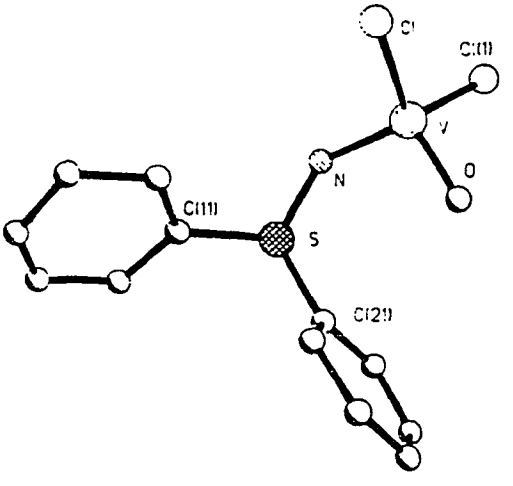

Figure 1: Perspective view of $Cl_2VO(NSPh_2)$[54]

1.4 Organouranium Oxo Complexes

Organo f-element oxo complexes are rare. Among the actinides, several complexes in which Cp_3An^+ (An = U or Th)[55] or Cp_2U^+ groups[56] are coordinated to polyoxoanions have been structurally characterized. The complexes, $(UO_2)_2U_2O_2(OC_6H_5)(THF)_4$[57], $U_4O_2(O_2CNEt_2)_4$[58], $U_3(O)(OCMe_3)_{10}$,[59] which contain μ_3-oxides have also been reported. A considerable number of lanthanide oxo derivatives are also known.[60-65] However, organo f-element hydroxy complexes are extremely rare. Only $[Cp_2Y(OH)(THF)]$[66], $\{[(Me_3Si)_2C_5H_3]_2Sm(\mu\text{-}OH)\}_2$[67], $[Cp_2Y(\mu\text{-}OH)]_2(PhC{=}CPh)$,[66] $[O(CH_2CH_2C_5H_4)_2Ln(N_2C_3HMe_2(\mu\text{-}OH)Ln(C_5H_4CH_2CH_2)_2O]$ (Ln = Y, Lu)[68] have been structurally characterized and no organo actinide hydroxy complexes are reported to date.

The oxo-centered organouranium-magnesium phosphoylide complex, $\{Cp^*U[\mu\text{-}(CH_2)P(Ph)_2(CH_2)]\}_2Mg\text{-}[CH_2PMePh_2]_2(\mu_3\text{-}O)(\mu_2\text{-}O)(\mu_2\text{-}Cl)_2$[69], contains two organouranium moieties and an organomagnesium group which are linked by μ_2- and μ_3-oxides. $[(Me_3SiC_5H_4)_3U]_2[\mu\text{-}O]$ has been structurally characterized.[70] The perspective diagram of the organouranium magnesium phosphoylide

structure is given in Figure 2 and that of $[(Me_3SiC_5H_4)U]_2[\mu\text{-}O]$ is shown in Figure 4. $[(Me_3SiC_5H_4)_3U_2][\mu\text{-}O]$ is synthesized according to following equation.

$$(Me_3SiC_5H_4)_3U + CO_2 \longrightarrow [(MeSiC_5H_4)U[\mu\text{-}O] + CO$$

Also, the complex, $[Cp_3U]_2[\mu\text{-}O]$ has been reported, but with no structural characterizations or detailed experimental data.[71]

In these compounds the bridging oxygen atom is derived from various sources such as O_2, H_2O, NO, N_2O, epoxybutane, pyridine oxide and CO_2.

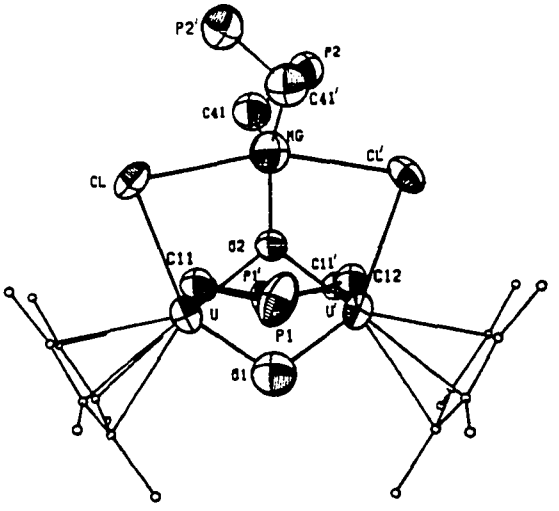

Figure 2: Perspective View of $\{Cp^*U[\mu\text{-}CH_2)P(Ph)_2(CH_2)]\}_2Mg[CH_2\text{-}PMePh_2](\mu_3\text{-}O)(\mu_2\text{-}O)(\mu_2\text{-}Cl)_2$[69]

1.5 Statement of the Problem

a) The interaction of S,S diphenylsulfilimine, $HNSPh_2$, which is isoelectronic with $[CHPR_3]^-$ and $HNPPh_3$ with $Cp^*_2UCl_2$ is proposed. No organometallic complexes containing $RNSPh_2/[NSPh_2]^-$ have been reported to date. The Cp^*_2U-imido complexes, $Cp^*_2UCl(NPPh_3)$ and $Cp^*_2U(NPPh_3)_2$ have been reported, but, with no structural characterization.[43] Therefore it is necessary to study the

reactivity of $Cp^*_2UCl_2$ and other Cp^*U compounds with $LiNSPh_2$ and $Me_3SiNSPh_2$ in order to evaluate if U-N multiple bonds are formed by these ligands.

b) Attempts to synthesize organouranium oxo complexes by hydrolysis of U-Cl bonds have not been succussful. It is possible that the availability of a reagent which contains both H_2O and a base that can absorb HCl, liberated during hydrolysis of $Cp^*_2UCl_2$, would offer an effective reagent for synthesizing organouranium oxo species. $HNSPh_2$ is available as a mono hydrate, $HNSPh_2 \cdot H_2O$, and it is a moderately strong base. Therefore the reaction of $Cp^*_2UCl_2$ with $HNSPh_2 \cdot H_2O$ is proposed.

The characterization of the products will be done by usual chemical and spectral analysis and by x-ray diffraction.

c) The reaction of Cp_3UCl with $Li(CH_2)_2PRR'$ forms $Cp_3U{=}CHPMeRR'$ which contains the only U=C multiple bond system found to date. The reaction of $Cp_3U{=}CHPMePh_2$ with one equivalent of phenylisocyanate produces an insertion product, $Cp_3U(PhNCO)CHPMePh_2$ which catalytically

dimerizes excess phenylisocyanate.[27] A further study of stoichiometric and catalytic reactivity of Cp_3U=CHPMeRR' with a series of heterocumulenes is proposed.

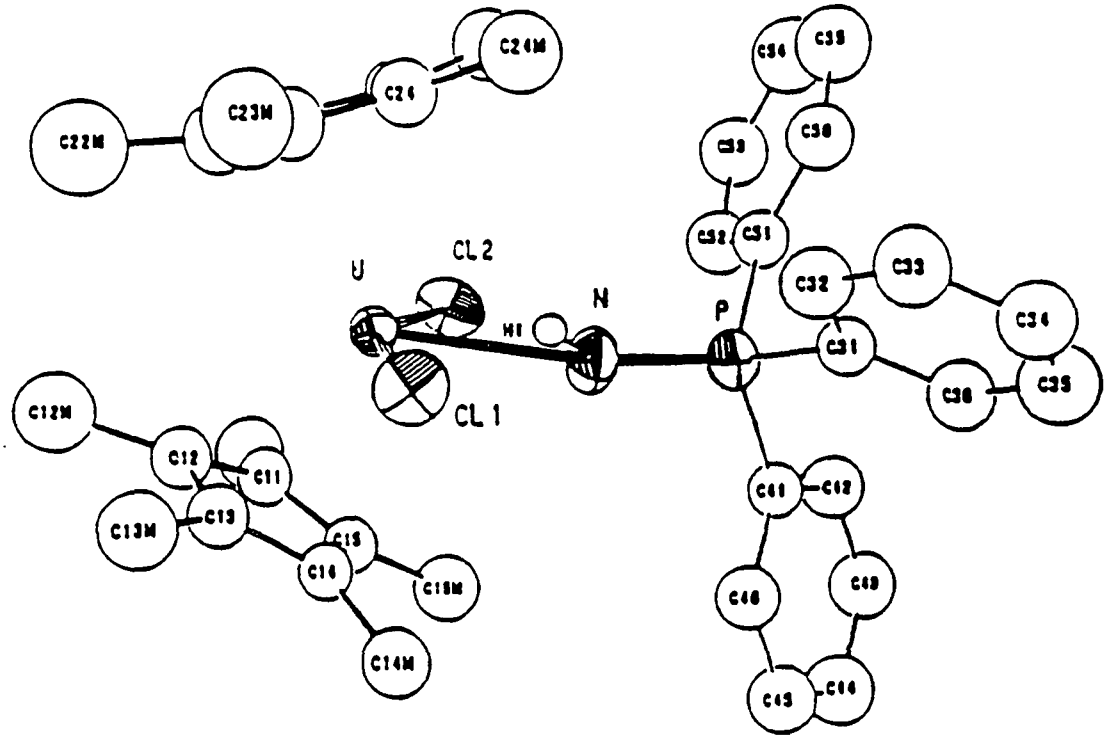

Figure 3: Perspective View of $Cp^*_2UCl_2(HNPPh_3)$[51]

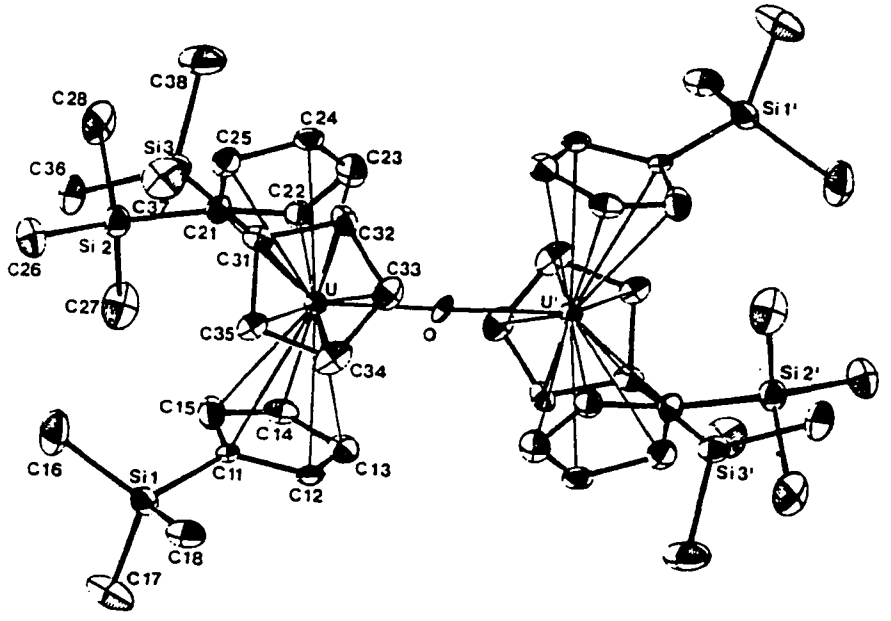

Figure 4: Perspective Diagram of $[(Me_3SiC_5H_4)_3U]_2[\mu\text{-}O]$[70]

Chapter 2

EXPERIMENTAL

2.1 Instrumentation

All ^{1}H-NMR spectra were obtained using a Nicolet QE 300 MHz spectrometer with a Nicolet microcomputer operating in the Fourier transform mode utilizing 16-100 transients. Infrared spectra of the products from the reactions of $Cp_3U{=}CHPMeR_2$ with heterocumulenes were recorded on a Perkin-Elmer 1430 spectrometer. A Nicolet-740 IR spectrometer operating in the Fourier transform mode was used for recording all other infrared spectra. The infrared spectra of $HNSPh_2$, $DNSPh_2$, $Cp^*_2UCl_2(HNSPh_2)$ and $Cp^*_2UCl_2(DNSPh_2)$ were obtained using a KBr solution cell and CCl_4 as the solvent whereas those of $Cp^*_2UCl(NSPh_2)$ and $Cp^*_2U(NSPh_2)_2$ were obtained by laying a thin film of the toluene solution onto a NaCl plate. The infrared spectrum of $Cp^*_2UCl(OH)(HNSPh_2)$ and $[Cp^*(Cl)(HNSPh_2)U\text{-}(\mu_3\text{-}OH)(\mu_2\text{-}O)_2\text{-}U(Cl)(HNSPh_2)_2]_2$ were obtained by laying a thin film of a THF solution onto a NaCl plate. The solvent was then allowed to evaporate in the glove box. In the case of the reactions of $Cp_3U{=}CHPMePh_2$ with heterocumulenes, infrared spectra were

run by using several drops of the liquid samples without using any solvent. Then the samples were sandwiched by a second NaCl plate before running the spectra. ^{1}H-NMR spectra were obtained in d_6-benzene, d_8-tetrahydrofuran, d_3-acetonitrile and/or d_8-toluene. Samples were prepared in the glove box in NMR tubes with ground glass joints and vacuum stopcocks. These were transferred to a vacuum line, frozen, evacuated and sealed. ^{1}H-NMR spectra were referenced to the internal deuterated solvent and recalculated relative to TMS. Positive chemical shifts are downfield of TMS.

2.2 Materials and Methods

All procedures were performed under a dry dinitrogen atmosphere using normal Schlenk techniques, a Vacuum Atmosphere glove box equipped with an HE-493 dri train or in a high vacuum line. Benzene, toluene, tetrahydrofuran, diethylether, pentane and hexane were dried and deoxygenated over sodium-benzophenone and were distilled under purified nitrogen gas immediately prior to use. $Cp_3U{=}CHPR_3$,[8] Ph_3PNH,[72] $Me_3SiNPPh_3$,[73] $Me_3SiNSPh_2$,[53] UCl_4,[74] $Cp^*_2UCl_2$,[75] $Cp^*_2UCl(CH_2)_2PR_2$[42] were synthesized using literature methods. $HNSPh_2$ was purchased from Aldrich

chemical company as $HNSPh_2 \cdot H_2O$ and dehydrated under high vacuum for three days at room temperature. $DNSPh_2$ was synthesized by hydrolysis of $Me_3SiNSPh_2$ with D_2O. $LiNSPh_2$ was synthesized by reacting $HNSPh_2$ with n-BuLi in tetrahydrofuran at -78°C and recrystallizing from tetrahydrofuran.

2.3 Syntheses and Reactions

2.3.1 Reaction of $Cp^*_2UCl_2$ with $HNSPh_2$

Synthesis of $Cp^*_2UCl_2(HNSPh_2)$

A reaction flask was charged with 230 mg (0.40 mmole) of $Cp^*_2UCl_2$ and 25 ml of toluene. To this solution, a solution of 80 mg (0.40 mmole) of $HNSPh_2$ in 30 ml of toluene was added slowly at -78°c under nitrogen. The sample was stirred for five hours during which the flask was allowed to warm slowly to room temperature. Then the dark orange solution was evaporated to dryness. The orange-red residue was extracted with 10 ml of toluene, filtered through a medium porosity frit, and reduced in volume to about 5 ml. Approximately 3 ml of pentane was added and the solution was stored at room temperature. After several days $Cp^*_2UCl_2(HNSPh_2)$ crystallized as red-orange plates on

the sides and bottom of the flask. These were isolated by filtration, washed with 2 x 0.5 ml pentane and dried under vacuum.

The microcrystalline material obtained by immediate evaporation of the toluene solution from the reaction above was rinsed with 2 ml of pentane, dried under strong vacuum and used for dertermining the percentage yield of the reaction. Yield: 240 mg (77%), microcrystalline product (based on the amount of $Cp^*_2UCl_2$ used). Elemental analysis; Observed: C = 48.20, H = 5.17, N = 1.31, Cl = 10.06, Calculated: C = 49.22, H = 5.30, N = 1.79, Cl = 9.08.

The ^{1}H-NMR spectrum of $Cp^*_2UCl_2(HNSPh_2)$ is shown in Figure 5 and data are summarized in Table 1. Figure 6 shows the expanded aromatic region of the spectrum. The spectrum contains a sharp singlet at 9.1 ppm for the Cp^* group, a doublet at -9.2 ppm for the ortho and triplets at 2.3 and 3.9 ppm for meta and para protons of the phenyl groups of the $HNSPh_2$ ligand. There is a singlet at -142 ppm for the imino hydrogen.

The calculated molecular weight of $Cp^*_2UCl_2(HNSPh_2)$ is 780.0. However the mass spectrum of $Cp^*_2UCl_2(HNSPh_2)$, Figure 7, table 2, does not contain a molecular ion peak. Rather, peaks arising from $Cp^*_2UCl_2$ (579 a.m.u.) and

$HNSPh_2$ (201 a.m.u.) are observed in the spectrum and indicate that $Cp^*_2UCl_2(HNSPh_2)$ dissociates in the gas phase in the mass spectrometer.

IR Spectra

In order to assign N-H stretch of $Cp^*_2UCl_2(HNSPh_2)$ unambiguously, the following experiments were carried out.

Synthesis of $DNSPh_2$

A reaction flask was charged with 2.0 g of $Me_3SiNSPh_2$ (7.0 mmole) and 10 ml of tetrahydrofuran. To this solution 15 ml of deuterium oxide was added slowly at room temperature under nitrogen and stirred for 15 mins. A few minutes after the addition was complete the solution became cloudy and a white crystalline material began to form. The solution along with the precipitate was then evaporated to dryness, rinsed with 1 ml of pentane, dried under vacuum and tested for identity by NMR.

The infrared spectrum of anhydrous $HNSPh_2$ in CCl_4, Figure 9, contains a strong absorption at 3306 cm^{-1} whereas that of $DNSPh_2$ in CCl_4, Figure 10, shows absorption peaks at 2448 cm^{-1}.

Synthesis of $Cp^*_2UCl_2(DNSPh_2)$

The same procedure mentioned above for the synthesis of $Cp^*_2UCl_2(HNSPh_2)$ was followed using 290 mg (0.50 mmole) of $Cp^*_2UCl_2$ and 101 mg (0.50 mmol) of $DNSPh_2$ to obtain 280 mg of $Cp^*_2UCl_2(DNSPh_2)$ (yield = 72%).

Figure 8 shows the infrared spectrum of $Cp^*_2UCl_2$. The infrared spectrum of $Cp^*_2UCl_2(HNSPh_2)$ in CCl_4, is given in Figure 11, Table 3, and contains an absorption peak at 3284 cm^{-1} whereas the spectrum of $Cp^*_2UCl_2(DNSPh_2)$ in CCl_4, Figure 12, Table 3, shows a single absorption peak at 2435 cm^{-1}. Based on these data, the peak at 3284 cm^{-1} in the infrared spectrum of $Cp^*_2UCl_2(HNSPh_2)$ is assigned as the N-H stretch of the $HNSPh_2$ group. This is 22 cm^{-1} lower than the the corresponding mode in uncomplexed $HNSPh_2$.

Attempted Dehydrochlorination of $Cp^*_2UCl_2(HNSPh_2)$

In order to see if $Cp^*_2UCl_2(HNSPh_2)$ undergoes thermal decomposition or dehydrochlorination the following experiments were carried out.

1) 50 mg (0.80 mmole) of $Cp^*_2UCl(HNSPh_2)$ was heated under vacuum at 100°C for 12 hrs. The ^{1}H-NMR spectrum of the sample obtained in toluene, was identical to that of $Cp^*_2UCl_2(HNSPh_2)$ and no evidence of any chemical reaction was evident.

2) A 50 mg (0.80 mmole) sample of $Cp^*_2UCl(HNSPh_2)$ was refluxed in toluene in a reaction flask for 24 hrs. The solution was then evaporated to dryness and ^{1}H-NMR spectrum of the red residue was obtained in deuterated toluene. The spectrum was identical to that of $Cp^*_2UCl(HNSPh_2)$ and no chemical reaction was observed.

2.3.2 Reaction of $Cp^*_2UCl_2$ with $LiNSPh_2$

Synthesis of $LiNSPh_2$

400 mg (2.0 mmole) of $HNSPh_2$ was dissolved in 25 ml of tetrahydrofuran and 8 ml of 0.6M n-BuLi was added slowly to this solution under nitrogen at room temperature. During the addition of n-BuLi, the solution turned yellow and gas bubbles formed. The solution was stirred for 15 mins and evaporated to dryness. The yellow crystalline $LiNSPh_2$ was washed with 2 ml of pentane, dried under vacuum and tested for identity by obtaining the ^{1}H-NMR spectrum. The ^{1}H-NMR spectrum, Figure 13, indicates that $LiNSPh_2$ forms a THF solvate. The spectrum contains broad signals between 7-8 ppm for the aromatic peaks of the $[NSPh_2]^-$ group and singlets at 1.76 ppm and 3.59 ppm for the tetrahydrofuran. The product can be successfully desolvated under high vacuum for three days.

Synthesis of $Cp^*_2UCl(NSPh_2)$

1) To 230 mg (0.40 mmole) of $Cp^*_2UCl_2$ in 25 ml of toluene was added a solution of 84 mg (0.40 mmole) of $LiNSPh_2$ in 25 ml of toluene under nitrogen. After stirring for 6

hrs at room temperature the red solution was filtered through a medium porosity frit and reduced in volume to about 5 ml. Approximately 3 ml of pentane was added and the solution was stored at room temperature. After two days dark red-black crystals had grown on the sides and the bottom of the flask. These were isolated and washed with 2 x 0.5 ml of pentane and dried under vacuum.

The reaction of 230 mg (0.40 mmole) with 84 mg (0.40 mmole) in toluene yields $Cp^*_2UCl(NSPh_2)$ as a microcrystalline material if the toluene is immediately evaporated to dryness. The solid residue was rinsed with 1 ml of pentane, tested for purity by NMR and used for determining the percentage yield of the reaction; Yield; 127 mg (72%) (based on the amount of $Cp^*_2UCl_2$ used in the synthesis). Molecular Weight; Calculated: 744.27, Reproducible mass spectra could not be obtained due to low volatility of the sample in the spectrometer.

Successful results were not obtained from elemental analysis due to the presence of traces of $Cp^*_2U(NSPh_2)_2$ as a contaminnat in the product.

The ^{1}H-NMR spectrum of $Cp^*_2UCl(NSPh_2)$ is given in Figure 14, Table 4, and in Figure 15 the aromatic region is expanded. The spectrum contains a sharp singlet for the Cp^* group at 2.15 ppm, a doublet at 14.1 ppm for the

ortho, and triplets at 8.4 and 8.5 ppm for the meta and para protons of the phenyl groups of the $[NSPh_2]^-$ group. The infrared spectrum is given in Figure 16 and data are summarized in Table 5.

Synthesis of $Cp^*_2U(NSPh_2)_2$

2) 230 mg of $Cp^*_2UCl_2$ (0.40 mmole) and 168 mg of $LiNSPh_2$ (0.80 mmole) were dissolved in 25 ml of toluene under nitrogen. The reaction mixture was stirred for 6 hrs, the dark red solution was filtered through a medium porosity frit, and the filtrate was evaporated to dryness leaving a dark red-brown residue. This residue was extracted with 10 ml of toluene and the resulting solution was reduced in volume to about 5 ml. A few drops of pentane were added to the solution. Over several weeks at room temperature dark red crystals formed on the sides and at the bottom of the flask.

The immediate evaporation of toluene from reaction of 230 mg (0.40 mmole) of $Cp^*_2UCl_2$ and 168 mg (0.80 mmole) of $LiNSPh_2$ in 25 ml of toluene, conducted as described above, formed $Cp^*_2U(NSPh_2)_2$ as a microcrystalline material. This was washed with 1 ml of pentane, dried under vacuum, tested for purity by NMR and used for

calculating the percentage yield. Yield; 224 mg (62%) microcrystalline material (based on the amount of $Cp^*_2UCl_2$ used). Elemental Analysis; Observed: C = 57.10, H = 5.40, N = 2.77, Calculated : C = 58.13, H = 5.54, N = 3.08)

Calculated molecular weight: 909.0. Reproducible mass spectra could not be obtained due to low volatility of the compound in the mass spectrometer.

A saturated solution of $Cp^*_2U(NSPh_2)_2$ in tetrahydrofuran formed dark prismatic crystals upon standing at room temperature for several weeks. They were mounted in 0.5 mm capillaries and used for determining the x-ray crystal structure. The ^{1}H-NMR spectrum of $Cp^*_2U(NSPh_2)_2$ is given in Figure 17, and data are summarized in Table 6. Figure 18 shows the expanded aromatic region of the spectrum. The spectrum contains a sharp singlet at -0.24 ppm for the Cp^* group and a doublet at 3.9 ppm, and triplets at 5.9 and 6.1 ppm for the aromatic protons of the $[NSPh_2]^-$ group. The infrared spectrum is shown in Figure 19 and the data are summarized in table 7.

2.3.3 Reaction of $Cp^*_2UCl_2$ with $Me_3SiNSPh_2$

NMR samples were prepared in toluene-d^8 using 29 mg (0.05 mmole) of $Cp^*_2UCl_2$ and 14 mg (0.05 mmole) of $Me_3SiNSPh_2$, and 29 mg (0.05 mmole) of $Cp^*_2UCl_2$ and 28 mg (0.10 mmole) of $Me_3SiNSPh_2$. ^{1}H-NMR spectra were obtained shortly after preparation. The samples were then heated to 100°C for 12 hrs and a second set of spectra were obtained. Finally spectra were taken after the samples were exposed to uv light for 12 hrs. No evidence of any chemical reaction between $Cp^*_2UCl_2$ and $Me_3SiNSPh_2$ was obtained from the NMR spectra under any condition.

2.3.4 Reactions of $Cp^*_2UCl(CH_2)_2R_2$ with $HNSPh_2$

NMR tube experiments

The following samples were prepared in deuterated toluene.

1) 76 mg (0.10 mmole) of $Cp^*_2UCl(CH_2)_2PPh_2$ and 20 mg (0.10 mmole) of $HNSPh_2$

2) 76 mg (0.10 mmole) of $Cp^*_2UCl(CH_2)_2PPh_2$ and 40 mg (0.20 mmole) of $HNSPh_2$

3) 70 mg (0.10 mmole) of $Cp^*_2UCl(CH_2)_2P(Ph)(Me)$ and 20 mg (0.10 mmole) of $HNSPh_2$

4) 70 mg (0.10 mmole) of $Cp^*_2UCl(CH_2)_2P(Ph)(Me)$ and 40 mg (0.20 mmole) of $HNSPh_2$

A light yellow precipitate formed in every case. The NMR spectra of the samples 1 and 3 contain peaks that are consistent with $Cp^*_2UCl(NSPh_2)$ and samples 2 and 4 contain peaks that are consistent with $Cp^*_2U(NSPh_2)_2$.

Large scale reactions

1) To 304 mg (0.40 mmole) of $Cp^*_2UCl(CH_2)_2PPh_2$ was added slowly 80 mg (0.40 mmole) of $HNSPh_2$ in about 25 ml of toluene under nitrogen. A yellow precipitate began to form as soon as the addition of $HNSPh_2$ was complete. After stirring for 3 hrs at room tempereature the red solution was filtered through a medium porosity frit and evaporated to dryness to obtain a dark red powder. This was rinsed with 2 ml of pentane, dried under vacuum and

used for determining the pecentage yield of $Cp^*_2UCl(NSPh_2)$ Yield; 193 mg (64%) powder. (based on the amount of $Cp^*_2UCl(CH_2)_2PPh_2$ used in the synthesis)

2) The procedure mentioned above was followed using 304 mg (0.40 mmole) of $Cp^*_2UCl(CH_2)_2PPh_2$ and 160 mg (0.80 mmole) of $HNSPh_2$. Yield; 254 mg (71%) crystalline material. (based on the amount of $Cp^*_2UCl(CH_2)_2PPh_2$ used in the synthesis)

2.3.5 Reaction of $HNSPh_2 \cdot H_2O$ With $Cp^*_2UCl_2$

1) An NMR sample was prepared in deuterated toluene using 29 mg (0.05 mmole) of $Cp^*_2UCl_2$ and 44 mg (0.20 mmole) of $HNSPh_2 \cdot H_2O$. The sample turned greenish yellow from dark red upon adding the $HNSPh_2 \cdot H_2O$. ^1H-NMR spectrum, Figure 20, indicates that a new compound forms which gives rise to a single sharp resonance at -2.15 ppm and broad peaks in the aromatic region. The NMR spectrum, Figure 21, of the same sample obtained after 1 week indicates the disappearance of the peak at -2.15 ppm and formation of new peaks at 0.98 ppm and 1.5 ppm which are due to Cp^*H. This observation suggests that the

reaction of $Cp^*_2UCl_2$ with $HNSPh_2 \cdot H_2O$ goes via an intermediate which further reacts to form Cp^*H and final products.

2) An NMR sample was prepared in deuterated toluene using 19 mg (0.03 mmole) of $Cp^*_2UCl_2$ and 22 mg (0.01 mmole) of $HNSPh_2 \cdot H_2O$. The ^1H-NMR spectrum, Figure 22, shows the presence of considerable amounts of $Cp^*_2UCl_2(HNSPh_2)$ and the same intermediate observed in the previous case.

3) 193 mg (0.30 mmole) of $Cp^*_2UCl_2$ and 219 mg (1.0 mmole) of $HNSPh_2 \cdot H_2O$ were dissolved in 25 ml of toluene under nitrogen. After stirring for three hours at room temperature the greenish yellow solution was filtered through a medium porosity frit and evaporated to dryness. The light green residue was washed with 5 ml of pentane and extracted with 15 ml of toluene. The dark green solution was reduced in volume to about 3 ml and stored at room temperature for several days during which dark red-black crystals formed at the bottom of the flask. A light green microcrystalline material had also formed in the sample. The crystals were mounted in 0.5 mm capillaries and used for determining the x-ray crystal

structure. According to the x-ray crystal structure, the formulation of the final product of this reaction is $[Cp^*(Cl)(HNSPh_2)U-(\mu_3-OH)(\mu_2-O)_2-U(Cl)(HNSPh_2)_2]_2$.

In an attempt to isolate the intermediate and the final product in a stoichiometric way, the following NMR and large scale reactions were carried out.

a) A series of ^{1}H-NMR spectra of a sample of sulfilimine hydrate was obtained in deuterated benzene, with variable pulse delay. The integrated intensity of the aromatic protons to the broad peak due to the exchanging NH and H_2O, does not vary with pulse delay and agrees with the formulation, $HNSPh_2 \cdot H_2O$. Figure 23 shows the ^{1}H-NMR spectrum of $HNSPh_2 \cdot H_2O$ in deuterated benzene with a pulse delay of 250 microsec.

b) The following NMR samples were prepared in deuterated benzene.

(1) 39 mg (0.05 mmole) of $Cp^*_2UCl_2(HNSPh_2)$ and 11 mg (0.05 mmole) of $HNSPh_2 \cdot H_2O$.

(2) 39 mg (0.05 mmole) of $Cp^*_2UCl_2(HNSPh_2)$ and 22 mg (0.10 mmole) of $HNSPh_2 \cdot H_2O$.

(3) 39 mg (0.05 mmole) of $Cp^*_2UCl_2(HNSPh_2)$ and 33 mg (0.15 mmole) of $HNSPh_2 \cdot H_2O$.

(4) 20 mg (0.025 mmole) of $Cp^*_2UCl_2(HNSPh_2)$ and 22 mg (0.10 mmole) of $HNSPh_2 \cdot H_2O$.

The ^1H-NMR spectra of these samples are given in Figures 24-27. The signal at -2.1 ppm indicates that the intermediate species forms in every case. Samples (1) and (2) formed large, light green, plate like crystals upon standing at room temperature over night. Crystals from these samples were mounted in 0.5 mm capillaries and used for x-ray crystallography. According to the crystal structure, the intermediate of this reaction is $Cp^*_2UCl(OH)(HNSPh_2)$.

c) To a solution of 193 mg (0.33 mmole) of $Cp^*_2UCl_2(HNSPh_2)$ was added slowly a solution of 73 mg (0.33 mmole) of $HNSPh_2 \cdot H_2O$ in 10 ml of benzene. The sample turned light green from dark orange and a white precipitate formed. The solution was filtered through a medium porosity frit and evaporated to dryness. The green oily residue thus obtained was kept under vacuum overnight in order to remove any unreacted water. The green residue was dissolved in 3 ml of benzene and stored

at room temperature for a week during which green microcrystals formed on the sides and at the bottom of the flask. These crystals were separated from the solution by filtration, dried under vacuum and used for obtaining infrared and low temperature ^{1}H-NMR spectra. The low temperature spectra of $Cp^*_2UCl(OH)(HNSPh_2)$ in deuterated THF were collected between +200 ppm and -200 ppm. The room temperature ^{1}H-NMR spectrum of $Cp^*_2UCl(OH)(HNSPh_2)$ immediately after it was prepared, is shown in Figure 28. The spectrum of the same sample at -60°C is given in Figure 29. The room temperature spectrum contains a sharp signal at -2.7 ppm for the Cp^* group and broad signals near -10.5 ppm, -0.5 ppm and -163 ppm. A small amount of $Cp^*_2UCl_2(HNSPh_2)$ is also present. When the sample temperature decreases the broad peaks at -10.5 ppm and -0.5 ppm significantly sharpen and resolve into three distinct peaks at -15.1, -0.5 and -2.0 ppm. They are assigned to the ortho, meta and para protons of the phenyl groups of the $HNSPh_2$ ligand of $Cp^*_2UCl(OH)(HNSPh_2)$. The broad signal at -163 ppm is assigned to the imino hydrogen. While the peak arising from O-H proton cannot be assigned unambiguously, three broad signals appear near 8.0 and 10.0 ppm when the sample is cooled. Figure 30 describes the variations

that occur in the aromatic region of the spectrum when cooling occurs. These resonances are assigned to the aromatic protons of the complex, $UO_2(HNSPh_2)$, which may arise from the partial decomposition of $Cp^*_2UCl(OH)(HNSPh_2)$. The ^1H-NMR spectrum of the same sample, obtained after several days, is given in Figure 31. The spectrum indicates that the predominant component in the system is $Cp^*_2UCl_2(HNSPh_2)$. Small amounts of $Cp^*_2UCl(OH)(HNSPh_2)$ and Cp^*H are also observed. A broad signal is also observed in the spectrum near 7.2 ppm which is assigned to the aromatic signals of $UO_2(HNSPh_2)$.

Green micro crystals form upon immediate evaporation of toluene from the reaction of 193 mg (0.33 mmole) of $Cp^*_2UCl_2(HNSPh_2)$ and 73 mg (0.33 mmole) of $HNSPh_2 \cdot H_2O$ conducted as described above. These were separated by filtration, rinsed with 2 ml of pentane, dried under vacuum tested for purity by NMR and used for calculating the percentage yield of the product. Yield: 120 mg (63.7%) (based on the amount of $Cp^*_2UCl_2(HNSPh_2)$ used). Elemental analysis; Observed: C = 43.35, H = 3.58, N = 2.98, Calculated; C = 50.42, H = 5.55, N = 1.84, Cl = 4.65. The difference in the observed and calculated elemental analyses is due to extremely low stability of

$Cp^*_2UCl(OH)(HNSPh_2)$. The infrared spectrum of $Cp^*_2UCl(OH)(HNSPh_2)$ is shown in Figure 32 and data are summarized in Table 8.

An NMR sample containing 30 mg (0.04 mmole) of $Cp^*_2UCl_2(HNSPh_2)$ and 33 mg (0.15 mmole) of $HNSPh_2 \cdot H_2O$ in deuterated toluene formed the final product, $[Cp^*(Cl)(HNSPh_2)U-(\mu_3-OH)(\mu_2-O)_2-U(Cl)(HNSPh_2)_2]_2$, as dark red-black microcrystals, upon standing at room temerature for three weeks. The crystals were isolated under nitrogen, washed with 0.5 ml of pentane and dried under vacuum. Low temperature ^{1}H-NMR spectra of this compound were collected in d_8-THF between +200 ppm and -200 ppm. The room temperature spectrum of $[Cp^*(Cl)(HNSPh_2)U-(\mu_3-OH)(\mu_2-O)_2-U(Cl)(HNSPh_2)_2]_2$ is given in Figure 33. While the peaks arising from the aromatic protons and the OH groups cannot be identified unambiguously, the spectrum contains a sharp singlet at 21.9 ppm for the Cp^* group, a small broad signal at -120 ppm for the NH and broad signals at 15.8, 6.5, -0.5, -1.5, -2.2, -3.7, -9.2 and -10.0 ppm.

There is also an unidentified sharp singlet at 22.6 ppm. When the temperature of the sample was decreased, the signals became considerably broader and no additional changes occurred in the spectra. The infrared spectrum

of this compound is shown in Figure 34 and data are summarized in Table 9. While it is difficult to assign the N-H and O-H stretches, broad signals appear between 3000 and 3500 cm^{-1} in the infrared spectra of both $Cp^*_2UCl(OH)(HNSPh_2)$ and $[Cp^*(Cl)(HNSPh_2)U-(\mu_3-OH)(\mu_2-O)_2-U(Cl)(HNSPh_2)_2]_2$.

2.3.6 Reaction of Cp_3UCl with $Me_3SiNPPh_3$

An NMR sample was prepared using 23 mg (0.05 mmole) of Cp_3UCl and 17 mg (0.05 mmole) of $Me_3SiNPPh_3$ in deuterated tetrahydrofuran. ^1H-NMR spectra of the sample were obtained periodically over a three day period. The sample was then heated in a warm water bath at 75°c overnight and the NMR spectrum was retaken.

Another NMR sample was prepared using 23 mg (0.05 mmole) of Cp_3UCl and 34 mg (0.10 mmole) of $Me_3SiNPPh_3$ in the same solvent and the spectra were obtained as mentioned above.

In both cases, no evidence of any chemical reaction was obtained from the NMR spectra.

2.3.7 Reaction of $Cp_3U=CHPR_3$ with $HNSPh_2$

The following NMR samples were prepared in deuterated toluene.

1) 32.3 mg (0.05 mmole) of $Cp_3U=CHPMePh_2$ and
   10.0 mg (0.05 mmole) of $HNSPh_2$.

2) 32.3 mg (0.05 mmole) of $Cp_3U=CHPMePh_2$ and
   20.0 mg (0.10 mmole) of $HNSPh_2$.

A yellow precipitate formed in both cases. The ^{1}H-NMR spectra indicate that Cp_3UNSPh_2 forms in both cases. Figure 35 shows the ^{1}H-NMR spectrum of the above reaction 1. The spectrum contains a sharp singlet for Cp group at -18.3 ppm, a doublet at 14.5 ppm for ortho, and triplets at 8.9 and 8.3 ppm for meta and para protons of the $[NSPh_2]^-$ group. The NMR samples were heated in a water bath at 75°C for 48 hrs and ^{1}H-NMR spectra were obtained. No evidence of further reactions was observed in both cases.

Both NMR samples formed dark red needle like crystals upon standing at room temperature for three weeks. They were selected, mounted in 0.5 mm capillaries

and used for x-ray crystallography. However, an accurate crystal structure for Cp_3UNSPh_2 could not be obtained due to disorder problems.

2.3.8 Reaction of $Cp_3U{=}CHPR_3$ with $HNPPh_3$

An NMR sample was prepared using 23.0 mg (0.05 mmole) of $Cp_3UCHPMePh_2$ and 27.6 mg (0.10 mmole) of $HNPPh_3$ in deuterated tetrahydrofuran. The ^{1}H-NMR spectrum, Figure 36, contains peaks that are consistent with $Cp_3U(NPPh_3)$ which is already reported in literature. It is also evident that $Cp_2U(NPPh_3)_2$ also forms in the system to some extent. An NMR experiment of $Cp_3UCHPMePh_2$ and $HNPPh_3$ with 1:4 ratio in d_8-THF, Figure 37, contains $Cp_2U(NPPh_3)_2$ as the major product. Attempted separations of the two complexes using large scale reactions were unsuccessful.

2.3.9 Reaction of UO_2Cl_2 with $Me_3SiNSPh_2$

1) An NMR sample was prepared in d_8-THF using 17.0 mg (0.05 mmole) of UO_2Cl_2 and 13.7 mg (0.05 mmole) of $Me_3SiNSPh_2$. The ^{1}H-NMR spectrum of $Me_3SiNSPh_2$ is given in Figure 38 and that of the reaction in Figure 39.

The spectrum of the reaction contains a new peak at 0.03 ppm which indicates that a new species formed.

2) To 68 mg (0.20 mmole) of UO_2Cl_2 in 25 ml of tetrahydrofuran was added a solution of 54.2 mg (0.20 mmole) of $Me_3SiNSPh_2$ in 15 ml of tetrahydrofuran. A dark yellow precipitate immdiately formed in the solution. After stirring for 30 mins the solution was filtered through a medium porosity frit. The yellow residue was rinsed with 5 ml of pentane and dried under vacuum. The ^{1}H-NMR spectrum of the yellow solid in deuterated THF, is given in Figure 40. The spectrum shows that it is a solvate. There are triplets at 1.8 and 3.6 ppm for THF and signals around 7.5 ppm for the phenyl groups of the product. The solid product was dissolved in 5 ml of acetonitrile and stored in the freezer for crystallization. No evidence of any crystallization was observed after 4 weeks.

2.3.10 Reaction of UO_2Cl_2 with $Me_3SiNPPh_3$

1) An NMR sample was prepared in d_8-THF using 17 mg (0.05 mmole) of UO_2Cl_2 and 17 mg (0.05 mmole) of $Me_3SiNPPh_3$. The ^{1}H-NMR spectrum of $Me_3SiNPPh_3$ in

deuterated THF is shown in Figure 41 and that of the reaction in Figure 42. According to Figure 42 a new Me_3Si species forms during this reaction. The sample was opened, a small amount of freshly distilled Me_3SiCl was added and the spectrum was retaken. The ^1H-NMR spectrum, Figure 43, shows that the new Me_3Si species that forms in the reaction is a different species from Me_3SiCl which shows a sharp singlet at 0.3 ppm.

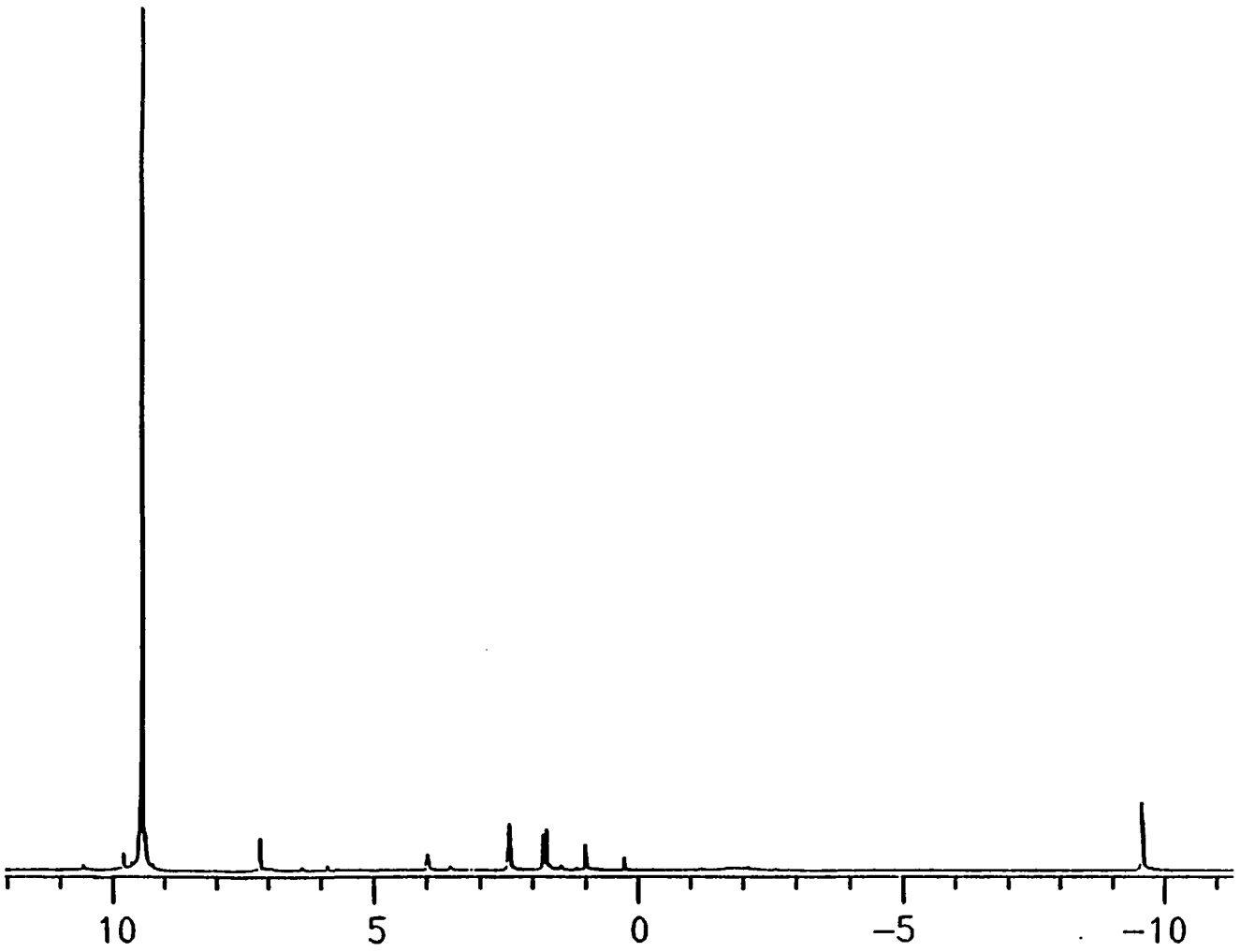

Figure 5: ^{1}H-NMR Spectrum of $Cp^{*}_{2}UCl_{2}(HNSPh_{2})$ in d_{6}-Benzene

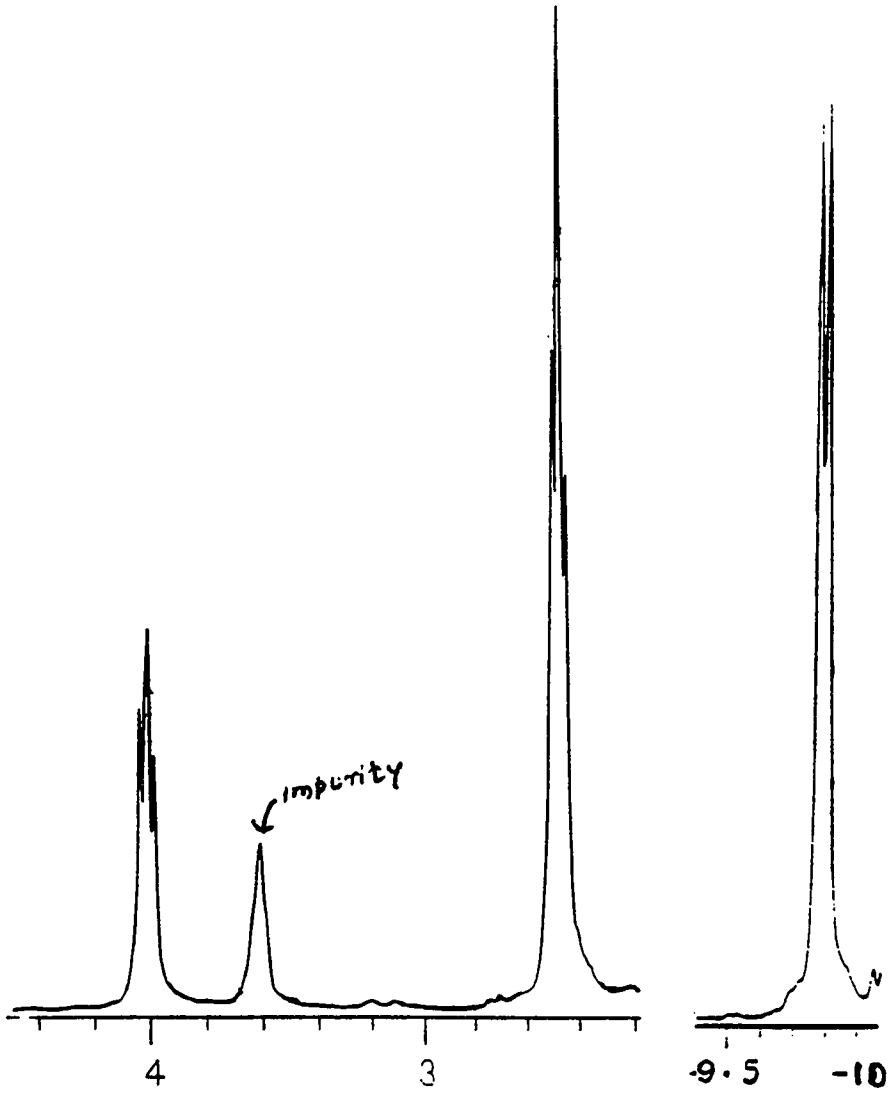

Figure 6: Expanded Aromatic Region of the ^{1}H-NMR Spectrum of $Cp^*_2UCl_2(HNSPh_2)$

TABLE 1

^{1}H-NMR Spectral Data for $Cp^*_2UCl_2(HNSPh_2)$

Chemical Shift (ppm)	Intensity (H)	Coupling Constant (Hz)	Assignment
9.43 s	30		UCp^*
3.85 t	2	$J_{C-H} = 7$	S-Ph(p)
2.31 t	4	$J_{C-H} = 7$	S-Ph(m)
-9.79 d	4	$J_{C-H} = 7$	S-Ph(o)
-142.00 s	1		N-H

s = singlet, d = doublet, t = triplet

a) Spectra obtained at 23°C in d_8-toluene.
b) Chemical shifts referenced to internal standard, then recalculated relative to TMS, negative shifts are upfield of TMS.

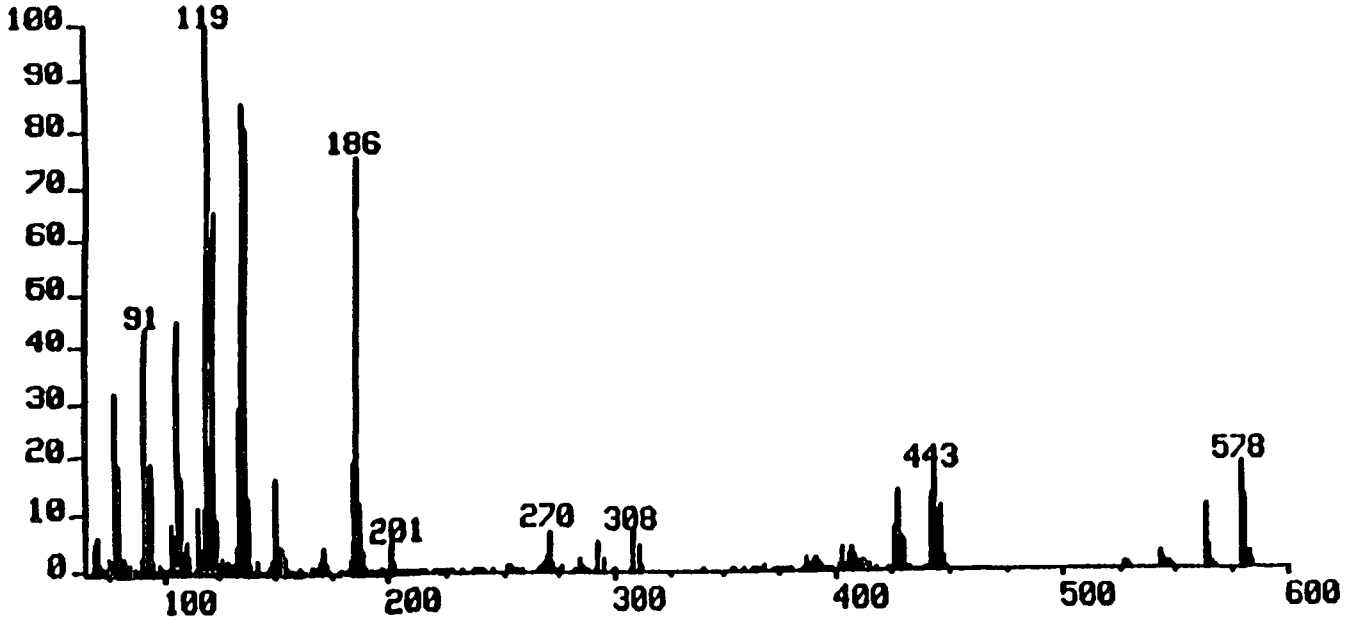

Figure 7: Mass Spectrum of $Cp^*_2UCl_2(HNSPh_2)$

TABLE 2

Mass Spectral Data of $Cp^*_2UCl_2(HNSPh)_2$

Peaks	Realtive Intensity	Possible Assignment
578	18	$Cp^*_2UCl_2$
443	17	Cp^*UCl_2
308	6	Cp^*UCl
270	7	$(Cp^*)_2$
201	5	$HNSPh_2$
186	75	SPh_2
119	100	
91	5	

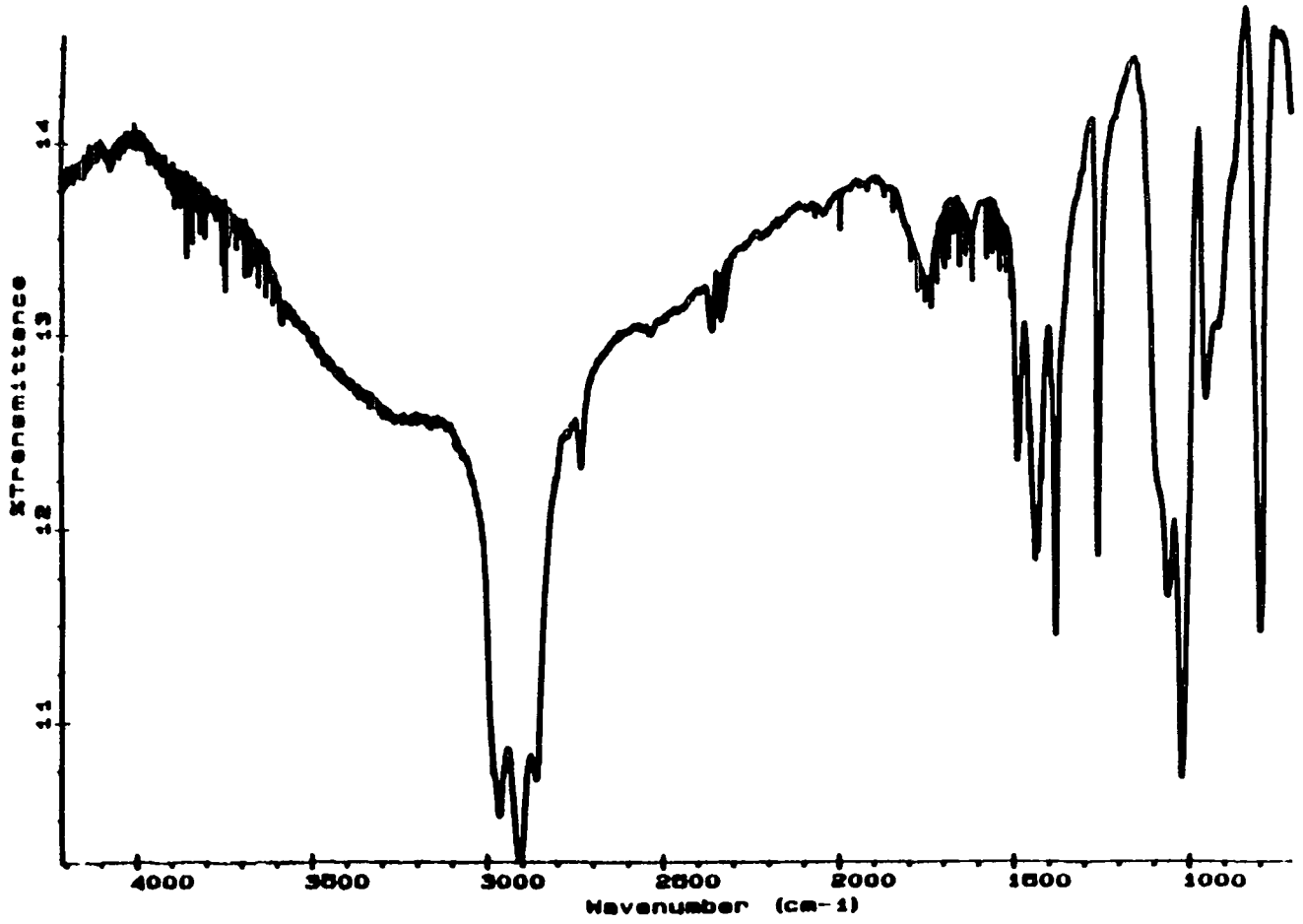

Figure 8: Infrared Spectrum of $Cp^*_2UCl_2$

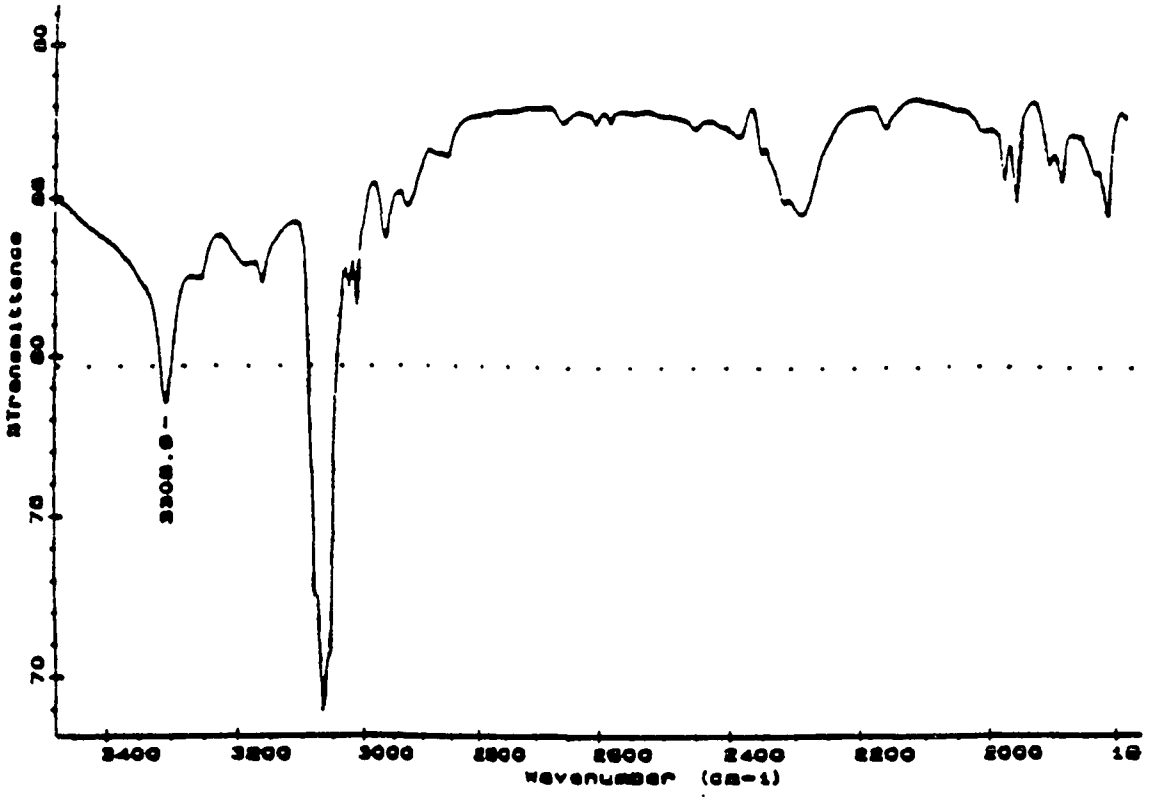

Figure 9: Infrared Spectrum of $HNSPh_2$

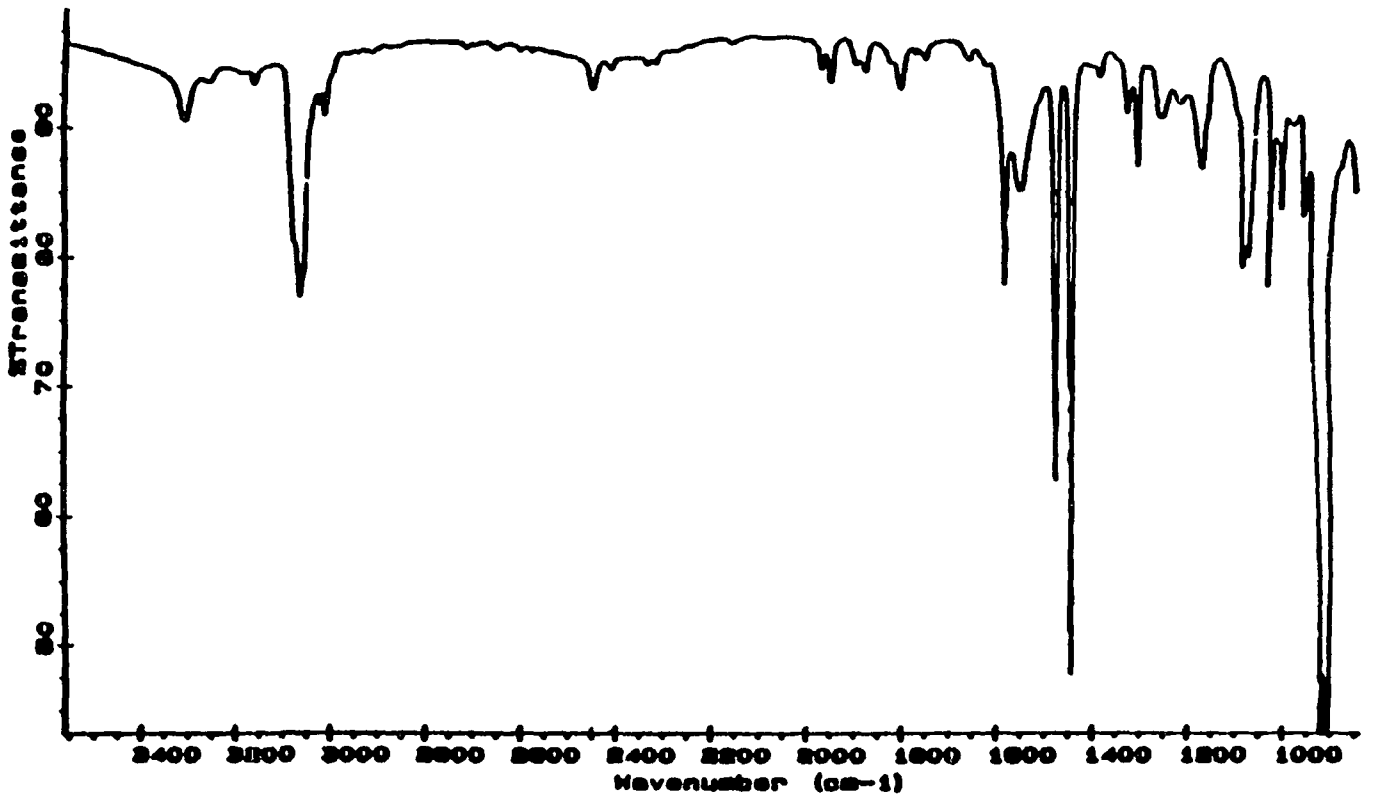

Figure 10: Infrared Spectrum of $DNSPh_2$

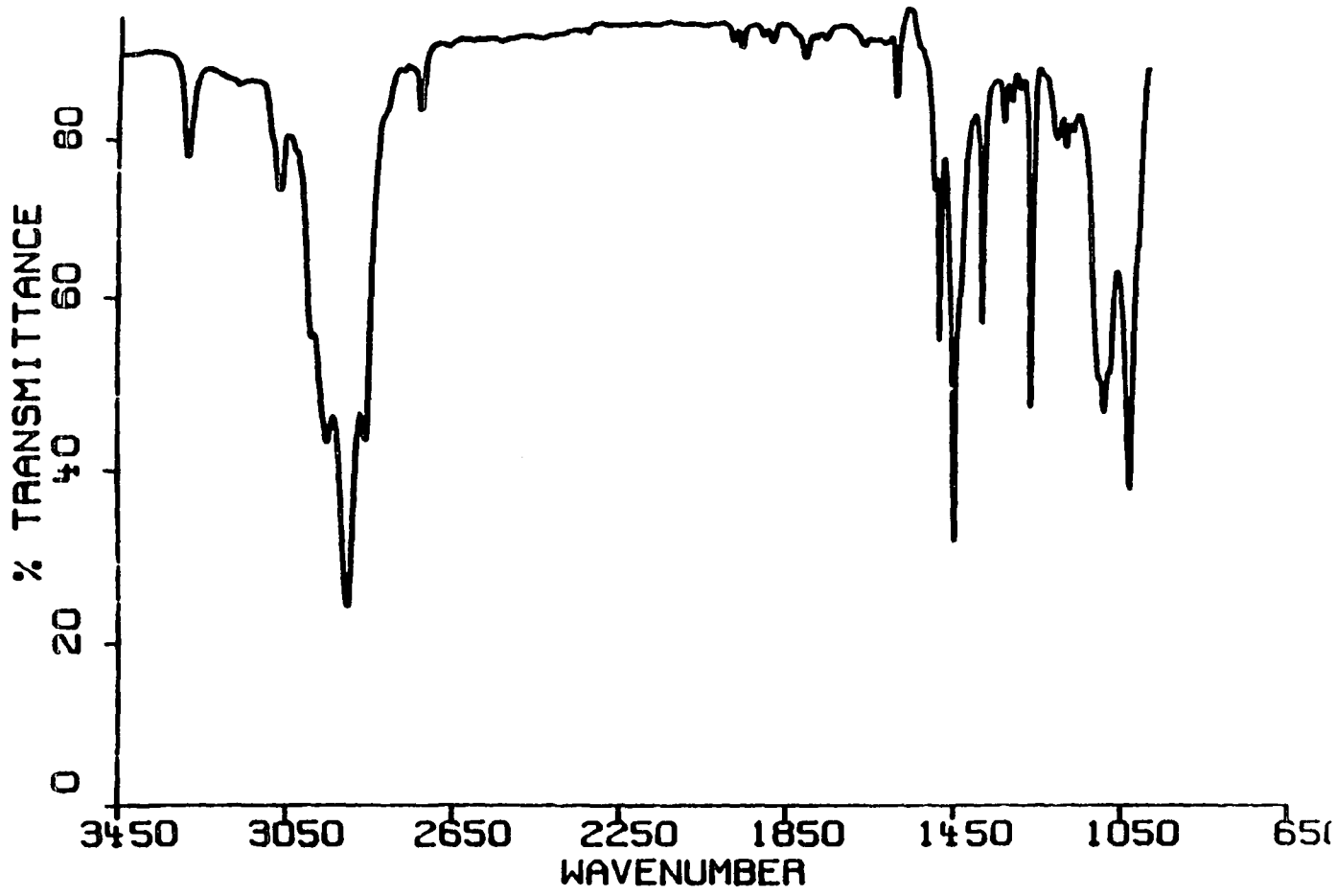

Figure 11: Infrared Spectrum of $Cp^*_2UCl_2(HNSPh_2)$

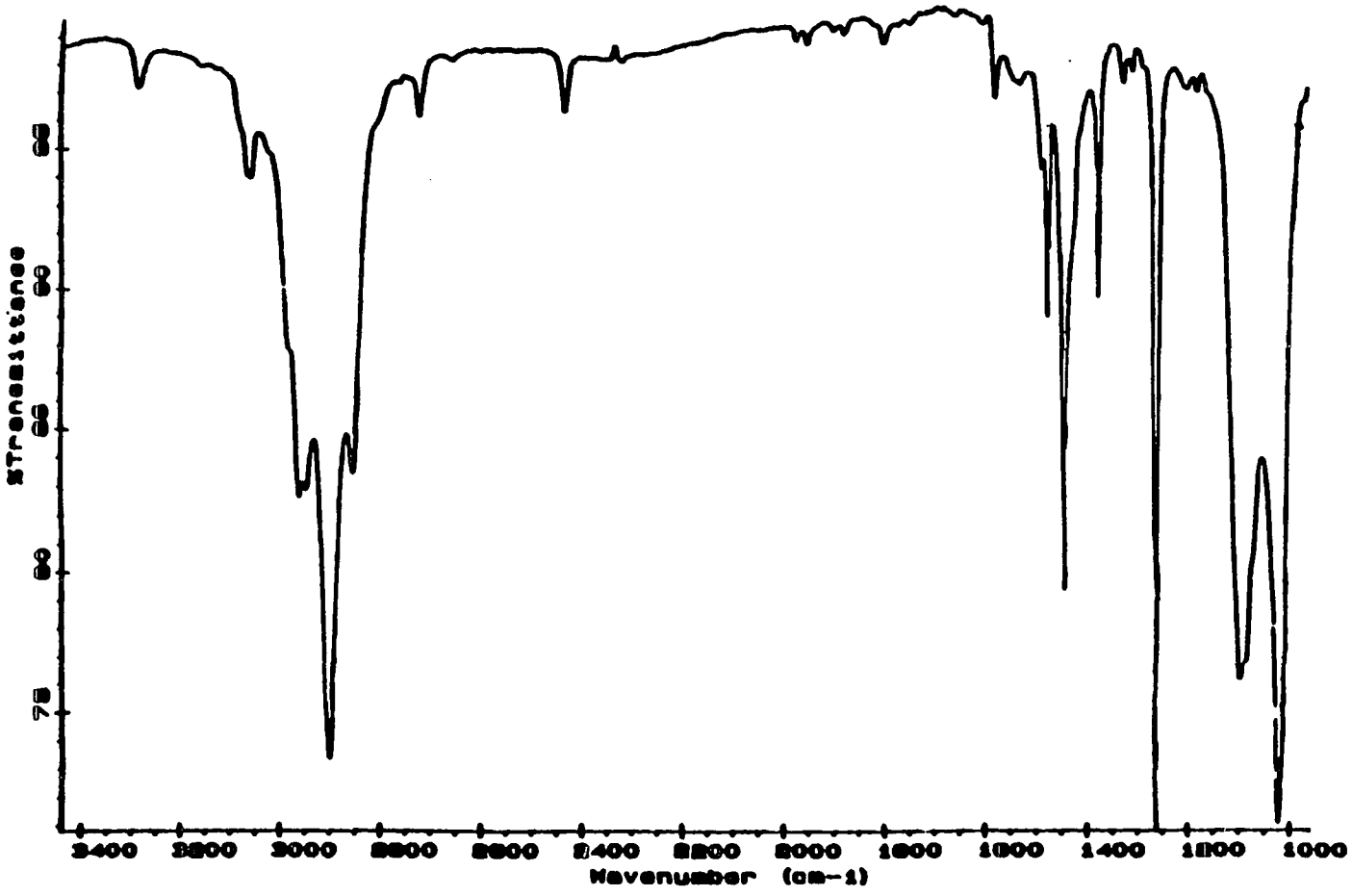

Figure 12: Infrared Spectrum of $Cp^*_2UCl_2(DNSPh_2)$

TABLE 3

Infrared Spectral Data of $Cp^*_2UCl_2(HNSPh_2)$

Frequencies	Possible Assignment
3284 w	N-H
3065 m	C-H(Ph)
2925 s	C-H(Cp^*)
2900 vs	C-H(Cp^*)
2830 s	C-H(Cp^*)
2700 w	
2435 w	N-D, $Cp^*_2UCl_2(DNSPh_2)$
1625 w	C=C(Ph)
1470 m	
1425 s	S-Ph[b]
1385 m	
1060 m	
1000 s	
990 w	
900 vs	

vs=very strong, s=strong, m=medium, w=weak

a) spectrum obtained as a solution in CCl_4.
b) planar ring deformation of phenyl group attached to sulfur.

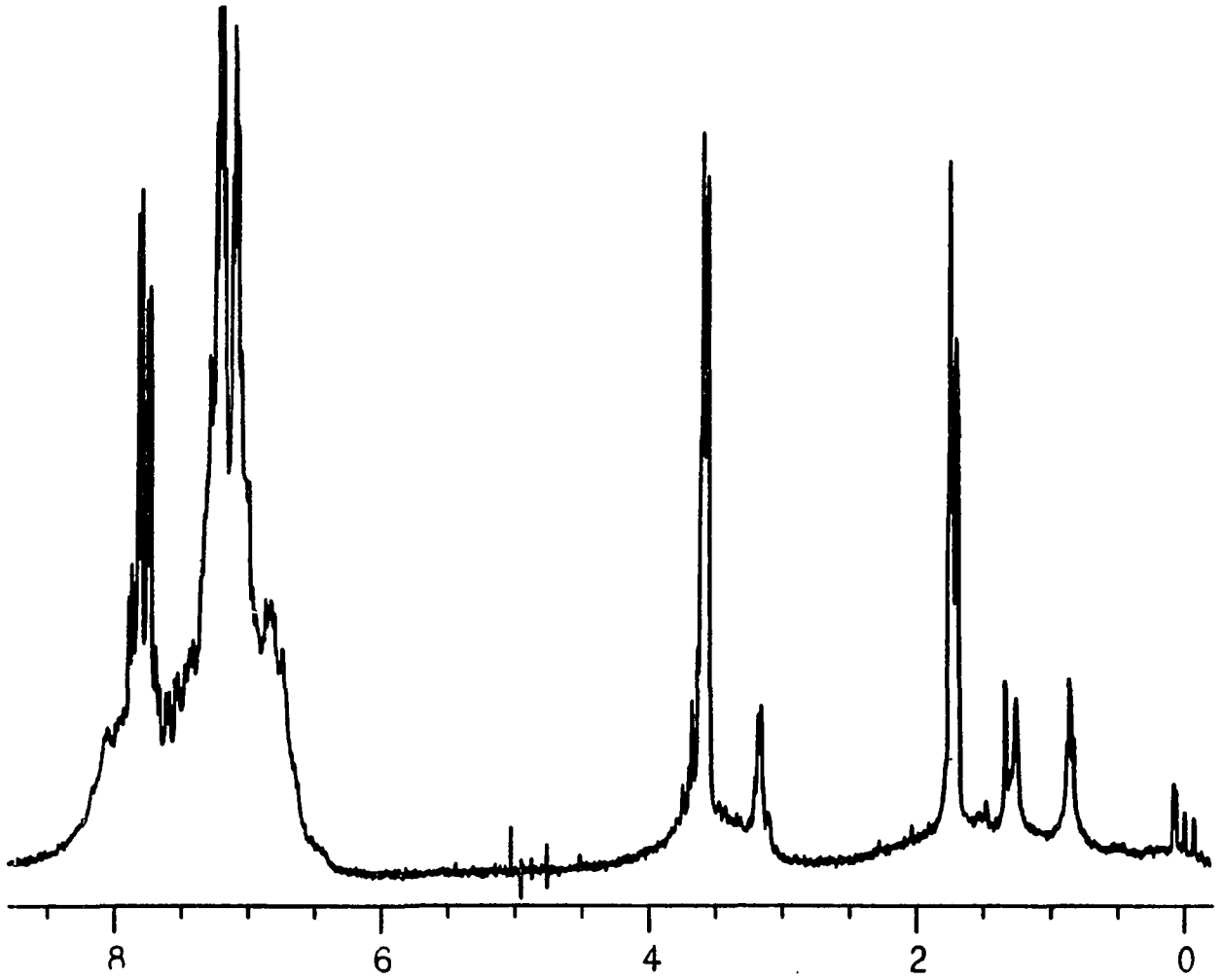

Figure 13: ^{1}H-NMR Spectrum of $LiNSPh_2$ in d_8-THF

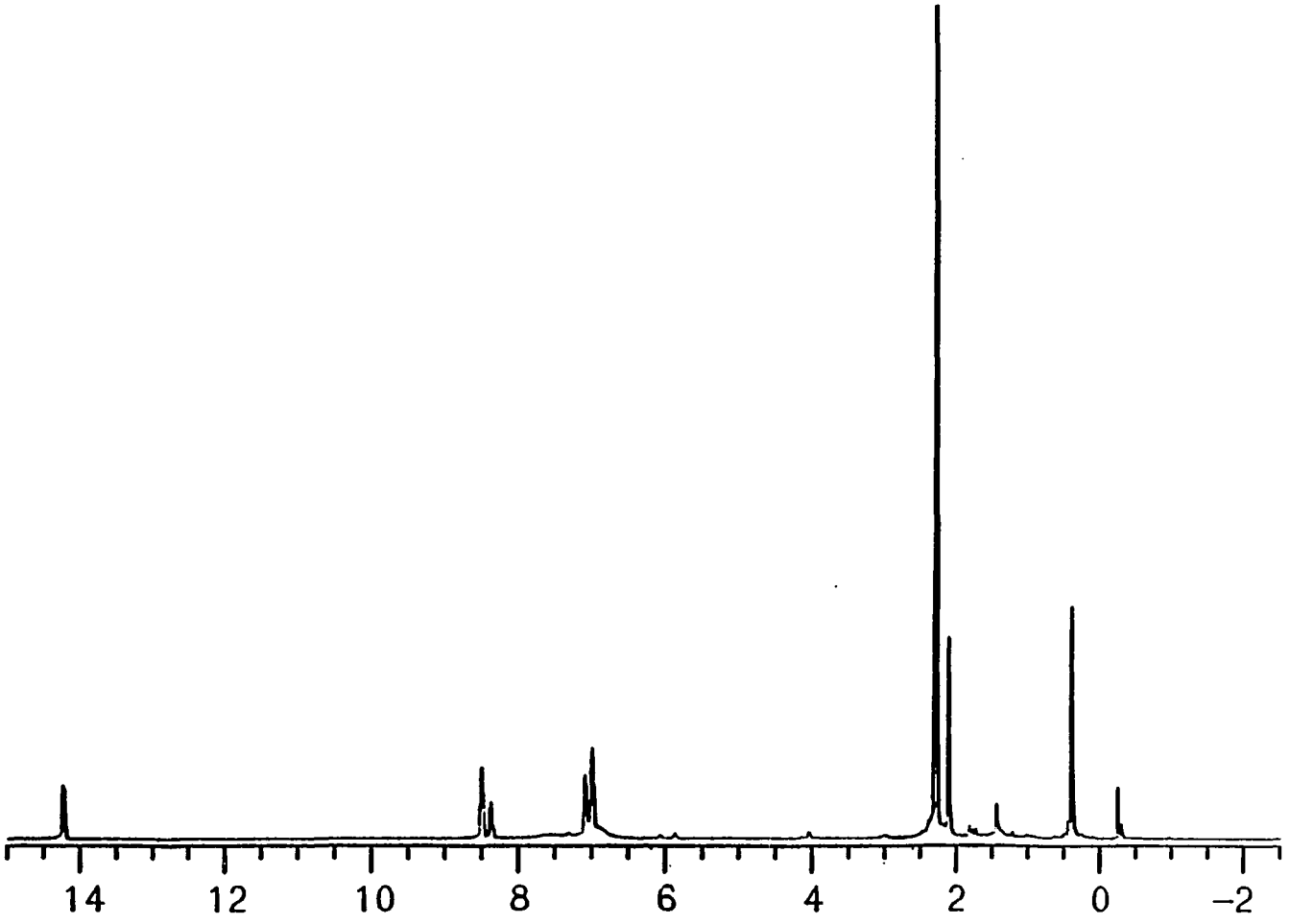

Figure 14: ^{1}H-NMR Spectrum of $Cp^{*}_{2}UCl(NSPh_{2})$ in d_{8}-Toluene

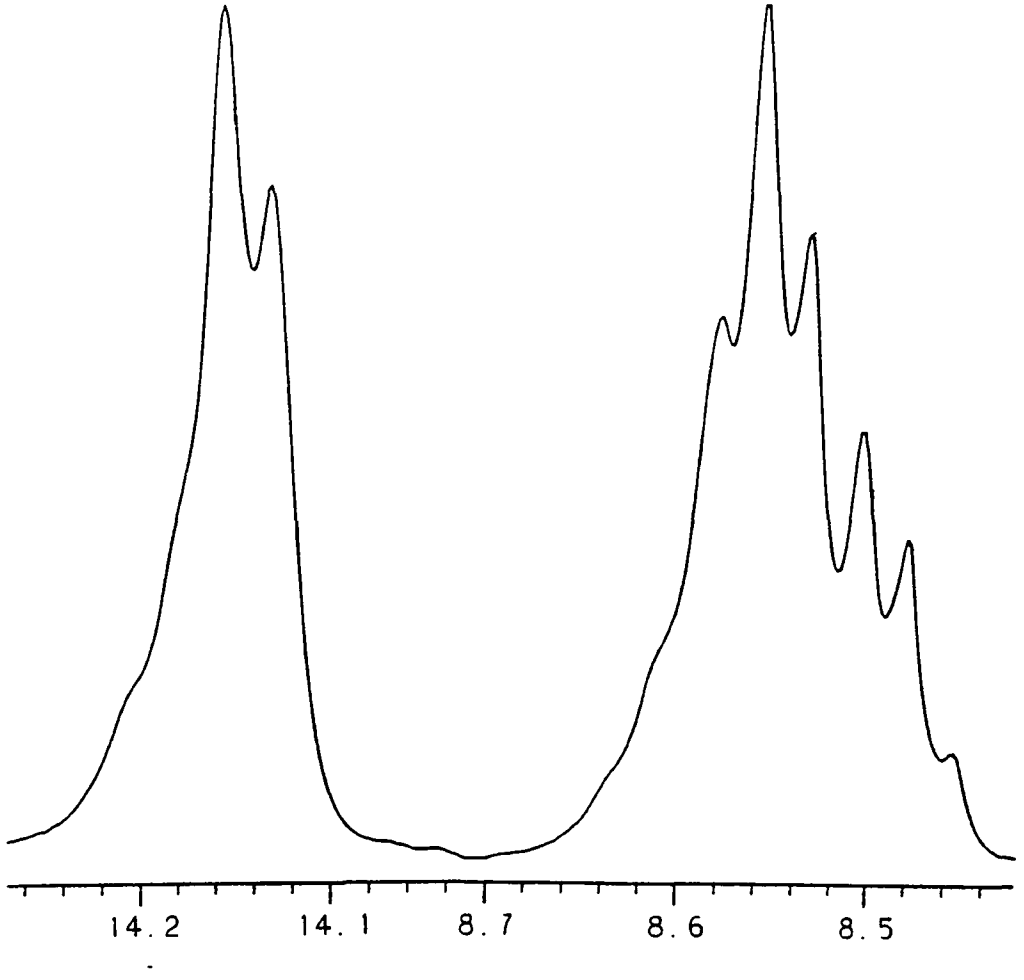

Figure 15: Expanded Aromatic Signals of $Cp^*_2UCl(NSPh_2)$

TABLE 4

^{1}H-NMR Spectral Data for $Cp^*_2UCl(NSPh_2)$

Chemical Shift (ppm)	Intensity (H)	Coupling constant (Hz)	Assignment
2.27 s	30		UCp^*
8.37 t	2	$J_{C-H} = 7$	S-Ph(P)
8.48 t	4	$J_{C-H} = 7$	S-Ph(m)
14.12 d	4	$J_{C-H} = 7$	S-Ph(o)

s = singlet, d = doublet, t = triplet

a) Spectra obtained at 23°C in d_8-toluene.
b) Chemical shifts referenced to internal standard, then recalculated relative to TMS.

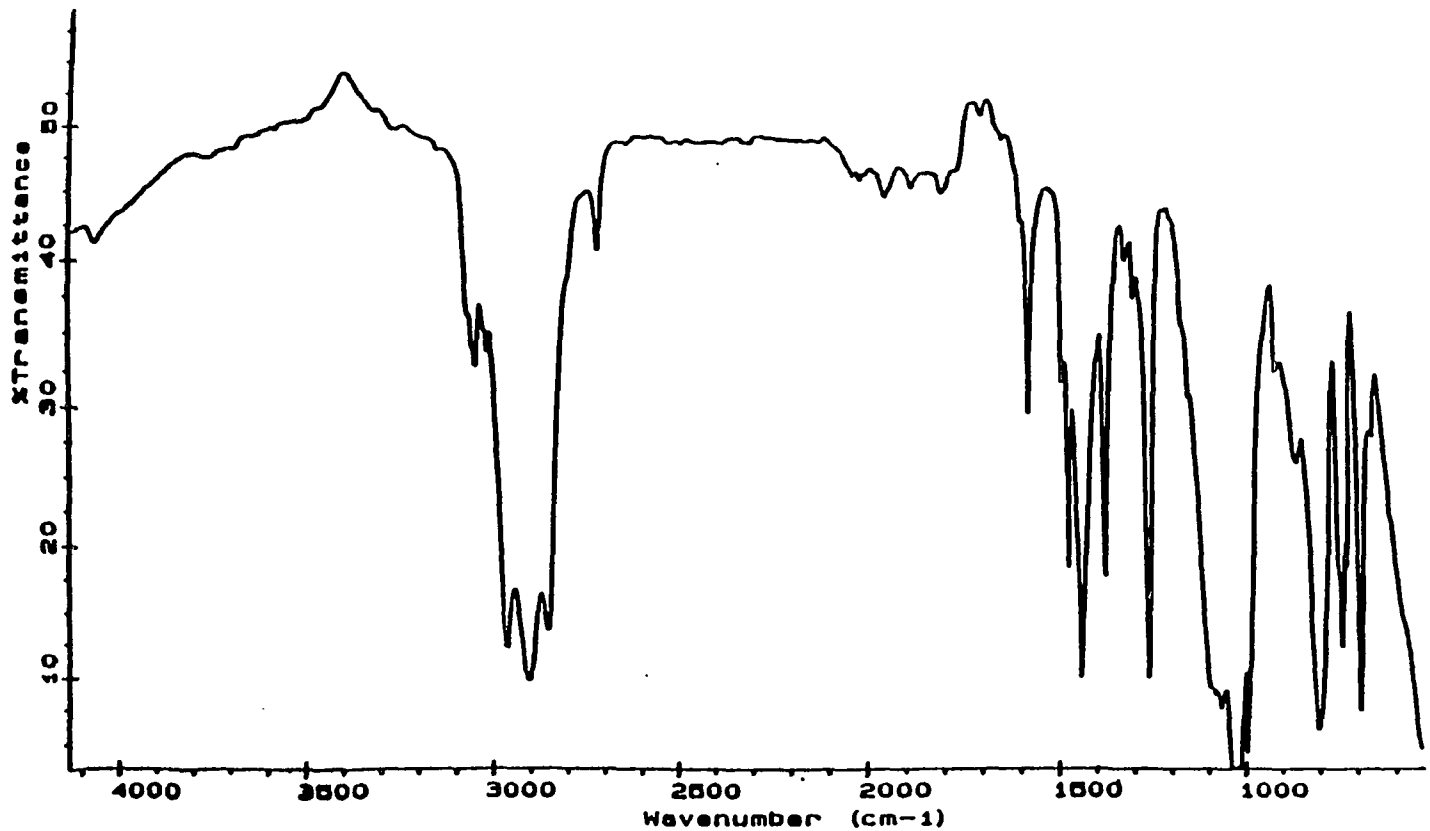

Figure 16: Infrared Spectrum of $Cp^*_2UCl(NSPh_2)$

TABLE 5

IR Spectral Data of $Cp^*_2UCl(NSPh_2)$

Frequencies	Possible Assignment
3010 vs	C-H(ph), C-H(Cp^*)
3000 w	C-H(ph), C-H(Cp^*)
2975 vs	C-H(ph), C-H(Cp^*)
2820 s	
2690 w	
1555 m	
1475 s	C=C(ph)
1450 v	S-Ph_b
1360 s	
1270 vs	
1025 vs	
1000 s	
800 vs	N-S
750 s	
695 s	

vs=very strong, s=strong, m=medium, w=weak

a) spectrum obtained as thin film on NaCl plates.
b) planar ring deformation of phenyl groups attached to sulfur.

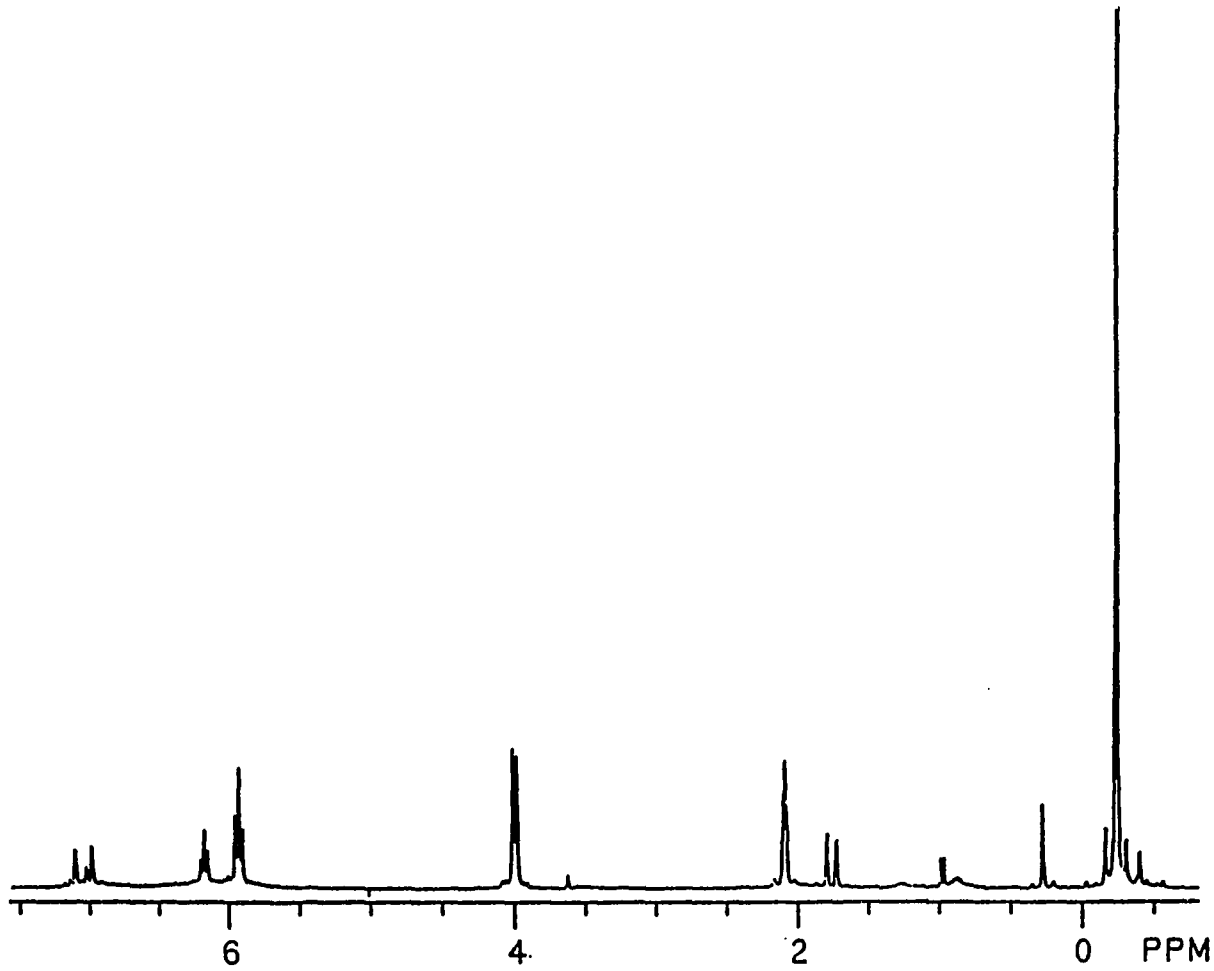

Figure 17: ^{1}H-NMR Spectrum of $Cp^{*}_{2}U(NSPh_{2})_{2}$ in d_{8}-Toluene

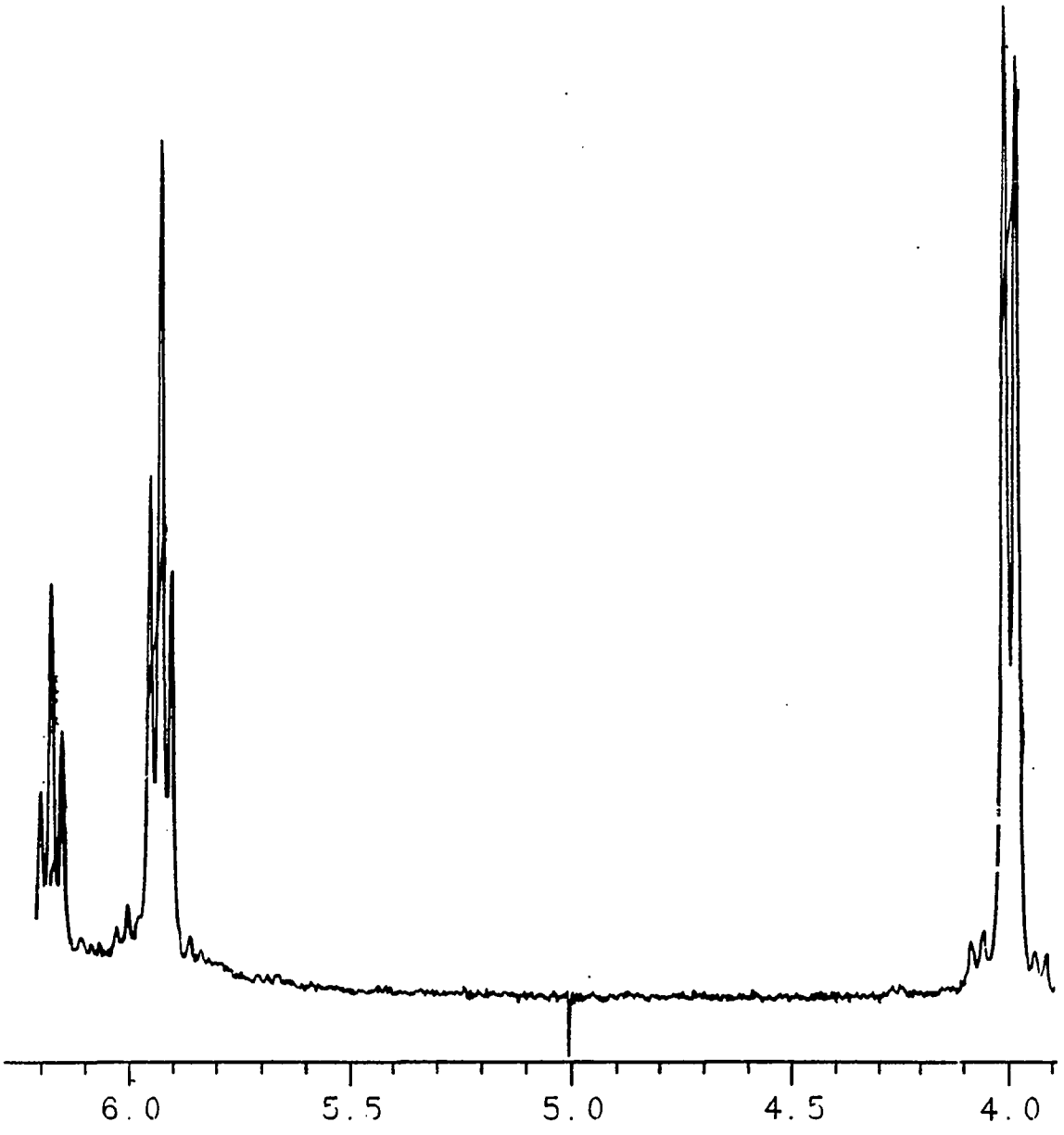

Figure 18: Expanded Aromatic Region of $Cp^*_2U(NSPh_2)_2$

TABLE 6

^{1}H-NMR Spectral Data for $Cp^*_2U(NSPh_2)_2$

Chemical Shift (ppm)	Intensity (H)	Coupling Constant (Hz)	Assignment
-0.24 s	30		U-Cp^*
6.18 t	4	J_{C-H} = 7	S-Ph(P)
5.93 t	8	J_{C-H} = 7	S-Ph(M)
3.93 d	8	J_{C-H} = 7	S-Ph(O)

s = singlet , d = doublet, t = triplet

a) Spectra obtained at 23°C in d_8-toluene.
b) chemical shifts referenced to internal standard, then recalculated to TMS, negative shifts are upfield of TMS.

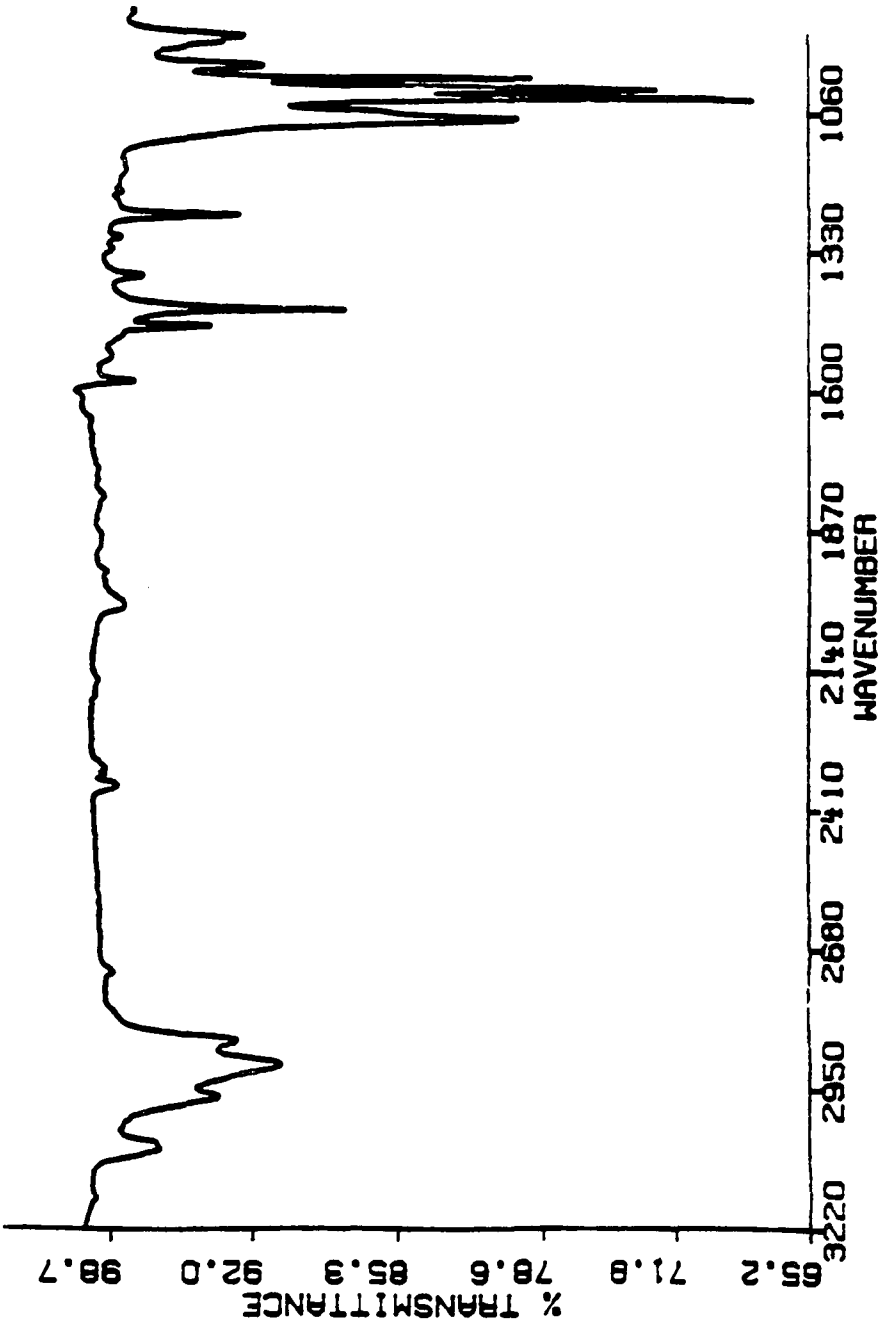

Figure 19: Infrared Spectrum of $Cp^*_2U(NSPh_2)_2$

TABLE 7

Infrared Spectral Data of $Cp^*_2U(NSPh_2)_2$

Frequencies (cm^{-1})	Possible Assignment
3075 m	C-H (Ph)
3010 m	C-H (Cp^*)
2890 m	C-H (Cp^*)
2860 m	C-H (Cp^*)
2300 w	
1965 w	
1585 w	C=C (Ph)
1465 w	C-H (Ph)[b]
1425 m	C-H (Ph)[b]
1300 w	
1080 s	
1000 vs	
990 s	

vs = very strong, s = strong, m = medium, w = weak

a) Spectrum obtained as a solution of CCl_4.
b) Planar rong deformation of phenyl group attached to sulfur.

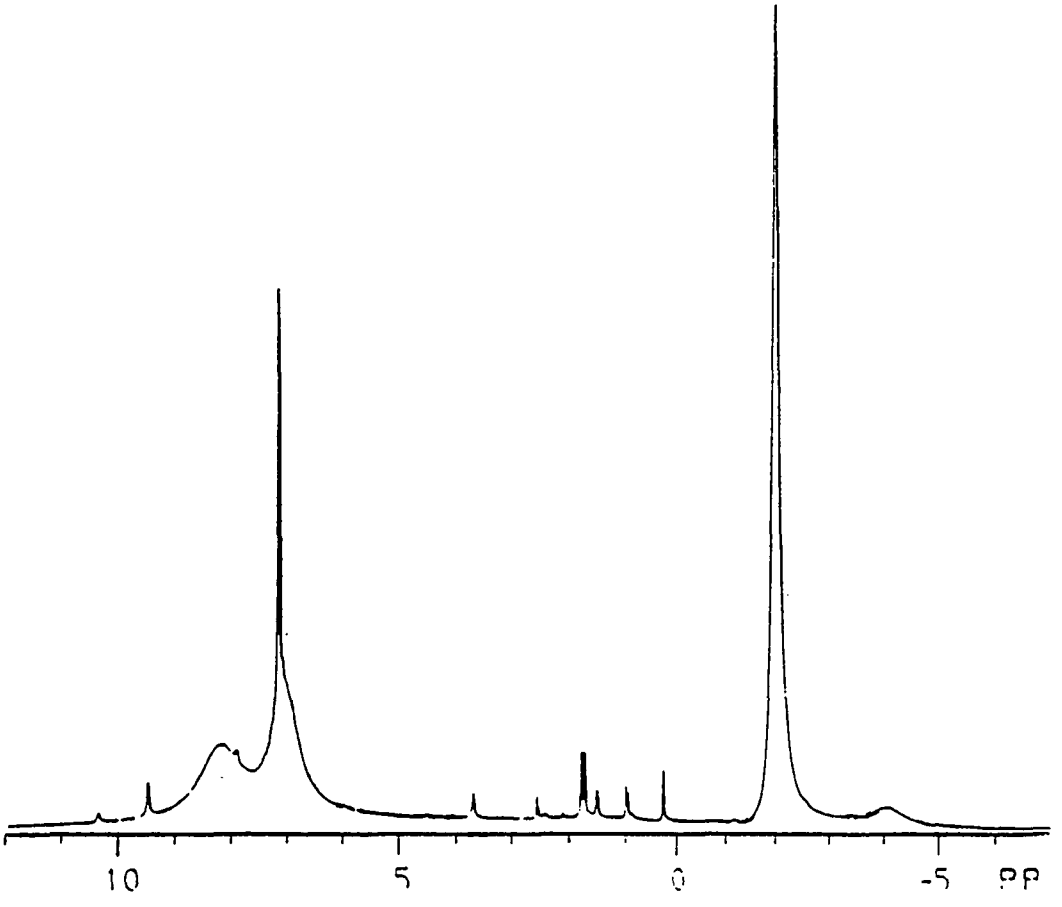

Figure 20: ^{1}H-NMR Spectrum of the Reaction of $Cp^*_2UCl_2$ and $HNSPh_2.H_2O$ (1:4) in d_6-Benzene Soon After the Sample was Prepared.

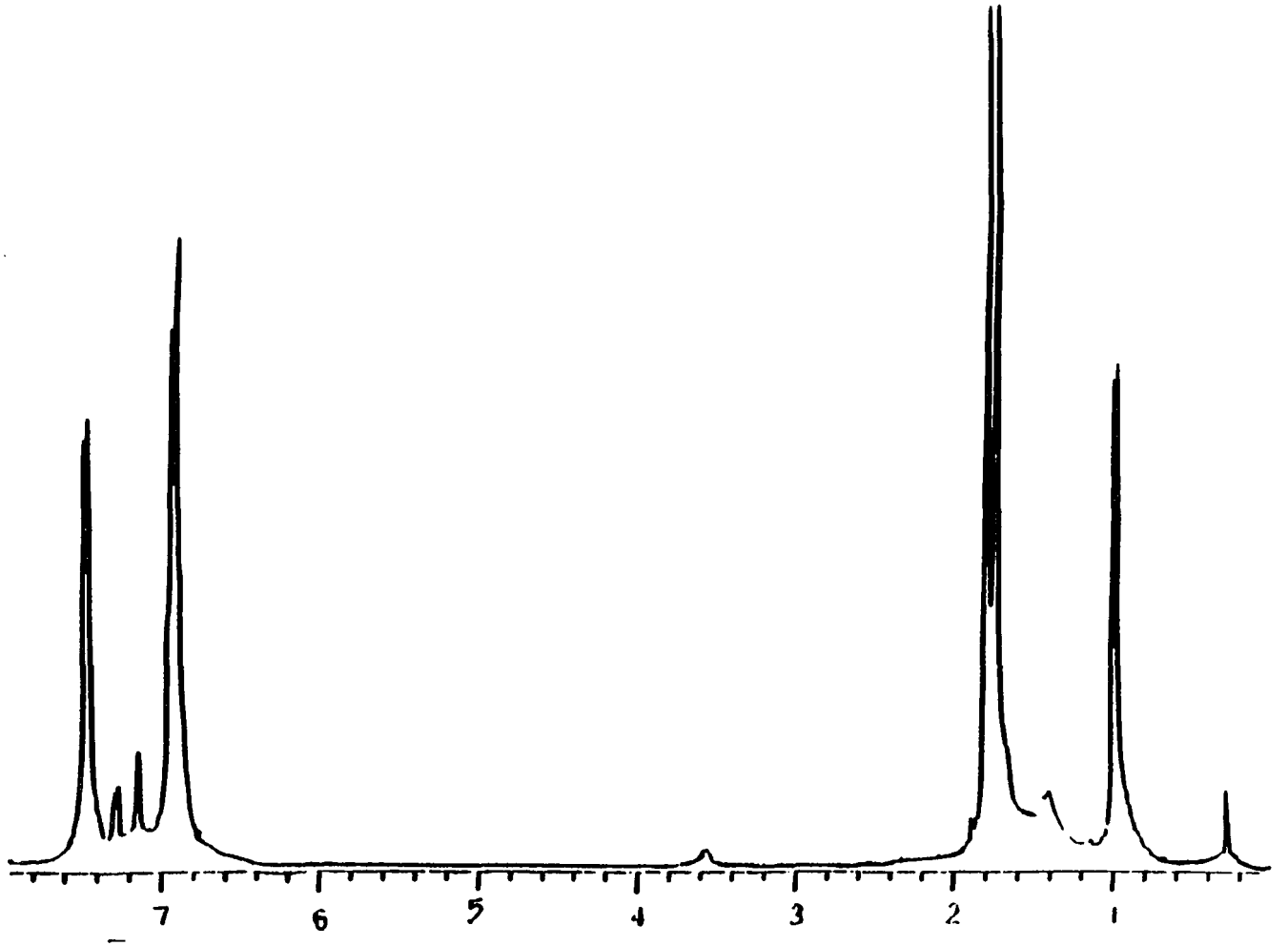

Figure 21: ^{1}H-NMR Spectrum of the Reaction of $Cp^*_2UCl_2$ and $HNSPh_2.H_2O$ (1:4) After One Week

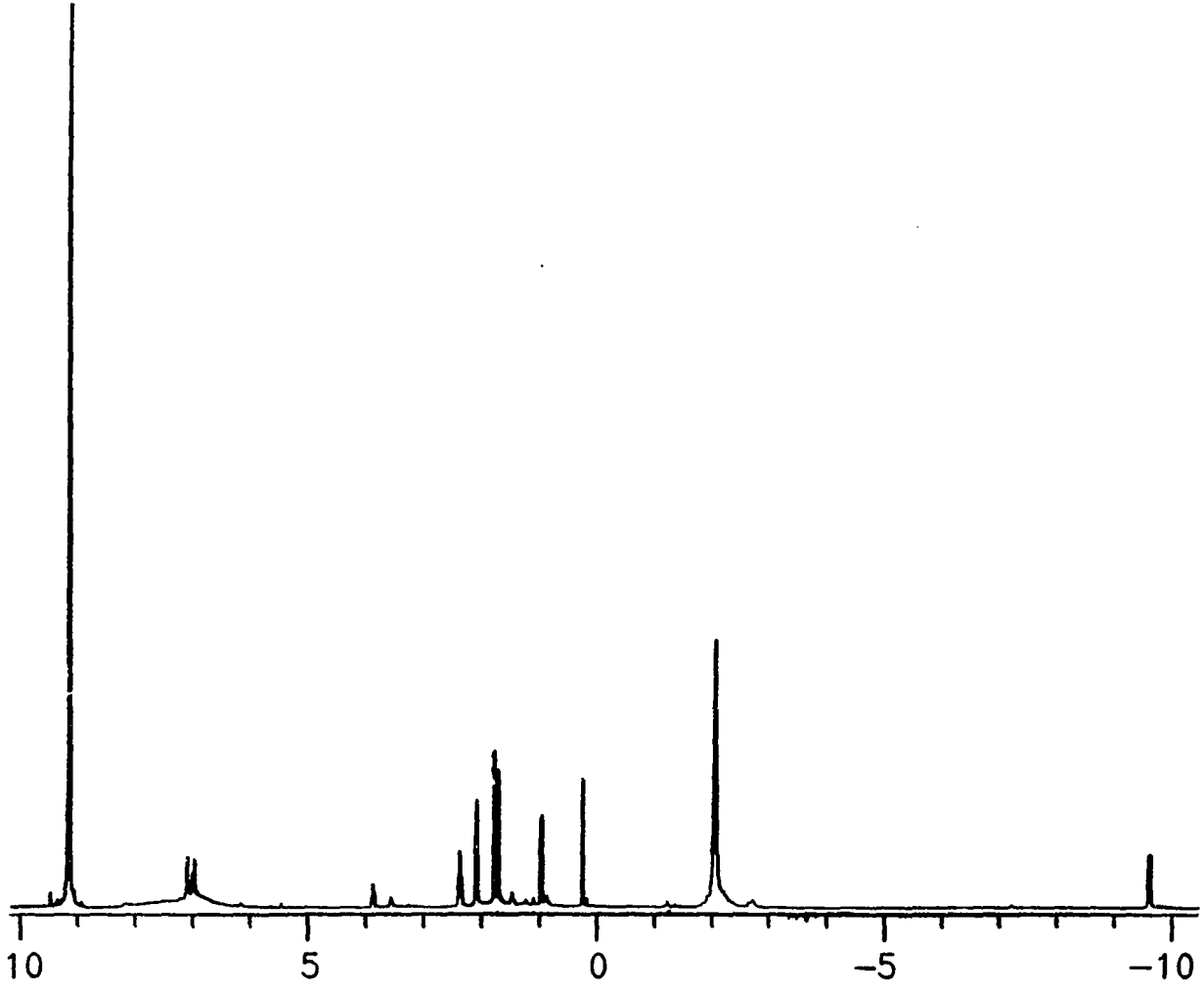

Figure 22: ^{1}H-NMR Spectrum of the Reaction of $Cp^{*}_{2}UCl_{2}$ and $HNSPh_{2}.H_{2}O$ (1:3) in d_{8}-Toluene

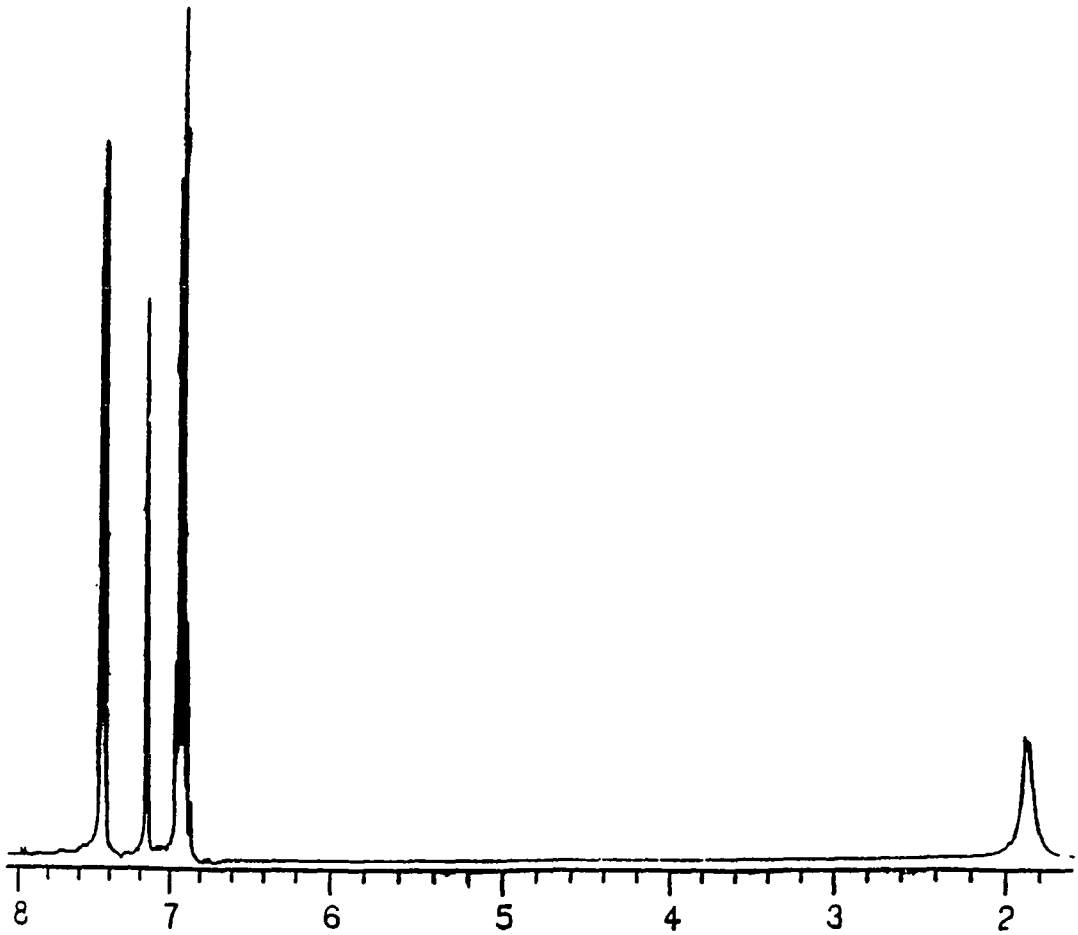

Figure 23: ^{1}H-NMR Spectrum of $HNSPh_2.H_2O$ in d_6-Benzene

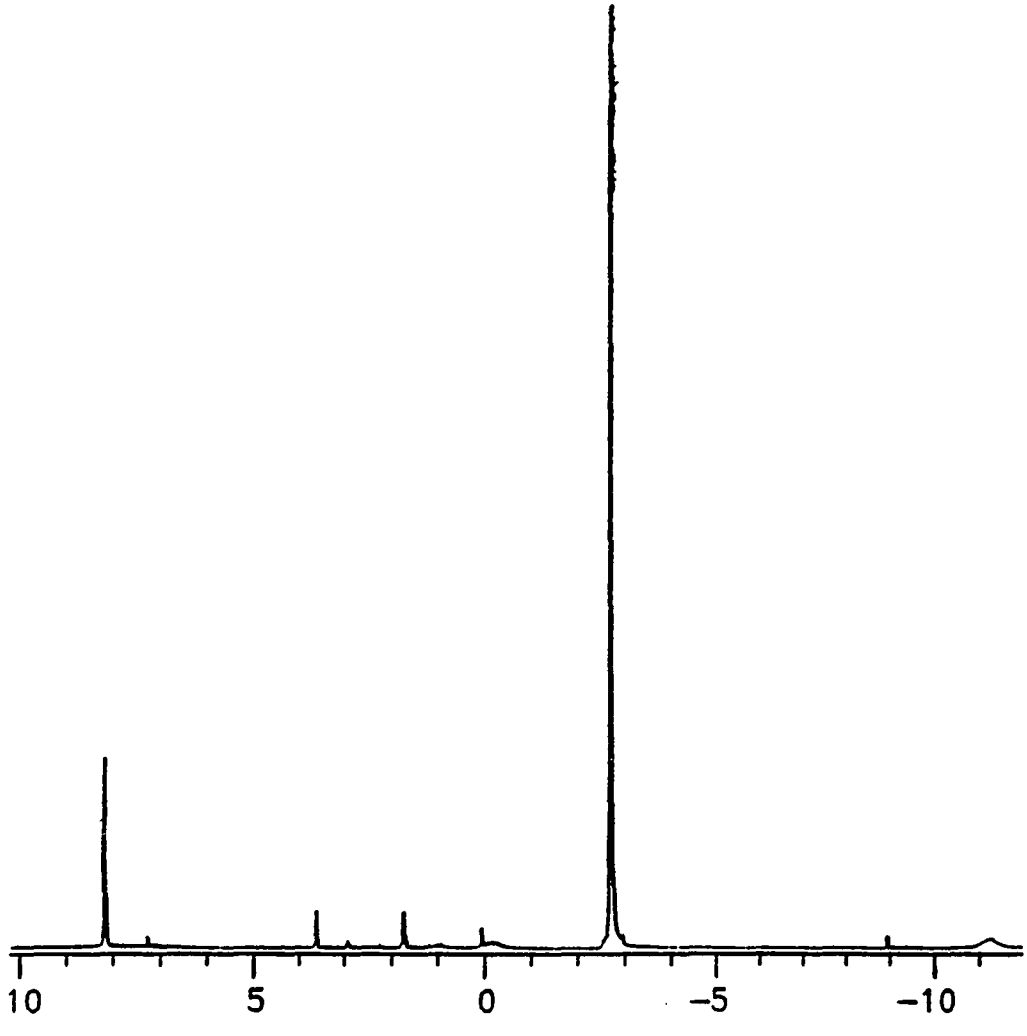

Figure 24: ^{1}H-NMR Spectrum of $Cp^*_2UCl_2(HNSPh_2)$ and $HNSPh_2 \cdot H_2O$ (1:1) in d_6-Benzene

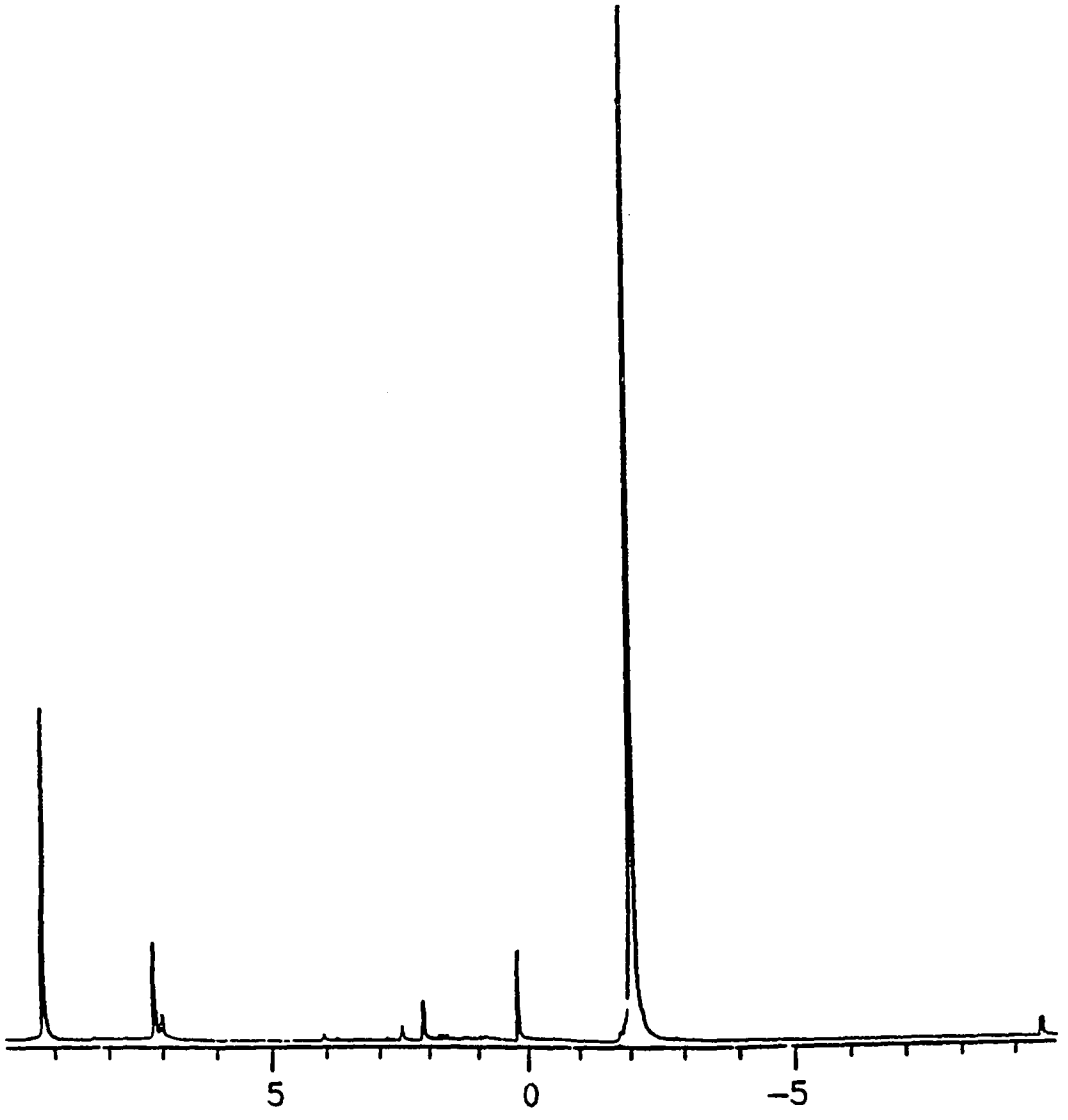

Figure 25: ^{1}H-NMR Spectrum of $Cp^{*}_{2}UCl_{2}(HNSPh_{2})$ and $HNSPh_{2}.H_{2}O$ (1:2) in d_{6}-Benzene

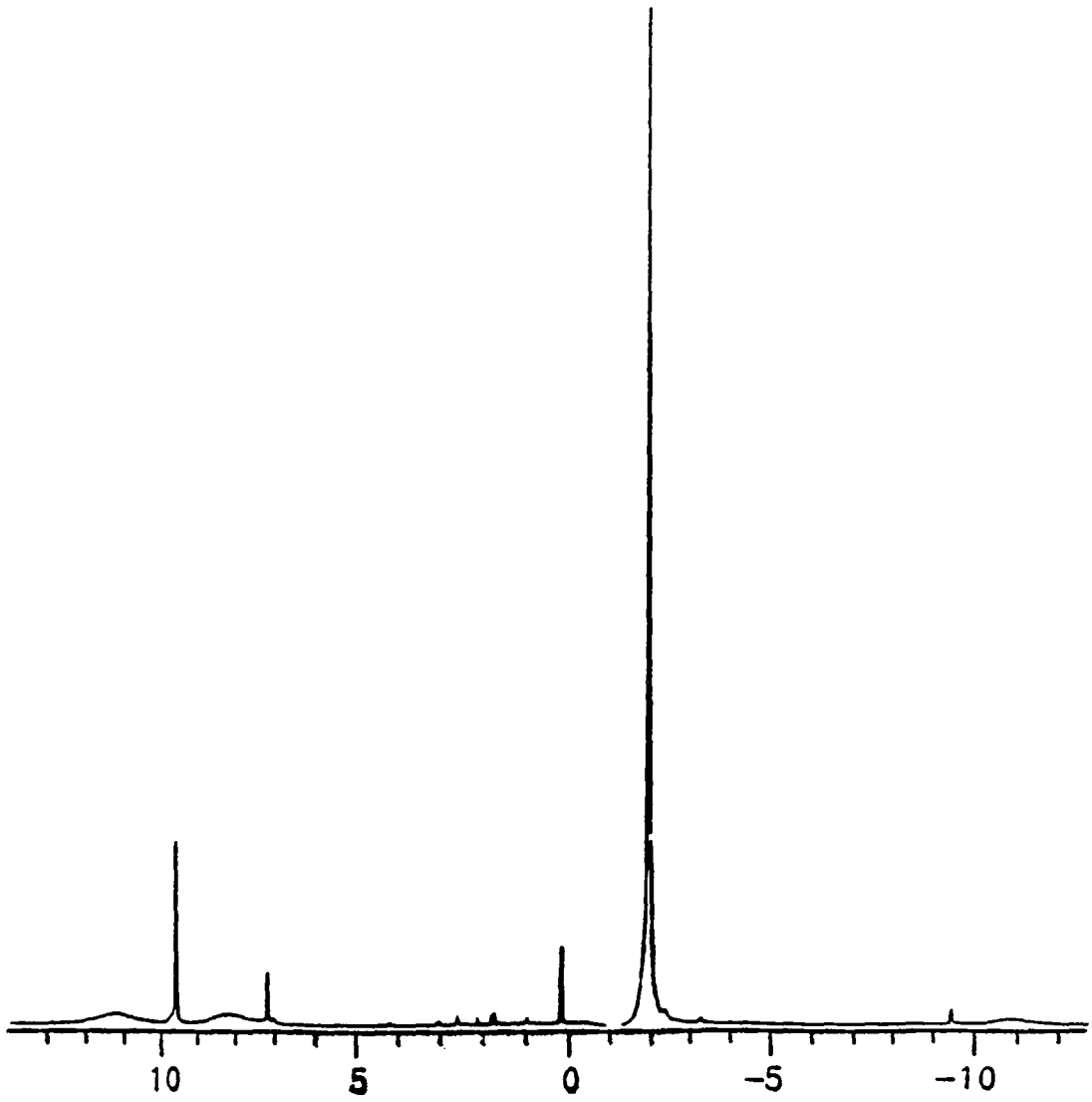

Figure 26: ^{1}H-NMR Spectrum of $Cp^{*}_{2}UCl_{2}(HNSPh_{2})$ and $HNSPh_{2}.H_{2}O$ (1:3) in d_{6}-Benzene

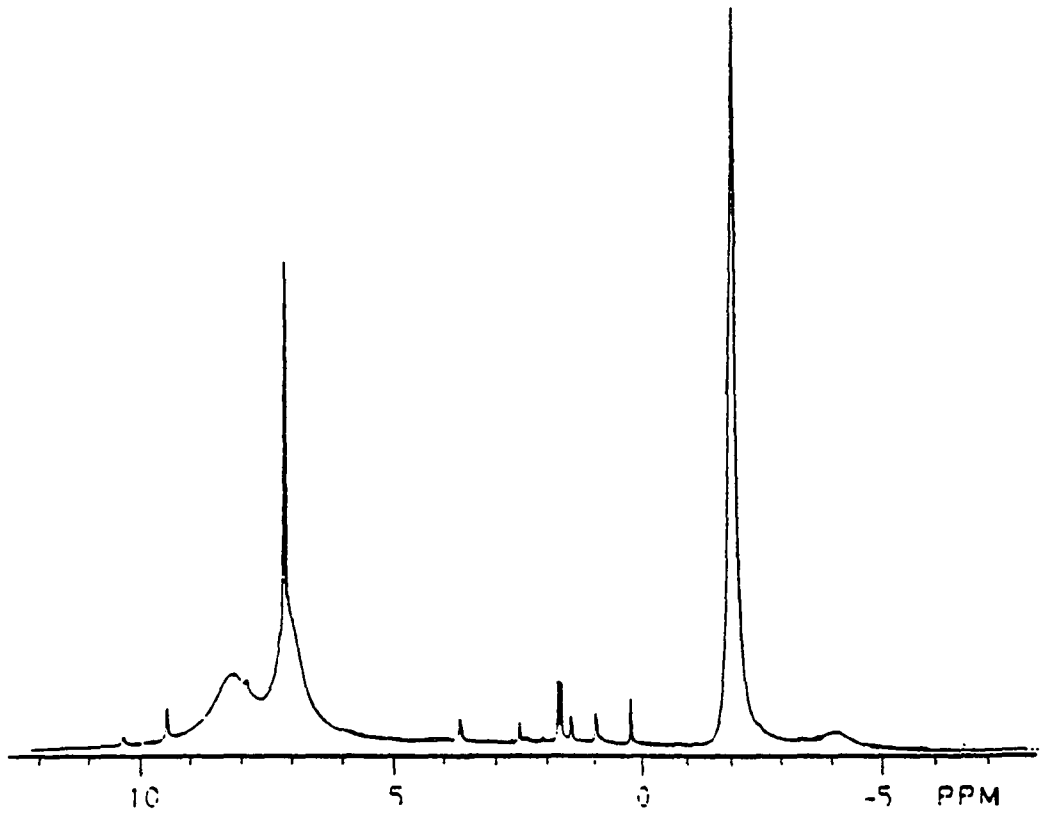

Figure 27: ^{1}H-NMR Spectrum of $Cp^*_2UCl_2(HNSPh_2)$ and $HNSPh_2.H_2O$ (1:4) in d_6-Benzene

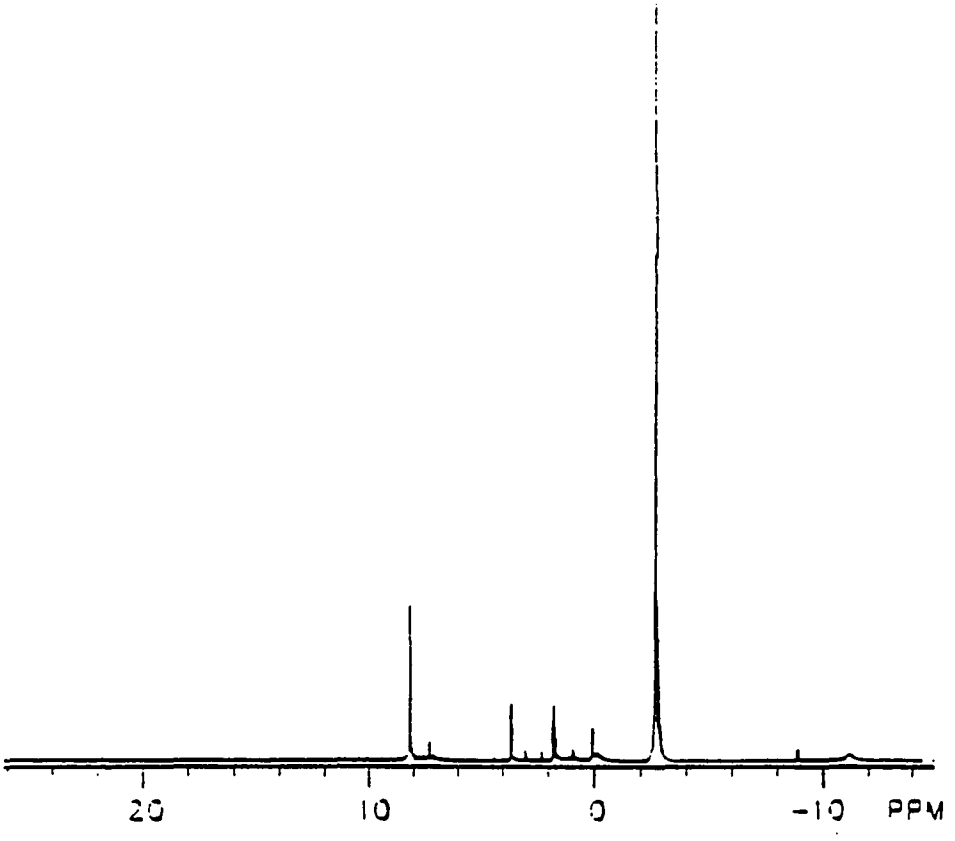

Figure 28: ^{1}H-NMR Spectrum of $Cp^*_2UCl(OH)(HNSPh_2)$ in d_8-THF at 23°C

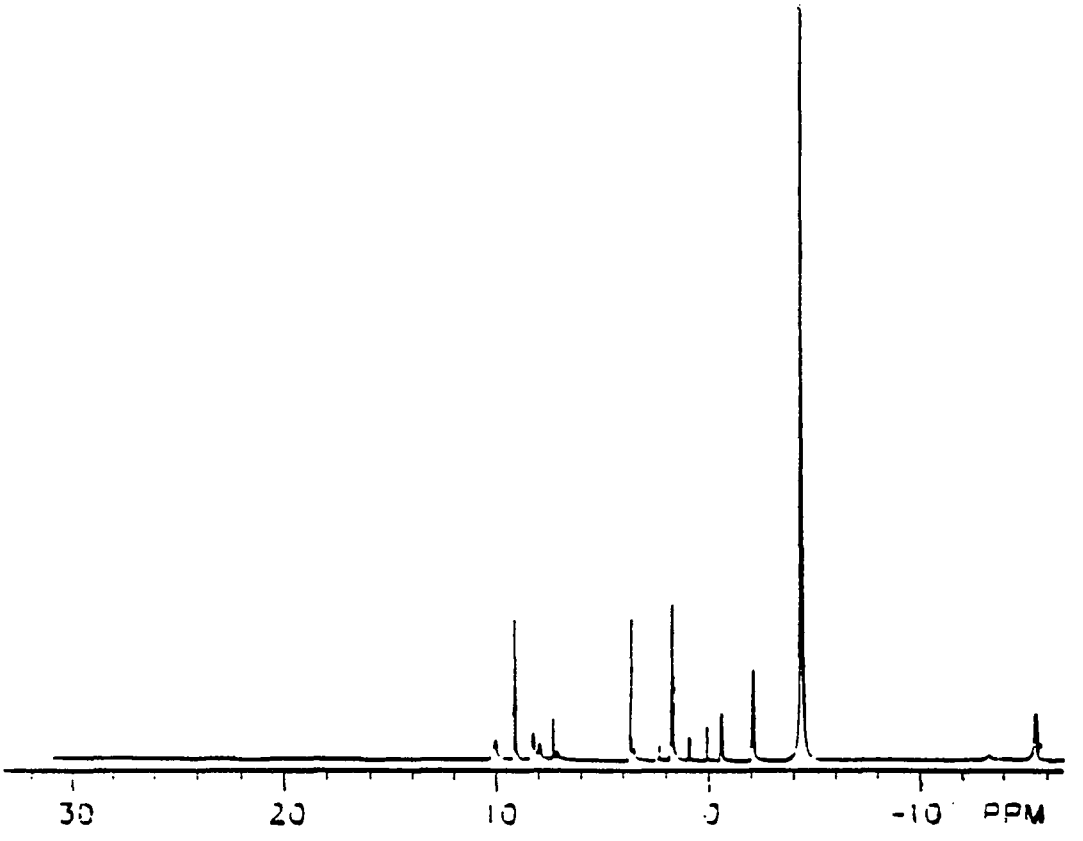

Figure 29: ^{1}H-NMR Spectrum of $Cp^*_2UCl(OH)(HNSPh_2)$ in d_8-THF at -60°c

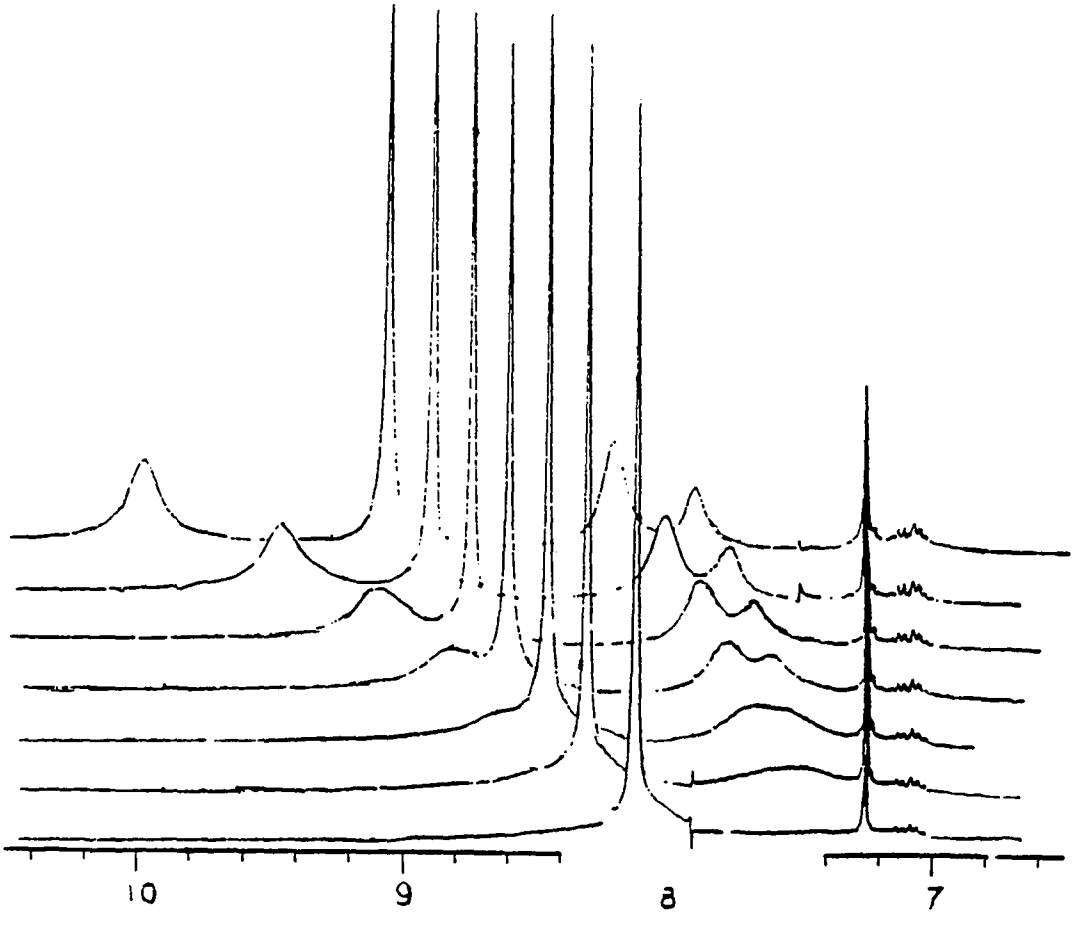

Figure 30: Variation of the Peaks in the Aromatic Region Among the Low Temperature ^{1}H-NMR Spectra of $Cp^*_2UCl(OH)(HNSPh_2)$

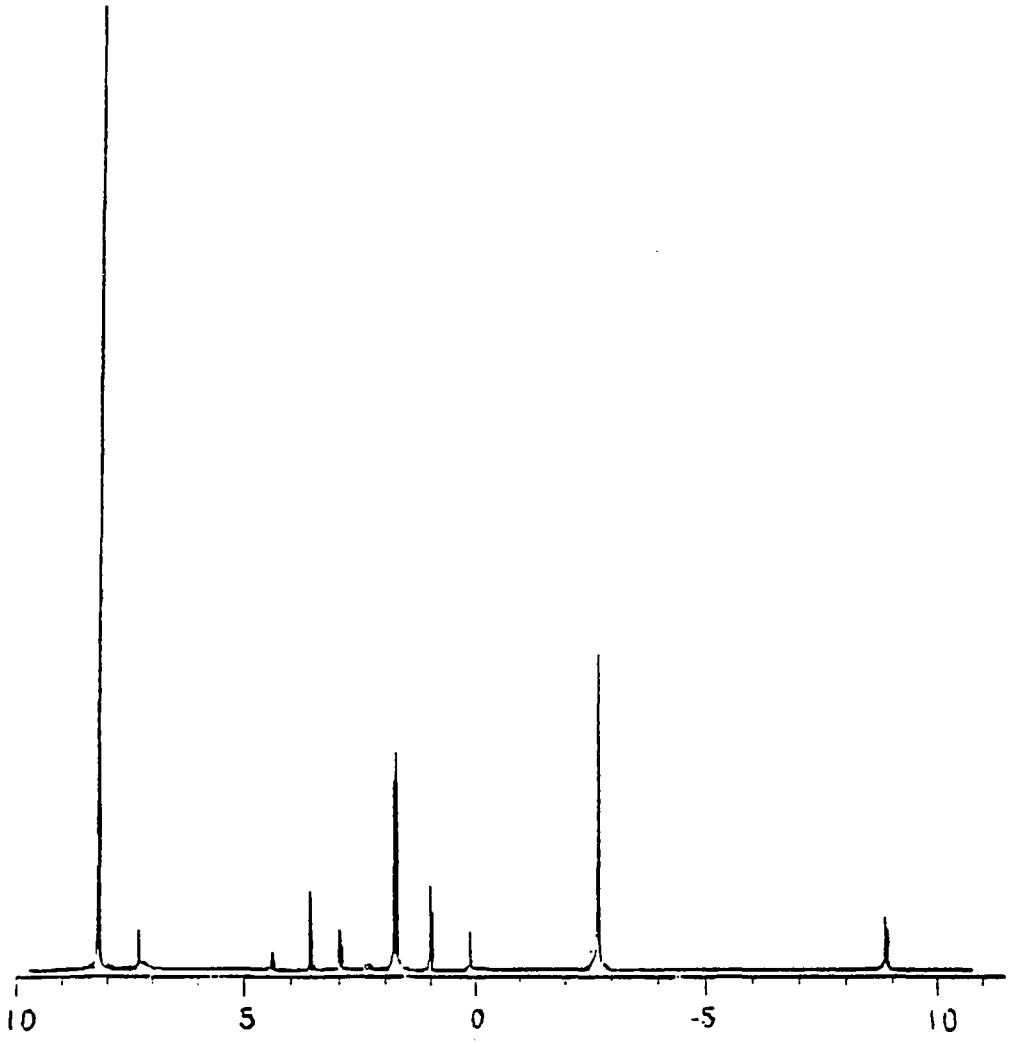

Figure 31: ^{1}H-NMR Spectrum of $Cp^*_2UCl(OH)(HNSPh_2)$ in d_8-THF a Week After the Sample was Prepared

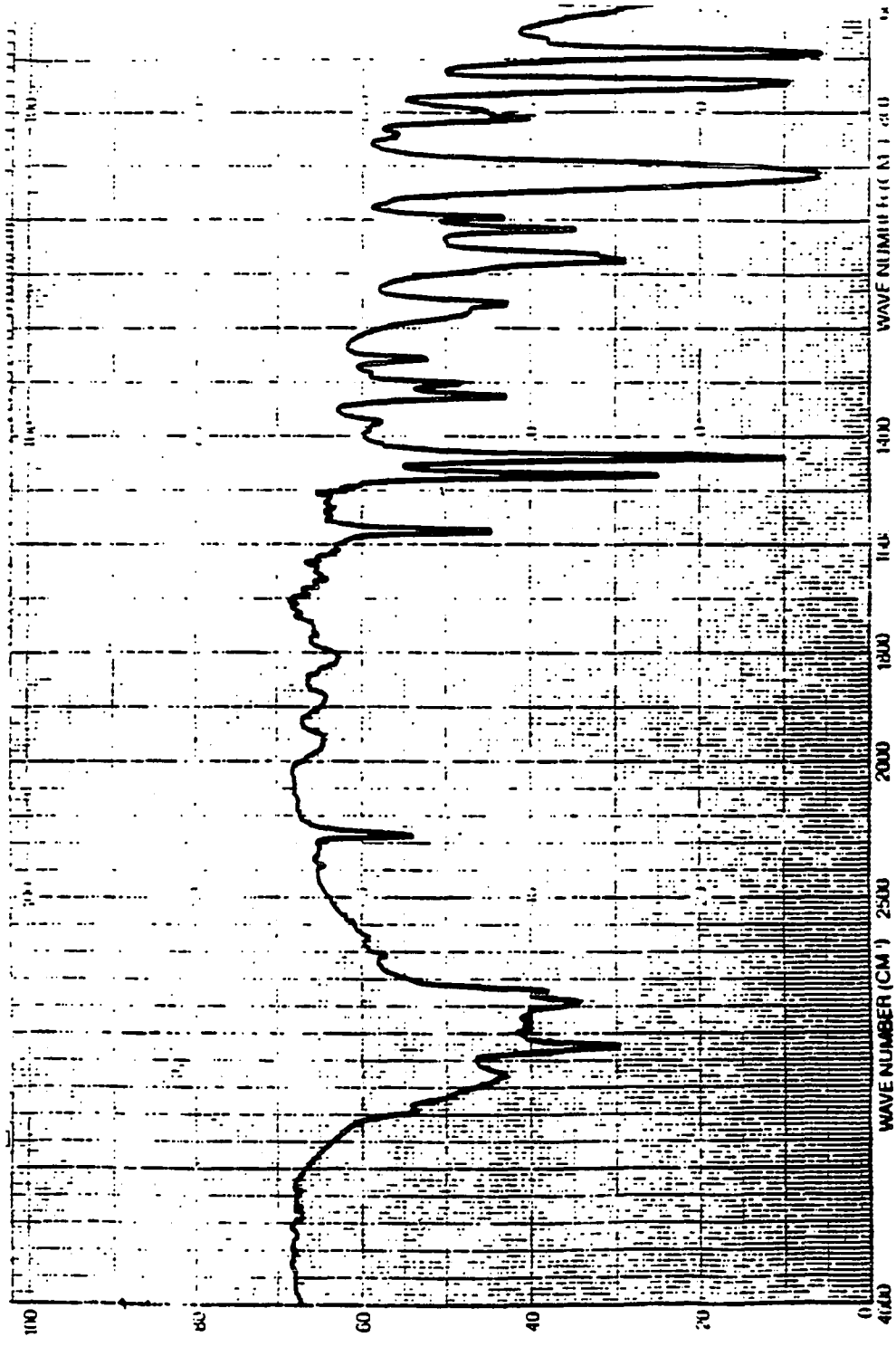

Figure 32: Infrared spectrum of $Cp^*_2UCl(OH)(HNSPh_2)$

TABLE 8

Infrared Spectral Data of $Cp^*_2UCl(OH)(HNSPh_2)$

Frequencies	Possible Assignment
3290 w	
3150 br	
3050 s	C-H(Ph)
2900 m	C-H(Cp^*)
2870 m	C-H(Cp^*)
2250 m	
1950 s	
1875 s	
1810 m	
1560 s	C=C(Ph)
1455 m	C-H(Ph)[a]
1440 s	C-H(Ph)[a]
1350 w	
1250 w	
1150 m	
1075 m	
1020 w	
990 w	
915 s	
810 m	
745 s	
690 s	

vs=very strong, s=strong, m=medium, w=weak

a) planar ring deformation of phenyl group attached to sulfur.

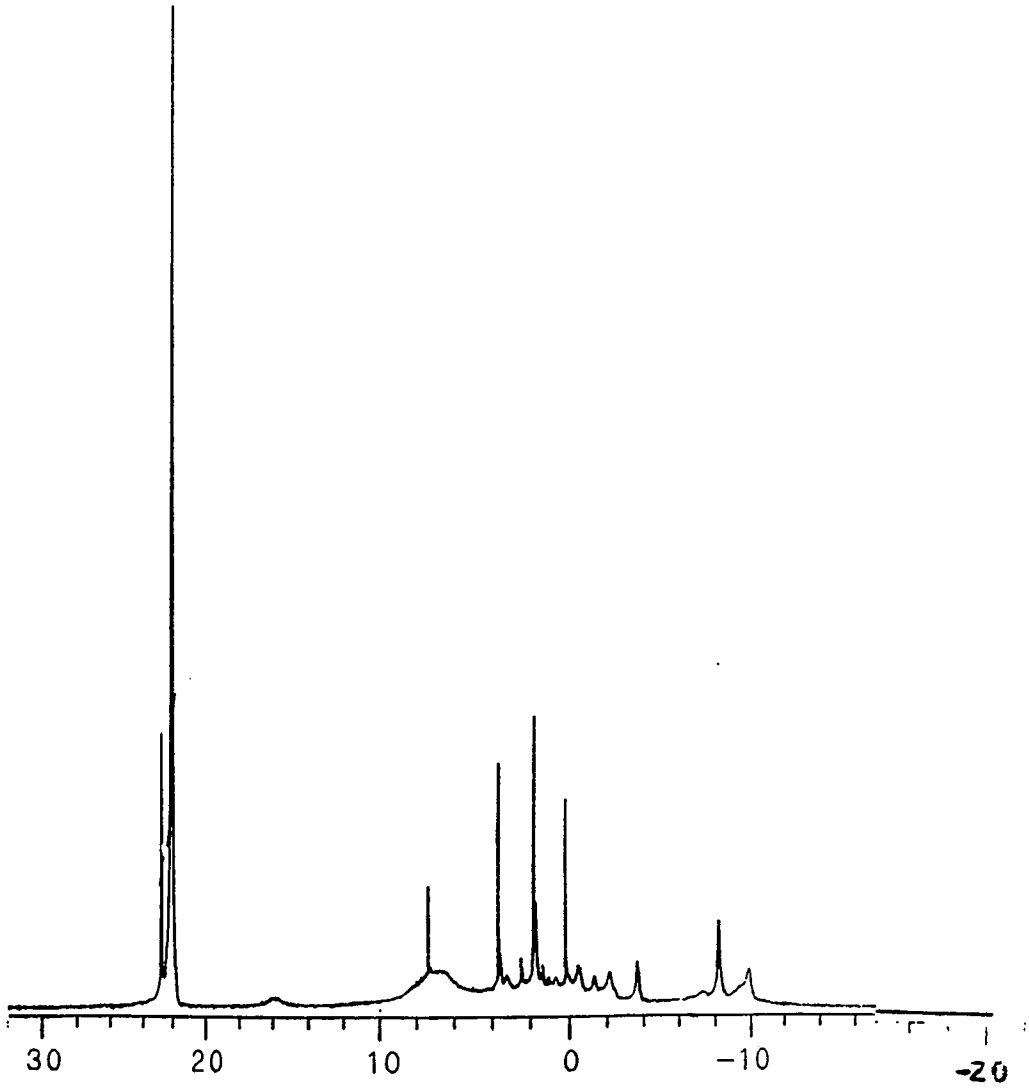

Figure 33: ^{1}H-NMR Spectrum of $[Cp^*(Cl)(HNSPh_2)U$
$-(\mu_3\text{-}OH)(\mu_2\text{-}O)_2\text{-}U(Cl)(HNSPh_2)_2]_2$ in d_8-THF

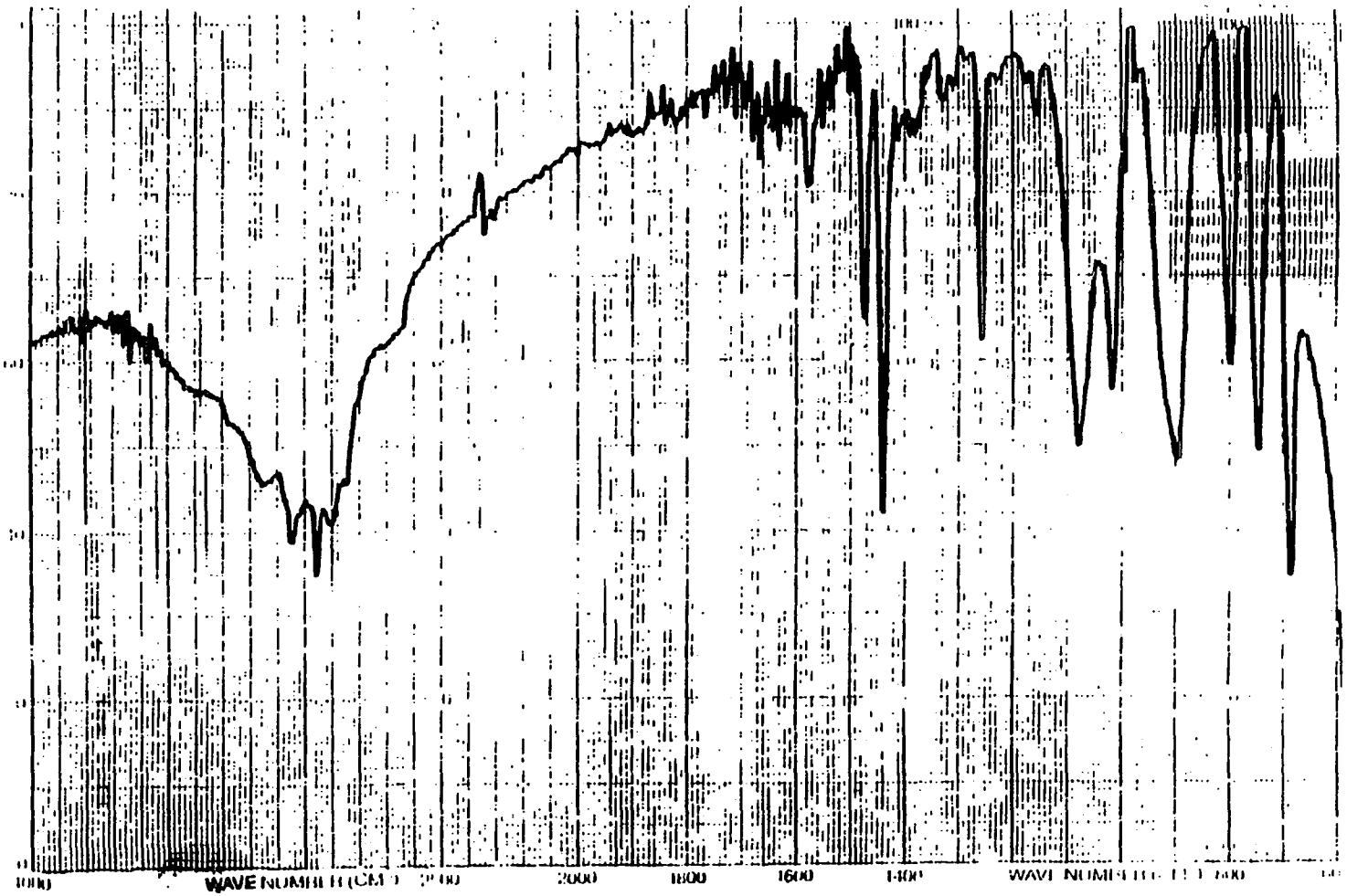

Figure 34: Infrared Spectrum of $[Cp^*(Cl)(HNSPh_2)U-(\mu_3-OH)(\mu_2-O)_2-U(Cl)(HNSPh_2)_2]_2$

TABLE 9

Infrared Spectral Data of $[Cp^*(Cl)(HNSPh_2)U-(\mu_3-OH)(\mu_2-O)_2-U(Cl)(HNSPh_2)_2]_2$

Frequencies	Possible Assignment
3280 w	
3155 br	
3040	C-H(Ph)
2950 m	C-H(Cp^*)
2910 m	C-H(Cp^*)
1580 m	C=C(Ph)
1475 s	C-H(Ph)[a]
1430 s	C-H(Ph)[a]
1410 m	
1390 s	
1380 m	
1305 m	
1330 s	
1260 w	
1060 vs	
1020 vs	
900 vs	
800 s	
740 m	
690 m	

vs=very strong, s=strong, m=medium, w=weak

a) planar ring deformation of phenyl group attached to sulfur.

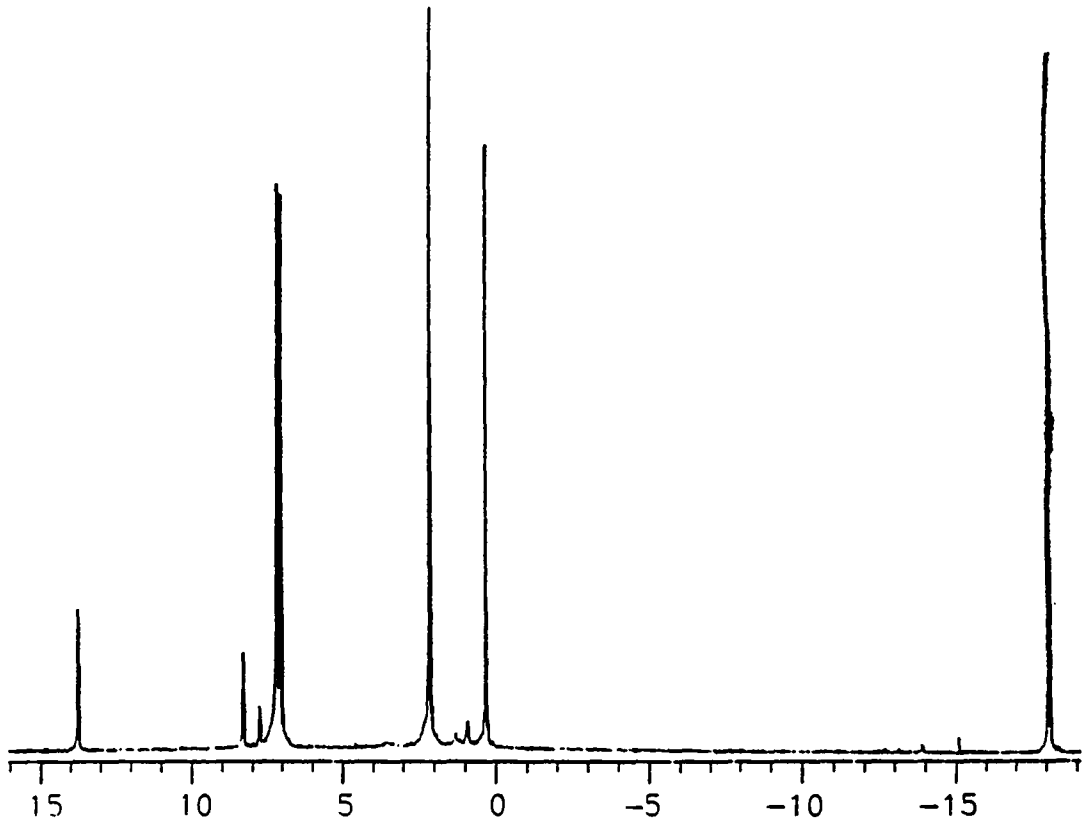

Figure 35: ^{1}H-NMR Spectrum of the Reaction of $Cp_3U{=}CHPMePh_2$ with $HNSPh_2$ in d_8-Toluene

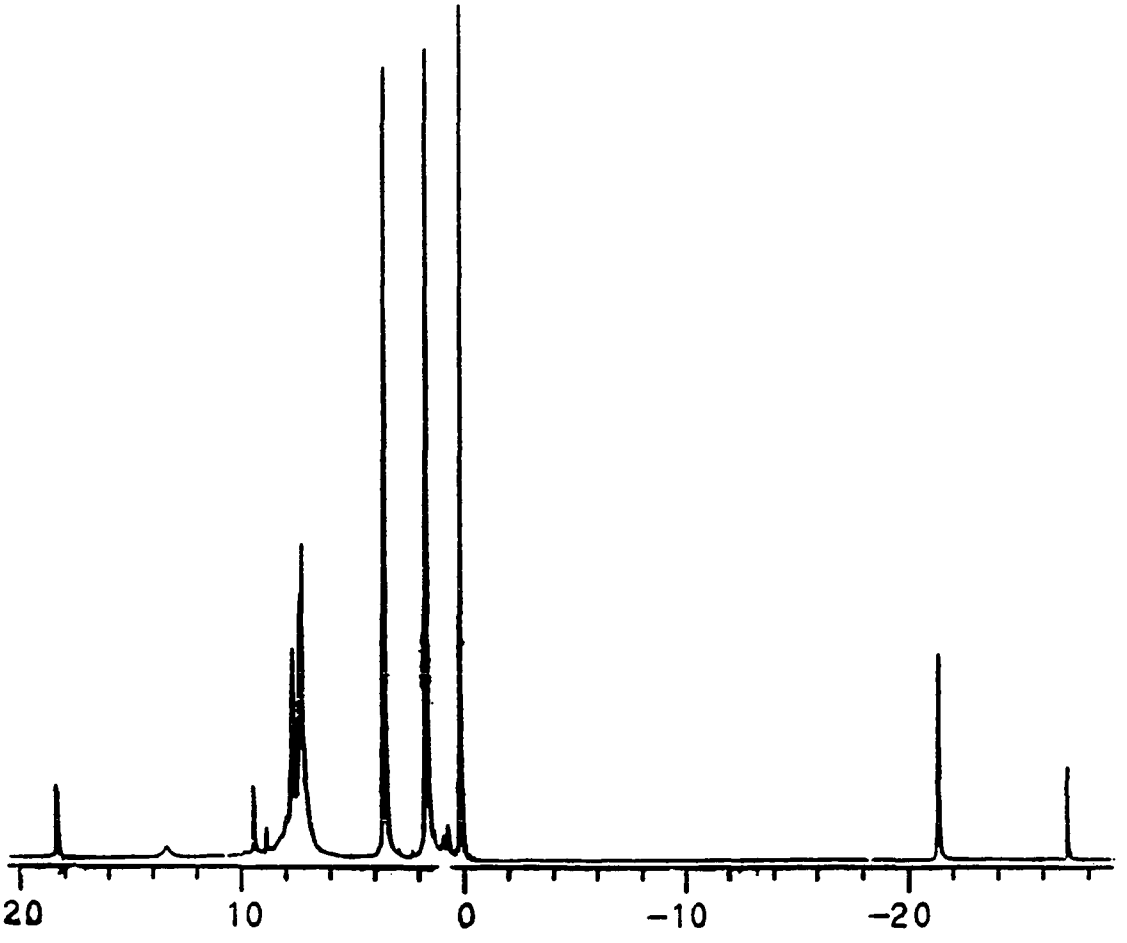

Figure 36: ^{1}H-NMR Spectrum of the Reaction of $Cp_3U{=}CHPMePh_2$ with 2 $HNPPh_3$ in d_8-THF

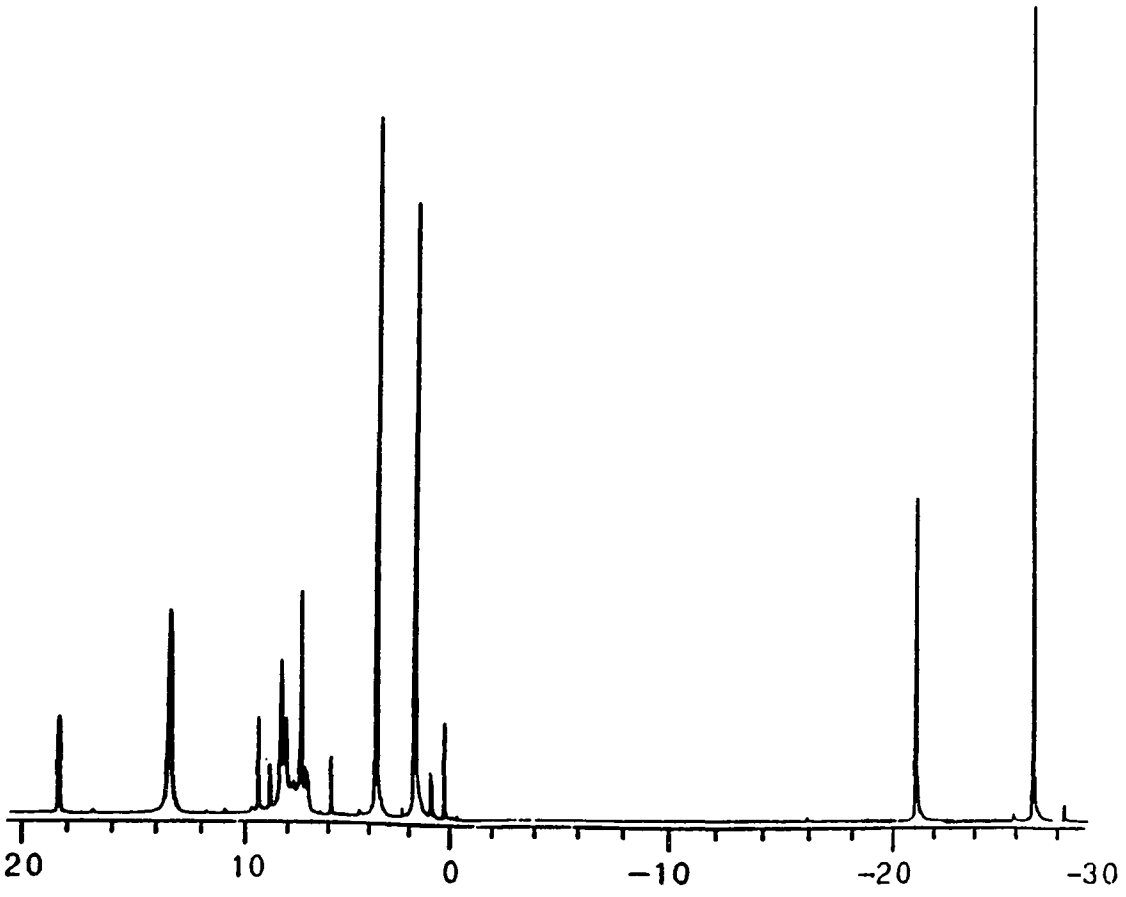

Figure 37: ^{1}H-NMR Spectrum of the Reaction of $Cp_3U{=}CHPMePh_2$ with 4 $HNPPh_3$ in d_8-THF

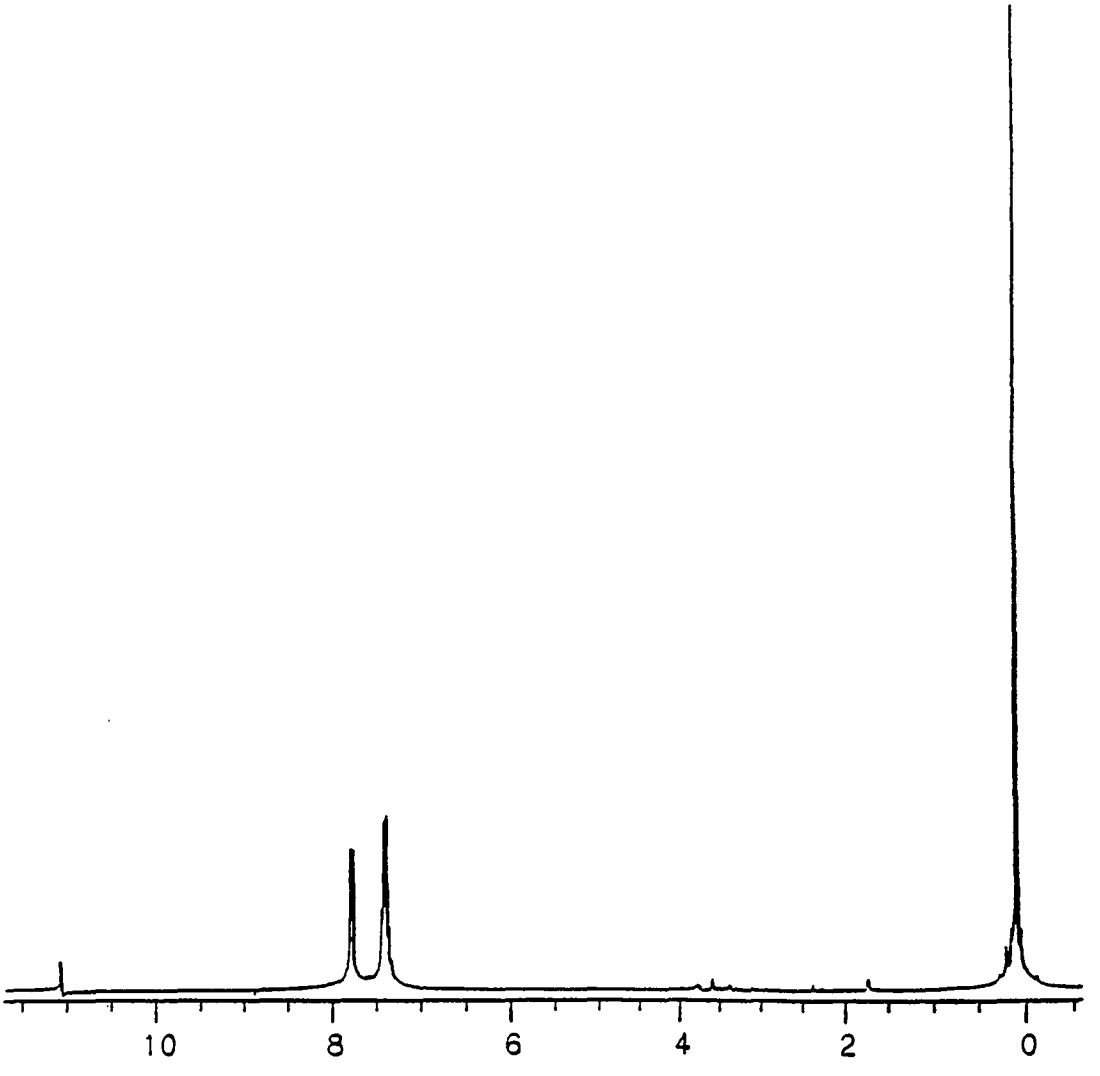

Figure 38: ^{1}H-NMR Spectrum of $Me_3SiNSPh_2$ in d_8-THF

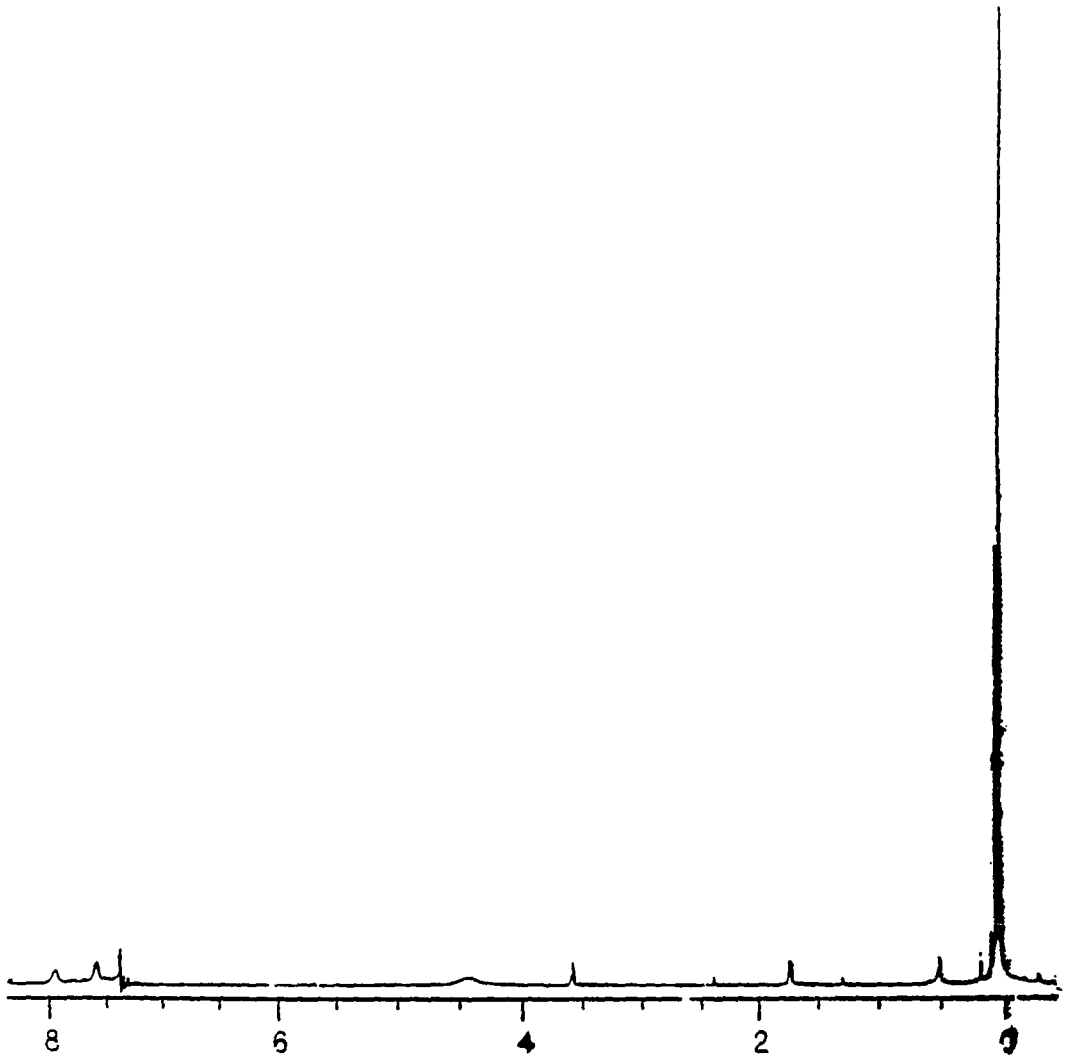

Figure 39: ^{1}H-NMR Spectrum of the Reaction of UO_2Cl_2 with Excess $Me_3SiNSPh_2$ in d_8-THF

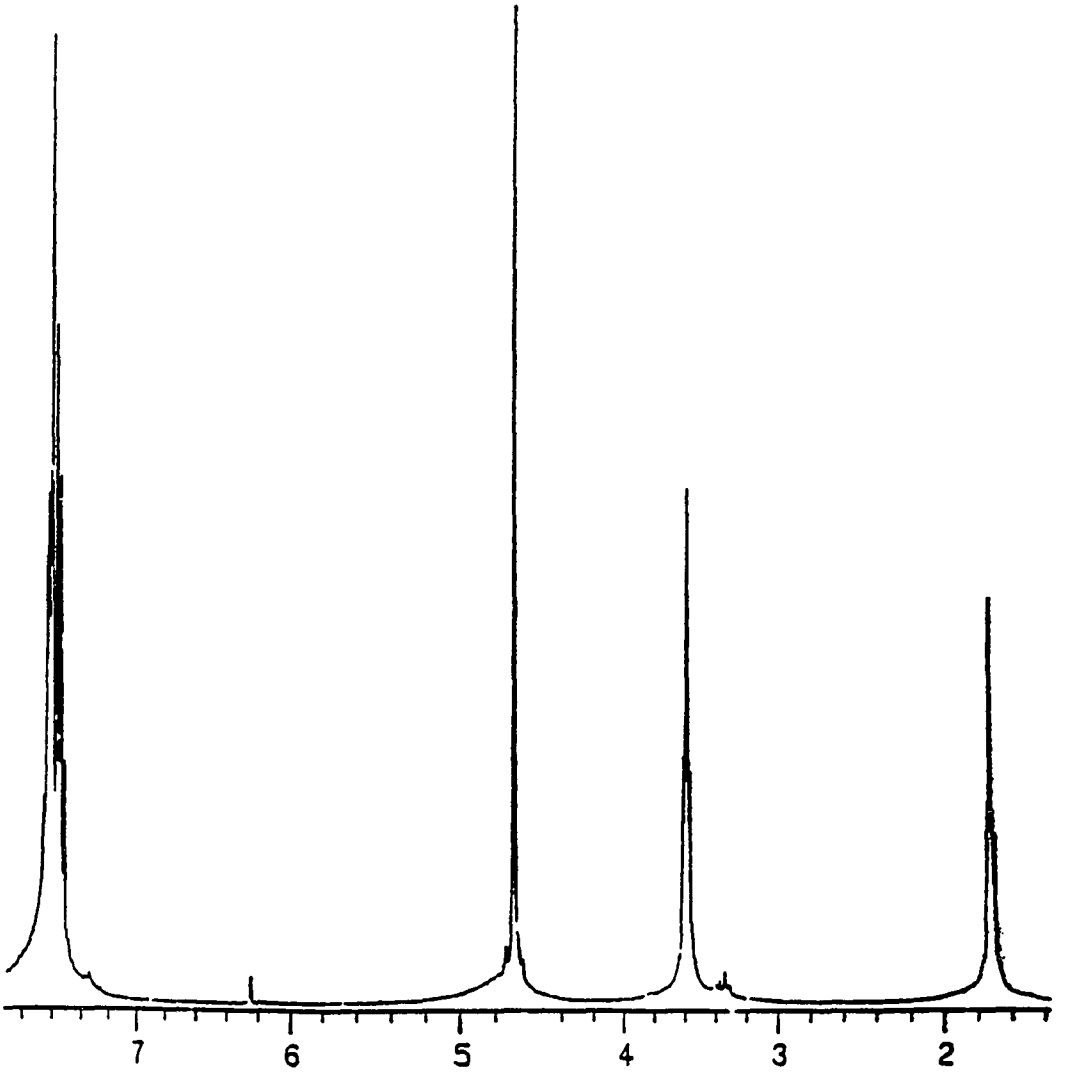

Figure 40: ^{1}H-NMR Spectrum of the Yellow Precipitate From the Reaction of UO_2Cl_2 with $Me_3SiNSPh_2$ in d_8-THF

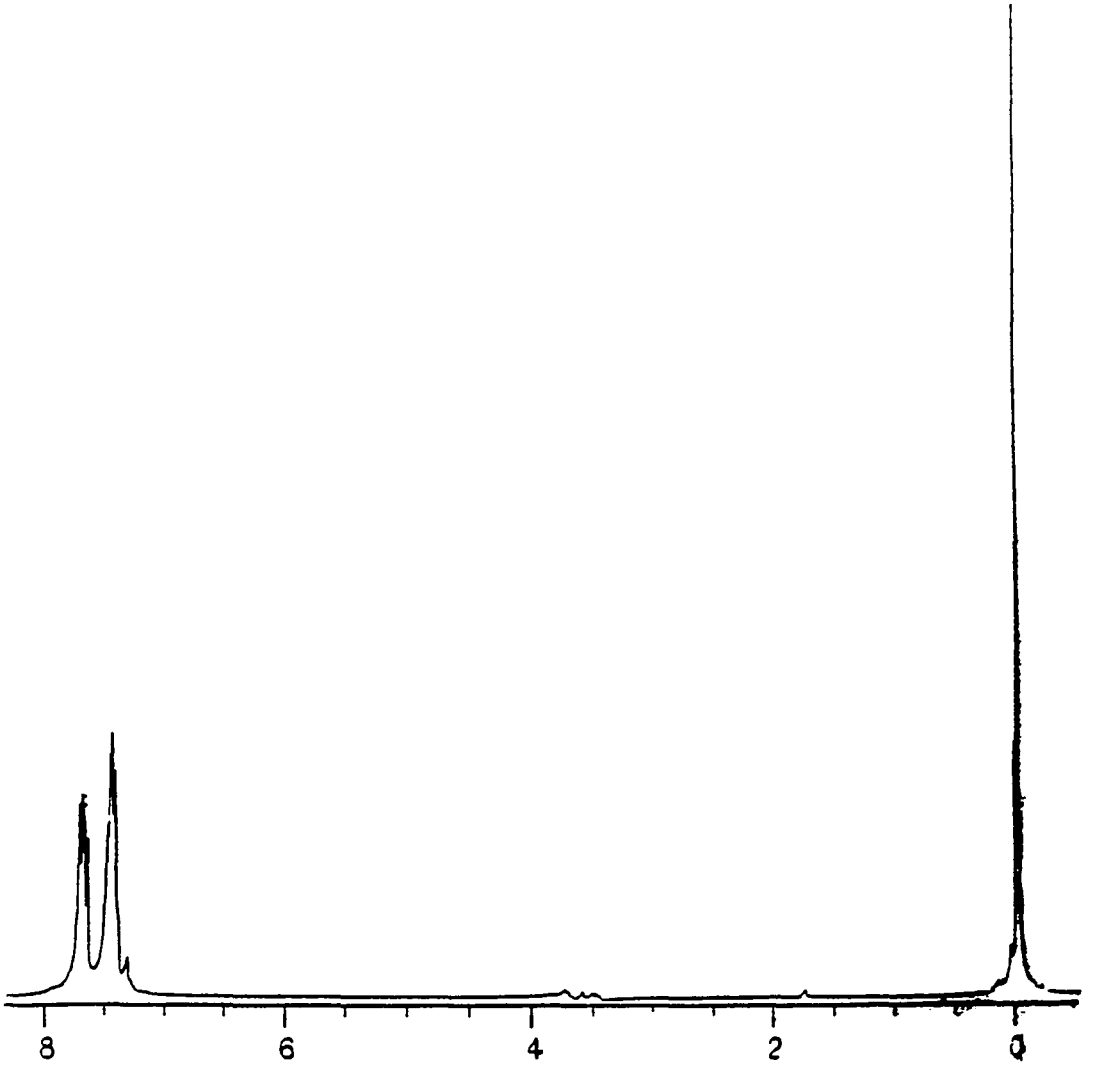

Figure 41: ^{1}H-NMR Spectrum of $Me_3SiNPPh_3$ in d_8-THF

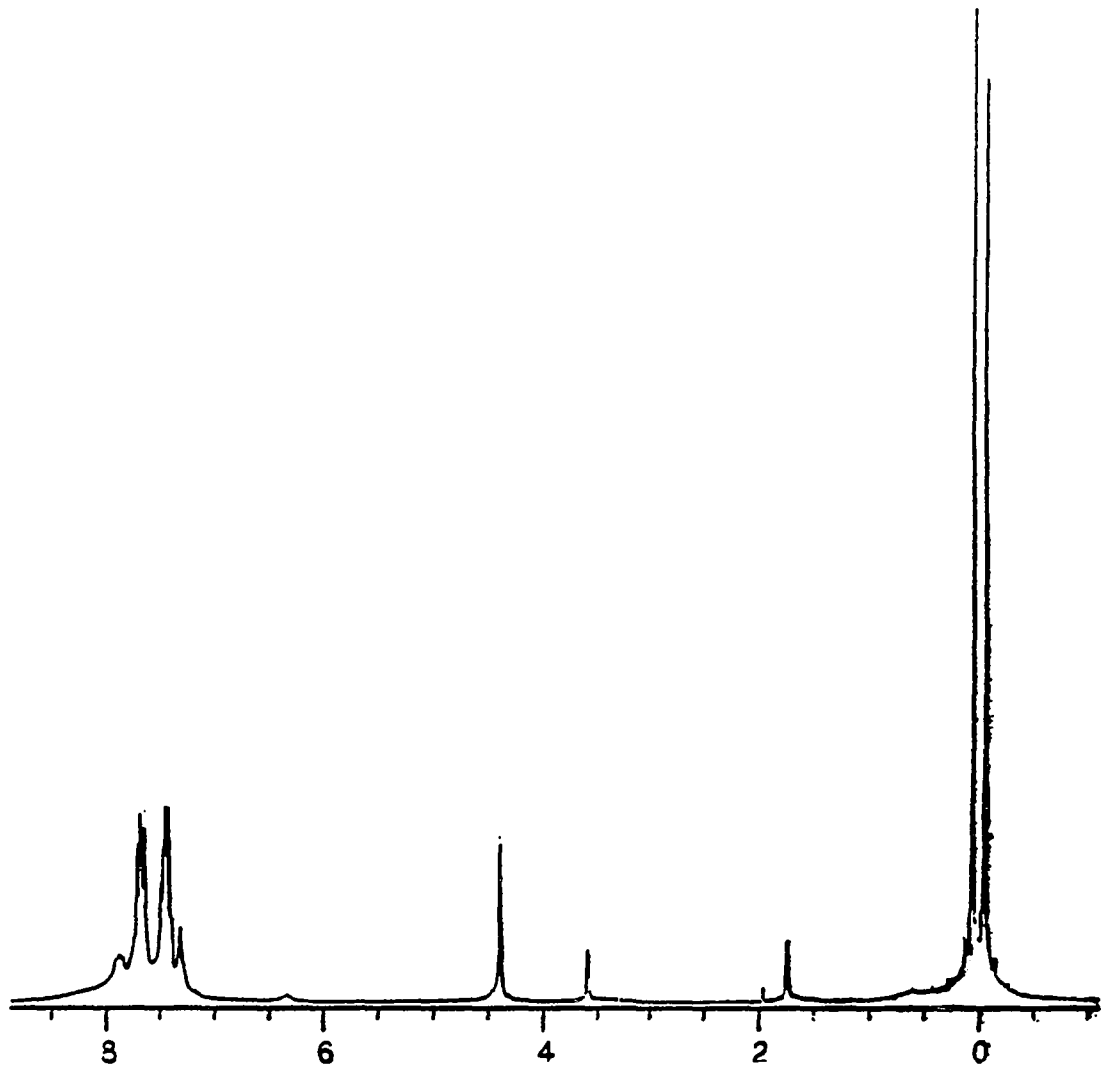

Figure 42: ^{1}H-NMR Spectrum of the Reaction of U_2OCl_2 with Excess $Me_3SiNPPh_3$ in d_8-THF

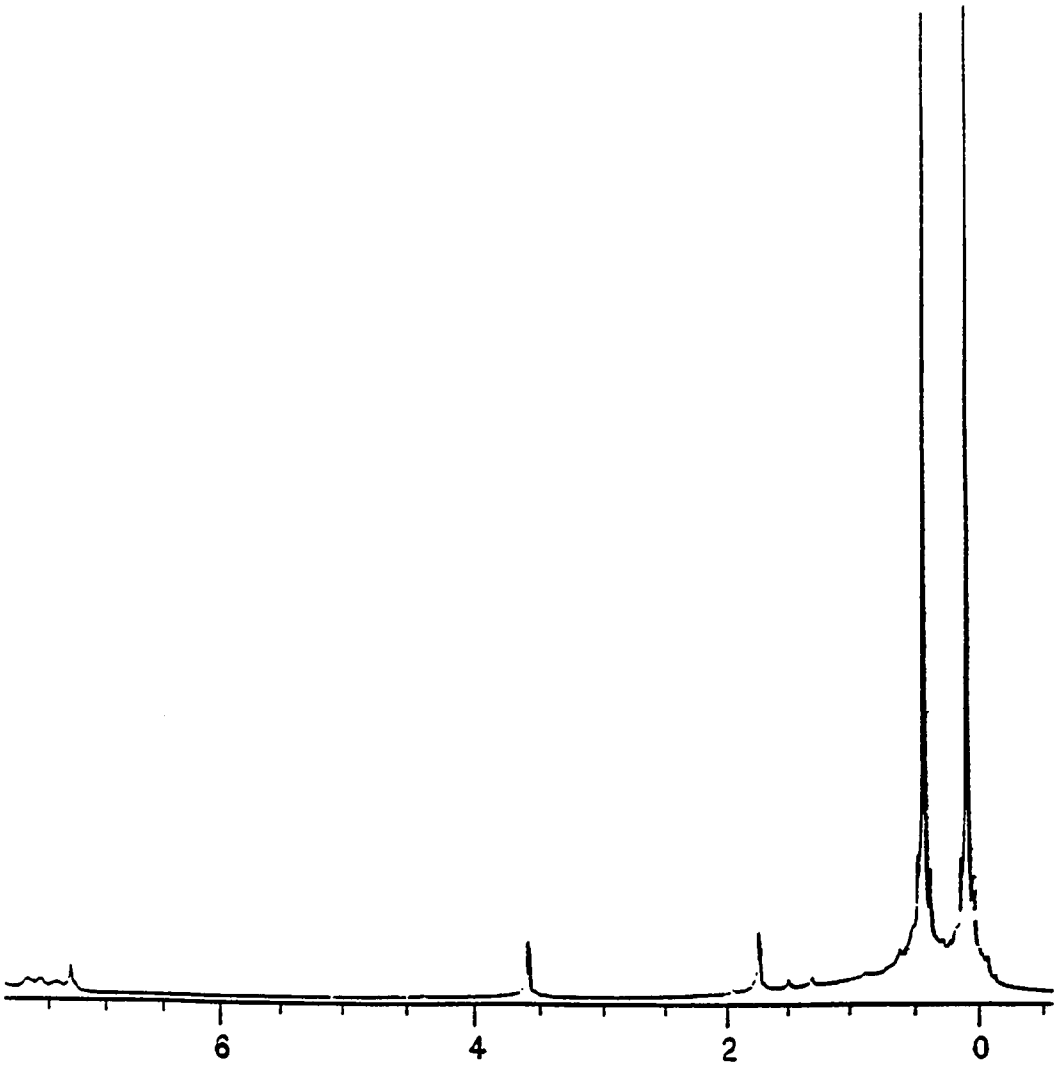

Figure 43: ^{1}H-NMR Spectrum of the Reaction of UO_2Cl_2 with Excess $Me_3SiNPPh_3$ in d_8-THF After Introducing Me_3SiCl

2.3.11 Reactions of $Cp_3U=CHPMePh_2$ with Heterocumulenes

The Reaction of $Cp_3U=CHPR_3$ with n-Butylisocyanate

About 15 mg (0.02 mmole) of $Cp_3U=CHP(CH_3)(C_6H_5)_2$ was added to 1 ml of n-butylisocyanate in the glove box. The solution immediately became dark red. The flask was stored at room temperature for two weeks. A small amount of a dark red precipitate initially appeared in the flask and the viscosity of the solution increased. The ^{1}H-NMR spectrum of this sample in d_8-toluene, Figure 44, contains paramagnetically shifted peaks which confirms that n-butylisocyanate indeed reacts with $Cp_3U=CHPMeR_2$. The reaction was monitored by taking infrared spectra and was allowed to continue until the n-butylisocyanate was completely consumed. Within three days the reaction was complete and the sample had turned into a dark brown semi solid material.

Figure 45 shows the infrared spectrum of pure n-butylisocyanate whereas that of the product is given in Figure 46 and data are summarized in Table 10. The peak at 2200 cm^{-1} for the N=C=O stretch of the starting material gradually disappears during the reaction and new peaks appear near 1700 cm^{-1}.

The infrared spectrum of the product contains three absorptions at 1690 cm^{-1}, 1700 cm^{-1} and 1710 cm^{-1} which correspond to the C=O stretches of the product. The mass spectrum of this material in $CHCl_3$, Figure 47, Table 11, contains a signal at 297 a.m.u. and signals which are consistent with a n-butylisocyanate trimer.(M.W. = 297).

The reaction of $Cp_3U=CHPR_3$ with excess n-propylisocyanate

A similar experiment was performed using 15 mg (0.02 mmole) of $Cp_3U=CHPMePh_2$ and 1 ml of n-propylisocyanate. Within three days n-propylisocyanate was completely consumed to give a red-brown semi-solid material. The progress of this reaction was monitored by taking infrared spectra, Figures 48-50, Table 12, periodically over several days. The spectra show the gradual disappearance of n-propylisocyanate while new peaks grow near 1700 cm^{-1} which are assigned to the C=O stretch of the reaction product. The mass spectrum of the mixture of the products in $CHCl_3$, Figure 51, Table 13, contains a signal at 255 a.m.u. and fragments which are consistent with a n-propylisocyanate trimer.(M.W. = 255)

The results from both mass and infrared spectra confirm that N-propylisocyanate undergoes catalytic trimerization in the presence of $Cp_3U{=}CHPMePh_2$.

Reaction of $Cp_3U{=}CHPR_3$ with excess t-butylisocyanate

About 150 mg (0.20 mmole) of $Cp_3U{=}CHPMePh_2$ was added to 1 ml of t-butylisocyanate. The solution turned dark red immediately. A red microcrystalline material formed instantly, but disappeared slowly over 8-10 hrs at room temperature. The ^{1}H-NMR spectrum, Figure 52, was obtained and the flask was kept at room temperature for two weeks during which the reaction was monitored by taking IR spectra. The ^{1}H-NMR spectrum contains paramagnetically shifted peaks. There was no evidence of any catalytic reactivity in the system.

The mass spectrum, Figure 53, Table 14, of the sample obtained in $CHCl_3$, shows no sign of polymerized t-butylisocyanate. A peak at 215 a.m.u. that corresponds to Ph_2MePO, is present in the mass spectrum.

The reaction of $Cp_3U=CHPR_3$ with phenylisothiocyanate.

150 mg (0.20 mmole) of $Cp_3U=CHPMePh_2$ was added to 1 ml of phenylisothiocyanate. The dark red solution thus obtained was allowed to stand at room temperature for two weeks. The mass spectrum, Figure 54, Table 15, of this sample shows no sign of polymerization. However peaks are observed at 232 a.m.u. and 194 a.m.u. which correspond to Ph_2MePS and PhN=C=NPh, respectively.

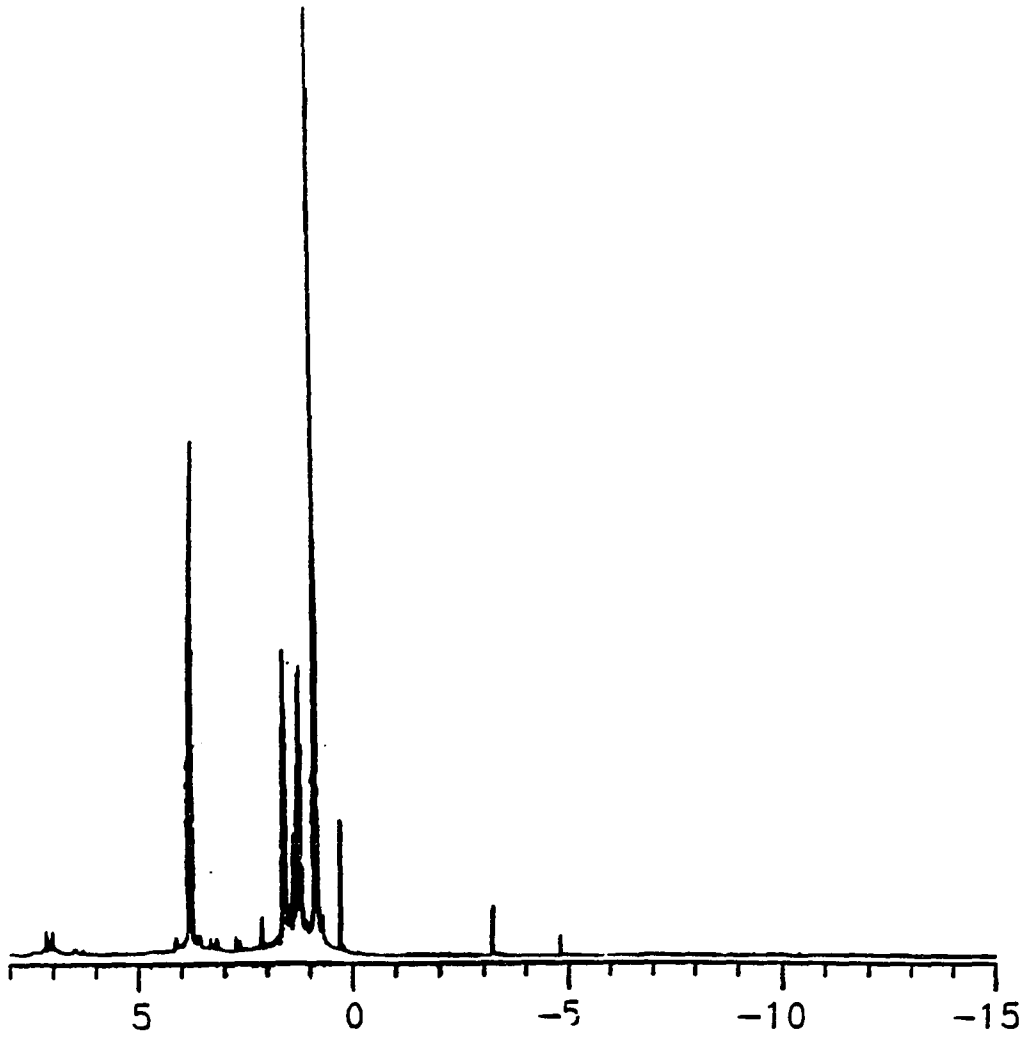

Figure 44: ^{1}H-NMR Spectrum of the Reaction of $Cp_3U{=}CHPMePh_2$ with Excess n-ButNCO in d_8-Toluene

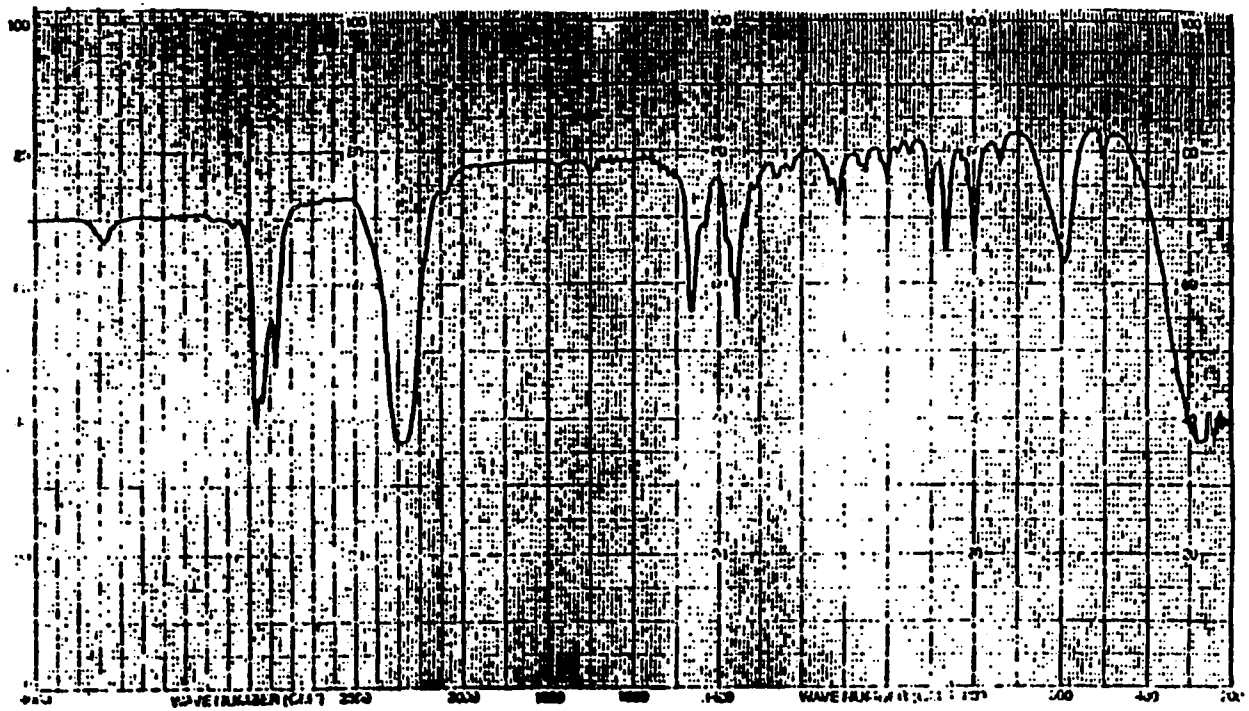

Figure 45: Infrared Spectrum of n-ButNCO

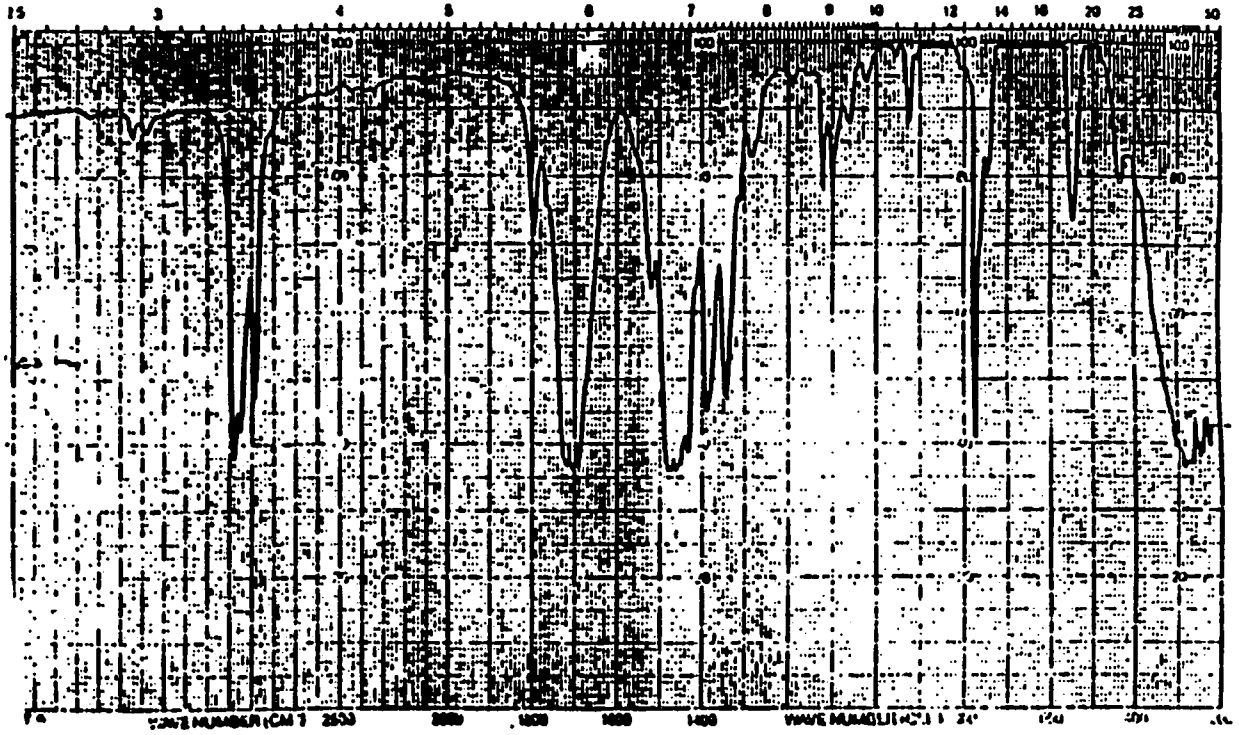

Figure 46: Infrared Spectrum of n-ButNCO Trimer

TABLE 10

Infrared Spectral Data of n-Butyl Isocyanate Trimer

Frequencies (cm^{-1})		Possible Assignment
2920	vs	C-H
2980	vs	C-H
2960	vs	C-H
1800	w	
1712	v	C=O
1700	v	C=O
1690	v	C=O
1450	v	C-H[b]
1390	s	C-H[b]
1345		
924		
775		
550		

vs=very strong, s=strong, m=medium, w=weak

a) Spectrum obtained as thin film on Nacl plates.
b) H-bending of alkyl groups.

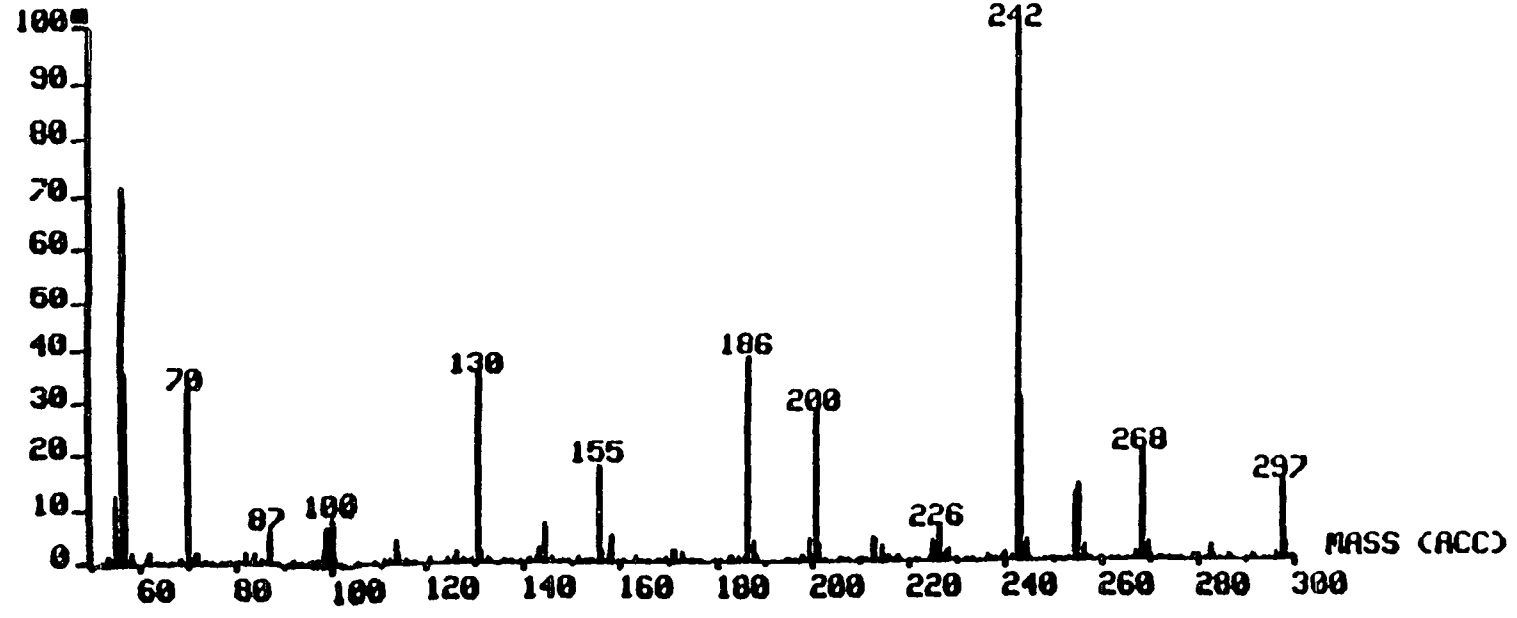

Figure 47: Mass Spectrum of n-ButNCO Trimer

TABLE 11

Mass Spectral Data of n-Butyl Isocyanate Trimer

Peaks	Relative Intensity	Possible Assignment
28	12	CO, N_2
57	35	n-butyl
70	31	
87	5	
100	8	
130	35	
155	17	
186	37	
200	27	
226	6	$(n\text{-butNCO})_3\text{-(ButN)}$
242	100	$(n\text{-ButNCO})_3\text{-(But)+2H}$
254	12	$(n\text{-ButNCO})_3\text{-(propyl)}$
268	19	$(n\text{-ButNCO})_3\text{-(ethyl)}$
297	14	$(n\text{-ButNCO})_3$

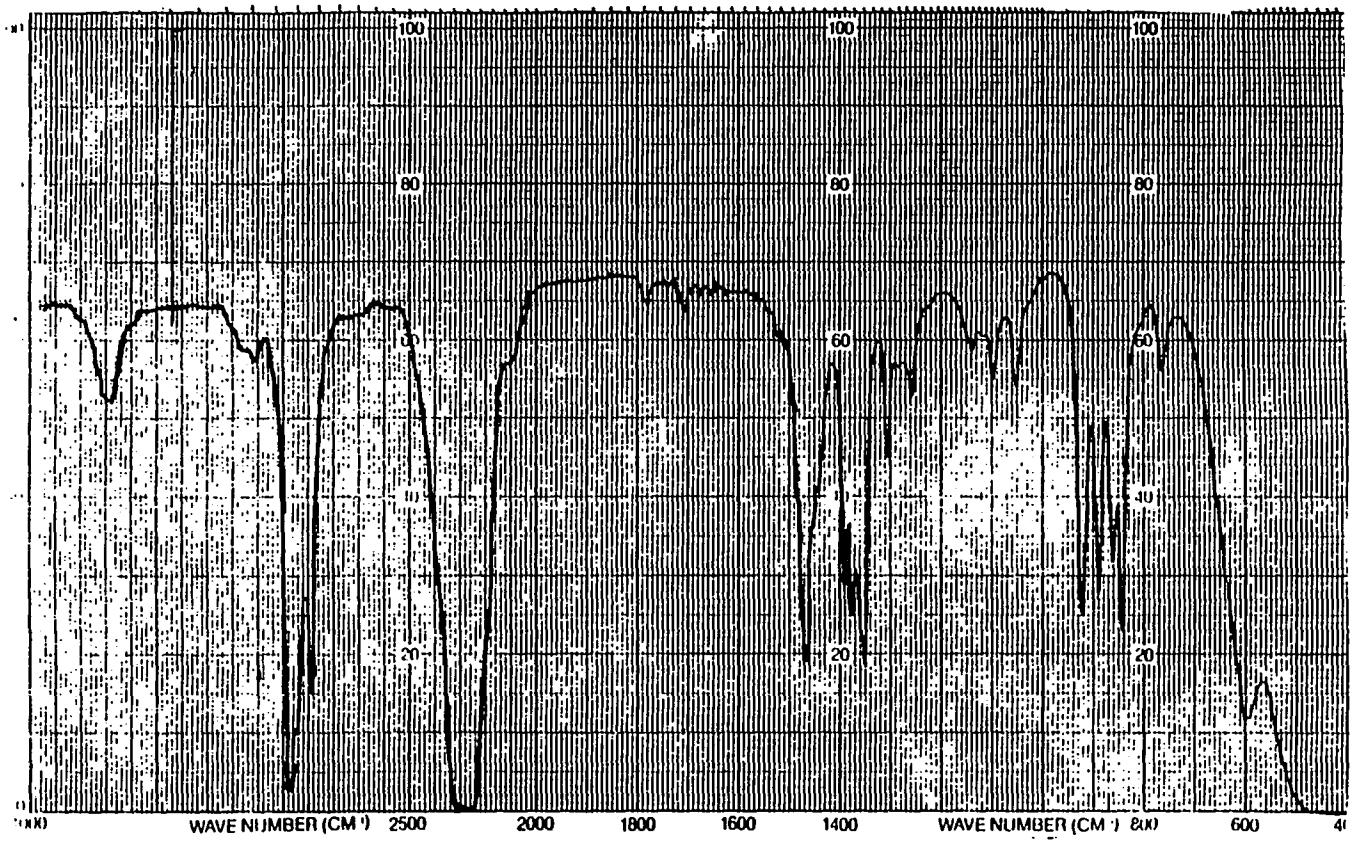

Figure 48: Infrared Spectrum of n-PrNCO

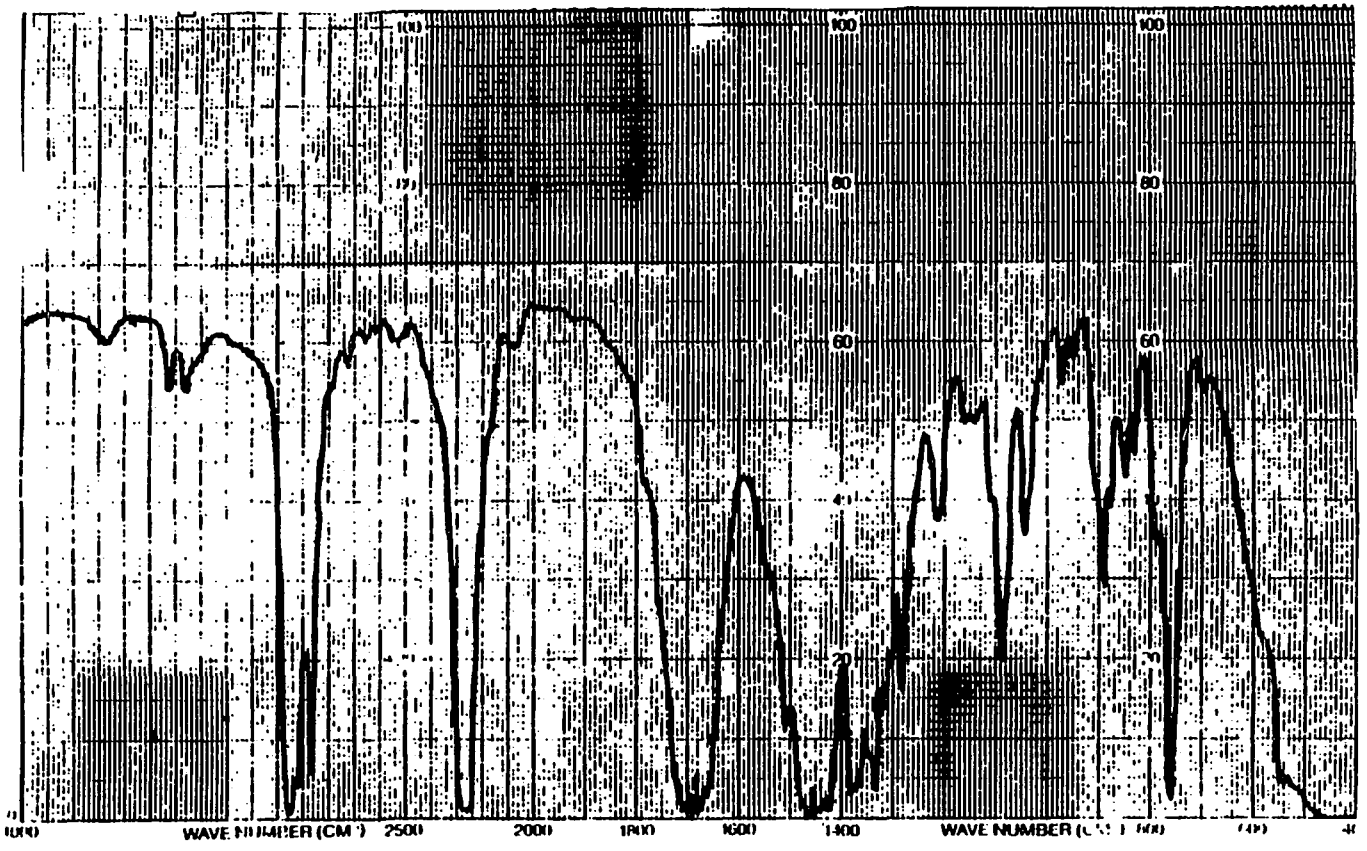

Figure 49: Infrared Spectrum of a Mixture of $Cp_3U{=}CHPMePh_2$ with Excess n-PrNCO After Two Days

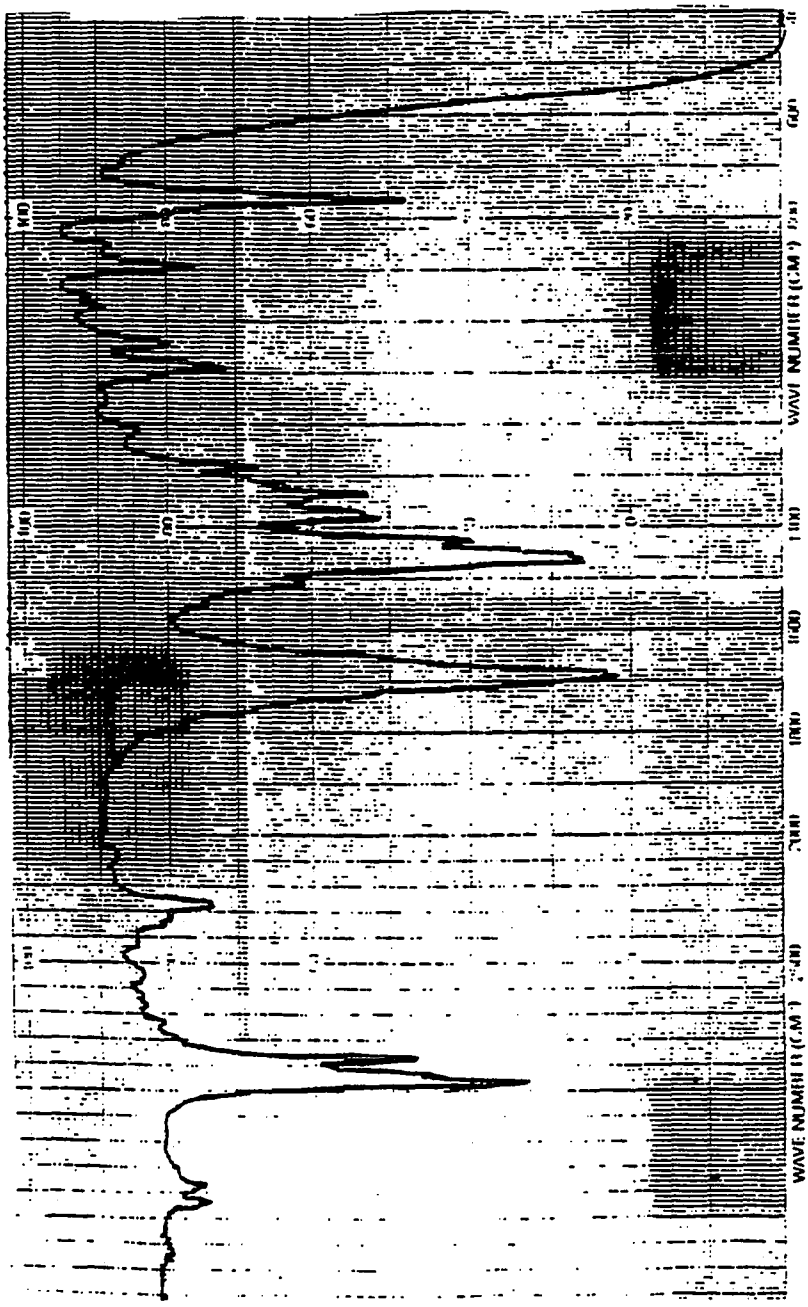

Figure 50: Infrared Spectrum of n-PrNCO Trimer

TABLE 12

Infrared Spectral Data of n-Propyl Isocyanate trimer

Frequencies(cm^{-1})	Possible Assignment
2925 vs	C-H
2980 vs	C-H
2965 vs	C-H
1700 vs	C=O
1480 vs	C-H[b]
1450 vs	C-H[b]
1445 vs	C-H[b]
1390 s	
1375 s	
1285 w	
1100 m	
1050 m	
900 m	
775 s	

vs = very strong, s = strong, m = medium, w = weak

a) Spectrum obtained as thin film in NaCl plates.

b) H-bending of alkyl groups.

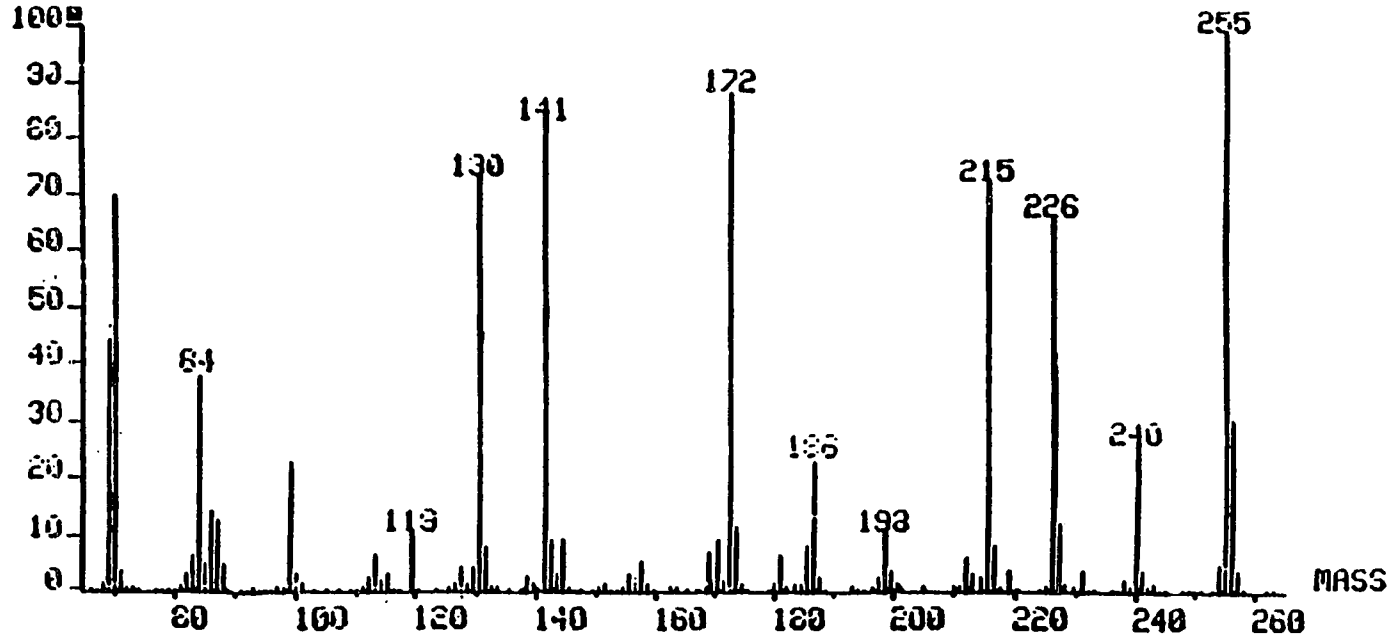

Figure 51: Mass Spectrum of n-PrNCO Trimer

TABLE 13

Mass Spectral Data of n-Propyl Isocyanate Trimer

Peaks	Relative Intensity	Possible Assignment
84	37	
99	34	
119	27	
130	71	
141	82	
172	88	$(PrNCO)_3$- (2Pr)+(3H)
186	25	
198	12	
215	70	$(PrNCO)_3$-(Pr)+(3H)
226	61	$(PrNCO)_3$-(Et)
240	27	$(PrNCO)_3$-(Me)
255	100	$(PrNCO)_3$

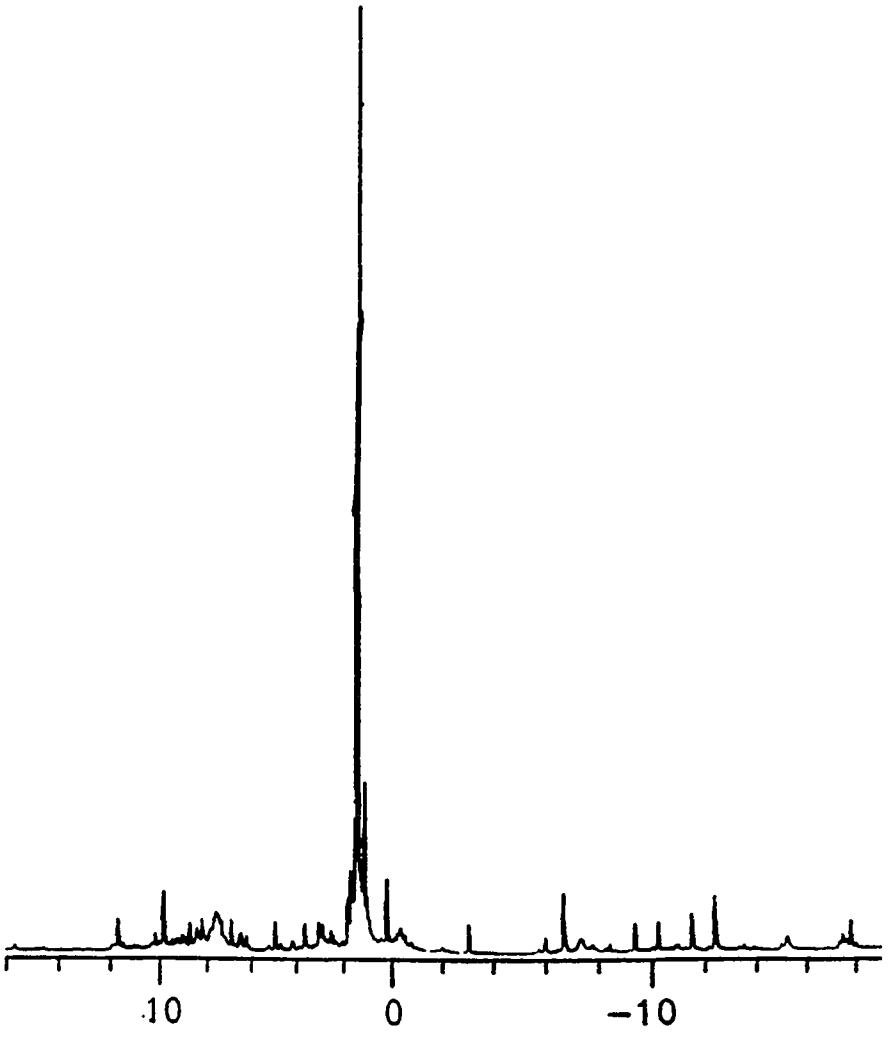

Figure 52: ^{1}H-NMR Spectrum of the Reaction of $Cp_3U{=}CHPMePh_2$ and t-ButNCO in d_8-Toluene

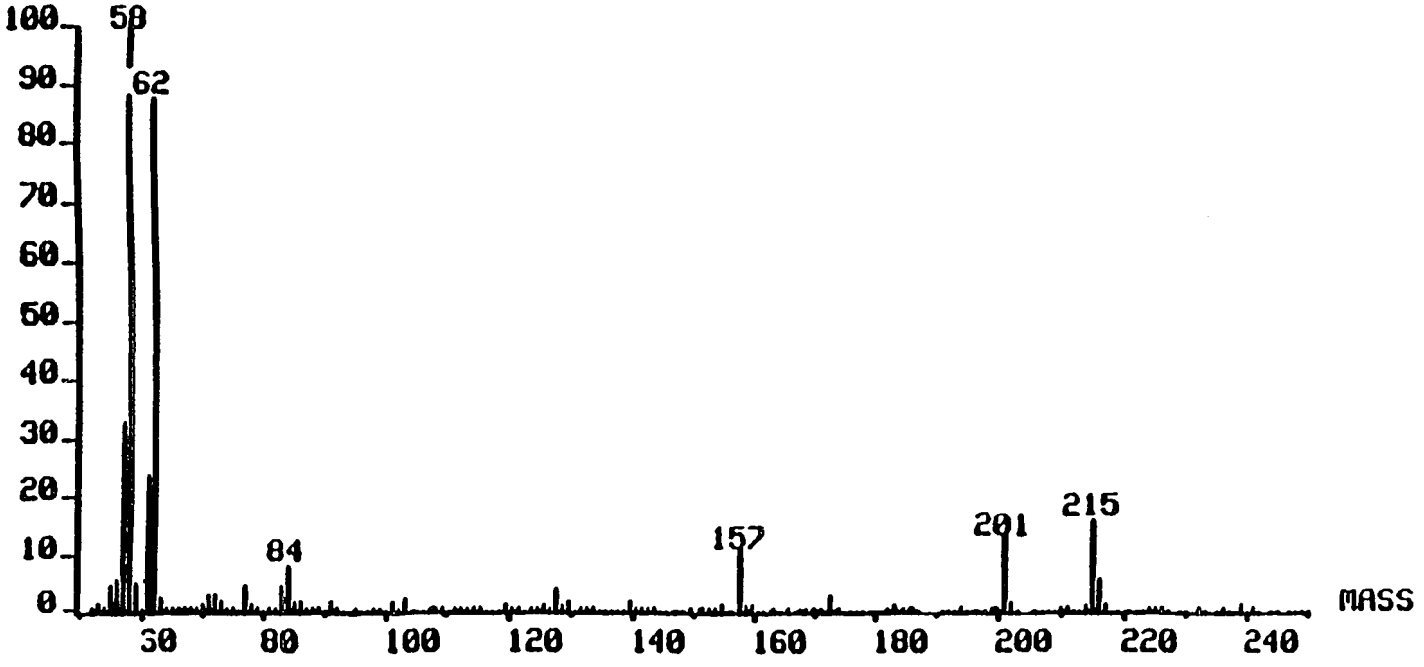

Figure 53: ^{1}H-NMR Spectrum of the Reaction of $Cp_3U{=}CHPMePh_2$ and t-ButNCO in d_8-Toluene

TABLE 14

Mass Spectral Data of The Products From The Reaction of t-Butyl Isocyanate With $Cp_3U=CHPMePh_2$

Peaks	Realtive Intensity	Possible Assignment
58	100	t-ButH
62	91	
84	9	
157	13	
201	18	$(Ph_2)PO$
215	19	$[(Ph_2)(Me)PO]-H$

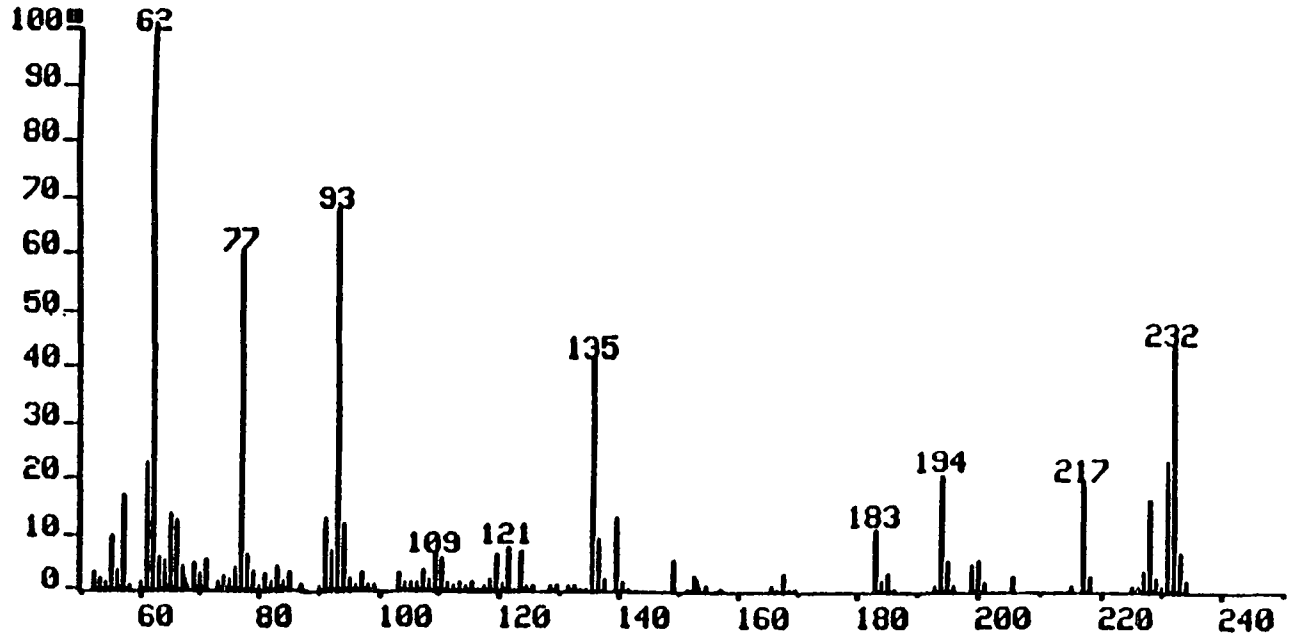

Figure 54: Mass Spectrum of the Product from the Reaction of $Cp_3U{=}CHPMePh_2$ with PhNCS

TABLE 15

Mass Spectral Data of the Product From The Reaction of Phenyl Isothiocyanate with $Cp_3U{=}CHPMePh_2$

Peaks	Relative Intensity	Possible Assignment
62	100	
77	60	Ph
93	70	
1	40	PhNCS
83	12	
194	17	PhN=C=NPh
217	20	(Ph_2PS)
232	45	Ph_2MePS

Chapter 3

DISCUSSION

3.1 Description of Reactions and Spectral Results

3.1.1 Reaction of $Cp^*_2UCl_2$ with $HNSPh_2$

When $Cp^*_2UCl_2$ is allowed to react with $HNSPh_2$ in a 1:1 molar ratio, a dark orange complex forms according to following equation.

$$Cp^*_2UCl_2 + HNSPh_2 \text{ -----> } Cp^*_2UCl_2(HNSPh_2)$$

This compound was characterized by elemental analysis, infrared, mass and ^{1}H-NMR spectroscopy and by X-ray diffraction. The ^{1}H-NMR spectrum, Figure 5, Table 1, exhibits a sharp singlet at δ 9.43 ppm for the Cp^* group (30H), a doublet at δ -9.79 ppm (4H, J_{C-H}=7Hz) and triplets at δ 2.31 ppm (4H, J_{C-H}=7H) and δ 3.85 ppm (2H, J_{C-H}=7Hz) for the ortho, meta and para protons of the SPh_2 group and a singlet at δ +142 ppm for the imino hydrogen of $HNSPh_2$. The peaks are scattered over a wide chemical shift range due to paramagnetic U(IV).

The infrared spectral data obtained over the range 3500-500 cm^{-1} are summarized in Table 3 and the spectrum

is shown in Figure 11. The characteristic absorptions of the Cp^* groups appear at 2925, 2900 and 2830 cm^{-1}. The band at 1425 cm^{-1} can be assigned to the C-H bending. The C-H stretch of the phenyl group occurs at 3065 cm^{-1} and the C=C stretch occurs at 1625 cm^{-1}. A signal for the N-H stretch in the infrared spectrum of $Cp^*_2UCl_2(HNSPh_2)$ is observed at 3284 cm^{-1}. This is 22 cm^{-1} smaller than the N-H stretching frequency of free $HNSPh_2$, 3306 cm^{-1}, of which the infrared spectrum is given in Figure 9.

In order to assign the N-H stretch unambiguously deuterium substitution on the N-H group of $HNSPh_2$ was carried out. $Me_3SiNSPh_2$ reacts with D_2O to yield $DNSPh_2$ according to the following reaction.

$$Me_3SiNSPh_2 + D_2O \text{ -------> } DNSPh_2 + (Me_3Si)_2O$$

The infrared spectrum of $DNSPh_2$ is shown in Figure 10. This contains a signal at 2448 cm^{-1} which is assigned to the D-N stretch. The calculated value for the D-N stretch is 2338 cm^{-1}.[76] The signal at 3304 cm^{-1} indicates that some $HNSPh_2$ is also present in the sample. The reaction of $Cp^*_2UCl_2$ with $DNSPh_2$ forms $Cp^*_2UCl_2(DNSPh_2)$.

$$Cp^*_2UCl_2 \quad + \quad DNSPh_2 \quad \text{-----} > \quad Cp^*_2UCl_2(DNSPh_2)$$

The infrared spectrum, Figure 12, of this complex shows a signal at 2435 cm^{-1} for the D-N stretch which is 13 cm^{-1} smaller than the D-N stretching frequency of free $DNSPh_2$, 2448 cm^{-1}. The differences between the expected and observed N-D stretching frequencies are in agreement with those of analogous compounds available in the literature.[77]

The mass spectrum, Figure 7, Table 2, does not contain a molecular ion peak, however, peaks are observed with m/e = 578 and 201 which correspond to $Cp^*_2UCl_2$ and $HNSPh_2$ respectively. Additional peaks occur at 443, 308, 270, 186 and 119 which correspond to the mass fragments of $Cp^*_2UCl_2$ and $HNSPh_2$. This is consistent with dissociation of $Cp^*_2UCl_2(HNSPh_2)$ upon heating.

If $Cp^*_2UCl_2(HNSPh_2)$ undergoes dehydrochlorination, $Cp^*_2UCl(NSPh_2)$ is expected to form. However, $Cp^*_2UCl_2(HNSPh_2)$ does not undergo dehydrochlorination upon heating under vacuum or reflux in toluene over a long period of time, as indicated by ^1H-NMR spectra. Interestingly, $Cp^*_2UCl_2(HNSPh_2)$ is stable even under reflux conditions in the presence of excess $HNSPh_2$ which is a moderately strong base. Similar to the sulfilimine

case, $Cp^*_2UCl_2(HNPPh_3)$ is stable in the presence of free $HNPPh_3$ even under reflux conditions. The transition metal phosphinimine complex, $Cp^*TaF_4.HNPPh_3$,[78] is also thermally stable and resistant to dehydrohalogenation.

Attempts to synthesize complexes containing a $[NSPh_2]^-$ ligand from reactions of $Me_3SiNSPh_2$ with $Cp^*_2UCl_2$ were also unsuccessful. This is a significant difference between transition metal chemistry and the f-element chemistry, as Me_3Si derivatives are commonly used in transition metal chemistry for replacing coordinated halides with other anions.[53,54,73]

$$Cp^*_2UCl_2 + Me_3SiNSPh_2 \longrightarrow Cp^*_2UCl(NSPh_2) + Me_3SiCl$$

But,

$$VOCl_3 + Me_3SiNSPh_2 \longrightarrow (Ph_2SN)V(O)Cl_2 + Me_3SiCl$$

3.1.2 Reaction of $Cp^*_2UCl_2$ With $LiNSPh_2$

In order to synthesize Cp^*_2U complexes of the $[NSPh_2]^-$ ligand, the reactivity of $Cp^*_2UCl_2$ with $LiNSPh_2$ was studied. When $HNSPh_2$ is treated with n-BuLi in THF

at -78°C, $LiNSPh_2$ forms as a yellow crystalline material according to following equation.

$$HNSPh_2 + n\text{-}BuLi \longrightarrow LiNSPh_2 + Bu\text{-}H$$

$LiNSPh_2$ reacts with $Cp^*_2UCl_2$ to form $Cp^*_2UCl(NSPh_2)$ and $Cp^*_2U(NSPh_2)_2$ as dark red complexes depending on the stoichiometry of the reactions:

$$Cp^*_2UCl_2 + LiNSPh_2 \longrightarrow Cp^*_2UCl(NSPh_2) + LiCl$$

$$Cp^*_2UCl_2 + 2\ LiNSPh_2 \longrightarrow Cp^*_2U(NSPh_2)_2 + 2LiCl$$

Both products were characterized by usual chemical and spectroscopic means and by x-ray diffraction.

These reactions are analogous to the reactions of $Cp^*_2UCl_2$ with $LiNPPh_3$ that produces $Cp^*_2UCl(NPPh_3)$ and $Cp^*_2U(NPPh_3)_2$[43]. The x-ray crystal structure of $Cp^*_2UCl_2(HNPPh_3)$[51] has been determined whereas $Cp^*_2UCl(NPPh_3)$ and $Cp^*_2U(NPPh_3)_2$ have been characterized only by ^{1}H-NMR spectroscopy[43].

The complexes, $Cp^*_2UCl(NSPh_2)$ and $Cp^*_2U(NSPh_2)_2$, also form by reactions of $HNSPh_2$ with the organouranium phosphoylide complex, $Cp^*_2UCl(CH_2)_2PR_2$.

$$Cp^*_2UCl(CH_2)_2PR_2 + HNSPh_2 \longrightarrow Cp^*_2UCl(NSPh_2) + MeR_2P{=}CH_2$$

$$Cp^*_2UCl(CH_2)_2PR_2 + 2\ HNSPh_2 \longrightarrow Cp^*_2U(NSPh_2)_2 + [Me_2R_2P]^+Cl^-$$

In the case of the 1:1 reaction between $Cp^*_2UCl(CH_2)_2PR_2$ and $HNSPh_2$, the phosphoylide which is a strong base, absorbs the imino hydrogen from $HNSPh_2$ to form $Cp^*_2UCl(NSPh_2)$ and the free phosphylide. Two equivalents of $HNSPh_2$ react with $Cp^*_2UCl(CH_2)_2PR_2$ to yield $Cp^*_2U(NSPh_2)_2$ and the phosphonium salt, $[Me_2R_2P]^+Cl^-$.

$Cp^*_2U(NSPh_2)_2$ can also be synthesized by reacting $Cp^*_2UCl_2(HNSPh_2)$ with $LiNSPh_2$ in the presence of $HNSPh_2$.

$$Cp^*_2UCl_2(HNSPh_2) + LiNSPh_2 + HNSPh_2 \longrightarrow Cp^*_2U(NSPh_2)_2 + LiCl + [H_2NSPh_2]^+Cl^-$$

Both, $Cp^*_2UCl(NSPh_2)$ and $Cp^*_2U(NSPh_2)_2$, were characterized by elemental analysis, infrared and ^{1}H-NMR spectroscopy and x-ray diffraction.

The ^{1}H-NMR spectrum of $Cp^*_2UCl(NSPh_2)$, Figure 14, Table 4, contains a sharp singlet at δ 2.27 ppm (30H) for the Cp^* group, a doublet at 14.12 ppm (4H, $J_{C\text{-}H}$=7Hz) and

two triplets 8.37 ppm (2H, J_{C-H}=7Hz) and δ 8.48 ppm (4H, J_{C-H}=7HZ) for the ortho, meta and para protons of the S-Ph_2 group. The ^{1}H-NMR spectrum of $Cp^*_2U(NSPh_2)_2$, Figure 17, Table 6, appears in the same general region, with a singlet for the Cp^* at δ -0.24 ppm (30H) for the Cp^* group, a doublet at δ 3.93 ppm (8H, J_{C-H}=7Hz) and triplets atδ 5.93 ppm (8H, J_{C-H}=7Hz) and 6.18 ppm (4H, J_{C-H}=7Hz) for the ortho, meta and para protons of the S-Ph_2 group. The contact shifts of the phenyl groups of $Cp^*_2UCl(NSPh_2)$ are downfield whereas those in $Cp^*_2UCl(NSPh_2)_2$ are upfield.

The infrared spectra of the two complexes are shown in Figures 16 and 19 and summarized in Tables 5 and 7. They are quite similar. The characteristic absorption peaks for the C-H stretch of Cp^* group of both products appear between 2890 cm^{-1} and 3010 cm^{-1}. The signal at 3055 cm^{-1} in the infrared spectrum of $Cp^*_2UCl(NSPh_2)$ is assigned to the C-H stretch of the phenyl group whereas the same band in $Cp^*_2U(NSPh_2)_2$ appears at 3065 cm^{-1}. The characteristic C=C stretch of the phenyl groups occurs at 1555 cm^{-1} in $Cp^*_2UCl(NSPh_2)$ and at 1585 cm^{-1} in $Cp^*_2U(NSPh_2)_2$. The signals for C-H bending in both complexes appear between 1400-1500 cm^{-1}. While it is

difficult to assign a signal for the N-S stretch unambiguously, strong absorption peaks occur between 900 cm^{-1} and 1100 cm^{-1} in both cases.

The U-Cl stretching bands were also not assigned in the infrared spectrum. Figures 55 and 56 summarize the chemistry involved in this section.

3.1.3 Reaction of $Cp^*_2UCl_2$ with $HNSPh_2 \cdot H_2O$

$Cp^*_2UCl_2$ reacts with excess $HNSPh_2 \cdot H_2O$ to form a yellowish green solution. The ^1H-NMR spectra, Figures 20-22, in which a resonance at -2.0 ppm grows and then disappears as the reaction progresses, indicate an unstable intermediate. This intermediate reacts further to form Cp^*H whose NMR peaks grow with time, as well as other products. Within several weeks the intermediate completely disappears and dark green-black crystals form in the solution. An x-ray structure of these crystals show the final product to be, $[Cp^*(Cl)(HNSPh_2)U-(\mu_3-OH)(\mu_2-O)_2-U(Cl)(HNSPh_2)_2]_2$.

$Cp^*_2UCl_2(HNSPh_2)$ also reacts with $HNSPh_2 \cdot H_2O$ to form the intermediate with an NMR signal at -2.0 ppm. From this reaction, crystals of the intermediate could be obtained and are shown to be $Cp^*_2UCl(OH)(HNSPh_2)$. In the

room temperature spectrum, Figure 28, the singlet at -2.0 ppm is assigned to the Cp^* group while broad signals appear near -10.5 and -0.5 ppm. The aromatic peaks can be identified in the low temperature spectra. The ^1H-NMR spectrum of $Cp^*_2UCl(OH)(HNSPh_2)$ at -60°C, Figure 29, contains signals at δ -0.2, -1.5 and -14.0 ppm for the aromatic protons and a broad signal at -163 ppm for the imino hydrogen whereas the hydroxy proton is not observed even at low temperature within the chemical shift range examined. The peak broadening at room temperature is mainly due to exchange of protons between the hydroxy and imino protons and the dissociation and re-association of the $HNSPh_2$ ligand. The reaction of $Cp^*_2UCl_2$ with $HNSPh_2 \cdot H_2O$ can be summarized as follows.

$$Cp^*_2UCl_2 + HNSPh_2 \longrightarrow Cp^*_2UCl_2(HNSPh_2)$$

$$Cp^*_2UCl_2(HNSPh_2) + HNSPh_2.H_2O \longrightarrow Cp^*_2UCl(OH)(HNSPh_2) + [H_2NSPh_2]^+Cl^-$$

$$4\ Cp^*_2UCl(OH)(HNSPh_2) + 2\ HNSPh_2.H_2O \longrightarrow 6\ Cp^*H + [Cp^*(Cl)(HNSPh_2)U\text{-}(\mu_3\text{-}OH)(\mu_2\text{-}O)_2\text{-}U(Cl)(HNSPh_2)_2]_2$$

Figures 28 and 31 show that $Cp^*_2UCl(OH)(HNSPh_2)$ is unstable in solution. In tetrahydrofuran, $Cp^*_2UCl(OH)(HNSPh_2)$ reacts to form $Cp^*_2UCl_2(HNSPh_2)$, Cp^*H and unidentified products that give broad signals around 7.5 ppm in the ^{1}H-NMR spectrum.

The following equation can be proposed for this reaction.

$$2\ Cp^*_2UCl(OH)(HNSPh_2) \longrightarrow Cp^*_2UCl_2(HNSPh_2) + 2\ Cp^*H + HNSPh_2 + "UO_2"$$

Infrared spectra of $Cp^*_2UCl(OH)(HNSPh_2)$ and $[Cp^*(Cl)(HNSPh_2)U\text{-}(\mu_3\text{-}OH)(\mu_2\text{-}O)_2\text{-}U(Cl)(HNSPh_2)_2]_2$, Figures 32 and 34, Tables 8 and 9, contain broad signals between 3000-3500 cm^{-1}. However, unambiguous assignment of OH and NH stretches in both cases was impossible.

3.1.4 Reaction of $Cp_3U{=}CHPR_3$ with $HNSPh_2$

This system was studied in collaboration with D. Afzal. The ability of the phosphoylide ligand of $Cp_3U{=}CHPMeR_2$ to abstract the imino hyrogen from $HNSPh_2$ is evident in the reaction of $HNSPh_2$ with $Cp_3U{=}CHPMeR_2$ which yields Cp_3UNSPh_2.

$Cp_3U{=}CHPMeR_2 + HNSPh_2 \longrightarrow Cp_3UNSPh_2 + MeR_2P{=}CH_2$

Figure 35 shows the ^{1}H-NMR spectrum of this compound. An analogous reaction occurs between $Cp_3U{=}CHPMeR_2$ and $HNPPh_3$.

$Cp_3U{=}CHPMeR_2 + HNPPh_3 \longrightarrow Cp_3UNPPh_3 + MeR_2P{=}CH_2$

Figure 36 contains peaks at δ 18.0 ppm, δ 9.0 ppm, δ 8.5 ppm and δ -20.7 ppm which are consistent with Cp_3UNPPh_3.[45] Interestingly, Cp_3UNSPh_2 is stable in the presence of excess $HNSPh_2$, whereas Cp_3UNPPh_3 reacts with excess $HNPPh_3$ to form $Cp_2U(NPPh_3)_2$ as indicated by the formation of a new sharp singlet at -26.3 ppm for the Cp group and peaks at 11.5 and 8.0 ppm for the aromatic protons.

$Cp_3UNPPh_3 + HNPPh_3 \longrightarrow Cp_2U(NPPh_3)_2 + CpH$

3.1.5 Reaction of UO_2Cl_2 with $Me_3SiNSPh_2$ and $Me_3SiNPPh_3$

The ^{1}H-NMR spectra indicate that UO_2Cl_2 reacts with both $Me_3SiNSPh_2$ and $Me_3SiNPPh_3$. New Me_3Si species form in both cases. According to spectrum in Figure 43, this Me_3Si product is not Me_3SiCl.

In contrast to this observation, transition metal oxy-halides are known to form Me_3SiX (X = F, Cl) during reaction with $Me_3SiNPPh_3$.[73, 79-82]

3.1.6 Reaction of $Cp_3U=CHPMeR_2$ with Heterocumulenes

As described in the introduction, small polar unsaturated molecules insert into the U=C bond in $Cp_3U=CHPMeR_2$. Previously, the reaction of $Cp_3U=CHPMePh_2$ with phenylisocyanate to form an insertion product was characterized. Therefore there was every expectation that n-butylisocyanate, n-propylisocynate, t-butyl isocyanate and phenylisothiocyanate would also insert into the U=C multiple bond. According to evidence available from NMR, infrared and mass spectroscopy, they indeed react with $Cp_3U=CHPR_3$. Excess n-butylisocyanate and n-propylisocyanate form cyclic trimers in the

presence of $Cp_3U{=}CHPR_3$ whereas with phenylisocyanate the cyclic dimer, $(PhNCO)_2$, is formed.

The catalyst responsible for the polymerization of the isocyanate has not yet been identified. However, the insertion product of the reaction between the isocyanate and $Cp_3U{=}CHPMeR_3$ probably is at least a precursor to the catalyst.

Both t-butylisocyanate and phenylisothiocyanate also react with $Cp_3U{=}CHPMeR_2$. However, no catalytic reactivity was observed in either case.

It is possible that the insertion products that form during the reactions of $Cp_3U{=}CHPMePh_2$ with t-butylisocyanate and phenylisothiocynate are unstable and undergo rapid decomposition.

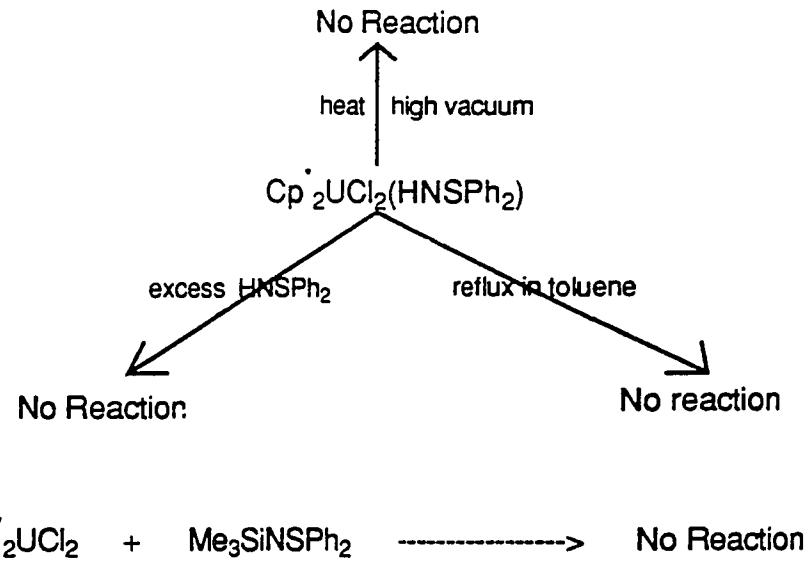

$Cp^*_2UCl_2 + Me_3SiNSPh_2 \dashrightarrow$ No Reaction

Figure 55: Summary of the Attempted Reactions Involving $Cp^*_2UCl_2(HNSPh_2)$

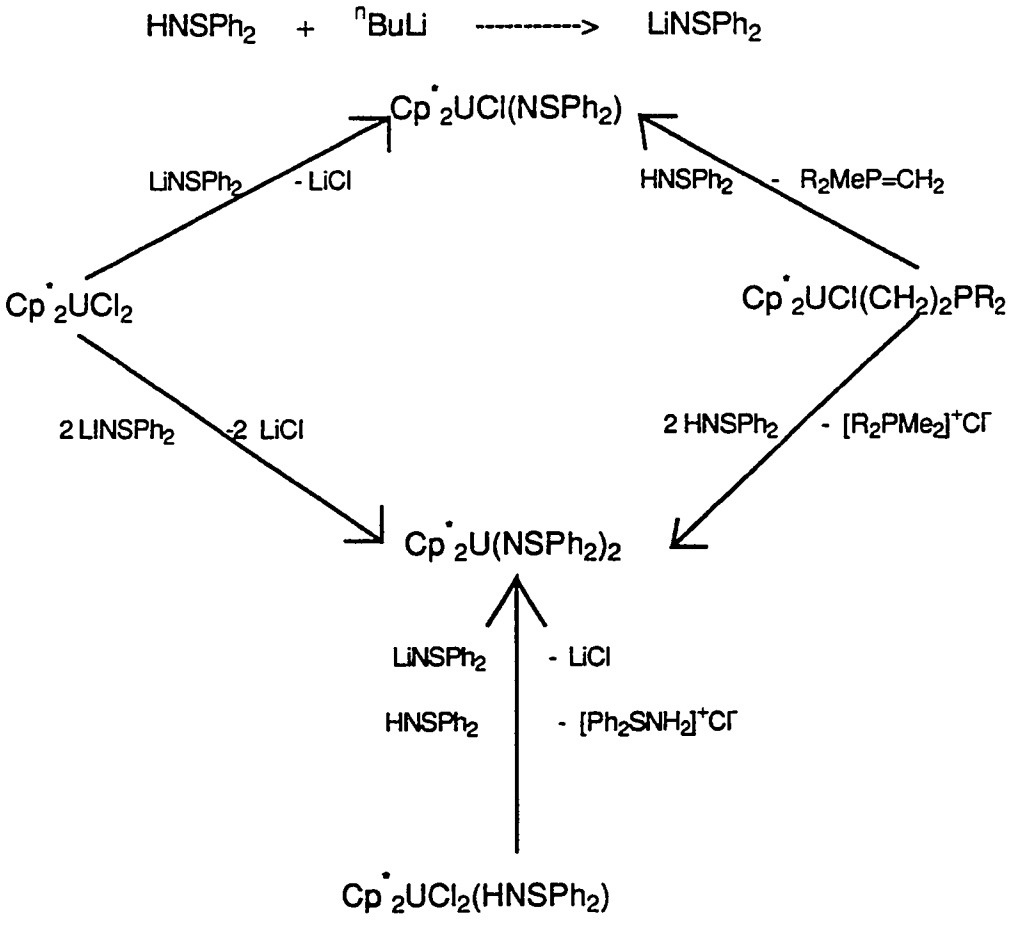

Figure 56: Scheme for the Synthesis of $Cp^*_2UCl(NSPh_2)$ and $Cp^*_2U(NSPh_2)_2$

3.2 X-ray Crystallography

3.2.1 Experimental

3.2.1.1 Collection and Reduction of X-Ray Data

Single crystals of $Cp^*_2UCl_2(HNSPh_2)$, $Cp^*_2UCl(NSPh_2)$, $Cp^*_2U(NSPh_2)_2$, $Cp^*_2UCl(OH)(HNSPh_2)$ and $[Cp^*(Cl)(HNSPh_2)U-(\mu_3-OH)(\mu_2-O)_2-U(Cl)(HNSPh_2)_2]_2$ from the preparations described in the experimental section, were selected, mounted and sealed in thin-walled glass capillaries under dinitrogen. A Nicolet R3 computer-controlled diffractometer with graphite monochrometized Mo Kα radiation ($K\alpha^1$ = 0.70930 A, $K\alpha^2$ = 0.71359 A) and a scintillation detector with pulse height analyzer was used for the measurement of diffraction intensities. During data collection, the intensities of three standard reflections were remeasured every 97 reflections. Corrections for Lorentz and polarization effects were applied using the program, XDISK and absorption correction was done using the program, XEMP, with a number of psi scans for each complex.[83] Atomic scattering factors for N°, S°, Cl°, O° and U° were supplied by SHELXTL PLUS.[84]

3.2.1.2 Structure Solution of $Cp^*_2UCl_2(HNSPh_2)$

The check reflections showed < 20% variation during data collection and data were corrected for this variation using the program, XDISK, before solving the structure. Cell constants were determined by least square methods from the centered angular coordinates of 25 reflections with 2-theta values between 15° and 26°. These were repeatedly re-centered during the data collection in order to compensate for the slight movement of the crystal within the capillary.

The structure was solved in the monoclinic space group, C2/c. The position of the uranium was determined by Patterson methods and the remaining atoms were located from a series of difference Fourier maps and least squares refinements using SHELXTL PLUS. All non-hydrogen atoms were refined anisotropically except for the ring carbons of the cyclopentadienyl and the phenyl groups which were refined isotropically as rigid bodies. [C-C(Cp^*) = 1.420 A, C-C(Ph) = 1.395 A] H atoms were not located in the crystal structure whereas all non-hydrogen atoms appeared in the first few difference Fourier syntheses.

After an empirical absorption correction using the program XEMP, with four psi scans with 2-theta values, 11.28, 17.25, 25.44 and 30.62, refinement converged to R = 8.61 and R_2 = 9.68. In the final refinement the positions and corresponding anisotropic and isotropic thermal parameters of all the non-hydrogen atoms were refined to yield R = 6.77 and R_g = 7.76. In the final cycle of refinement the maximum parameter shift was 21% of standard deviation for one of the Cp^* methyl carbon atoms. The final positional and thermal parameters are listed in Tables 18-20. The bond lengths and bond angles are listed in Table 17.

3.2.1.3 Structure solution of $Cp^*_2UCl(NSPh_2).1/2\ C_5H_{12}$

The check reflections showed <10% variation during data collection and data were corrected for this variation using the program, XDISK, before solving the structure. For the absorption correction the program XEMP was used with six psi scans with the 2-theta values, 7.17°, 16.56°, 20.93°, 26.79°, 30.66°, 36.43°. Cell constants were determined by least square methods from the centered angular coordinates of 28 reflections with 2-theta values between 8° and 29°.

The monoclinic structure was solved in the space group P2 1/n. The position of the uranium was determined by Patterson methods and the remaining atoms were located from a series of difference Fourier maps and least square refinements using SHELXTL PLUS. All non-hydrogen atoms were refined anisotropically except for the ring carbons of the phenyl groups which were refined isotropically as rigid bodies. [C-C(Ph) = 1.395 A] H atoms were not located in the crystal structure. A pentane molecule is also present in the crystal structure. After several cycles of least squares refinements and an empirical absorption correction, R = 7.54 and R_2 = 8.35 were obtained.

In the final refinement, the positions and corresponding isotropic and anisotropic thermal parameters of all the non-hydrogen atoms were refined to yield R = 6.55 and R_g = 7.85. The final cycle of refinement yielded a maximum parameter shift of 13% of its standard deviation for one of the Cp^* methyl carbon atoms and a maximum shift of 40% for one of the carbon atoms of the pentane molecule. The final positional and thermal parameters are listed in Tables 26-28. The bond lengths and bond angles are listed in the Table 25.

3.2.1.4 Structure Solution of $Cp^*_2U(NSPh_2)_2$

The check reflections showed less than 2% variation during data collection and data were corrected using the program, XDISK, before solving the stucture. For the absorption correction, the program XEMP was used with seven psi scans with the 2-theta values, 11.56°, 17.12°, 17.63°, 25.80°, 34.63°, 44.32°, and 50.15°. Cell constants were determined by least squares methods from the centered angular coordinates of 23 reflections with 2-theta values between 16° and 41°.

The monoclinic structure was solved in the space group C2/c. The position of the uranium was determined by Patterson methods and the remaining atoms were located from a series of difference Fourier maps and least square refinements using SHELXTL PLUS. The molecule lies on a crystallographic two fold axis so that the asymmetric unit is one half of the molecule. All non-hydrogen atoms were refined anisotropically except for the ring carbons of the cyclopentadienyl and the phenyl groups which were refined isotropically as rigid bodies. [C-C(Cp^*) = 1.420 A, C-C(Ph) = 1.395 A] All non-hydrogen atoms were revealed in the first few difference Fourier syntheses. After several cycles of least squares refinements and an

empirical absorption correction, R = 6.52 and R_2 = 7.67 were obtained. H atoms were added to the structure at calculated positions at this stage and more least square refinements were performed on the structure.

In the final refinement, the positions and corresponding isotropic and anisotropic thermal parameters of all the atoms were refined to yield R = 4.54 and R_g = 5.20. The final cycle of refinement yielded a maximum parameter shift of 3% of its standard deviation for one of the Cp^* methyl carbon atoms. The final positional and thermal parameters are listed in Tables 32-35. The bond lengths and bond angles are listed in Table 31.

3.2.1.5 Structure Solution of $Cp^*_2UCl(OH)(HNSPh_2).C_6H_6$

The check reflections showed about 12% variation in intensity during the data collection and data were corrected for this variation by using the program, XDISK. For the corrections for absorption effects the program, XEMP, was used with five psi scans with 2-theta values, 11.42, 17.24, 23.28, 31.71 and 37.88. Cell constants

were determined by least square methods from the centered angular coordinates of 16 reflections with 2-theta values between 8° and 19°.

The structure was solved in the monoclinic space group, P2(1)/c. The positions of the two uranium atoms were determined by direct methods and the remaining atoms were located from a series of difference Fourier maps and least square refinements using SHELXTL PLUS. All non-hydrogen atoms were refined anisotropically except for the ring carbons of the cyclopentadienyl, phenyl groups and the oxygen which were refined isotropically. The cyclopentadienyl and the phenyl groups were treated as rigid bodies. [C-C(Cp^*) = 1.420 A, C-C(Ph) = 1.395 A] Hydrogen atoms were not located in the crystal structure whereas all non-hydrogen atoms were revealed in the first few difference Fourier syntheses.

After several cycles of least squares refinements R = 10.65 and R_2 = 10.65 were obtained. After an empirical absorption correction and more least squares refinements R = 9.23 and R_2 = 9.23 were recorded. The anisotropic refinement of selected non-hydrogen atoms with further least squares refinements yielded R = 6.64 and R_2 = 7.41. H atoms were added to the structure at

calculated positions at this stage and more least squares refinements were performed on the structure.

In the final refinement, the positions and corresponding isotropic and anisotropic thermal parameters of all the atoms were refined to yield $R = 6.53$ and $R_g = 7.28$. The final cycle of refinement yielded a maximum parameter shift of 37% of its standard deviation for one of the benzene carbon atoms. The final positional and thermal parameters are listed in Tables 40-43. The bond lengths and bond angles are listed in Tables 38 and 39.

3.2.1.6 Structure Solution of $[Cp^*(Cl)(HNSPh_2)U\text{-}(\mu_3\text{-}OH)(\mu_2\text{-}O)_2\text{-}U(Cl)(HNSPh_2)_2]_2 \cdot 4C_7H_8$

The check reflections showed less than 5% variation in intensity during the data collection and data were corrected for this variation using the program, XDISK, before solving the structure. For the corrections for absorption effects the program, XEMP was used with four psi scans with 2-theta values, 8.43, 14.06, 22.77, and 27.01. Cell constants were determined by least square methods from the centered angular coordiantes of 14 reflections with 2-theta values between 6° and 24°.

The structure was solved in the triclinic space group, P 1 bar. The positions of the two uranium atoms were determined by Pattersen methods and the remaining atoms were located from a series of difference Fourier maps and least square refinements using SHELXTL PLUS. Two disordered toluene molecules were also identified in the asymmetric unit. All non-hydrogen atoms were refined anisotropically except for the ring carbons of the cyclopentadienyl, phenyl groups and the toluene carbons which were refined isotropically. The cyclopentadienyl and the phenyl groups were treated as rigid bodies. [C-C(Cp^*) = 1.420 A, C-C(Ph) = 1.395 A] Hydrogen atoms were not located in the crystal structure whereas all non-hydrogen atoms were revealed in the first few difference Fourier syntheses.

After several cycles of least squares refinements R = 9.37 and R_2 = 11.20 were obtained. After an empirical absorption correction and more least squares refinements R = 6.56 and R_2 = 8.71 were recorded. The anisotropic refinement of selected non-hydrogen atoms with further least squares refinements yielded R = 5.75 and R_2 = 8.02. At this stage the toluene carbons were introduced. As both toluene molecules appeared to be disordered, new carbon atoms were introduced at

calculated positions and least squares refinements were carried out with occupancy refinements using free variables. Each toluene molecule is disordered over three positions as shown in Figures 73 and 74. The disorder in the toluene 1, [C(71)-C(76)], occurs nearly in the same plane where the relative distances between the centroids, X1A-X1B, X1A-X1C and X1B-X1C are 1.58, 1.07 and 2.62 A respectively. The disorder in toluene 2 , [C(81)-C(86)], involves three different planes where the distances between the centroids, X1A-X1B, X1A-X1C and X1B-X1C are 1.01, 2.16 and 1.98 A, respectively. Further least squares refinements then yielded the values, R = 5.67 and R_2 = 7.97.

H atoms were added to the structure at calculated positions at this stage for all the Cp^* methyl groups and the phenyl groups, except for the toluenes, and more least square refinements were performed on the structure.

In the final refinement, the positions and corresponding isotropic and anisotropic thermal parameters of all the atoms were refined to yield R = 5.64 and R_g = 7.91. The final cycle of refinement yielded a maximum parameter shift of 31% of its standard deviation for one of the toluene carbon atoms whereas all the parameter shifts for the atoms in [Cp^*(Cl)($HNSPh_2$)U-

$(\mu_3\text{-OH})(\mu_2\text{-O})_2\text{-U(Cl)(HNSPh}_2)_2]_2$ were less than 3%. The final positional and thermal parameters are listed in Tables 47-51. The bond lengths and bond angles are listed in Tables 45 and 46.

3.2.2 Description of Crystal Structures

3.2.2.1 The Structures of $Cp^*_2UCl_2(HNSPh_2)$ and $Cp^*_2UCl(OH)(HNSPh_2)$

The crystal structure of the adduct $Cp^*_2UCl_2(HNSPh_2)$ contains one molecule in the asymmetric unit and the unit cell contains eight adduct molecules. There are two nearly equivalent $Cp^*_2UCl(OH)(HNSPh_2)$ molecules and two benzenes in the asymmetric unit of the crystal. Least square plane calculations were performed on these benzene molecules with respect to their neighboring phenyl groups. The dihedral angles between the benzene molecule, $(C_1\text{-}C_6)$, and the phenyl groups of the first $Cp^*_2UCl(OH)(HNSPh_2)$ molecule, $(C_{51}\text{-}C_{56})$ and $(C_{61}\text{-}C_{66})$, are 24.8° and 72.7° respectively, while the dihedral angles between the other benzene molecule, $(C_{91}\text{-}C_{96})$, and the phenyl groups of the second $Cp^*_2UCl(OH)(HNSPh_2)$ molecule, $(C_{71}\text{-}C_{76})$ and $(C_{81}\text{-}C_{86})$, are 39.6° and 55.0°. The differences in these dihedral angles indicate that the

two benzenes are symmetrically non-equivalent. This accounts for the presence of two $Cp^*_2UCl(OH)(HNSPh_2)$ molecules in the asymmetric unit. The unit cell consists of eight molecules of $Cp^*_2UCl(OH)(HNSPh_2)$ and eight benzene molecules. The packing diagram of $Cp^*_2UCl(OH)(HNSPh_2)$, Figure 72, shows alternating layers of $Cp^*_2UCl(OH)(HNSPh_2)$ and benzene molecules. The $Cp^*_2UCl(OH)(HNSPh_2)$ molecules in different layers are held together by intermolecular H bonds which form between the hydroxide and the chloride ligands of adjacent molecules. The O(1)-Cl(2) distance in the asymmetric unit is 3.27 A while the O(2)-Cl(1) distance is 3.32 A.

The perspective drawings of $Cp^*_2UCl_2(HNSPh_2)$[85] and $Cp^*_2UCl(OH)(HNSPh_2)$[85] are shown in Figures 57 and 68. The crystal data are summarized in Tables 16 and 37, and bond lengths and angles are given in Tables 17, 38 and 39. Similar to $Cp^*_2UCl_2(HNPPh_3)$, both $Cp^*_2UCl_2(HNSPh_2)$ and $Cp^*_2UCl(OH)(HNSPh_2)$ are of the Cp_2ML_3 type, with uranium being bound by two Cp^* rings, two chlorides and the nitrogen of the $HNSPh_2$ ligand in $Cp^*_2UCl_2(HNSPh_2)$, while the gross structure of $Cp^*_2UCl(OH)(HNSPh_2)$ can be derived by substituting a chloride with OH^-. If each Cp^* group is assigned three coordination sites, chloride one, hydroxide one and nitrogen one, uranium is in ninefold

coordination in both cases. Analogous bond lengths and angles of $Cp^*_2UCl_2(HNSPh_2)$, $Cp^*_2UCl(OH)(HNSPh_2)$ and $Cp^*_2UCl_2(HNPPh_3)$[51] are compared in Tables 22 and 23.

The equatorial girdles of all of these complexes are planar within experimental uncertainties and the external Cl-U-Cl or Cl-U-O angles are equal to the sum of the respective Cl-U-N or O-U-N interior angles. The smaller Cl-U-Cl angle in $Cp^*_2UCl_2(HNSPh_2)$ probably reflects the fact that the sulfilimine ligand is somewhat smaller than the phosphine imine. While the standard deviations for the Cp-U-Cp angles cannot not be determined accurately, they can be estimated based on those of U-C-C(Me) angles in corresponding complexes. In $Cp^*_2UCl_2(HNSPh_2)$, the Cp-U-Cp angles is 130.7(4)° while the average Cp-U-Cp angle in $Cp^*_2UCl(OH)(HNSPh_2)$ is 136(1)°. These angles are in the same range as that in $Cp^*_2UCl_2(HNPPh_3)$, 134.3(3)°.

The U-N-S atoms in $Cp^*_2UCl_2(HNSPh_2)$ form an angle of 134(1)°, consistent with a nearly sp^2 hybridized nitrogen atom with trigonal planar geometry. The same angle in $Cp^*_2UCl(OH)(HNSPh_2)$, 129.5(9)°, also argues for sp^2 nitrogen hybridization. The U-N-P angle in $Cp^*_2UCl_2(HNPPh_3)$, 155.8(6)°, which is significantly wider

than the U-N-S angle in $Cp^*_2UCl_2(HNSPh_2)$, may also indicate that the SPh_2 group is sterically less demanding than the PPh_3 moiety.

There are two different U-Cl distances in $Cp^*_2UCl_2(HNSPh_2)$, 2.648(8) A and 2.693(8) A. They both are longer than the U-Cl distances found in Cp_3UCl,[86] 2.56(2) A, $[UCl_2(dmso)_6][UCl_6]$,[87] 2.60(2) A (anion), $UCl_4.(hmpa)_2$,[88] 2.58(1) A and 2.60(1) A and $UCl_4(tppo)_2$,[89] 2.609(4) A and 2.626(3) A. This difference is probably due to steric crowding created by the bulky Cp^* groups and $HNSPh_2$ ligand on the uranium center. A similar situation is observed in $Cp^*_2UCl_2(HNPPh_3)$[51] where the U-Cl distances are comparable to those of $Cp^*_2UCl_2(HNSPh_2)$. The U-Cl distance of $Cp^*_2UCl(OH)(HNSPh_2)$, 2.745(5) A, is very long and may be the result of OH^- being a better donor than is Cl^-.

None of the hydrogens were located in the crystal structure of $Cp^*_2UCl_2(HNSPh_2)$. However, if the imino hydrogen is placed in its predicted position in $Cp^*_2UCl_2(HNSPh_2)$, it is directed toward Cl(1), the chloride which makes the longer U-Cl bond, 2.693(8) A. The N-Cl(1) separation, 3.001 A, which is within the range observed for N-H---Cl hydrogen bonds,[90] is in agreement with this argument. The longer U-Cl distance

probably reflects such a N-H--Cl(1) interaction. A similar proposal has been made for $Cp^*_2UCl_2(HNPPh_3)$. The N-Cl separation of 3.002 A in $Cp^*_2UCl(OH)(HNSPh_2)$, with the imino hydrogen directed towards Cl, also indicates a possible H-bonding situation.

In $Cp^*_2UCl_2(HNSPh_2)$, the N-S-C(31) and N-S-C(41) dihedral angles with respect to the U, N, Cl(1), Cl(2) least squares plane, are 36.5° and 68.8°. The corresponding angles in the two molecules of $Cp^*_2UCl(OH)(HNSPh_2)$, 51.6°, 53.7° and 48.5°, 56.8°, are significantly different from those of $Cp^*_2UCl_2(HNSPh_2)$. In $Cp^*_2UCl_2(HNPPh_3)$, the N-P-C(31), N-P-C(41) and N-P-C(51) dihedral angles with respect to the U, N, Cl(1), Cl(2) least squares plane are 16.0°, 80.1° and 135.4° respectively. This indicates that the conformation around the S in $Cp^*_2UCl_2(HNSPh_2)$ has rotated about 60° around the N-S bond, compared to that of P in $Cp^*_2UCl_2(HNPPh_3)$.

While the Cp-U-Cp angles in the two molecules in the asymmetric unit of $Cp^*_2UCl(OH)(HNSPh_2)$, 135.5° and 136.3°, are very similar, the corresponding U-N distances, 2.41(2) A and 2.51(2) A, are significantly different from each other. The U-N distance in $Cp^*_2UCl_2(HNSPh_2)$ is 2.44(3) A and that in $Cp^*_2UCl_2(HNPPh_3)$ is 2.43(1) A.

These bond lengths fall in the upper portion of U-N distances as would be expected for sterically crowded molecules.

According to the molecular orbital studies of $HNPH_3$ carried out by K. Lammertsma,[52] the electron density of nitrogen is somewhat delocalized towards the PH_3 group as the result of strong polarization of PH_3 orbitals towards the imino group. The $HNSPh_2$ case can be expected to be similar to that of phosphorous in $HNPH_3$ with the sulfur orbitals being lower in energy. Therefore the sulfur orbitals in $HNSPh_2$ show a better energy match for interacting with the nitrogen orbitals so that the extent of delocalization of electron density on the nitrogen towards sulfur in $HNSPh_2$ would be greater than the delocalization towards phosphorous in $HNPH_3$. Therefore, $HNPPh_3$ can be expected to be a better donor ligand than $HNSPh_2$. However, the overriding effect in $HNPH_3$ is a large Coulombic interaction which makes the P-N bond extremely polar. Similarly, the following resonance forms can be written for $HNSPh_2$ where the resonance form A is more important than B.

A B

This indicates that the nitrogen in $HNSPh_2$ can act as a strong electron donor.

The U-O bond length in $Cp^*_2UCl(OH)(HNSPh_2)$,[85] 2.11(1) A, is very similar to that of $[(Me_3SiC_5H_4)_3U]_2[\mu\text{-}O)$,[70] 2.105(3) A. This distance is similar to that in the cation $[(C_9H_7)UBr(MeCN)_4]_2[\mu\text{-}O]^{2+}$,[91] 2.057(1) A. The U-O distances in the $\{Cp^*U[\mu\text{-}CH_2)P(Ph)_2(CH_2)]\}_2Mg[CH_2PMePh_2](\mu_3\text{-}O)(\mu_2\text{-}O)(\mu_2\text{-}Cl)_2$ hydrolysis product,[69] 2.13(2) A and 2.18(2) A, also lie in the same range.

3.2.2.2 The Structures of $Cp^*_2UCl(NSPh_2)$ and $Cp^*_2U(NSPh_2)_2$

The asymmetric unit in the crystal structure of $Cp^*_2UCl(NSPh_2)$ contains one molecule of $Cp^*_2UCl(NSPh_2)$ and half of a pentane molecule which lies on a center of inversion. Thus the unit cell consists of four molecules of $Cp^*_2UCl(NSPh_2)$ and two pentane molecules.

The asymmetric unit of the $Cp^*_2U(NSPh_2)_2$ complex contains a uranium coordinated by a Cp^* group and an $[NSPh_2]^-$ group. The uranium atom lies on a crystallographic twofold axis so that the asymmetric unit is only one half of the molecule whereas the unit cell contains four $Cp^*_2U(NSPh_2)_2$ molecules.

The perspective drawings of $Cp^*_2UCl(NSPh_2)$ and $Cp^*_2U(NSPh_2)_2$ are given in Figures 60 and 63. The crystal data are summarized in Tables 24 and 30, and bond lengths and angles are given in Tables 25 and 31. Similar to $Cp^*_2UCl_2(HNSPh_2)$ and $Cp^*_2UCl(OH)(HNSPh_2)$, both $Cp^*_2UCl(NSPh_2)$ and $Cp^*_2U(NSPh_2)_2$ belong to the bent metallocene family. Both complexes are eightfold coordinated and of the Cp_2ML_2 type.

The U-N-S angles of $Cp^*_2UCl(NSPh_2)$, 164.4(9)°, and $Cp^*_2U(NSPh_2)_2$, 151.9(3)°, are both considerably wider than that in $Cp^*_2UCl_2(HNSPh_2)$. This is expected because both contain only a dicoordinated nitrogen. The U-Cl bond in $Cp^*_2UCl(NSPh_2)$, 2.609(6) A, is significantly shorter than those in $Cp^*_2UCl_2(HNSPh_2)$, $Cp^*_2UCl(OH)(HNSPh_2)$, and $Cp^*_2UCl_2(HNPPh_3)$ and is normal for tetravalent uranium. The U-N distances in $Cp^*_2UCl(NSPh_2)$, 2.10(1) A and $Cp^*_2U(NSPh_2)_2$, 2.138(5) A, are among the shortest found for Cp^*_2U-(N-donor) complexes. This no doubt reflects the strong donor power of the $[NSPh_2]^-$ ligand. The U-N distance in Cp_3UNPPh_3,[45] 2.07(2) A, is comparable to those reported here.

The Cl-U-N angle in $Cp^*_2UCl(NSPh_2)$, 96.4(4)°, is very similar to the N-U-N angle in $Cp^*_2U(NSPh_2)_2$, 96.8(3)°. These angles are significantly narrower than the Cl-U-Cl

angle in $Cp^*_2UCl_2(HNSPh_2)$, 145.9(3)° and the average Cl-U-O angles in $Cp^*_2UCl(OH)(HNSPh_2)$, 147.2(3)°. This is consitant with less sterically crowded uranium centers in $Cp^*_2UCl(NSPh_2)$ and $Cp^*_2U(NSPh_2)_2$.

The N-S-C(31) and N-S-C(41) dihedral angles in $Cp^*_2UCl(NSPh_2)$ with respect to the U-N-S least squares plane, 18.5° and 87.5°, are not significantly different from the corresponding N-S-C angles in $Cp^*_2U(NSPh_2)_2$, 24.6° and 82.1°. This indicates that the conformations around sulfur in both cases are similar.

The ring centroid-U-ring centroid angles, 131°, 134°, 133° and 138°, and the average U-C(Cp^*) distances, 2.77(2)A , 2.73(5) A, 2.804(4) A, and 2.78(1) A, in the complexes, $Cp^*_2UCl_2(HNSPh_2)$, $Cp^*_2UCl(NSPh_2)$, $Cp^*_2U(NSPh_2)_2$ and $Cp^*_2UCl(OH)(HNSPh_2)$, respectively, are within the ranges found for other actinide complexes.[43,92-96]

3.2.2.3 The Structure of $[Cp^*(Cl)(HNSPh_2)U-(\mu_3-OH)(\mu_2-O)_2-U(Cl)(HNSPh_2)_2]_2$

The asymmetric unit contains two uranium atoms, three oxygens, one Cp^* group and three $HNSPh_2$ molecules. The molecule encloses an inversion center so that the asymmetric unit is only one half of the molecule.

The unit cell contains one molecule of $[Cp^*(Cl)(HNSPh_2)U-(\mu_3-OH)(\mu_2-O)_2-U(Cl)(HNSPh_2)_2]_2$ and four disordered toluenes.

Both $Cp^*_2UCl_2$ and $Cp^*_2UCl_2(HNSPh_2)$ react with excess $HNSPh_2 \cdot H_2O$ to form a product which has the formula, $[Cp^*(Cl)(HNSPh_2)U-(\mu_3-OH)(\mu_2-O)_2-U(Cl)(HNSPh_2)_2]_2$. A perspective diagram of this molecule is shown in Figure 72. Figure 73 shows a view of the molecule from which the phenyl groups attached to sulfur have been removed for clarity. The molecule contains four uranium atoms which are joined by four doubly bridging and two triply bridging oxygen atoms. U1 and U1A are coordinated by a sulflimine molecule, a chloride and a Cp^* group whereas U2 and U2A are coordinated by two neutral sulfilimine ligands and a chloride. Even though the H atom on the N in any of the $HNSPh_2$ ligands was not located in the crystal structure, the U-N bond lengths which range between 2.47(1)-2.57(2) A and the U-N-S bond angles which lie between 128.5(8)-130.5(9)°, indicate that they are indeed neutral sulfilimine ligands. These bond distances and angles fall in the same range as those found in $Cp^*_2UCl_2(HNSPh_2)$ and $Cp^*_2UCl(OH)(HNSPh_2)$. Although no hydrogen atoms were located on any of the oxygens, on the basis of charge balance, the molecule is required to have

2 OH^- and 4 O^{2-} ligands. Based on symmetry, the two triply bridging oxygens are recognized as the OH^- ligands and the 4 doubly bridging oxides are identified as O^{2-} ligands.

Atoms U1 and U1A are hexa coordinate. Assigning one coordination site to the Cp^* group, one for chloride and one for the sulfilimine group, the geometry is octahedral. Atoms U2 and U2A are hepta coordinate and the basic stereochemistry is pentagonal bipyramidal.

The average U-C(Cp^*) distance, 2.80(1) A, is in the range observed for other Cp^*-U complexes.[92-96] The U(1)-Cl(1) and U(2)-Cl(2) distances, 2.745(6) A and 2.803(4) A, are significantly longer than that for a terminal chloride, where the bond distance is normally about 2.6 A[97]. This observation is consistent with highly sterically crowded uranium and the strong donor power of the OH^- and O^{2-} ligands. The U(2)-Cl(2) distance, 2.803(4) A, is significantly longer than the U(1)-Cl(1) distance, 2.745(6) A. The U(1)-N(11) distance, 2.47(1) A, is considerably shorter than the U(2)-N(22) distance 2.57 A, but similar to the U(2)-N(21) distance 2.50(1) A. This difference is most probably due to larger steric crowding in U(2) created by the hepta coordination.

According to Table 53, the N(11)-S(11), N(21)-S(21) and N(22)-S(22) distances in $[Cp^*(Cl)(HNSPh_2)U-(\mu_3-OH)(\mu_2-O)_2U(Cl)(HNSPh_2)_2]_2$, 1.58(1), 1.61(2) and 1.60(2) are very similar to the N-S distances in other actinide and transition metal sulfilimine, $RNSPh_2$, and sulfilimide, $[NSPh_2]^-$, complexes. This demonstrates that the deprotonation of the imino hydrogen in $HNSPh_2$ has no effect on the N-S distance.

The large U-U distances, 3.802(7) A, 3.533(5) A and 3.555(6) A which are significantly longer than twice the metallic radius of uranium, 1.426 A, indicate that no metal-metal bonding occurs in the compound. This is in agreement with other complexes in which uranium atoms are held in close proximity by bridging ligands. For comparison, the U-U distances in $[Cp^*(Cl)(HNSPh_2)U-(\mu_3-OH)(\mu_2-O)_2-U(Cl)(HNSPh_2)_2]_2$ are significantly longer than that in the magnesium complex,[69] 3.437(3) A, and fall in the same range as those in $[Cp_2U]_2[(CH)PPh_2(CH_2)]_2$,[10] 3.82(1) A, in $[Cp_2U]_2[OTiW_5O_{19}]_2^{4-}$,[55] 3.782(2) A, in $U_3(O)(OCMe_3)$,[98] 3.57(3) A and in $U_4O_2(O_2CNEt_2)_4$,[58] 3.702(1) A, 3.777(1) A and 4.021(1) A.

The U-O bond lengths in the complex range between 1.96(1)-2.355(9) A. Among these, the two axial U(2)-O(1) and U(2)-O(3) distances, 1.96(1) A and 1.97(1)

A, are the shortest found among tetravalent uranium complexes. These distances are comparable with the estimated Th-O distance, 1.91 A, for tetravelent thorium in ThO_2.[99,100] For comparison, the U-O distances in $\{Cp^*U[\mu\text{-}CH_2)P(Ph)_2(CH_2)]\}_2Mg[CH_2PMePh_2]_2(\mu_3\text{-}O)(\mu_2\text{-}O)(\mu_2\text{-}Cl)_2$[69] are 2.13(2) A and 2.18(2) A, in $(Cp_3U)_2(\mu\text{-}O)$[70] is 2.035(3) A, and in $U_4O_2(O_2CNEt_2)_4$[58] the U-O distances vary between 2.147(7) A and 2.682(7) A. The extremely short U-O distances along with the near linear O(1)-U(2)-O(3) angle, 175.0(4)°, in $[Cp^*(Cl)(HNSPh_2)U\text{-}(\mu_3\text{-}OH)(\mu_2\text{-}O)_2\text{-}U(Cl)(HNSPh_2)_2]_2$, show a close similarity to those in uranyl complexes.[101-107] For example, the coordination geometry around uranium in $UO_2(CH_2OHCOO)_2$[101] is pentagonal bipyramidal in which the two apical oxygen atoms belong to the uranyl group. The apical U-O distances, 1.740(5) A and 1.754(4) A, are significantly shorter than those in $[Cp^*(Cl)(HNSPh_2)U\text{-}(\mu_3\text{-}OH)\text{-}(\mu_2\text{-}O)_2\text{-}U(Cl)(HNSPh_2)_2]_2$. The O-U-O angle of 177.8(3)° is somewhat similar to that in the sulfilimine complex. In $[UO_2(hfa)_2]_3$,[107] the uranium shows pentagonal bipyramidal geometry with an axial uranyl moiety and resembles the coordination geometry around U(2) in $[Cp^*(Cl)(HNSPh_2)U\text{-}(\mu_3\text{-}OH)(\mu_2\text{-}O)_2\text{-}U(Cl)(HNSPh_2)_2]_2$.

The structure of $[Cp^*(Cl)(HNSPh_2)U-(\mu_3-OH)(\mu_2-O)_2-U(Cl)(HNSPh_2)_2]_2$ resembles that of the mixed valent uranium complex, $(UO_2)_2U_2O_2(OC_6H_5)_{10}(THF)_4$,[57] Figure 78. which also contains a planar tetrauranium unit connected by doubly and triply bridging oxygens. All uranium atoms in this complex show pentagonal bipyramidal geometry and they are interconnected by doubly bridging phenoxide groups and triply bridging oxides. The triply and doubly bridging oxygens in the phenoxide complex lie approximately in the same plane with the four uraniums whereas in the sulfilimine complex the triply bridging oxygens, O(2) and O(2A), occupy positions which are well above and below the U_4 plane. U(1) and U'(1) in this structure are in the +6 oxidation state and contain apical oxides, O(1), O(2) and O'(1), O'(2), respectively, whereas U(2) and U'(2) are in the +5 oxidation state. The apical U-O distances, 1.76(1) A and 1.76(2) A, in the phenoxide complex are significantly shorter than the axial U-O distances, 1.96(1) A and 1.97(1) A, on U(2) in the sulfilimine complex. The average U-O distance for the doubly bridging oxides in $(UO_2)_2U_2O_2(OC_6H_5)_{10}(THF)_4$,[57] 2.42(2) A, is considerably longer than that in the sulfilimine complex, 2.12(1) A. The average U-O-U angle for the doubly bridging oxides in the sulfilimine

complex, 112.5(6)°, is significantly wider than the corresponding U-O-U angle in the phenoxide complex, 105.4(7)°. The U-O distances for the triply bridging oxides in the sulfilimine complex, 2.20(1) A, 2.30(1) A and 2.355(9) A are somewhat longer than the corresponding distances in the phenoxide complex, 2.08(2) A, 2.25(2) A and 2.31(2) A. This is consistent with the μ_3-O being an OH^-. The geometry around each triply bridging oxide in the phenoxide complex is nearly planar whereas that in the sulfilimine complex is pyramidal where the average U-O-U angle is 104.9(3)°. For comparison, the U-O-U angles, are 108(1)° and 104(1)° in $\{Cp^*U[\mu CH_2)P(Ph)_2(CH_2)]\}_2Mg[CH_2PMePh_2](\mu_3\text{-}O)(\mu_2\text{-}O)(\mu_2\text{-}Cl)_2$ and 180° in $(Cp_3U)_2(\mu\text{-}O)$.

In addition to $[Cp^*(Cl)(HNSPh_2)U\text{-}(\mu_3\text{-}OH)(\mu_2\text{-}O)_2\text{-}U(Cl)(HNSPh_2)_2]_2$[85] and $(UO_2)_2U_2O_2(OC_6H_5)_{10}(THF)_4$[57], only very few oxo-uranium clusters are reported. $U_4O_2(O_4CNEt_4)_4$[58] contains two U_3O units joined by a shared triangle edge. $U_3(O)(OCMe_3)_{10}$[98] contains an isolated U_3O unit whereas $[Cp_2U]_2[OTiW_5O_{19}]_2$[55] contains a poly oxo anion coordinated to uranium.

Uranium dioxide has the fluorite structure where each U^{4+} ion is symmetrically surrounded by eight O^{2-} ions with the U-O distance of nearly 2.37 A[108-110] which is

considerably larger than the average U-O distance in $[Cp^*(Cl)(HNSPh_2)U-(\mu_3-OH)(\mu_2-O)_2-U(Cl)(HNSPh_2)_2]_2$, 2.21(1) A. Therefore the structure of the sulfilimine complex is significantly different from that of uranium dioxide. However, it belongs to a commonly observed structural type in inorganic chemistry. The crystal structures of UO_3, $Ca(UO_2)O_2$ and UO_2F_2[111] contain a hexagonal layer of the type shown in Figure 79 which is similar to that in $[Cp^*(Cl)(HNSPh_2)U-(\mu_3-OH)(\mu_2-O)_2-U(Cl)(HNSPh_2)_2]_2$ and $(UO_2)_2U_2O_2(OC_6H_5)_{10}(THF)_4$. In the structure of UO_3, the uranium has two colinear neighbors at 1.9 A and six more distant neighbors with a U-O distance of 2.3 A. All these U-O distances are very similar to those in $[Cp^*(Cl)(HNSPh_2)U-(\mu_3-OH)(\mu_2-O)_2-U(Cl)(HNSPh_2)_2]_2$.

Quite similar layers occur in a number of uranates, CaU_4O, $SrUO_4$, Li_2UO_4, Na_2UO_4 and K_2UO_4.[111] The structures of these complexes could be derived from the fluorite structure. The crystal structure of NH_4CdCl_3, Figure 80, also resembles them and contains $[CdCl_3]^-$ chains which form hexagonal layers of edge-shared octahedra.[112]

Chapter 4

CONCLUSION

There are only a few structurally characterized complexes known to contain the ligand, $[NSPh_2]^-$. In addition to the transition metal complexes, $F_4W(NSPh_2)_2$,[53] $Ph_2S{=}NV(O)Cl_2$[54] and $(Ph_2S{=}NFeCl_2)_2$,[54] the organo uranium sulfilimine complexes described in this study, are the only sulfilimine complexes to be structurally characterized to date.

The sulfilimine complexes described in this study show a wide range of U-N distances. These are listed in Table 52. The complexes, $Cp^*_2UCl_2(HNSPh_2)$, $Cp^*_2UCl(OH)(HNSPh_2)$ and $[Cp^*(Cl)(HNSPh_2)U\text{-}(\mu_3\text{-}OH)(\mu_2\text{-}O)_2\text{-}U(Cl)(HNSPh_2)_2]_2$, contain neutral sulfilimine ligands and their U-N distances range between 2.41(2) A-2.57(1) A. Except for those in $[Cp^*(Cl)(HNSPh_2)U\text{-}(\mu_3\text{-}OH)(\mu_2\text{-}O)_2\text{-}U(Cl)(HNSPh_2)_2]_2$, all other U-N distances given in Table 52 are among the shortest found for organo uranium complexes of neutral nitrogen donor ligands. For comparison, the U-N distance in $Cp^*_2UCl_2(Pz)$ is 2.607(8) A,[91]. The U-N distances are 2.61(2) A and 2.58(2) A in $Cp_3U(NCMe)_2^+$,[50] and 2.68(2) A for the U-(NCMe) distance in $Cp_3U(NCS)(NCMe)$.

$Cp^*_2UCl(NSPh_2)$ contains the shortest U-N distance that has been found among Cp^*_2U complexes while $Cp^*_2U(NSPh_2)_2$ is the only structurally characterized organo actinide bis-imide complex known to date.

It has been shown that the metal-nitrogen triple bond is approximately 0.41 A longer than the appropriate Pauling metallic radius.[113] While the metallic radius of tetravalent uranium has not been tabulated by Pauling,[114] 1.60 A can be estimated by subtracting the difference in ionic radii between U(IV) and Th(IV), 0.05 A, from the metallic radius of thorium, 1.65 A. Subtraction of 1.60 A from the U-N bond length of each complex would give information about nature of the U-N bond. The metal-nitrogen bond distances in structurally characterized sulfilimide complexes are summarized in Table 52. The differences in the M-N bond length and the Pauling radius of the corresponding metal vary between 0.50 A and 0.89 A and indicate that none of the complexes listed in Table 52, contain M-N triple bonds. The 0.50 A difference in $Cp^*_2UCl(NSPh_2)$, $F_4W(NSPh_2)_2$ and $Cl_2VO(NSPh_2)$ is consistent with a bond order of 2.3[113] which is the highest among those listed in Table 52. The 0.80-0.89 A differences in $Cp^*_2UCl_2(HNSPh_2)$, $Cp^*_2UCl(OH)(HNSPh_2)$, $[Cp^*(Cl)(HNSPh_2)U-(\mu_3-OH)(\mu_2-O)_2-U(Cl)(HNSPh_2)_2]_2$ and

$Cp^*_2UCl_2(HNPPh_3)$ indicate that they do not show any multiple bonding.

The relative orientation of Cp^* groups in the Cp^*_2U complexes are of interest. Those in $Cp^*_2UCl_2(HNSPh_2)$ and $Cp^*_2UCl(OH)(HNSPh_2)$, Figures 69 and 70 respectively, show eclipsed configuration, presumably because of the Cl-U-Cl and Cl-U-O angles, 145.9(3)° and 147.4(3)° and the crowding which may occur between Cl and Cp^* methyl groups. A similar situation is observed in $Cp^*_2UCl_2(HNPPh_3)$. The Cp^* groups in $Cp^*_2UCl(NSPh_2)$ are somewhat staggered whereas those in $Cp^*_2U(NSPh_2)_2$ are almost perfectly staggered. Thus, the staggered orientation of the rings appears to be preferred when the equatorial plane has small steric crowding in Cp^*_2U complexes.

The C-Me(Cp^*) distances in the Cp^* groups of all the sulfilimine complexes described in this study are very similar and range from 1.46(2) A in $Cp^*_2UCl(OH)(HNSPh_2)$ to 1.69(6) A in $Cp^*_2UCl(NSPh_2)$. There is one close contact between methyl groups on opposite Cp^* groups at the apex of the Cp^*-U-Cp^* angle which is less than 3.6 A, the sum of the Van der Waals radii for two carbon atoms (1.80 A +1.80 A), in $Cp^*_2UCl_2(HNSPh_2)$, $Cp^*_2UCl(OH)(HNSPh_2)$, $Cp^*_2UCl(NSPh_2)$ and $Cp^*_2U(NSPh_2)_2$. These distances are

listed in Table 54. Consequently, the Cp^* methyl groups bend away from the C_5 plane and away from the metal center. Thus, the Cp^* groups in these complexes adopt a dish like shape. All off-plane displacements for the Cp^* methyl groups in these complexes are listed in Tables 55-58. For example, in $Cp^*_2UCl_2(HNSPh_2)$, the greatest off-plane displacement is by C(12M), 0.34 A, presumably because of 3.10 A nonbonded contact with C(21M). Similar situations are observed in $Cp^*_2UCl(NSPh_2)$ and $Cp^*_2U(NSPh_2)_2$.

Hydrolysis of organo transition metal halides has been an effective way of synthesizing organo transition metal oxo-cluster complexes.[115-118] In contrast to the large number of organo transition metal oxides only a few hydroxy complexes have been reported. The niobium complex, $[Cp^*_3Nb_3(OH)_2(\mu_2\text{-}OH)(\mu_3\text{-}OH)(\mu_2\text{-}O)_2(\mu_3\text{-}O)Cl]Cl$[119] and the zirconium complex, $[Cp^*ZrCl]_3(\mu_3\text{-}O)(\mu_3\text{-}OH)(\mu\text{-}OH)_3.2(THF)$[120] are oxo-bridged trimetallic clusters that are structurally very similar to that of $[Cp^*(Cl)(HNSPh_2)U\text{-}(\mu_3\text{-}OH)(\mu_2\text{-}O)_2\text{-}U(Cl)(HNSPh_2)_2]_2$. $Cp^*_2UCl(OH)(HNSPh_2)$ and $[Cp^*(Cl)(HNSPh_2)U\text{-}(\mu_3\text{-}OH)(\mu_2\text{-}O)_2\text{-}U(Cl)(HNSPh_2)_2]_2$ are the first organoactinide hydroxy complexes to be characterized. The reproducibility and the convenience of their synthesis provides a new method

for the synthesis of oxide and hydroxide complexes of f-block elements.

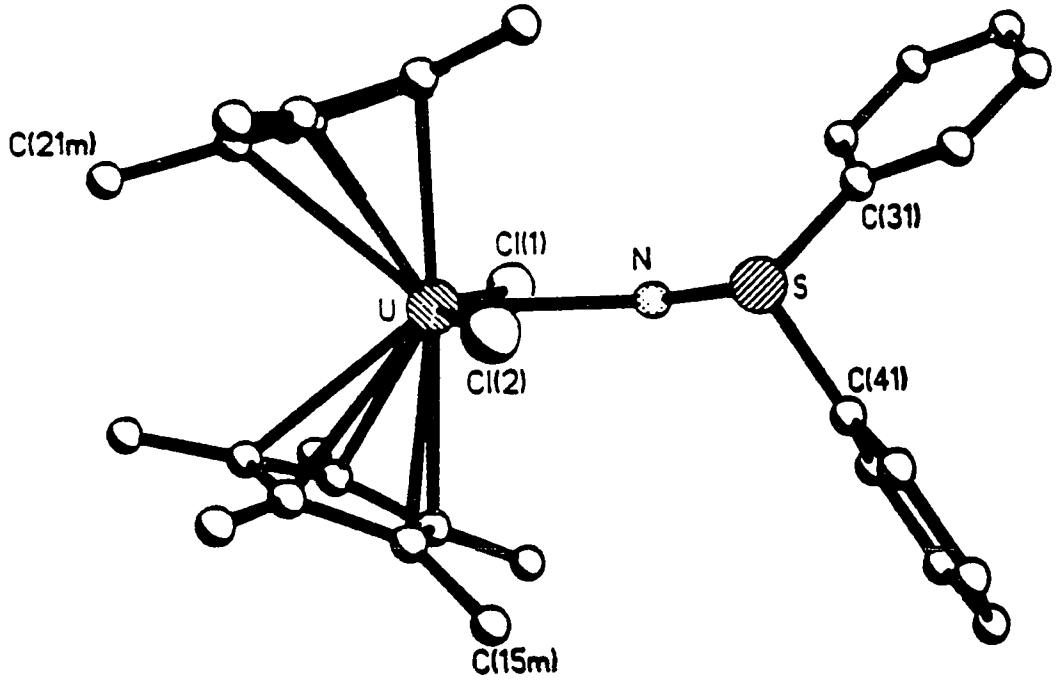

Figure 57: Perspective View of $Cp^*_2UCl_2(HNSPh_2)$

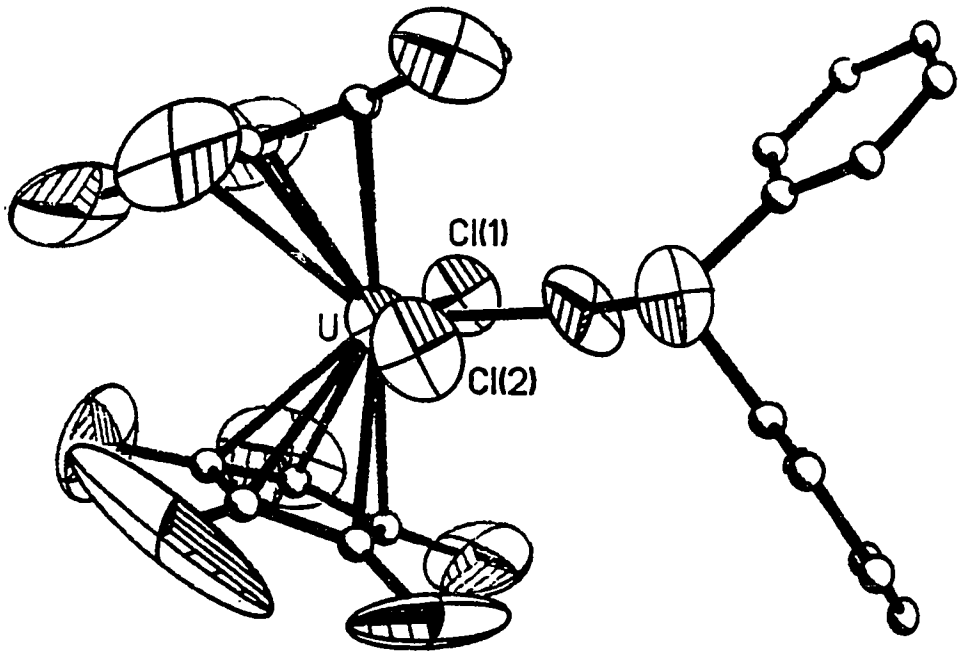

Figure 58: Perspective View of $Cp^*_2UCl_2(HNSPh_2)$ with the Thermal Ellipsoids

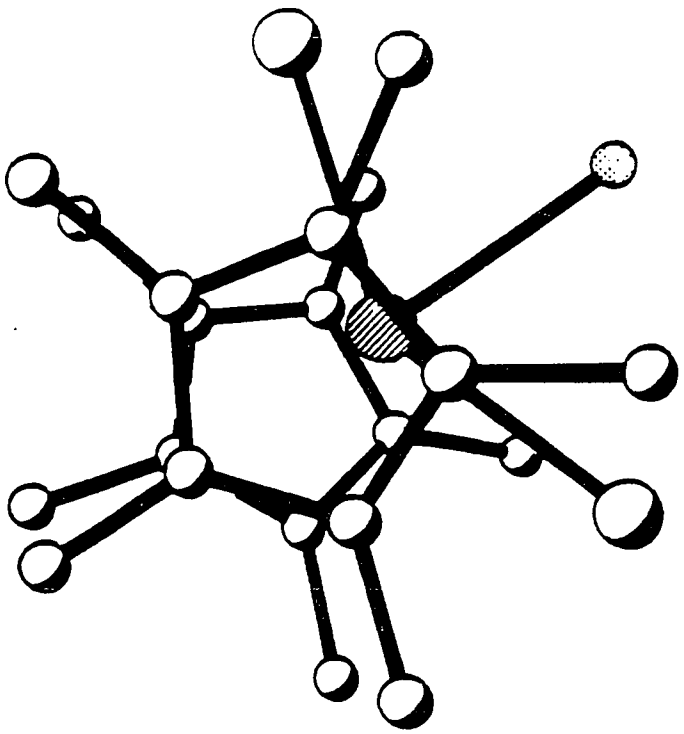

Figure 59: Eclipsed Configuration of the Cp^* Groups of $Cp^*_2UCl_2(HNSPh_2)$

TABLE 16

Summary of Crystal Data for $Cp^*_2UCl_2(HNSPh_2)$

Formula	$C_{32}H_{41}Cl_2NSU$
Formula Weight	739.3
crystal dimensions	0.2 x 0.8 x 0.4
crystal system	monoclinic
space group	C2/c
a,°A	23.83(3)
b,°A	9.92(1)
c,°A	27.29(3)
β,°A	94.36(4)
V,°A^3	6430(12)
z	8
crystal shape	rectangular plate
crystal color	reddish orange
D(cacd), Mg/M^3	1.504
abs. coeff.(μ),mm^{-1}	5.037
abs. corr. factor range	0.813 - 0.354
radiation (Mo, K^α), °A	0.71073
scan rate,°	4.0 to 35.0
total observations	2620
unique observations	1955
unique data with F > 6.0σ (F)	1310
no. of parameters	214
over determination ratio	6.12
R	0.0655
R_g	0.0800

$$R = \Sigma (|F_o - F_c|) / \Sigma (F)_o$$

$$R_g = [\Sigma (|F_o - F_c|^2) / \Sigma (F_o^2)]^{1/2}$$

TABLE 17

Bond Distances and Angles for $Cp^*_2UCl_2(HNSPh_2)$

Bond Distance, (°A)		Bond Angle, (°)	
U-Cl(1)	2.693(8)	Cl(2)-U-Cl(1)	145.9(3)
U-Cl(2)	2.648(8)	N-U-Cl(1)	71.3(6)
U-N	2.44(3)	N-U-Cl(2)	74.7(6)
N-S	1.55(2)	U-N-S	134(1)
S-C(31)	1.79(2)	N-S-C(31)	108.1(7)
S-C(41)	1.78(2)	N-S-C(41)	108.3(7)
U-C(11)	2.75(2)	C(31)-S-C(41)	98(1)
U-C(12)	2.80(2)	Cp(1)-U-Cp(2)[a]	130.7
U-C(13)	2.79(2)	Cp(2)-U-N	113.0
U-C(14)	2.74(2)	Cp(1)-U-Cl(1)	96.4
U-C(15)	2.71(2)	Cp(1)-U-Cl(2)	96.5
U-C(21)	2.89(2)	Cp(2)-U-Cl(1)	98.3
U-C(22)	2.80(2)	Cp(1)-U-N	116.3
U-C(23)	2.69(2)		
U-C(24)	2.72(2)		
U-C(25)	2.84(2)		
U-Cp(1)[a]	2.52		
U-Cp(2)	2.48		

[a]Cp(1) and Cp(2) represent the centroids of the C(11)-C(15) and the C(21)-C(25) rings, respectively.

TABLE 18

Positional Parameters of Anisotropically Refined Atoms for $Cp^*_2UCl_2(HNSPh_2)$

atom	x	y	z
U	0.1025(1)	0.3163(1)	0.1165(1)
N	0.004(1)	0.384(3)	0.1148(9)
S	-0.0385(4)	0.401(1)	0.1548(3)
Cl(1)	0.0590(4)	0.318(1)	0.0225(3)
Cl(2)	0.0841(4)	0.367(1)	0.2091(3)
C(11M)	0.2226(8)	0.474(2)	0.1969(6)
C(12M)	0.2621(8)	0.352(2)	0.0888(6)
C(13M)	0.1824(8)	0.446(2)	0.0118(6)
C(14M)	0.0958(8)	0.646(2)	0.0542(6)
C(15M)	0.1234(8)	0.670(2)	0.1663(6)
C(21M)	0.2296(6)	0.066(2)	0.1232(7)
C(22M)	0.1420(6)	0.040(2)	0.0309(7)
C(23M)	0.0168(6)	0.018(2)	0.0745(7)
C(24M)	0.0278(6)	0.058(2)	0.1835(7)
C(25M)	0.1601(6)	0.076(2)	0.2190(7)

TABLE 19

Thermal Parameters of Anisotropically Refined Atoms
for $Cp^*_2UCl_2(HNSPh_2)$

atom	U(11)	U(22)	U(33)	U(23)	U(13)	U(12)
U	0.059(1)	0.070(1)	0.050(1)	-0.002(1)	0.005(1)	0.003(1)
N	0.07(2)	0.15(3)	0.09(2)	-0.03(2)	0.07(2)	-0.03(2)
S	0.079(8)	0.14(1)	0.059(5)	0.009(6)	0.010(5)	0.011(7)
Cl(1)	0.095(7)	0.119(8)	0.053(5)	-0.004(6)	0.003(4)	-0.007(8)
Cl(2)	0.099(8)	0.15(1)	0.048(5)	-0.016(5)	0.006(5)	-0.007(7)
C(11M)	0.37(9)	0.6(1)	0.21(5)	0.29(7)	-0.27(6)	-0.41(9)
C(12M)	0.11(4)	0.18(6)	0.33(7)	0.06(5)	0.12(4)	0.07(4)
C(13M)	0.23(6)	0.23(6)	0.15(4)	-0.05(4)	0.15(4)	-0.07(5)
C(14M)	0.20(5)	0.08(4)	0.17(4)	0.08(3)	-0.02(4)	-0.01(3)
C(15M)	0.33(7)	0.07(3)	0.15(4)	-0.07(3)	0.14(4)	-0.08(4)
C(21M)	0.17(6)	0.07(5)	0.8(2)	-0.08(7)	0.22(8)	0.03(4)
C(22M)	0.25(6)	0.13(4)	0.12(3)	0.02(3)	0.13(4)	0.03(4)
C(23M)	0.11(3)	0.07(3)	0.15(3)	-0.01(3)	-0.04(3)	-0.07(3)
C(24M)	0.15(4)	0.14(4)	0.07(2)	-0.01(3)	0.04(2)	-0.04(4)
C(25M)	0.26(5)	0.13(4)	0.09(3)	0.04(3)	-0.13(3)	0.01(4)

TABLE 20

Positional and Thermal Parameters of Isotropically Refined Atoms for $Cp^*_2UCl_2(HNSPh_2)$

Atom	x	y	z	U
C(11)	0.1929(8)	0.475(2)	0.1481(6)	0.12(1)
C(12)	0.2095(8)	0.421(2)	0.1032(6)	0.11(1)
C(13)	0.1738(8)	0.476(2)	0.0643(6)	0.11(1)
C(14)	0.1353(8)	0.565(2)	0.0852(6)	0.09(1)
C(15)	0.1471(8)	0.564(2)	0.1370(6)	0.10(1)
C(21)	0.1670(6)	0.070(2)	0.1279(7)	0.14(2)
C(22)	0.1304(6)	0.059(2)	0.0846(7)	0.09(1)
C(23)	0.0742(6)	0.057(2)	0.0986(7)	0.10(1)
C(24)	0.0761(6)	0.068(2)	0.1506(7)	0.07(1)
C(25)	0.1334(6)	0.076(2)	0.1687(7)	0.12(1)
C(31)	-0.1036(8)	0.325(2)	0.1325(9)	0.067(9)
C(32)	-0.1127(8)	0.268(2)	0.0859(9)	0.12(2)
C(33)	-0.1644(8)	0.208(2)	0.0717(9)	0.14(2)
C(34)	-0.2070(8)	0.206(2)	0.1041(9)	0.11(1)
C(35)	-0.1979(8)	0.263(2)	0.1507(9)	0.11(1)
C(36)	-0.1461(8)	0.323(2)	0.1649(9)	0.11(1)
C(41)	-0.0612(9)	0.572(2)	0.1521(9)	0.07(1)
C(42)	-0.0663(9)	0.632(2)	0.1977(9)	0.09(1)
C(43)	-0.0839(9)	0.765(2)	0.2004(9)	0.12(1)
C(44)	-0.0964(9)	0.839(2)	0.1573(9)	0.11(1)
C(45)	-0.0912(9)	0.779(2)	0.1117(9)	0.09(1)
C(46)	-0.0736(9)	0.645(2)	0.1091(9)	0.08(1)

TABLE 21

Selected Intramolecular Non-Bonded Distances (°A)
for $Cp^*_2UCl_2(HNSPh_2)$

Atom	Atom	Distance	Atom	Atom	Distance
Cl(1)	-N	3.001	Cl(2)	-C(15)	3.221
Cl(1)	-C(45)	3.919	Cl(2)	-C(15M)	3.380
Cl(1)	-C(46)	3.651	Cl(2)	-C(11M)	3.508
Cl(1)	-C(13)	3.283	Cl(2)	-C(24)	3.369
Cl(1)	-C(14)	3.425	Cl(2)	-C(25)	3.336
Cl(1)	-C(13M)	3.234	Cl(2)	-C(24M)	3.393
Cl(1)	-C(14M)	3.459	Cl(2)	-C(25M)	3.403
Cl(1)	-C(22)	3.460	C(13M)	-Cl(1)	3.722
Cl(1)	-C(23)	3.325	C(11M)	-C(34)	3.891
Cl(1)	-C(22M)	3.390	C(11M)	-C(35)	3.707
Cl(1)	-C(23M)	3.480	C(11M)	-C(14)	3.670
Cl(2)	-N	3.093	C(12M)	-C(14)	3.680
Cl(2)	-C36	3.665	C(12M)	-C(44)	3.680
Cl(2)	-C(42)	3.699	C(14M)	-C(12)	3.685
Cl(2)	-C(11)	3.361	C(24M)	-C(21)	3.754

TABLE 22

Comparison of Bond Lengths, (°A), of $Cp^*_2UCl_2(HNSPh_2)$ and $Cp^*_2UCl_2(HNPPh_3)$ and $Cp^*_2UCl(OH)(HNSPh_2)$

Bond	$Cp^*_2UCl_2(HNSPh_2)$	$Cp^*_2UCl_2(HNPPh_3)$	$Cp^*_2UCl(OH)(HNSPh_2)$ (mole. 1)	(mole. 2)
U-N	2.44(3)	2.43(1)	2.41(2)	2.51(2)
U-Cl(1)	2.693(8)	2.730(4)	2.742(5)	2.759(5)
U-Cl(2)(O)	2.648(8)	2.658(4)	2.10(1)[a]	2.11(1)[b]
U-C(11)	2.75(2)	2.79(1)	2.79(1)[c]	2.733(9)[d]
U-C(12)	2.80(2)	2.81(1)	2.80(1)[c]	2.76(1)[d]
U-C(13)	2.79(2)	2.78(1)	2.774(9)[c]	2.82(1)[d]
U-C(14)	2.74(2)	2.75(1)	2.76(1)[c]	2.834(9)[d]
U-C(15)	2.71(2)	2.75(1)	2.77(1)[c]	2.780(9)[d]
U-C(21)	2.89(2)	2.75(1)	2.815(9)[e]	2.83(1)[f]
U-C(22)	2.80(2)	2.79(1)	2.78(1)[e]	2.77(1)[f]
U-C(23)	2.69(2)	2.80(1)	2.73(1)[e]	2.73(1)[f]
U-C(24)	2.72(2)	2.77(1)	2.73(1)[e]	2.76(1)[f]
U-C(25)	2.84(2)	2.74(1)	2.785(9)[e]	2.82(1)[f]
U-Cp(1)	2.52	2.50	2.50	2.49
U-Cp(2)	2.48	2.49	2.51	2.51

a) U(1)-O(1) distance in molecule one
b) U(2)-O(2) distance in molecule two
c) U-C distances for the (C11-C15) Cp ring in molecule 1
d) U-C distances for the (C31-C35) Cp ring in molecule 2
e) U-C distances for the (C21-C25) Cp ring in molecule 1
f) U-C distances for the (C41-C45) Cp ring in molecule 2

TABLE 23

Comparison of Bond Angles, (°) of $Cp^*_2UCl_2(HNSPh_2)$ $Cp^*_2UCl_2(HNPPh_3)$ and $Cp^*_2UCl(OH)(HNSPh_2)$

Angle	$Cp^*_2UCl_2(HNSPh_2)$	$Cp^*_2UCl_2(HNPPh_3)$	$Cp^*_2UCl(OH)(NSPh_2)$ (Mole. 1)	(Mole. 2)
Cl-U-Cl(O)	145.9(3)	151.0(1)	147.4(3)	146.9(3)
N-U-Cl(O)	71.3(6)	72.5(3)	76.4(4)	76.0(5)
N-U-Cl	74.7(6)	78.5(3)	71.0(3)	70.9(4)
U-N-S(P)	134(1)	155.8(6)	130.4(8)	127.5(9)
Cp(1)-U-Cp(2)	130.7	134.3	135.5	136.3
Cp(1)-U-Cl	96.4	98	96.5	95.5
Cp(1)-U-Cl(O)	96.5	91	97.1	96.8
Cp(2)-U-Cl	98.3	97	94.1	95.3
Cp(2)-U-Cl(O)	96.8	96	96.7	96.8
Cp(1)-U-N	116.3	115	112.3	113.7
Cp(2)-U-N	113	110	111.9	109.9

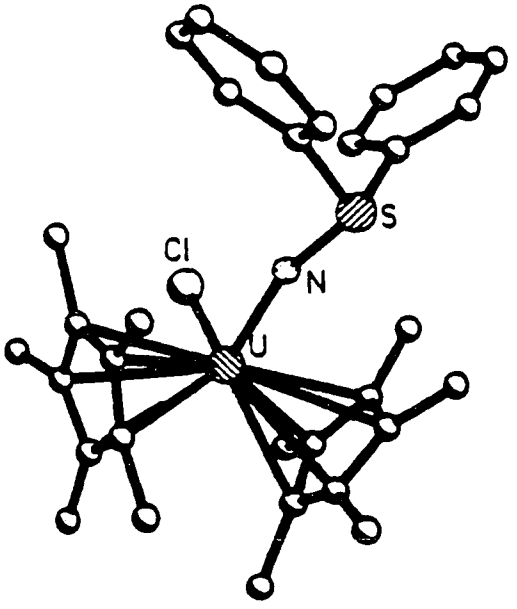

Figure 60: Perspective View of $Cp^*_2UCl(NSPh_2)$

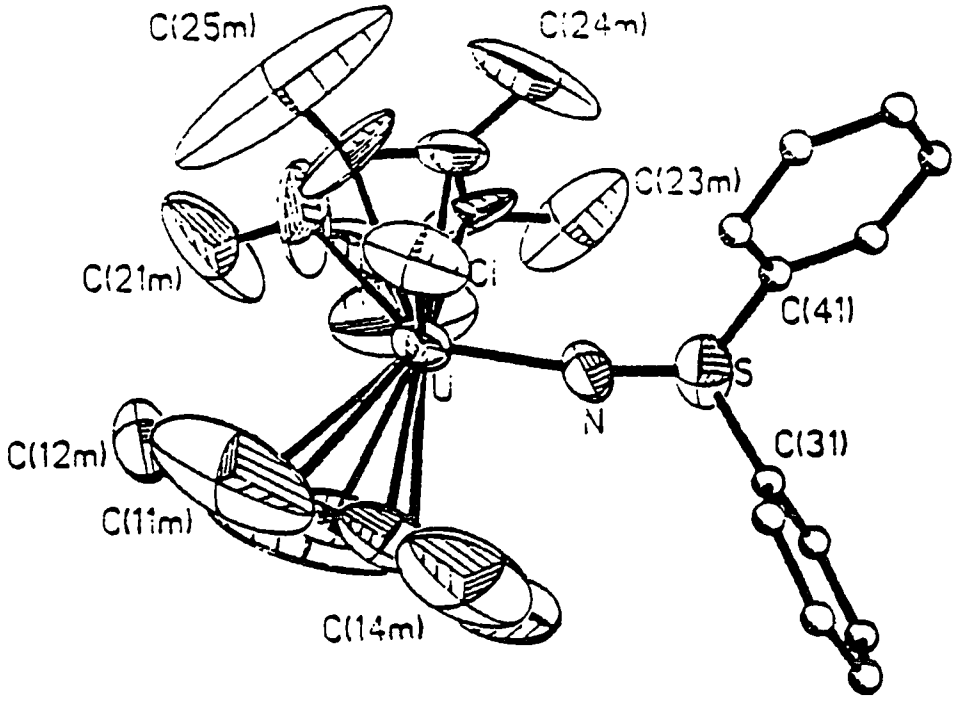

Figure 61: Perspective View of $Cp^*_2UCl(NSPh_2)$ with Thermal Ellipsoids

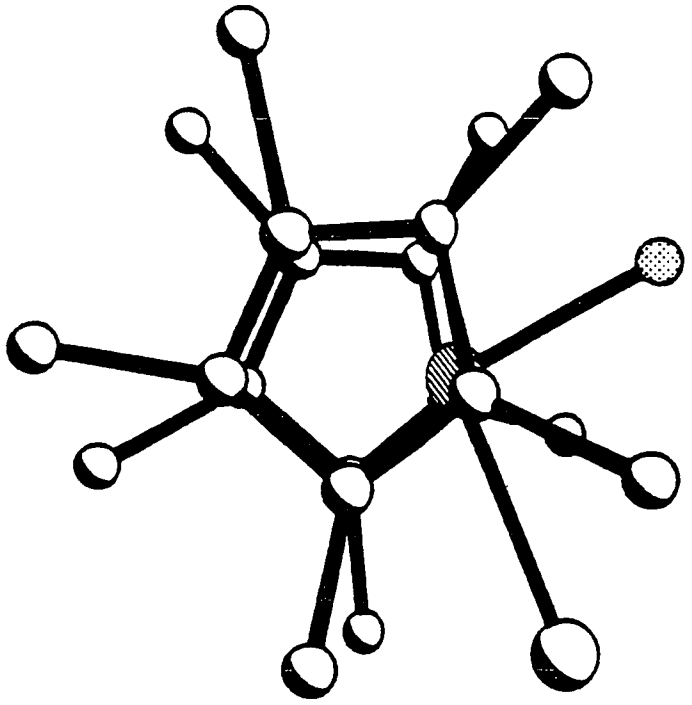

Figure 62: Configuration of the Cp^* groups of $Cp^*_2UCl(NSPh_2)$

TABLE 24

Summary of Crystal Data for $Cp^*_2UCl(NSPh_2).1/2\ C_5H_{12}$

Formula	$C_{34.5}H_{46}ClNSU$
Formula Weight	780.3
crystal dimensions,mm	0.5 x 0.1 x 1.0
crystal system	monoclinic
space group	P2 1/n
a,°A	12.120(5)
b,°A	13.249(6)
c,°A	21.644(8)
β,°	95.57(3)
V,°A^3	3445(2)
Z	4
crystal shape	rectangular prsims
cryst color	reddish black
D(calcd),Mg/M^3	1.504
abs coeff(μ),mm^{-1}	4.625
abs corr factor range	0.106-0.058
radiatn (Mo K_α),°A	0.71073
scan rate,°/min	1.5 - 15.0
scan type	omega
2-theta range,°	4.0 to 40.0
total observations	3673
unique observations	3149
unique data with F > 2.0σ(F)	2530
no. of parameters	267
over determination ratio	9.5
R	0.0655
R_G	0.0800

$$R = \Sigma(|F_o - F_c|)/\Sigma(F_o)$$

$$R_g = [\Sigma(|F_o - F_c|^2)/\Sigma(F_o^2)]^{1/2}$$

TABLE 25

Bond Distances and Angles for $Cp^*_2UCl(NSPh_2)$

Bond distance, (°)A		Bond Angle, (°)	
U-Cl	2.609(6)	Cl-U-N	96.4(4)
U-N	2.10(1)	U-N-S	164.4(9)
N-S	1.55(1)	N-S-C(31)	108.1(7)
S-C(31)	1.77(1)	N-S-C(41)	108.3(8)
S-C(41)	1.78(1)	C(31)-S-C(41)	98.7(6)
U-C(11)	2.76(3)	Cp(1)-U-N	107.0[a]
U-C(12)	2.75(4)	Cp(1)-U-Cl	103.7
U-C(13)	2.71(3)	Cp(2)-U-Cl	103.9[a]
U-C(14)	2.73(2)	Cp(2)-U-N	106.6
U-C(15)	2.71(3)	Cp(1)-U-Cp(2)	133.2[a]
U-C(21)	2.77(5)		
U-C(22)	2.71(3)		
U-C(23)	2.73(3)		
U-C(24)	2.70(2)		
U-C(25)	2.73(3)		
U-Cp(1)[a]	2.48		
U-Cp(2)[a]	2.48		

[a]Cp(1) and Cp(2) represent the centroids of the C(11)-C(15) and the C(21)-C(25) rings, respectively.

TABLE 26

Positional Parameters of the Anisotropically Refined Atoms for $Cp^*_2UCl(NSPh_2)$

atom	x	y	z
U	0.0065(1)	0.0072(1)	0.2193(1)
N	-0.140(1)	-0.045(1)	0.1664(7)
S	-0.2632(4)	-0.0731(4)	0.1430(2)
Cl	0.0503(5)	0.1473(3)	0.1414(3)
C(11)	0.210(2)	-0.60(2)	0.192(2)
C(12)	0.205(3)	-0.90(3)	0.254(2)
C(13)	0.127(3)	-0.161(2)	0.2537(2)
C(14)	0.083(2)	-0.181(2)	0.196(2)
C(15)	0.133(3)	-0.118(2)	0.158(1)
C(11M)	0.281(3)	0.007(2)	0.154(3)
C(12M)	0.298(3)	-0.037(4)	0.298(4)
C(13M)	0.123(5)	-0.216(4)	0.317(2)
C(14M)	0.000(2)	-0.265(2)	0.181(3)
C(15M)	0.105(3)	-0.125(3)	0.088(1)
C(21)	0.036(3)	0.098(5)	0.336(2)
C(22)	-0.042(4)	0.034(3)	0.337(1)
C(23)	-0.136(2)	0.062(2)	0.301(1)
C(24)	-0.110(2)	0.149(2)	0.2727(9)
C(25)	-0.004(3)	0.172(2)	0.294(1)
C(21M)	0.119(3)	0.065(4)	0.392(2)
C(22M)	-0.085(4)	-0.069(3)	0.373(2)
C(23M)	-0.259(3)	0.023(3)	0.288(2)
C(24M)	-0.186(3)	0.222(3)	0.227(1)
C(25M)	0.060(6)	0.262(4)	0.289(3)
C(50)	1.000	0.500	0.000
C(51)	0.93(1)	0.44(1)	-0.003(8)
C(52)	0.921(7)	0.419(6)	0.071(4)

TABLE 27

Thermal Parameters of the Anistropically Refined Atoms for $Cp^*_2UCl(NSPh_2)$

atom	U(11)	U(22)	U(33)	U(12)	U(13)	U(23)
U	0.046(1)	0.051(1)	0.063(1)	0.008(1)	0.014(1)	-0.001(1)
N	0.047(9)	0.076(9)	0.06(1)	0.015(8)	-0.005(7)	-0.006(8)
S	0.054(3)	0.109(4)	0.058(3)	0.000(3)	0.016(3)	-0.010(3)
Cl	0.109(5)	0.083(3)	0.122(5)	0.024(3)	0.066(4)	0.035(3)
C(11)	0.02(1)	0.04(1)	0.29(5)	0.02(1)	0.05(2)	0.03(2)
C(12)	0.12(3)	0.11(3)	0.18(3)	0.09(2)	-0.05(3)	-0.04(3)
C(13)	0.16(3)	0.09(2)	0.09(2)	0.07(2)	0.04(2)	0.03(2)
C(14)	0.07(1)	0.06(1)	0.14(2)	0.02(1)	0.02(2)	-0.03(2)
C(15)	0.10(2)	0.12(2)	0.08(2)	0.05(2)	0.06(2)	0.02(2)
C(11M)	0.17(4)	0.17(3)	0.6(1)	0.04(2)	0.25(5)	0.13(4)
C(12M)	0.10(3)	0.42(7)	0.8(1)	0.12(4)	-0.18(5)	-0.49(9)
C(13M)	0.7(1)	0.32(5)	0.18(4)	0.36(7)	0.24(6)	0.15(4)
C(14M)	0.104(2)	0.05(2)	0.67(8)	-0.3(2)	0.06(3)	-0.10(3)
C(15M)	0.23(4)	0.31(5)	0.10(2)	0.16(4)	0.04(2)	-0.03(3)
C(21)	0.08(2)	0.38(8)	0.10(3)	0.03(3)	-0.04(2)	-0.13(4)
C(22)	0.26(5)	0.18(3)	0.04(2)	0.17(4)	-0.00(2)	0.01(2)
C(23)	0.14(2)	0.06(1)	0.13(2)	-0.04(2)	0.11(2)	-0.07(2)
C(24)	0.09(2)	0.05(1)	0.08(1)	0.03(1)	0.01(1)	-0.02(1)
C(25)	0.16(3)	0.11(2)	0.12(2)	-0.12(2)	0.09(2)	-0.07(2)
C(21M)	0.23(4)	0.49(7)	0.18(4)	0.26(5)	-0.13(3)	-0.18(5)
C(22M)	0.40(7)	0.16(3)	0.17(4)	0.02(4)	0.17(4)	-0.00(3)
C(23M)	0.15(3)	0.26(4)	0.29(5)	-0.12(3)	0.17(3)	-0.19(4)
C(24M)	0.31(4)	0.25(4)	0.12(2)	0.24(4)	0.00(3)	-0.02(2)
C(25M)	0.8(1)	0.35(6)	0.46(7)	-0.44(7)	0.55(8)	-0.33(6)
C(50)	0.13(6)	0.2(1)	1.0(5)	0.02(6)	-0.1(2)	-0.2(2)
C(51)	0.4(2)	0.4(1)	0.5(2)	0.2(1)	-0.3(1)	-0.3(1)
C(52)	0.23(6)	0.23(5)	0.30(7)	0.04(4)	0.05(5)	0.02(5)

TABLE 28

Positional and Thermal Parameters of Isotropically Refined Atoms for $Cp^*_2UCl(NSPh_2)$

Atom	x	y	z	U
C(31)	-0.263(1)	-0.1620(8)	0.0819(5)	0.0064(5)
C(32)	-0.318(1)	-0.2536(8)	0.0882(5)	0.0077(5)
C(33)	-0.314(1)	-0.3291(8)	0.0436(5)	0.0091(6)
C(34)	-0.256(1)	-0.3131(8)	-0.0071(5)	0.0087(6)
C(35)	-0.202(1)	-0.2215(8)	-0.0134(5)	0.0083(6)
C(36)	-0.206(1)	-0.1460(8)	0.0311(5)	0.0068(5)
C(41)	-0.326(1)	0.0302(9)	0.0987(6)	0.0093(6)
C(42)	-0.261(1)	0.1054(9)	0.0764(6)	0.0093(6)
C(43)	-0.312(1)	0.1859(9)	0.0421(6)	0.0126(9)
C(44)	-0.428(1)	0.1913(9)	0.0301(6)	0.0132(9)
C(45)	-0.493(1)	0.1161(9)	0.0525(6)	0.0133(9)
C(46)	-0.442(1)	0.0356(9)	0.0868(6)	0.0119(8)

TABLE 29

Selected Intramolecular Non-Bonded Distances
for $Cp^*_2UCl(NSPh_2)$

Atom	Atom	Distance	Atom	Atom	Distance
Cl	-N	3.528	C(11M)	-C(13)	3.765
Cl	-C(11)	3.458	C(15M)	-N	3.758
Cl	-C(15)	3.656	C(15M)	-C(13)	3.582
Cl	-C(11M)	3.341	C(14M)	-N	3.373
Cl	-C(15M)	3.872	C(13)	-N	3.849
Cl	-C(35)	3.656	C(14)	-N	3.246
Cl	-C(42)	3.890	C(15)	-N	3.474
Cl	-C(24)	3.647	C(32)	-N	3.765
Cl	-C(25)	3.469	C(36)	-N	3.222
C(11M)	-Cl	3.341	C(15M)	-C(12)	3.667
C(11M)	-C(14)	3.655			

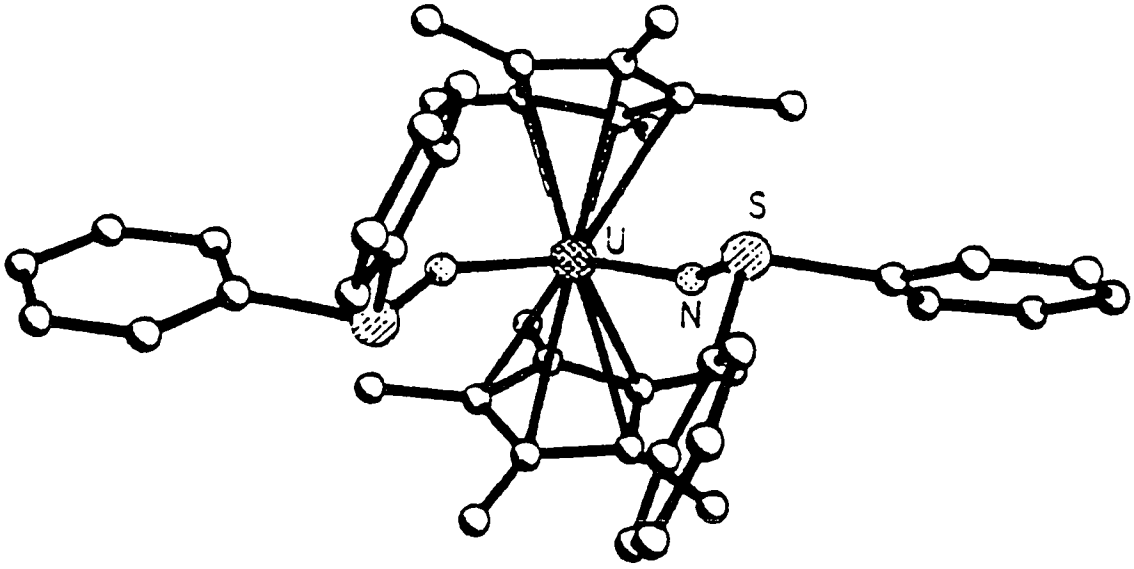

Figure 63: Perspective View of $Cp^*_2U(NSPh_2)$

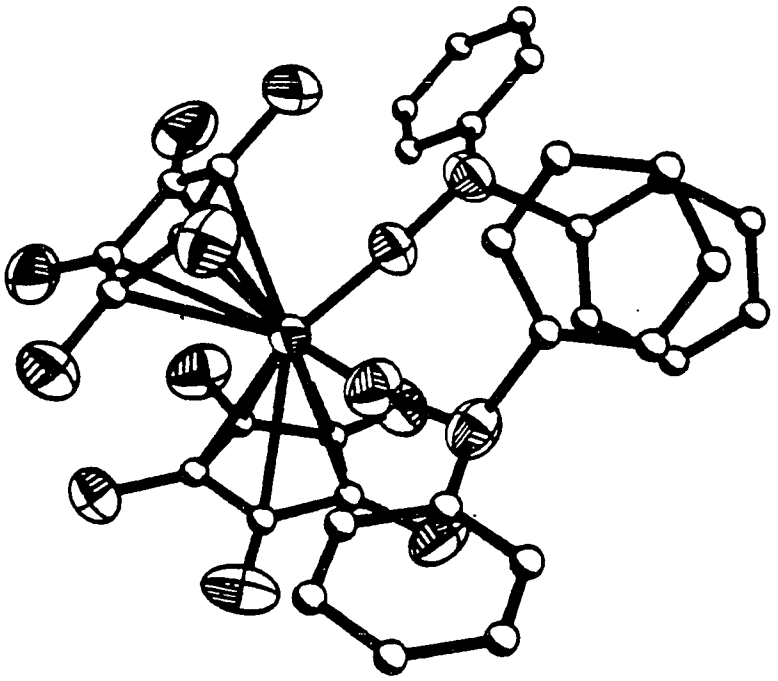

Figure 64: Perspective View of $Cp^*_2U(NSPh_2)$ with Thermal Ellipsoids

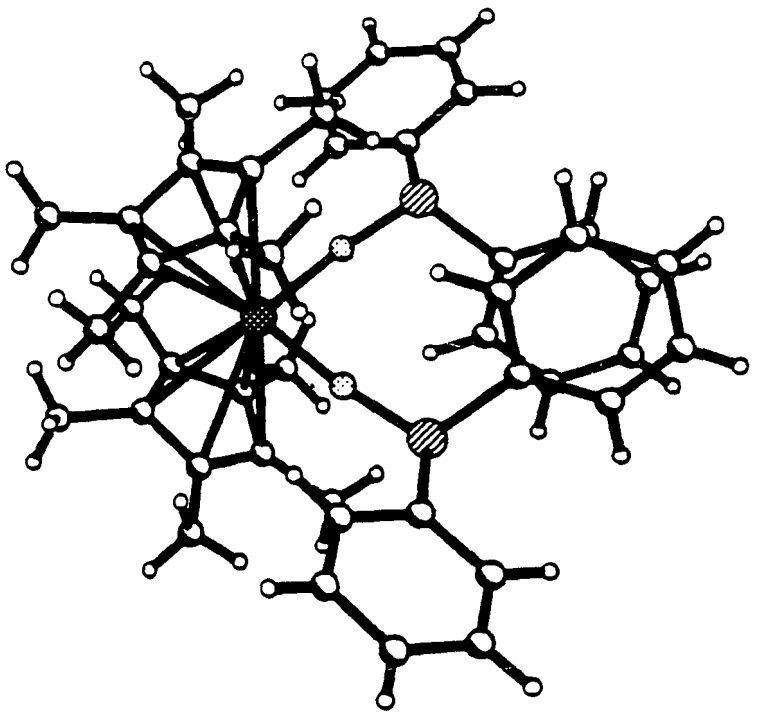

Figure 65: Perspective View of $Cp^*_2(NSPh_2)_2$ with the Hydrogen Atoms

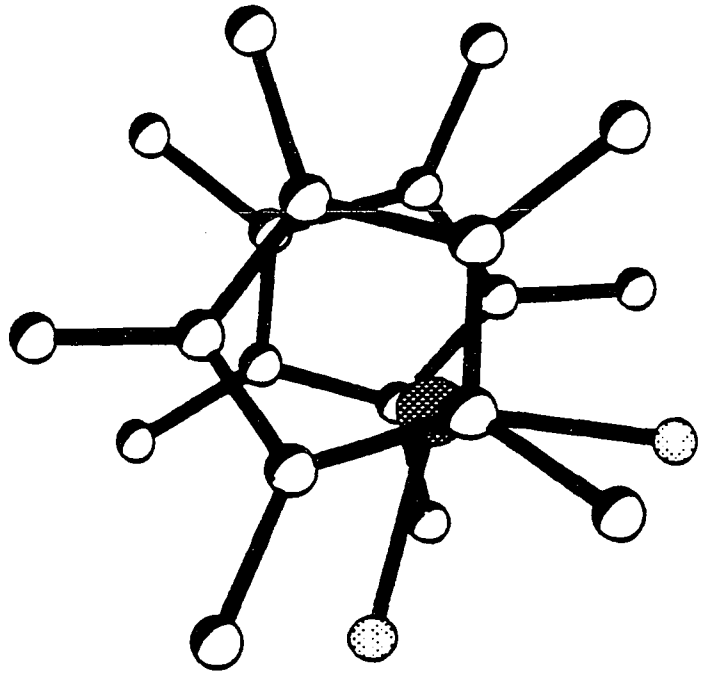

Figure 66: Staggared Configuration of the Cp^* Groups of $Cp^*_2U(NSPh_2)_2$

TABLE 30

Summary of Crystal Data for $Cp^*_2U(NSPh_2)_2$

Formula	$C_{44}H_{50}N_2S_2U$
Formula Weight	909.0
crystal dimensions, mm	1.3 x 0.5 x 0.5
crystal system	monoclinic
space group	c2/c
a, °A	15.70(1)
b, °A	13.00(1)
c, °A	19.13(1)
β, °	92.98(6)
V, °A^3	3898(5)
Z	4
crystal shape	dark red blocks
crystal color	reddish orange
D(calcd), Mg/M^3	1.549
abs. coeff.(μ), mm^{-1}	4.083
abs. corr. factor range	0.049-0.106
radiation, (Mo K_α), °A	0.71073
scan rate, °/min	1.5-15.0
scan type	omega
2theta range, °	4.0 to 65.0
total observations	7741
unique observations	7048
unique data with F > 2.0σ(F)	6345
number of parameters	121
over determination ratio	52.4
R	0.0454
R_G	0.0656

$$R = \Sigma(|F_o - F_c|)/\Sigma(F_o)$$

$$R_g = [\Sigma(|F_o - F_c|^2)/\Sigma(F_o^2)]^{1/2}$$

TABLE 31

Bond Distances and Angles for $Cp^*_2U(NSPh_2)_2$

Bond Distance, (°)A		Angle, (°)	
U-N	2.138(5)	U-N-S	151.9(3)
N-S	1.556(5)	N-S-C(11)	110.0(2)
S-C(11)	1.794(4)	N-S-C(21)	107.9(2)
S-C(21)	1.811(4)	N-U-NA	96.8(3)
U-C(31)	2.800(4)	C(11)-S-C(21)	98.7(2)
U-C(32)	2.787(4)	Cp(1)-U-Cp(2)	130.0
U-C(33)	2.798(4)	Cp(1)-U-N	104.1
U-C(34)	2.817(4)	Cp(2)-U-N	108.5
U-C(35)	2.819(4)	Cp(1)-U-NA	108.5
U-Cp(1)[a]		Cp(2)-U-NA	104.1
U-Cp(2)[a]			

[a]Cp(1) and Cp(2) represent the centroid of the C31-C35 and C(41)-C(45) rings.

TABLE 32

Positional Parameters of Anisotropically Refined for Atoms for $Cp^*_2U(NSPh_2)_2$

atom	x	y	z
U	0.0000	0.3390(1)	0.2500
S	0.1258(1)	0.5485(1)	0.3207(1)
N	0.0721(3)	0.4482(3)	0.3122(3)
C(31M)	0.0591(5)	0.3665(6)	0.0593(3)
C(32M)	0.2033(4)	0.4304(5)	0.1746(4)
C(33M)	0.2230(4)	0.2475(7)	0.2854(3)
C(34M)	0.1062(4)	0.0670(4)	0.2295(4)
C(35M)	-0.0111(5)	0.1475(6)	0.0999(4)

TABLE 33

Thermal Parameters of Anistropically Refined Atoms for $Cp^*_2U(NSPh_2)_2$

Atom	U11	U22	U33	U13	U12	U23
U	0.040(1)	0.034(1)	0.049(1)	0.000	0.000(1)	0.000
S	0.064(1)	0.055(1)	0.059(1)	-0.014(1)	0.007(1)	-0.010(1)
N	0.064(2)	0.057(2)	0.074(3)	-0.012(2)	0.004(2)	-0.017(2)
C(31M)	0.088(4)	0.076(3)	0.057(3)	0.013(3)	0.013(3)	0.004(2)
C(32M)	0.060(3)	0.073(3)	0.101(4)	-0.018(3)	0.031(3)	-0.021(3)
C(33M)	0.054(3)	0.111(5)	0.077(3)	0.022(3)	-0.012(2)	-0.011(3)
C(34M)	0.074(3)	0.052(3)	0.105(4)	0.014(2)	0.011(3)	0.010(3)
C(35M)	0.069(4)	0.085(4)	0.085(4)	-0.016(3)	-0.006(3)	-0.024(3)

TABLE 34

Positional and Thermal Parameters for Isotropically Refined Non Hydrogen Atoms for $Cp^*_2U(NSPh_2)_2$

Atom	x	y	z	U
C(11)	0.0598(2)	0.6523(3)	0.3477(2)	0.059(1)
C(12)	0.0884	0.7537	0.3444	0.088(2)
C(13)	0.0351	0.8343	0.3623	0.109(3)
C(14)	-0.0469	0.8135	0.3834	0.088(2)
C(15)	-0.0755	0.7121	0.3867	0.092(2)
C(16)	-0.0222	0.6315	0.3688	0.073(1)
C(21)	0.1941(2)	0.5364(3)	0.3995(2)	0.058(1)
C(22)	0.2518	0.6131	0.4209	0.075(1)
C(23)	0.3093	0.5961	0.4778	0.089(2)
C(24)	0.3090	0.5024	0.5134	0.091(2)
C(25)	0.2512	0.4257	0.4920	0.086(2)
C(26)	0.1938	0.4427	0.4351	0.075(1)
C(31)	0.0831(2)	0.3085(2)	0.1256(1)	0.054(1)
C(32)	0.1485	0.3365	0.1762	0.054(1)
C(33)	0.1593	0.2542	0.2247	0.056(1)
C(34)	0.1006	0.1753	0.2040	0.055(1)
C(35)	0.0535	0.2089	0.1428	0.055(1)

TABLE 35

Positional and Thermal Parameters for Hydrogen Atoms of $Cp^*_2U(NSPh_2)_2$

Atom	x	y	z	U
H(11)	-0.0418	0.5617	0.3711	0.156(14)
H(12)	0.1448	0.7680	0.3299	0.156(14)
H(13)	0.0548	0.9041	0.3600	0.156(14)
H(14)	-0.0836	0.8690	0.3957	0.156(14)
H(15)	-0.1319	0.6978	0.4012	0.156(14)
H(25)	0.2510	0.3612	0.5164	0.156(14)
H(24)	0.3485	0.4907	0.5526	0.156(14)
H(23)	0.3490	0.6489	0.4926	0.156(14)
H(22)	0.2520	0.6775	0.3965	0.156(14)
H(21)	0.1540	0.3899	0.4203	0.156(14)
H(311)	0.0613	0.3247	0.0181	0.112(7)
H(312)	0.0043	0.3991	0.0601	0.112(7)
H(313)	0.1029	0.4181	0.0590	0.112(7)
H(321)	0.2530	0.4149	0.1493	0.112(7)
H(322)	0.1743	0.4885	0.1535	0.112(7)
H(323)	0.2202	0.4464	0.2224	0.112(7)
H(331)	0.2623	0.1911	0.2836	0.112(7)
H(332)	0.2543	0.3110	0.2906	0.112(7)
H(333)	0.1878	0.2386	0.3245	0.112(7)
H(341)	0.1538	0.0305	0.2120	0.112(7)
H(342)	0.1100	0.0659	0.2797	0.112(7)
H(343)	0.0541	0.0347	0.2128	0.112(7)
H(351)	0.0185	0.1063	0.0672	0.112(7)
H(352)	-0.0440	0.1036	0.1286	0.112(7)
H(353)	-0.0485	0.1946	0.0747	0.112(7)

TABLE 36

Selected Intramolecular Non-Bonded Distances
for $Cp^*_2U(NSPh_2)_2$

Atom	Atom	Distance	Atom	Atom	Distance
N	-NA	3.197	C(31M)	-C(34)	3.751
N	-C(11)	2.748	C(32M)	-S	3.463
N	-C(16)	3.034	C(32M)	-C(24)	3.682
N	-C(31A)	3.309	C(33M)	-N	3.579
N	-C(32)	3.261	C(34M)	-C(34A)	3.817
N	-C(32A)	3.772	C(34M)	-C(32)	3.717
C(31M)	-NA	3.455	C(35M)	-C(33)	3.756
C(31M)	-C(16A)	3.765	C(35M)	-C(32)	3.750
C(31M)	-C(33)	3.754			

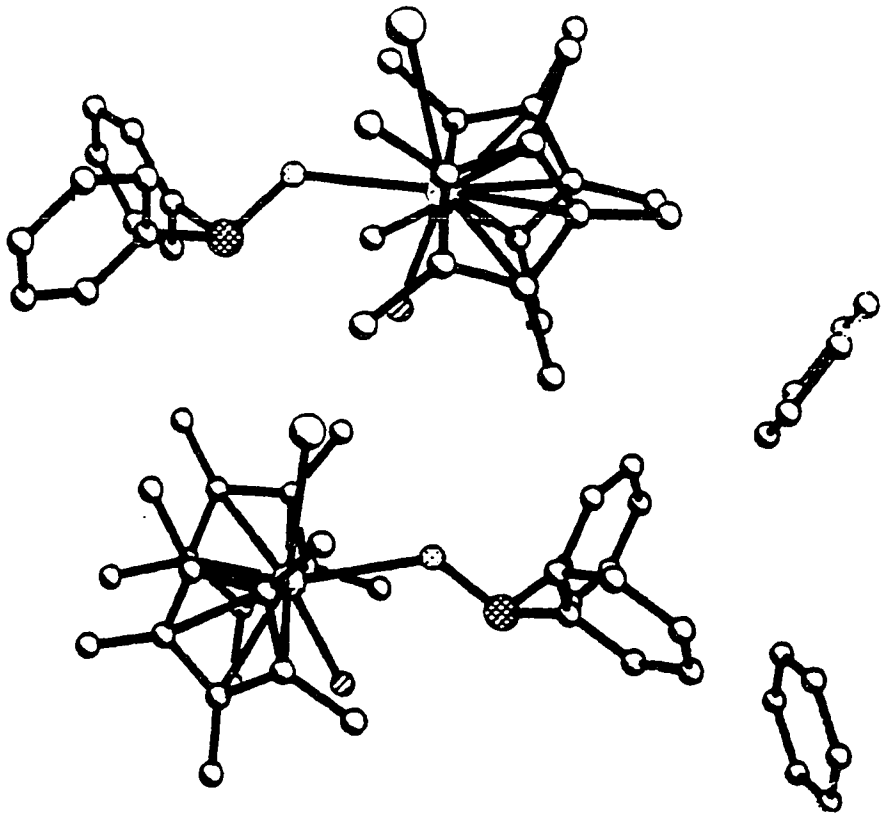

Figure 67: A Diagram of the Assymetric Unit in the Crystal Structure of $Cp^*_2UCl(OH)(HNSPh_2)\cdot C_6H_6$

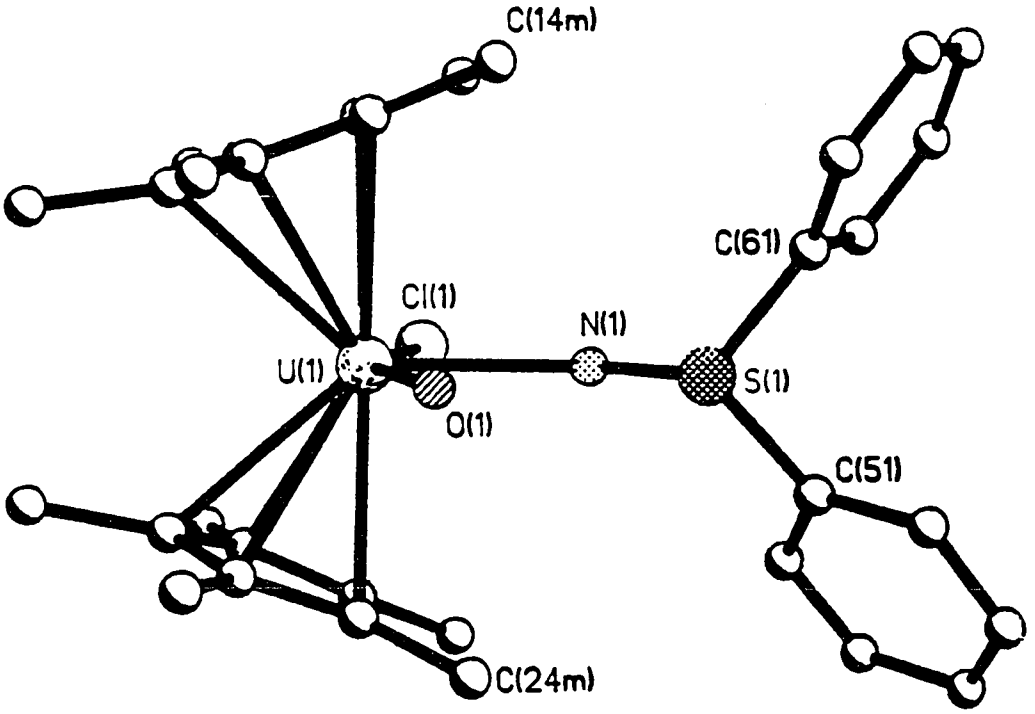

Figure 68: Perspective View of $Cp^*_2UCl(OH)(HNSPh_2)$

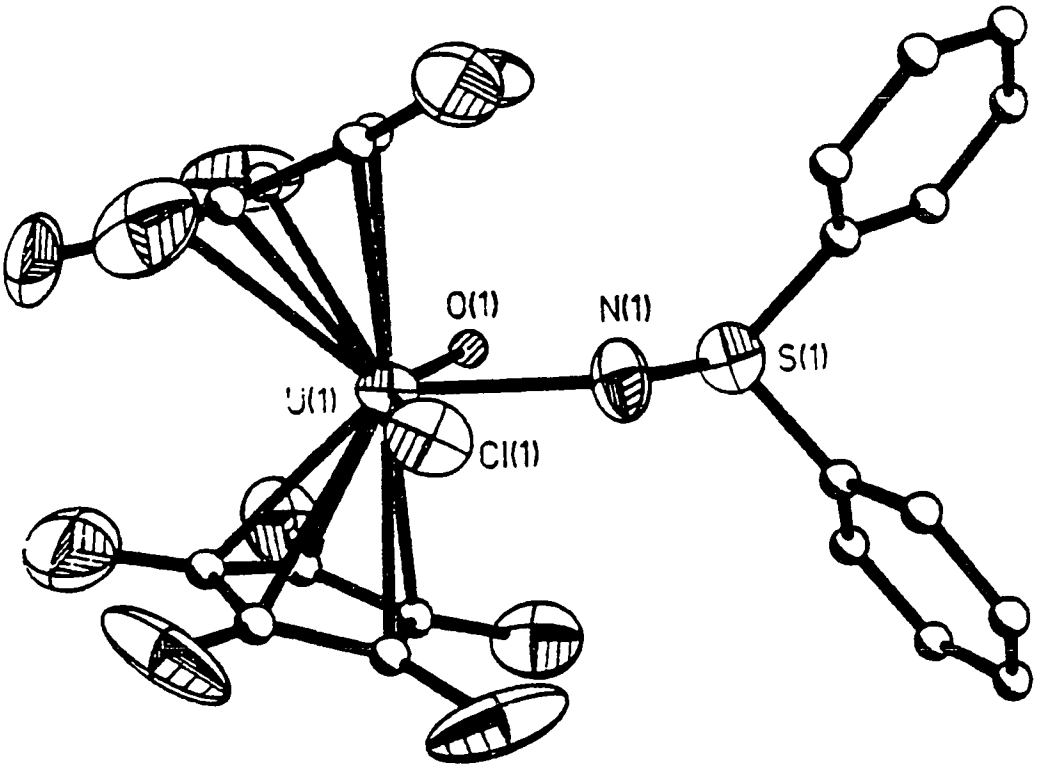

Figure 69: Perspective View of $Cp^*_2UCl(OH)(HNSPh_2)$ with Thermal Ellipsoids

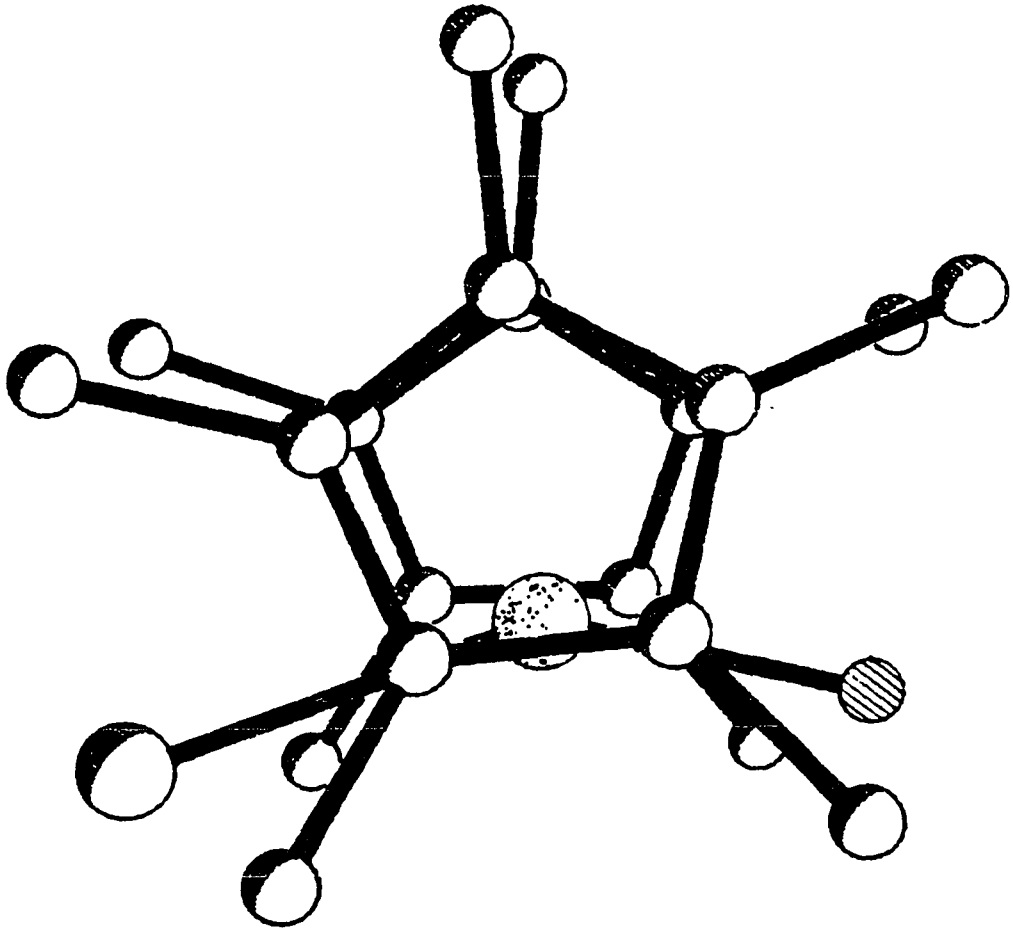

Figure 70: Eclipsed Configuration of the Cp^* Groups in $Cp^*_2UCl(OH)(HNSPh_2)$

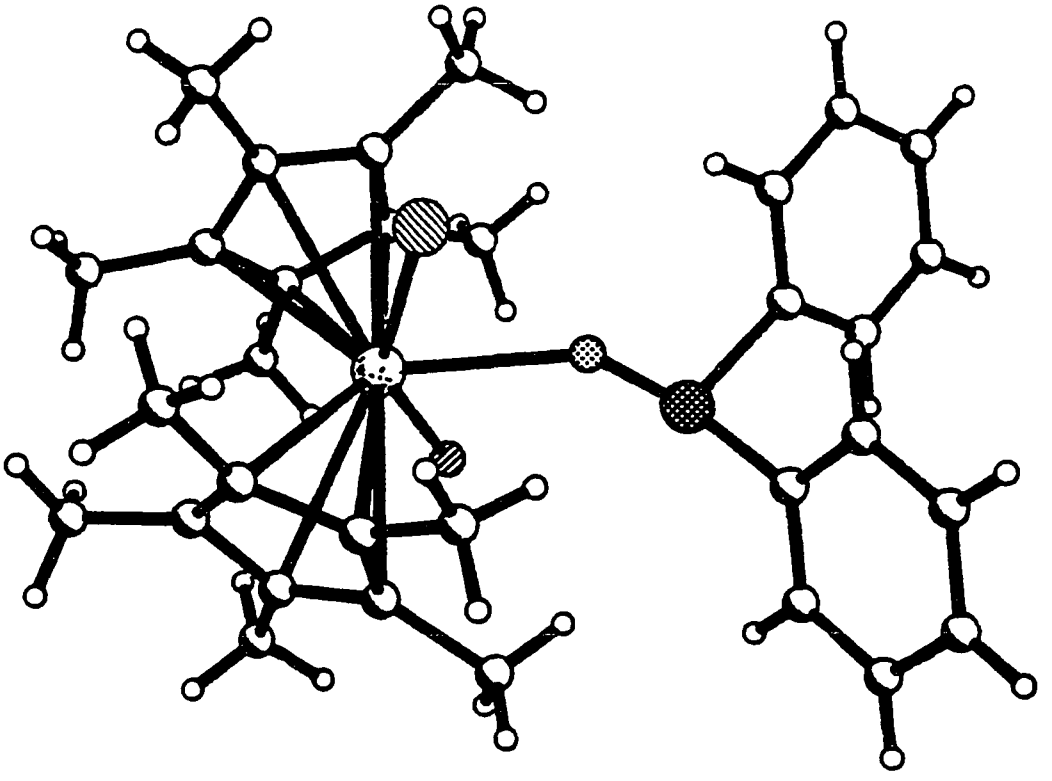

Figure 71: Perspective View of $Cp^*_2UCl(OH)(HNSPh_2)$ with Hydrogen Atoms

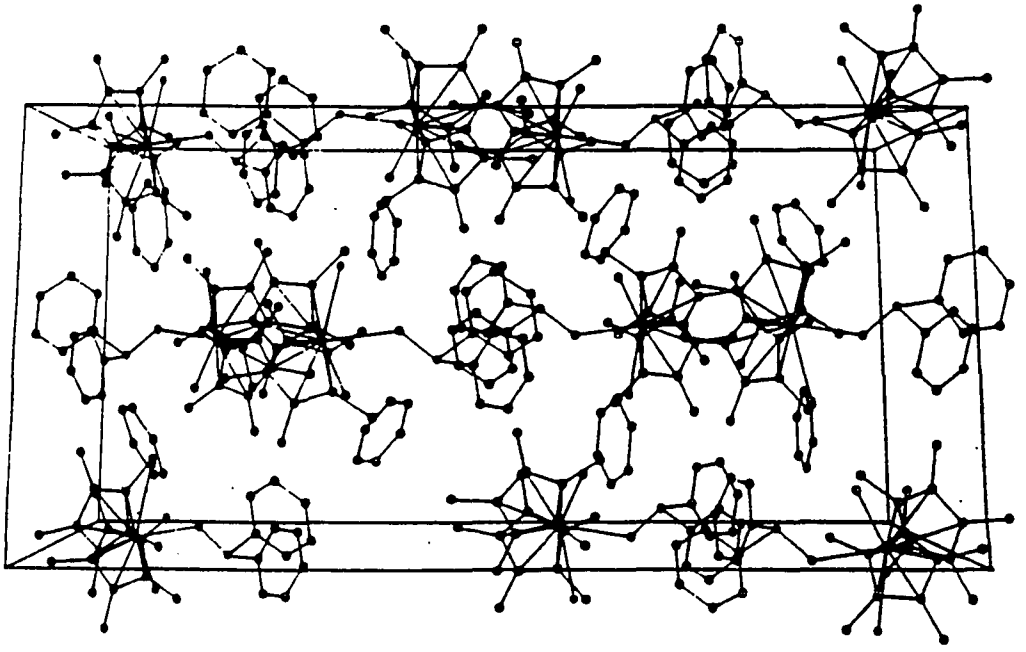

Figure 72: Packing Diagram of $Cp^*_2UCl(OH)(HNSPh_2)\cdot C_6H_6$

TABLE 37

Summary of Crystal Data for $Cp^*_2UCl(OH)(HNSPh_2).C_6H_6$

Formula	$C_{38}H_{46}NOSU$
Formula Weight	838.3
crystal dimensions, mm	1.0 x 0.5 x 0.5
crystal system	monoclinic
space group	P(2)1/c
a,°A	14.503(5)
b,°A	30.10(1)
c,°A	17.048(9)
β,°	102.20(3)
V,°A^3	7273(5)
Z	8
crystal shape	Blocks
crystal color	Greenish Yellow
D(calcd), Mg/M^3	1.531
abs. coeff.(μ), mm^{-1}	4.389
abs. corr. factor range	0.107-0.212
radiation, (Mo K_α), °A	0.71073
scan rate, °/min	1.5-15.0
scan type	omega
2-theta range, °	3.0 to 45.0
total observations	10321
unique observations	9343
unique data with F > 2.0σ(F)	6280
number of parameters	440
over determination ratio	14.3
R	0.0653
R_G	0.0933

$$R = \Sigma (|F_o - F_c|)/\Sigma(F_o)$$

$$R_g = [\Sigma(|F_o - F_c|^2)/\Sigma(F_o^2)]^{1/2}$$

TABLE 38

Bond Distances for $Cp^*_2UCl(OH)(HNSPh_2)$, (°)A

Molecule 1		Molecule 2	
U(1)-N(1)	2.41 (2)	U(2)-N(2)	2.51(2)
U(1)-Cl(1)	2.742 (5)	U(2)-Cl(2)	2.759(5)
U(1)-O(1)	2.10 (1)	U(2)-O(2)	2.11(1)
U(1)-C(11)	2.79 (1)	U(2)-C(31)	2.733(9)
U(1)-C(12)	2.80 (1)	U(2)-C(32)	2.76(1)
U(1)-C(13)	2.774 (9)	U(2)-C(33)	2.82(1)
U(1)-C(14)	2.76 (1)	U(2)-C(34)	2.834(9)
U(1)-C(15)	2.77 (1)	U(2)-C(35)	2.780(9)
U(1)-C(21)	2.815 (9)	U(2)-C(41)	2.83(1)
U(1)-C(22)	2.78 (1)	U(2)-C(42)	2.77(1)
U(1)-C(23)	2.73 (1)	U(2)-C(43)	2.73(1)
U(1)-C(24)	2.73 (1)	U(2)-C(44)	2.76(1)
U(1)-C(25)	2.785 (9)	U(2)-C(45)	2.82(1)
N(1)-S(1)	1.60 (2)	N(2)-S(2)	1.54(2)
S(1)-C(51)	1.80 (1)	S(2)-C(72)	1.76(1)
S(1)-C(61)	1.74 (1)	S(2)-C(81)	1.76(1)
U(1)-Cp(1)	2.50	U(2)-Cp(1)	2.51
U(1)-Cp(2)	2.49	U(2)-Cp(2)	2.51

TABLE 39

Bond Angles for $Cp^*_2UCl(OH)(HNSPh_2)$, (°)

Molecule 1		Molecule 2	
N(1)-U(1)-Cl(1)	71.0(3)	N(2)-U(2)-Cl(2)	70.9(4)
N(1)-U(1)-O(1)	76.4(4)	N(2)-U(2)-O(2)	76.0(5)
Cl(1)-U(1)-O(1)	147.4(3)	Cl(2)-U(2)-O(2)	146.9(3)
U(1)-N(1)-S(1)	130.4(8)	U(2)-N(2)-S(2)	127.5(9)
N(1)-S(1)-C(51)	110.8(6)	N(2)-S(2)-C(72)	109.1(7)
N(1)-S(1)-C(61)	109.5(7)	N(2)-S(2)-C(81)	107.3(7)
C(51)-S(1)-C(61)	96.6(5)	C(72)-S(2)-C(81)	98.0(5)
Cp(1)-U(1)-Cp(2)	135.5	Cp(1)-U(2)-Cp(2)	136.3

TABLE 40

Positional Parameters of Anisotropically Refined Atoms for $Cp^*_2UCl(OH)(HNSPh_2).C_6H_6$

atom	x	y	z	u
U(1)	-0.4816(1)	0.3257(1)	0.2611(1)	0.036(1)
N(1)	-0.5063(9)	0.4050(5)	0.2598(8)	0.052(4)
S(1)	-0.4388(3)	0.4449(2)	0.2457(3)	0.054(2)
Cl(1)	-0.6562(3)	0.3427(2)	0.2921(3)	0.056(2)
C(11M)	-0.569(2)	0.2565(9)	0.416(1)	0.113(5)
C(12M)	-0.393(2)	0.2124(8)	0.359(1)	0.135(5)
C(13M)	-0.245(1)	0.2796(7)	0.350(1)	0.096(5)
C(14M)	-0.300(1)	0.3737(7)	0.430(1)	0.081(5)
C(15M)	-0.503(2)	0.360(1)	0.466(1)	0.117(5)
C(21M)	-0.7049(1)	0.2582(7)	0.169(1)	0.089(5)
C(22M)	-0.511(2)	0.2070(6)	0.174(1)	0.115(5)
C(23M)	-0.366(1)	0.2703(8)	0.113(1)	0.100(5)
C(24M)	-0.474(2)	0.3612(7)	0.059(1)	0.092(5)
C(25M)	-0.682(1)	0.3540(7)	0.087(1)	0.078(5)
U(2)	0.0145(1)	0.4235(1)	0.2466(1)	0.035(1)
N(2)	-0.013(1)	0.3414(7)	0.2507(8)	0.064(4)
S(2)	0.0572(3)	0.3039(1)	0.2425(3)	0.054(2)
Cl(2)	-0.1616(3)	0.4081(2)	0.2785(3)	0.059(2)
C(31M)	0.190(1)	0.3814(7)	0.423(1)	0.078(5)
C(32M)	-0.011(1)	0.4004(6)	0.457(1)	0.071(5)
C(33M)	-0.078(1)	0.4941(9)	0.398(1)	0.114(5)
C(34M)	0.088(2)	0.5435(6)	0.334(1)	0.094(5)
C(35M)	0.251(1)	0.4715(8)	0.337(1)	0.105(5)
C(41M)	-0.201(2)	0.4906(8)	0.145(1)	0.104(5)
C(42M)	-0.190(2)	0.3910(9)	0.078(1)	0.105(5)
C(43M)	0.017(2)	0.3784(7)	0.048(1)	0.079(5)
C(44M)	0.130(2)	0.4646(8)	0.087(1)	0.106(5)
C(45M)	0.001(2)	0.5376(7)	0.138(1)	0.129(5)

TABLE 41

Thermal Parameters of Anisotropically Refined Atoms for $Cp^*_2UCl(OH)(HNSPh_2)\cdot C_6H_6$

Atom	U11	U22	U33	U12	U13	U23
U(1)	0.035(1)	0.043(1)	0.030(1)	0.002(1)	0.006(1)	0.001(1)
N(1)	0.039(6)	0.036(7)	0.077(7)	-0.010(5)	0.005(6)	0.004(5)
S(1)	0.051(3)	0.054(3)	0.060(3)	0.000(2)	0.014(2)	0.002(2)
Cl(1)	0.044(2)	0.068(3)	0.057(3)	0.007(2)	0.014(2)	0.008(2)
C(11M)	0.074(8)	0.166(9)	0.097(8)	-0.037(8)	0.011(7)	0.086(8)
C(12M)	0.198(4)	0.099(9)	0.077(8)	0.023(9)	-0.039(9)	-0.001(8)
C(13M)	0.066(8)	0.087(8)	0.121(9)	0.023(8)	-0.011(8)	0.023(8)
C(14M)	0.056(8)	0.109(9)	0.072(8)	-0.010(8)	0.001(7)	-0.003(8)
C(15M)	0.091(8)	0.202(9)	0.061(8)	0.025(8)	0.025(7)	-0.056(8)
C(21M)	0.065(8)	0.114(9)	0.089(8)	-0.0950(7)	0.017(7)	-0.026(8)
C(22M)	0.182(9)	0.033(8)	0.105(9)	0.001(8)	-0.024(9)	-0.009(7)
C(23M)	0.062(8)	0.187(9)	0.054(8)	0.053(8)	0.021(7)	-0.009(8)
C(24M)	0.151(9)	0.105(8)	0.029(7)	-0.021(8)	0.039(7)	0.010(7)
C(25M)	0.071(8)	0.074(8)	0.075(8)	0.019(7)	-0.018(7)	0.004(7)
U(2)	0.035(1)	0.039(1)	0.031(1)	-0.02(1)	0.004(1)	0.000(1)
N(2)	0.067(7)	0.052(8)	0.078(7)	0.007(6)	0.025(6)	-0.006(6)
S(2)	0.057(3)	0.043(3)	0.064(3)	0.000(2)	0.018(2)	0.005(2)
Cl(2)	0.041(2)	0.075(3)	0.063(3)	-0.014(2)	0.015(2)	-0.004(2)
C(31M)	0.068(8)	0.099(8)	0.060(8)	0.014(8)	-0.005(7)	0.015(7)
C(32M)	0.086(8)	0.064(8)	0.067(8)	-0.033(7)	0.025(7)	0.006(7)
C(33M)	0.054(8)	0.178(9)	0.108(8)	0.032(8)	0.013(7)	-0.096(8)
C(34M)	0.173(9)	0.042(7)	0.065(8)	-0.028(8)	0.020(8)	0.003(7)
C(35M)	0.066(8)	0.157(9)	0.090(8)	-0.078(8)	0.010(7)	-0.022(8)
C(41M)	0.109(9)	0.105(8)	0.081(8)	0.073(8)	-0.021(8)	-0.005(8)
C(42M)	0.066(8)	0.185(9)	0.052(8)	-0.031(8)	-0.015(7)	-0.026(8)
C(43M)	0.102(8)	0.098(8)	0.043(7)	0.023(8)	0.029(7)	0.010(7)
C(44M)	0.124(9)	0.142(9)	0.063(8)	-0.049(8)	0.043(7)	0.035(8)
C(45M)	0.202(9)	0.079(8)	0.082(8)	-0.033(9)	-0.024(9)	0.032(8)

TABLE 42

Positional and Thermal Parameters of the Isotropically Refined Atoms for $Cp^*_2UCl(OH)(HNSPh_2)\cdot C_6H_6$

Atom	x	y	z	u
O(1)	-0.3577(8)	0.3515(4)	0.2330(6)	0.052(3)
C(11)	-0.4821(6)	0.2806(3)	0.4042(7)	0.059(4)
C(12)	-0.4099	0.2597	0.3728	0.069(5)
C(13)	-0.3354	0.2906	0.3762	0.060(4)
C(14)	-0.3615	0.3308	0.4097	0.049(4)
C(15)	-0.4521	0.3245	0.4271	0.044(4)
C(21)	-0.6146(6)	0.2776(3)	0.1487(6)	0.053(4)
C(22)	-0.5275	0.2549	0.1554	0.064(4)
C(23)	-0.4654	0.2828	0.1238	0.050(4)
C(24)	-0.5141	0.3229	0.0975	0.046(4)
C(25)	-0.6064	0.3196	0.1129	0.041(3)
C(51)	-0.4998(8)	0.4826(3)	0.1713(6)	0.053(4)
C(52)	-0.5935	0.4756	0.1327	0.077(5)
C(53)	-0.6360	0.5034	0.0700	0.083(5)
C(54)	-0.5848	0.5381	0.0458	0.077(5)
C(55)	-0.4911	0.5451	0.0844	0.083(5)
C(56)	-0.4486	0.5173	0.1472	0.070(5)
C(61)	-0.4243(8)	0.4816(3)	0.3261(5)	0.058(4)
C(62)	-0.3334	0.4882	0.3715	0.075(5)
C(63)	-0.3187	0.5171	0.4371	0.081(5)
C(64)	-0.3948	0.5392	0.4572	0.063(4)
C(65)	-0.4858	0.5326	0.4118	0.075(5)
C(66)	-0.5005	0.5038	0.3463	0.074(5)
O(2)	0.1409(8)	0.3955(4)	0.2261(6)	0.051(3)
C(31)	0.1298(7)	0.4233(3)	0.3958(6)	0.052(4)
C(32)	0.0384	0.4302	0.4111	0.046(4)
C(33)	0.0091	0.4738	0.3853	0.059(4)
C(34)	0.0823	0.4938	0.3540	0.049(4)
C(35)	0.1570	0.4626	0.3605	0.055(4)
C(41)	-0.1126(7)	0.4697(3)	0.1254(7)	0.059(4)
C(42)	-0.1088	0.4253	0.0981	0.058(4)
C(43)	-0.0173	0.4180	0.0831	0.048(4)
C(44)	0.0353	0.4578	0.1011	0.061(4)
C(45)	-0.0236	0.4898	0.1272	0.067(5)
C(71)	0.0007(6)	0.2511(4)	0.3564(6)	0.075(5)
C(72)	0.0752	0.2706	0.3290	0.051(4)
C(73)	0.1674	0.2658	0.3729	0.067(5)
C(74)	0.1851	0.2416	0.4443	0.076(5)

Table 42(Continued)

Positional and Thermal Parameters of Isotropically Refined Atoms for $Cp^*_2UCl(OH)(HNSPh_2)\cdot C_6H_6$

atom	x	y	z	u
C(75)	0.1105	0.2221	0.4717	0.079(5)
C(76)	0.0184	0.2268	0.4278	0.095(6)
C(81)	-0.0044(7)	0.2649(3)	0.1741(6)	0.055(4)
C(82)	-0.0981	0.2701	0.1341	0.070(5)
C(83)	-0.1403	0.2386	0.0 778	0.077(5)
C(84)	-0.0889	0.2019	0.0615	0.079(5)
C(85)	0.0049	0.1966	0.1015	0.092(6)
C(86)	0.0471	0.2281	0.1578	0.067(5)
C(91)	0.315(1)	0.1114(5)	0.221(1)	0.177(8)
C(92)	0.218	0.1084	0.193	0.159(8)
C(93)	0.157	0.1216	0.242	0.143(7)
C(94)	0.193	0.1376	0.319	0.155(8)
C(95)	0.291	0.1405	0.347	0.0177(8)
C(96)	0.352	0.1274	0.298	0.160(8)
C(1)	-0.329(1)	0.1136(5)	0.2019(9)	0.137(7)
C(2)	-0.321	0.0954	0.2784	0.157(8)
C(3)	-0.241	0.1048	0.3382	0.149(8)
C(4)	-0.171	0.1324	0.3216	0.131(7)
C(5)	-0.179	0.1507	0.2452	0.131(7)
C(6)	-0.258	0.1413	0.1853	0.138(7)

TABLE 43

Positional and Thermal Parameters of the Hydrogen Atoms for $Cp^*_2UCl(OH)(HNSPh_2)\cdot C_6H_6$

Atom	x	y	z	u
H(11A)	-0.6088	0.2767	0.4377	0.204(9)
H(11B)	-0.5518	0.2321	0.4522	0.204(9)
H(11C)	-0.6035	0.2456	0.3651	0.204(9)
H(12A)	-0.4492	0.1957	0.3580	0.204(9)
H(12B)	-0.3431	0.2015	0.4008	0.204(9)
H(12C)	-0.3745	0.2092	0.3080	0.204(9)
H(13A)	-0.2044	0.3051	0.3575	0.204(9)
H(13B)	-0.2588	0.2711	0.2948	0.204(9)
H(13C)	-0.2140	0.2554	0.3823	0.204(9)
H(14A)	-0.2418	0.3701	0.4127	0.204(9)
H(14B)	-0.2869	0.3786	0.4872	0.204(9)
H(14C)	-0.3337	0.3988	0.4035	0.204(9)
H(15A)	-0.5632	0.3491	0.4721	0.204(9)
H(15B)	-0.5128	0.3862	0.4320	0.204(9)
H(15C)	-0.4658	0.3681	0.5174	0.204(9)
H(21A)	-0.7537	0.2803	0.1590	0.204(9)
H(21B)	-0.6927	0.2494	0.2240	0.204(9)
H(21C)	-0.7246	0.2328	0.1353	0.204(9)
H(22A)	-0.5622	0.1952	0.1947	0.204(9)
H(22B)	-0.4531	0.2036	0.2133	0.204(9)
H(22C)	-0.5060	0.1913	0.1260	0.204(9)
H(23A)	-0.3488	0.2416	0.1357	0.204(9)
H(23B)	-0.3210	0.2920	0.1387	0.204(9)
H(23C)	-0.3652	0.2696	0.0564	0.204(9)
H(24A)	-0.5203	0.3843	0.0467	0.204(9)
H(24B)	-0.4565	0.3514	0.0107	0.204(9)
H(24C)	-0.4191	0.3725	0.0956	0.204(9)
H(25A)	-0.7387	0.3450	0.1037	0.204(9)
H(25B)	-0.6952	0.3569	0.0296	0.204(9)
H(25C)	-0.6615	0.3821	0.1111	0.204(9)
H(52A)	-0.6288	0.4516	0.1494	0.142(9)
H(53A)	-0.7005	0.4986	0.0434	0.142(9)
H(54A)	-0.6141	0.5573	0.0026	0.142(9)
H(55A)	-0.4559	0.5691	0.0678	0.15(1)
H(56A)	-0.3841	0.5221	0.1737	0.142(9)
H(62A)	-0.2810	0.4730	0.3577	0.142(9)
H(63A)	-0.2561	0.5216	0.4683	0.142(9)
H(64A)	-0.3847	0.5591	0.5023	0.142(9)

TABLE 43 (Continued)

Positional and Thermal Parameters of the Hydrogen Atoms for $Cp^*_2UCl(OH)(HNSPh_2)\cdot C_6H_6$

atom	x	y	z	u
H(65A)	-0.5382	0.5479	0.4257	0.142(9)
H(66A)	-0.5631	0.4992	0.3151	0.142(9)
H(31A)	0.2486	0.3835	0.4068	0.204(9)
H(31B)	0.1561	0.3555	0.3998	0.204(9)
H(31C)	0.2009	0.3791	0.4808	0.204(9)
H(32A)	0.0222	0.3728	0.4674	0.204(9)
H(32B)	-0.0740	0.3948	0.4269	0.204(9)
H(32C)	-0.0149	0.4142	0.5073	0.204(9)
H(33A)	-0.0837	0.5236	0.3758	0.204(9)
H(33B)	-0.0766	0.4957	0.4545	0.204(9)
H(33C)	-0.1310	0.4766	0.3721	0.204(9)
H(34A)	0.1440	0.5488	0.3134	0.204(9)
H(34B)	0.0902	0.5608	0.3812	0.204(9)
H(34C)	0.0336	0.5517	0.2937	0.204(9)
H(35A)	0.2899	0.4454	0.3467	0.204(9)
H(35B)	0.2824	0.4957	0.3682	0.204(9)
H(35C)	0.2401	0.4790	0.2809	0.204(9)
H(41A)	-0.1876	0.5207	0.1623	0.204(9)
H(41B)	-0.2195	0.4739	0.1872	0.204(9)
H(41C)	-0.2508	0.4902	0.0982	0.204(9)
H(42A)	-0.2449	0.4027	0.0931	0.204(9)
H(42B)	-0.1709	0.3640	0.1072	0.204(9)
H(42C)	-0.2031	0.3849	0.0215	0.204(9)
H(43A)	-0.0307	0.3557	0.0413	0.204(9)
H(43B)	0.0731	0.3678	0.0831	0.204(9)
H(43C)	0.0301	0.3858	-0.0032	0.204(9)
H(44A)	0.1507	0.4940	0.1037	0.204(9)
H(44B)	0.1284	0.4612	0.0307	0.204(9)
H(44C)	0.1718	0.4431	0.1168	0.204(9)
H(45A)	-0.0488	0.5530	0.1560	0.204(9)
H(45B)	0.0085	0.5499	0.0880	0.204(9)
H(45C)	0.0586	0.5408	0.1773	0.204(9)
H(71A)	-0.0628	0.2543	0.3262	0.142(9)
H(73A)	0.2187	0.2793	0.3540	0.142(9)
H(74A)	0.2485	0.2384	0.4746	0.142(9)
H(75A)	0.1227	0.2054	0.5208	0.142(9)
H(76A)	-0.0329	0.2134	0.4467	0.142(9)
H(82A)	-0.1335	0.2954	0.1453	0.142(9)

TABLE 43 (Continued)

Positional and Thermal Parameters of Hydrogen Atoms for $Cp^*_2UCl(OH)(HNSPh_2)\cdot C_6H_6$

atom	x	y	z	u
H(83A)	-0.2048	0.2422	0.0503	0.142(9)
H(84A)	-0.1179	0.1802	0.0228	0.142(9)
H(85A)	0.0403	0.1713	0.0903	0.142(9)
H(86A)	0.1116	0.2245	0.1853	0.142(9)
H(91A)	0.3573	0.1024	0.1874	0.150
H(92A)	0.1929	0.0974	0.1398	0.150
H(93A)	0.0899	0.1196	0.2224	0.150
H(94A)	0.1512	0.1466	0.3525	0.150
H(95A)	0.3156	0.1516	0.4001	0.150
H(96A)	0.4186	0.1295	0.3176	0.150
H(1C)	-0.3835	0.1072	0.1608	0.150
H(2C)	-0.3691	0.0764	0.2898	0.150
H(3A)	-0.2354	0.0922	0.3908	0.150
H(4A)	-0.1160	0.1389	0.3628	0.150
H(5A)	-0.1304	0.1697	0.2338	0.150
H(6A)	-0.2642	0.1538	0.1328	0.150

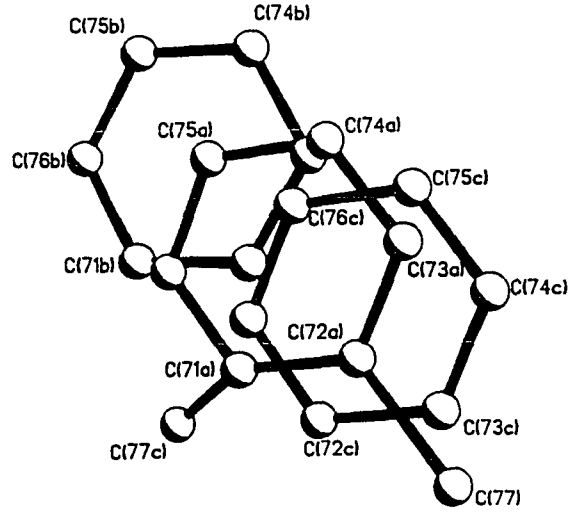

Figure 73: In-plane Disorder of Toluene-1 in $[Cp^*(Cl)(HNSPh_2)U-(\mu_3-OH)(\mu_2-O)_2-U(Cl)(HNSPh_2)_2]_2 \cdot 2C_7H_8$

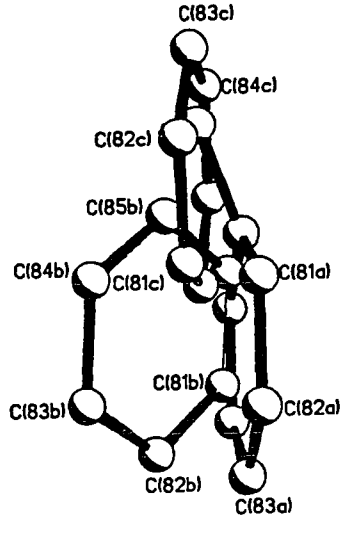

Figure 74: Off-Plane Disorder of Toluene-2 in $[Cp^*(Cl)(HNSPh_2)U-(\mu_3-OH)(\mu_2-O)_2-U(Cl)(HNSPh_2)_2]_2$

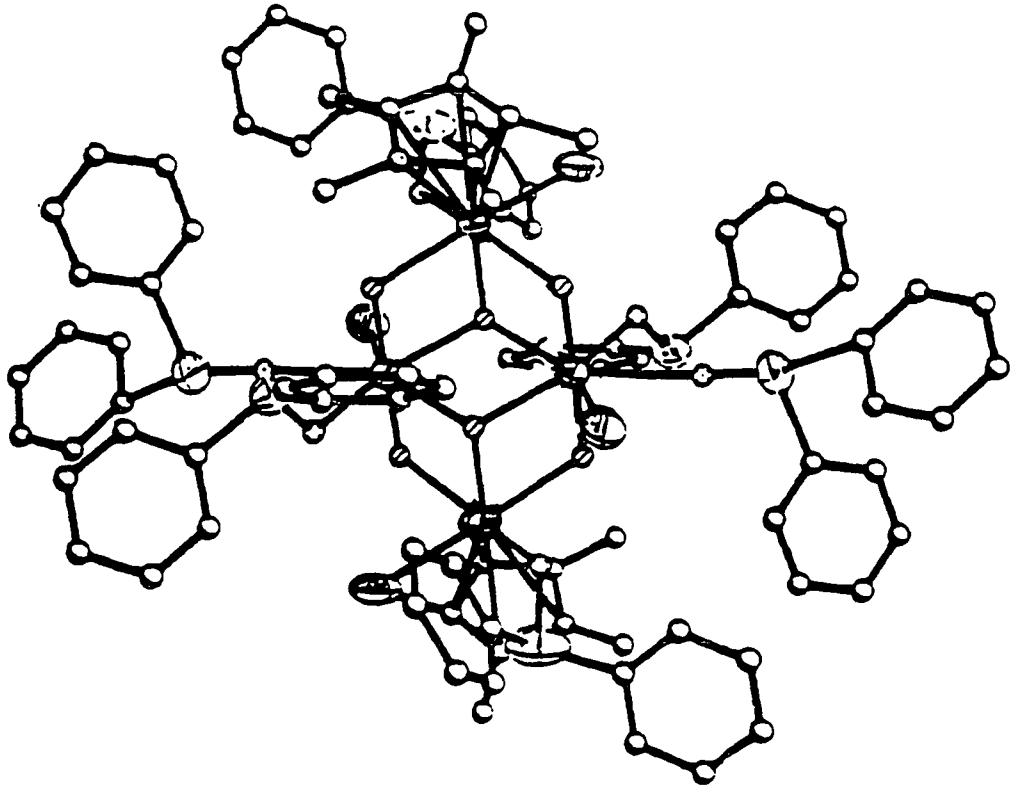

Figure 75: Perspective View of $[Cp^*(Cl)(HNSPh_2)U-(\mu_3\text{-}OH)(\mu_2\text{-}O)_2\text{-}U(Cl)(HNSPh_2)_2]_2$

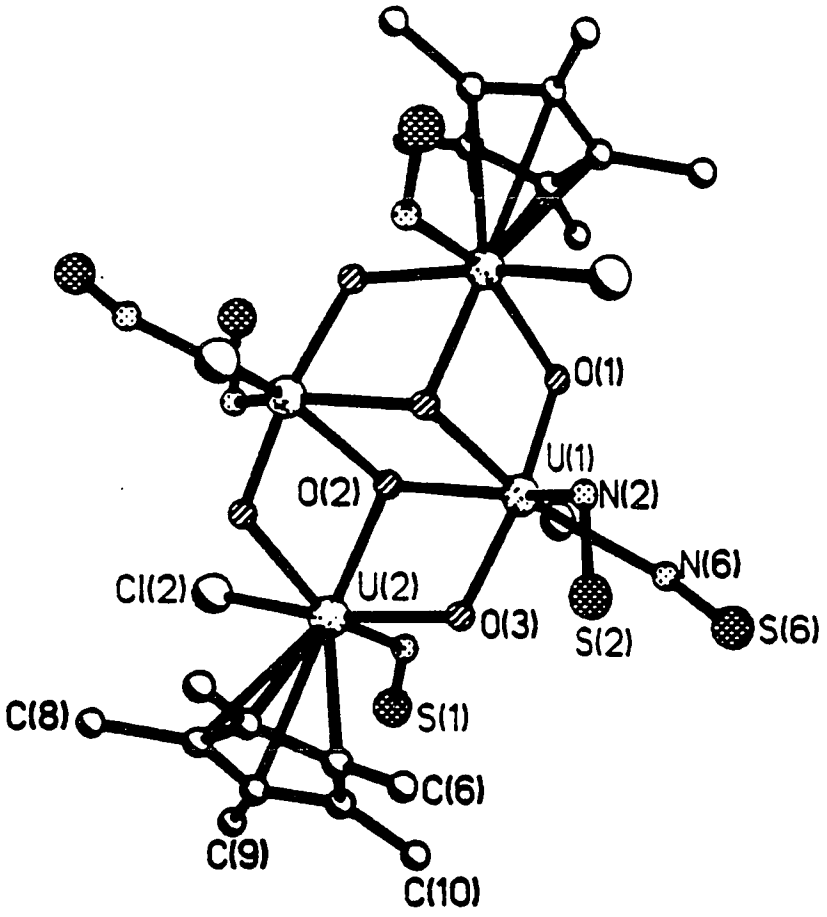

Figure 76: Perspective View of $[Cp^*(Cl)(HNSPh_2)U-(\mu_3-OH)(\mu_2-O)_2-U(Cl)(HNSPh_2)_2]_2$ with the Phenyl Groups Removed

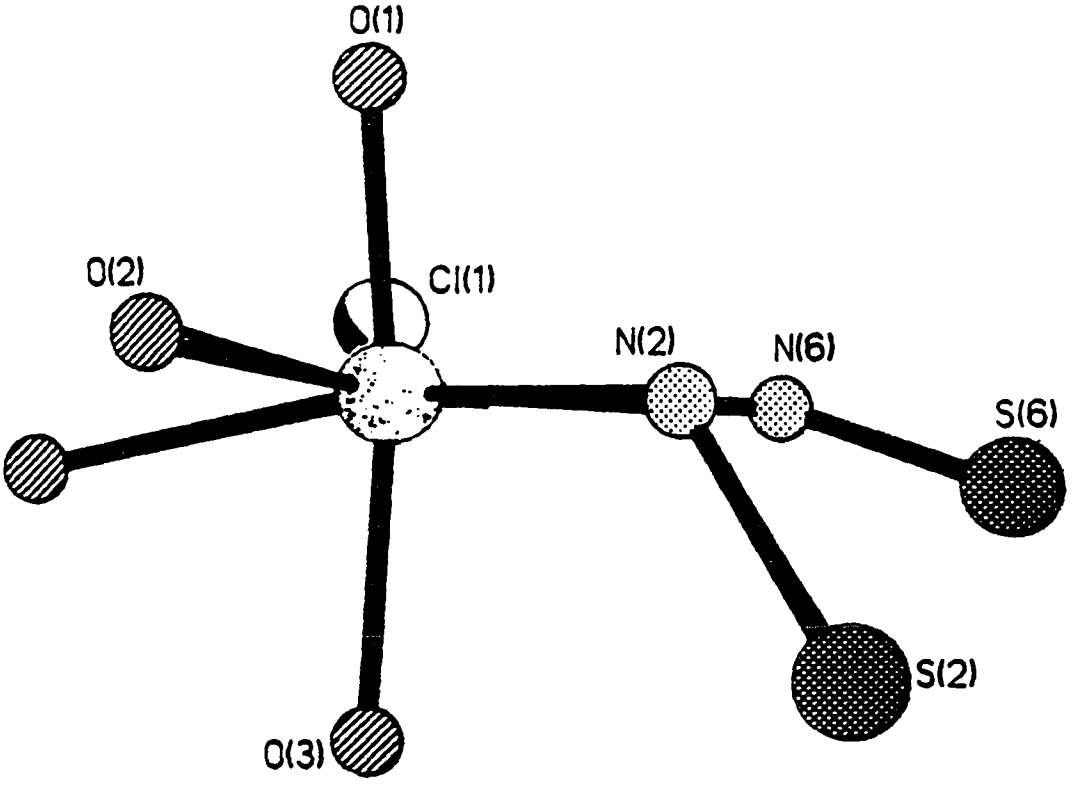

Figure 77: Pentagonal Bipyramidal Stereochemistry Around U(1) in $[Cp^*(Cl)(HNSPh_2)U-(\mu_3-OH)(\mu_2-O)_2-U(Cl)(HNSPh_2)_2]_2$

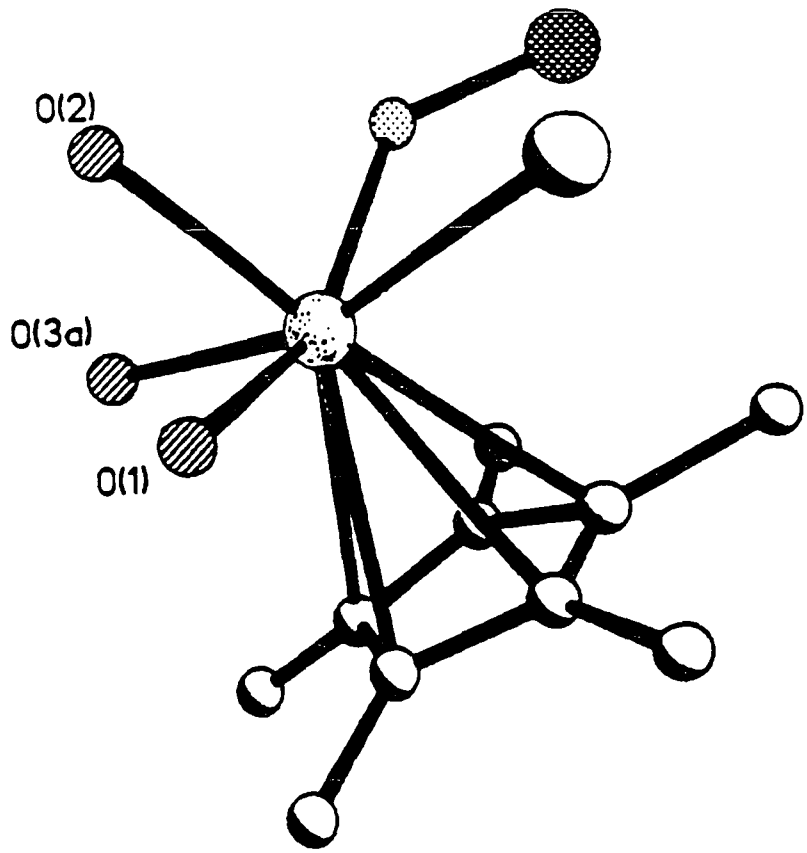

Figure 78: Octahedral Stereochemistry Around U(2) in $[Cp^*(Cl)(HNSPh_2)U-(\mu_3-OH)(\mu_2-O)_2-U(Cl)(HNSPh_2)_2]_2$

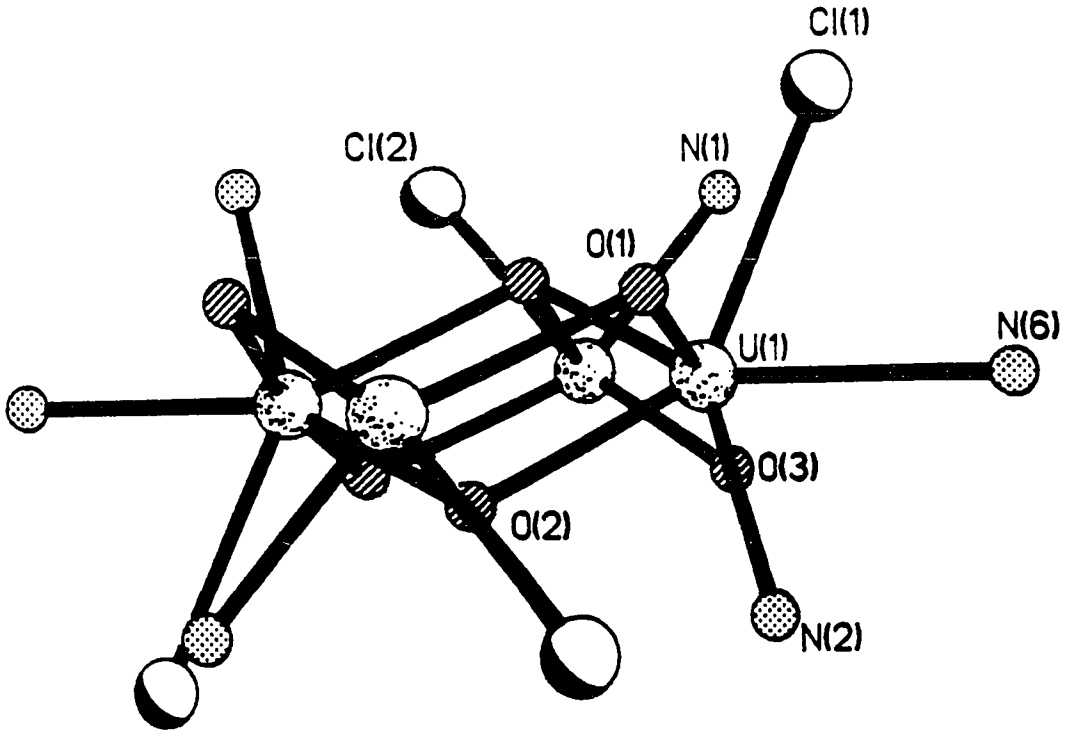

Figure 79: The Side View of the Core of

$[Cp^*(Cl)(HNSPh_2)U-(\mu_3-OH)(\mu_2-O)_2-U(Cl)(HNSPh_2)_2]_2$

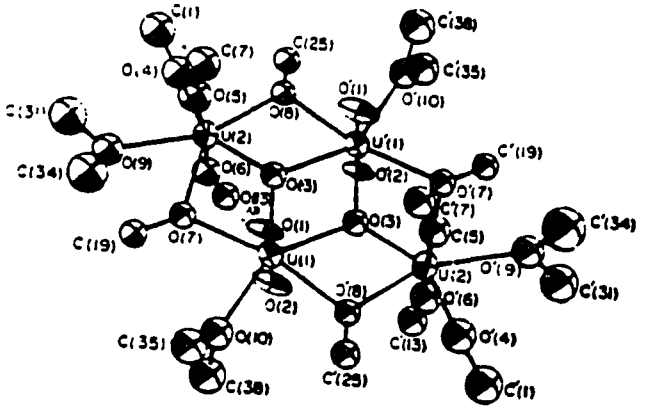

Figure 80: Perspective View of $(UO_2)_2U_2O_2(OC_6H_5)_{10}(THF)_4$[57]

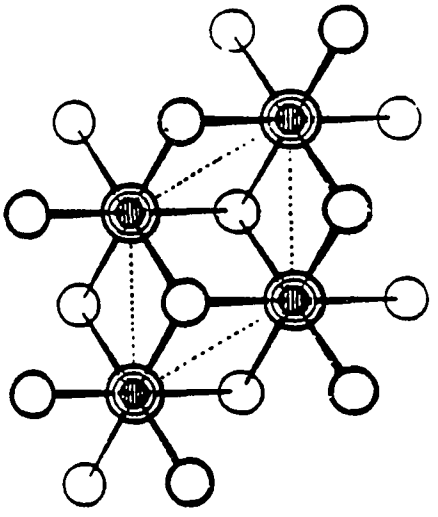

Figure 81: The Layer Structure of UO_3[111]

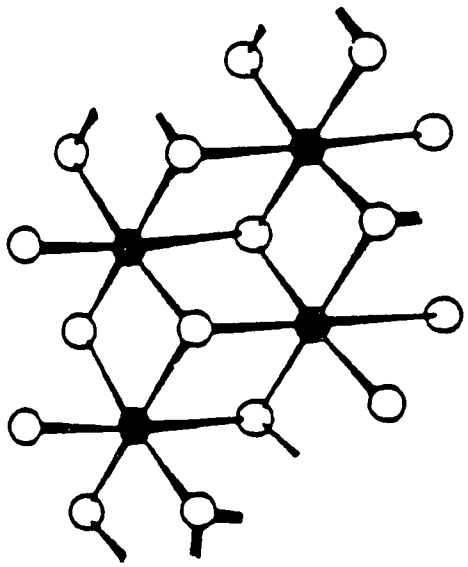

Figure 82 : The $[CdCl_3^-]_n$ Layers of $[NH_4][CdCl_3]$[112]

TABLE 44

Summary of Crystal Data for
$[Cp^*(Cl)(HNSPh_2)U-(\mu_3-OH)(\mu_2-O)_2-U(Cl)(HNSPh_2)_2]_2 \cdot 2C_7H_8$

Formula	$C_{120}H_{130}N_6S_6O_6Cl_4U_4$
Formula Weight	3038.6
crystal dimensions, mm	0.5 x 0.5 x 0.5
crystal system	triclinic
space group	P -1
a, °A	14.093(7)
b, °A	15.36(1)
c, °A	16.153(5)
α, °	89.46(4)
β, °	64.63(3)
γ, °	74.22(5)
V, $°A^3$	3018(3)
Z	1
crystal shape	Cube
crystal color	Dark Red-Black
D(calcd), Mg/M^3	1.672
abs. coeff.( ), mm^{-1}	5.596
radiation, (Mo K_α), °A	0.71073
scan rate, °/min	4.88-14.65
scan type	omega
2-theta range, °	3.0 to 45.0
total observations	8586
unique observations	7849
unique data with F > 6.0σ(F)	5008
number of parameters	263
over determination ratio	19.0
R	0.0564
R_G	0.0791

$$R = \Sigma (|F_o - F_c|)/\Sigma(F_o)$$
$$R_g = [\Sigma(|F_o - F_c|^2)/\Sigma(F_o^2)]^{1/2}$$

TABLE 45

Bond Distances for

$[Cp^*(Cl)(HNSPh_2)U-(\mu_3-OH)(\mu_2-O)_2-U(Cl)(HNSPh_2)_2]_2$

Bond	Distance, (A)	Bond	Distance, (A)
U(1)-Cl(1)	2.745(6)	U(2)-Cl(2)	2.803(4)
U(1)-N(11)	2.47(1)	U(2)-N(21)	2.50(1)
U(2)-N(22)	2.57(2)	U(1)-O(3)	2.30(1)
U(1)-O(1A)	2.27(1)	U(2)-O(2)	2.355(9)
U(2)-O(2A)	2.30(1)	U(1A)-O(2)	2.20(1)
U(2)-O(1)	1.96(1)	U(2)-O(3)	1.97(1)
U(1)-C(1)	2.75(1)	U(1)-C(2)	2.79(1)
U(1)-C(3)	2.85(1)	U(1)-C(4)	2.84(1)
U(1)-C(5)	2.79(1)	N(11)-S(11)	1.58(1)
N(21)-S(21)	1.61(2)	N(22)-S(22)	1.60(2)
S(11)-C(51)	1.76(2)	S(11)-C(61)	1.80(2)
S(22)-C(11)	1.77(2)	S(21)-C(36)	1.77(1)
S(21)-C(41)	1.770(9)	S(22)-C(21)	1.75(1)

TABLE 46

Bond Angles for
$[Cp^*(Cl)(HNSPh_2)U-(\mu_3-OH)(\mu_2-O)_2-U(Cl)(HNSPh_2)_2]_2$

	Angle, (°)		Angle, (°)
U(1)-N(11)-S(11)	130.5(9)	U(2)-N(21)-S(21)	128.5(8)
U(2)-N(22)-S(22)	129.8(6)	Cl(1)-U(1)-N(11)	79.2(4)
Cl(2)-U(2)-N(21)	141.8(3)	Cl(2)-U(2)-N(22)	67.7(3)
N(11)-S(11)-C(51)	110.1(9)	N(11)-S(11)-C(61)	109.7(9)
N(21)-S(21)-C(36)	108.6(8)	N(21)-S(21)-C(41)	107.8(7)
N(22)-S(22)-C(11)	110.3(8)	N(22)-S(22)-C(21)	110.1(8)
C(51)-S(11)-C(61)	98.0(7)	C(36)-S(21)-C(41)	100.9(5)
C(11)-S(22)-C(21)	98.5(7)	O(1)-U(2)-O(3)	175.0(4)
O(3)-U(1)-O(1A)	104.8(4)	O(2)-U(2)-O(2A)	71.1(3)
O(2)-U(2)-O(3)	102.0(4)	O(1)-U(2)-O(2)	73.2(4)
O(3)-U(1)-O(2A)	70.4(4)	U(1)-O(3)-U(2)	111.3(6)
U(2)-O(1)-U(1A)	113.6(4)	U(2)-O(2)-U(2A)	108.9(3)
U(2)-O(2)-U(1A)	102.1(3)	U(1A)-O(2)-U(2A)	103.8(5)
Cl(2)-U(2)-O(1)	88.8(3)	Cl(2)-U(2)-O(3)	94.2(3)

TABLE 47

Positional and Thermal Parameters of Isotropicaly Refined Atoms for $[Cp^*(Cl)(HNSPh_2)U\text{-}(\mu_3\text{-}OH)(\mu_2\text{-}O)_2\text{-}U(Cl)(HNSPh_2)_2]_2 \cdot 2C_7H_8$

Atom	x	y	z	u
C(1)	-0.1682(8)	0.0980(6)	-0.2060(7)	0.063(4)
C(2)	-0.1686	0.1856	-0.1780	0.061(4)
C(3)	-0.0828	0.2097	-0.2513	0.058(4)
C(4)	-0.0294	0.1370	-0.3247	0.074(4)
C(5)	-0.0822	0.0679	-0.2967	0.064(4)
C(11)	-0.110(1)	0.3025(8)	-0.1965(8)	0.083(5)
C(12)	-0.0434	-0.2576	-0.2609	0.114(5)
C(13)	-0.0442	-0.2506	-0.3467	0.145(6)
C(14)	-0.1115	-0.2885	-0.3681	0.143(6)
C(15)	0.1780	-0.3385	-0.3037	0.131(6)
C(16)	-0.1772	-0.3405	-0.2179	0.120(5)
C(21)	-0.094(1)	-0.4142(8)	-0.0728(9)	0.112(5)
C(22)	-0.181	-0.4355	-0.0009	0.130(6)
C(23)	-0.172	-0.5260	0.0154	0.162(6)
C(24)	-0.077	-0.5953	-0.0401	0.118(5)
C(25)	0.010	-0.5740	-0.1121	0.145(6)
C(26)	0.001	-0.4834	-0.1284	0.136(6)
C(31)	-0.417(1)	-0.2236(8)	0.0556(7)	0.101(5)
C(32)	-0.476	-0.2826	0.1019	0.116(5)
C(33)	-0.494	-0.2955	0.1923	0.131(6)
C(34)	-0.452	-0.2494	0.2364	0.146(6)
C(35)	-0.393	-0.1905	0.1901	0.117(5)
C(36)	-0.375	-0.1777	0.0997	0.067(4)
C(41)	-0.3884(8)	0.0027(6)	0.0918(6)	0.065(4)
C(42)	-0.3455	0.0706	0.1047	0.069(4)
C(43)	-0.4128	0.1604	0.1355	0.083(4)
C(44)	-0.5230	0.1825	0.1532	0.088(5)
C(45)	-0.5658	0.1147	0.1402	0.106(5)
C(46)	-0.4985	0.0248	0.1095	0.083(4)
C(51)	0.262(1)	-0.148(1)	-0.4786(9)	0.091(5)
C(52)	0.246	-0.128	-0.5570	0.160(6)
C(53)	0.247	-0.197	-0.6132	0.146(6)

TABLE 47 (Continued)

Positional and Thermal Parameters of Isotropically Refined Atoms for $[Cp^*(Cl)(HNSPh_2)U\text{-}(\mu_3\text{-}OH)(\mu_2\text{-}O)_2\text{-}U(Cl)(HNSPh_2)_2]_2 \cdot 2C_7H_8$

atom	x	y	z	u
C(54)	0.264	-0.286	-0.5911	0.177(6)
C(55)	0.279	-0.306	-0.5128	0.202(6)
C(56)	0.278	-0.237	-0.4565	0.146(6)
C(61)	0.3855(9)	-0.0875(7)	-0.4184(8)	0.071(4)
C(62)	0.4744	-0.1140	-0.5058	0.107(5)
C(63)	0.5811	-0.1291	-0.5160	0.127(5)
C(64)	0.5990	-0.1179	-0.4388	0.112(5)
C(65)	0.5102	-0.0914	-0.3514	0.112(5)
C(66)	0.4035	-0.0762	-0.3413	0.108(5)
C(45)	-0.391	-0.241	0.048	0.13(2)
C(50)	-0.379(2)	0.001(2)	0.091(2)	0.067(1)
C(51)	-0.489	0.023	0.103	0.061(1)
C(52)	-0.562	0.115	0.132	0.16(2)
C(53)	-0.524	0.183	0.149	0.07(1)
C(54)	-0.413	0.160	0.137	0.12(2)
C(55)	-0.341	0.069	0.108	0.07(1)
C(60)	-0.097(3)	-0.304(3)	-0.211(3)	0.11(2)
C(61)	-0.163	-0.347	-0.226	0.14(2)
C(62)	-0.173	-0.343	-0.309	0.160(2)
C(63)	-0.117	-0.295	-0.376	0.10(2)
C(64)	-0.050	-0.252	-0.361	0.11(2)
C(65)	-0.040	-0.256	-0.279	0.11(2)
C(75)	0.091(6)	-0.475(6)	0.012(7)	0.50(2)
C(70)	0.050	-0.391	0.067	0.156(2)
C(71)	-0.016	-0.383	0.162	0.400(2)
C(73)	-0.041	-0.459	0.202	0.344(2)
C(72)	0.000	-0.543	0.147	0.23(2)
C(74)	0.067	-0.551	0.052	0.31(2)

TABLE 48

Positional Parameters of Anisotropically Refined Atoms for $[Cp^*(Cl)(HNSPh_2)U\text{-}(\mu_3\text{-}OH)(\mu_2\text{-}O)_2\text{-}U(Cl)(HNSPh_2)_2]_2 \cdot 2C_7H_8$

atom	x	y	z	u
U(1)	0.0197(1)	0.0617(1)	-0.1812(1)	0.044(1)
U(2)	-0.0033(1)	-0.1147(1)	-0.0382(1)	0.040(1)
Cl(1)	0.1815(4)	0.1452(3)	-0.2594(3)	0.075(2)
Cl(2)	0.1998(4)	-0.2203(3)	-0.1759(3)	0.075(2)
O(1)	0.0446(9)	-0.1632(7)	0.0547(8)	0.055(4)
O(2)	-0.0815(8)	0.0029(6)	0.0850(7)	0.042(3)
O(3)	-0.0546(9)	-0.0552(6)	-0.1265(7)	0.050(4)
N(11)	0.165(1)	-0.604(1)	-0.3022(9)	0.073(4)
S(11)	0.2470(5)	-0.0558(4)	-0.4054(3)	0.087(3)
N(21)	-0.194(1)	-0.1210(9)	0.0630(9)	0.058(4)
S(21)	-0.2953(4)	-0.1063(3)	0.0382(3)	0.065(2)
N(22)	0.011(1)	-0.2693(8)	-0.090(1)	0.060(4)
S(22)	-0.1133(5)	-0.2985(3)	-0.0860(4)	0.074(2)
C(1M)	-0.259(2)	0.052(2)	-0.155(2)	0.111(5)
C(2M)	-0.252(2)	0.245(2)	-0.095(2)	0.115(5)
C(3M)	-0.064(2)	0.300(1)	-0.248(2)	0.103(5)
C(4M)	0.058(2)	0.140(1)	-0.420(1)	0.086(5)
C(5M)	-0.056(2)	-0.016(2)	-0.354(2)	0.108(5)

TABLE 49

Thermal Parameters of Anisotropically Refined Atoms for
$[Cp^*(Cl)(HNSPh_2)U-(\mu_3-OH)(\mu_2-O)_2-U(Cl)(HNSPh_2)_2]_2 \cdot 2C_7H_8$

Atom	U11	U22	U33	U12	U13	U23
U(1)	0.046(1)	0.053(1)	0.043(1)	-0.023(1)	-0.022(1)	0.014(1)
U(2)	0.043(1)	0.041(1)	0.047(1)	-0.022(1)	-0.023(1)	0.010(1)
Cl(1)	0.070(3)	0.096(3)	0.073(3)	-0.048(2)	-0.032(2)	0.034(2)
Cl(2)	0.061(3)	0.071(3)	0.083(3)	-0.018(2)	-0.024(2)	0.005(2)
O(1)	0.050(5)	0.047(4)	0.077(5)	-0.023(4)	-0.032(4)	0.032(4)
O(2)	0.035(4)	0.045(4)	0.061(5)	-0.016(4)	-0.032(4)	0.013(4)
O(3)	0.057(5)	0.048(4)	0.056(5)	-0.032(4)	-0.026(4)	0.019(4)
N(11)	0.074(6)	0.101(6)	0.044(5)	-0.032(5)	-0.024(5)	0.024(5)
S(11)	0.083(3)	0.097(3)	0.056(3)	-0.003(3)	-0.022(3)	0.009(2)
N(21)	0.045(5)	0.086(5)	0.060(5)	-0.043(5)	-0.025(4)	0.022(5)
S(21)	0.062(3)	0.080(3)	0.073(3)	-0.043(3)	-0.036(2)	0.017(2)
N(22)	0.070(5)	0.047(5)	0.074(5)	-0.026(5)	-0.037(5)	0.002(5)
S(22)	0.089(3)	0.069(3)	0.089(3)	-0.049(2)	-0.046(3)	0.016(2)
C(1M)	0.087(6)	0.168(6)	0.113(6)	-0.071(6)	-0.057(6)	0.081(6)
C(2M)	0.107(6)	0.156(6)	0.097(6)	-0.029(6)	-0.063(5)	-0.011(6)
C(3M)	0.127(6)	0.086(6)	0.145(6)	-0.029(6)	-0.108(5)	0.035(6)
C(4M)	0.102(6)	0.110(6)	0.046(6)	-0.048(6)	-0.022(5)	0.029(5)
C(5M)	0.127(6)	0.124(6)	0.109(6)	-0.030(6)	-0.090(5)	0.006(6)

TABLE 50

Positional and Thermal Parameters of the Hydrogen Atoms for $[Cp^*(Cl)(HNSPh_2)U-(\mu_3-OH)(\mu_2-O)_2-U(Cl)(HNSPh_2)_2]_2 \cdot 2C_7H_8$

Atom	x	y	z	u
H(1MA)	-0.3072	-0.0848	-0.0947	0.206(7)
H(1MB)	-0.2254	-0.0098	-0.1490	0.206(7)
H(1MC)	-0.2998	0.0517	-0.1894	0.206(7)
H(2MA)	-0.2340	0.3000	-0.0916	0.206(7)
H(2MB)	-0.2560	0.2143	-0.0421	0.206(7)
H(2MC)	-0.3223	0.2590	-0.0965	0.206(7)
H(3MA)	-0.0026	0.3025	-0.3039	0.206(7)
H(3MB)	-0.0498	0.3080	-0.1962	0.206(7)
H(3MC)	-0.1287	0.3468	-0.2415	0.206(7)
H(4MA)	0.0818	0.0834	-0.4573	0.206(7)
H(4MB)	0.1192	0.1509	-0.4143	0.206(7)
H(4MC)	0.279	0.1889	-0.4475	0.206(7)
H(5MA)	-0.1033	-0.0510	-0.3194	0.206(7)
H(5MB)	0.0191	-0.0502	-0.3729	0.206(7)
H(5MC)	-0.0676	-0.0007	-0.4076	0.206(7)
H(12A)	0.0030	-0.2316	-0.2462	0.287(7)
H(13A)	0.0016	-0.2197	-0.3910	0.287(7)
H(14A)	-0.1120	-0.2837	-0.4272	0.287(7)
H(15A)	-0.2244	-0.3596	-0.3184	0.287(7)
H(16A)	-0.2230	-0.3714	-0.1735	0.287(7)
H(22B)	-0.2465	-0.3878	0.0373	0.287(7)
H(23A)	-0.2318	-0.5407	0.0649	0.287(7)
H(24A)	-0.0711	-0.6576	-0.0289	0.287(7)
H(25A)	0.0750	-0.6216	-0.1503	0.287(7)
H(26A)	0.0604	-0.4688	-0.1779	0.287(7)
H(31A)	-0.4045	-0.2147	-0.0066	0.287(7)
H(32A)	-0.5048	-0.3142	0.0715	0.287(7)

TABLE 50(Continued)

Positional and Thermal Parameters of the Hydrogen Atoms for $[Cp^*(Cl)(HNSPh_2)U-(\mu_3-OH)(\mu_2-O)_2-U(Cl)(HNSPh_2)_2]_2 \cdot 2C_7H_8$

Atom	x	y	z	u
H(33A)	-0.5349	-0.3360	0.2242	0.287(7)
H(34A)	-0.4643	-0.2583	0.2986	0.287(7)
H(35A)	-0.3639	-0.1589	0.2205	0.287(7)
H(42A)	-0.2697	0.0554	0.0925	0.287(7)
H(43A)	-0.3833	0.2071	0.1444	0.287(7)
H(44A)	-0.5693	0.2444	0.1743	0.287(7)
H(45A)	-0.6416	0.1299	0.1524	0.287(7)
H(46A)	-0.5280	-0.0218	0.1006	0.287(7)
H(52A)	0.2342	-0.0665	-0.5722	0.287(7)
H(53A)	0.2359	-0.1831	-0.6671	0.287(7)
H(54A)	0.2641	-0.3336	-0.6298	0.287(7)
H(55A)	0.2908	-0.3676	-0.4975	0.287(7)
H(56A)	0.2892	-0.2509	-0.4026	0.287(7)
H(62A)	0.4620	-0.1217	-0.5589	0.287(7)
H(63A)	0.6422	-0.1473	-0.5761	0.287(7)
H(64A)	0.6725	-0.1283	-0.4458	0.287(7)
H(65A)	0.5225	-0.0837	-0.2983	0.287(7)
H(66A)	0.3424	-0.0579	-0.2811	0.287(7)

TABLE 51

Positional and Thermal Parameters for the Carbon Atoms of the Toluene Molecules in the Crystal Structure of $[Cp^*(Cl)(HNSPh_2)U-(\mu_3-OH)(\mu_2-O)_2-U(Cl)(HNSPh_2)_2]_2 \cdot 2C_7H_8$

Atom	x	y	z	u
C(71A)	0.543(2)	0.403(2)	0.186(2)	0.195(6)
C(72A)	0.464	0.421	0.278	0.182(6)
C(73A)	0.356	0.471	0.300	0.207(6)
C(74A)	0.327	0.504	0.231	0.281(7)
C(75A)	0.406	0.486	0.139	0.182(6)
C(76A)	0.514	0.436	0.116	0.185(6)
C(77)	0.488(5)	0.368(5)	0.365(4)	0.379(7)
C(77C)	0.640(6)	0.386(6)	0.132(6)	0.058(7)
C(71B)	0.527(5)	0.439(4)	0.088(4)	0.205(7)
C(72B)	0.459	0.449	0.182	0.108(7)
C(73B)	0.350	0.503	0.218	0.113(7)
C(74B)	0.309	0.546	0.159	0.223(7)
C(75B)	0.377	0.536	0.064	0.249(7)
C(76B)	0.486	0.482	0.029	0.145(7)
C(73C)	0.451(5)	0.407(4)	0.346(4)	0.137(7)
C(74C)	0.344	0.461	0.369	0.050(7)
C(75C)	0.317	0.499	0.300	0.103(7)
C(76C)	0.398	0.484	0.209	0.151(7)
C(71C)	0.505	0.430	0.186	0.063(7)
C(72C)	0.532	0.392	0.255	0.053(7)
C(81A)	0.714(3)	0.606(3)	0.439(3)	0.371(7)
C(82A)	0.627	0.627	0.415	0.446(7)
C(83A)	0.620	0.563	0.359	0.314(7)
C(84A)	0.699	0.478	0.327	0.317(7)
C(85A)	0.786	0.457	0.351	0.266(7)
C(86A)	0.793	0.521	0.407	0.302(7)

TABLE 51 (Continued)

Positional and Thermal Parameters for the Carbon Atoms of the Toluene Molecules in the Crystal Structure of $[Cp^*(Cl)(HNSPh_2)U\text{-}(\mu_3\text{-}OH)(\mu_2\text{-}O)_2\text{-}U(Cl)(HNSPh_2)_2]_2 \cdot 2C_7H_8$

Atom	x	y	z	u
C(81B)	0.736(4)	0.464(3)	0.325(3)	0.064(7)
C(82B)	0.701	0.539	0.285	0.146(7)
C(83B)	0.737	0.6154	0.284	0.069(7)
C(84B)	0.809	0.616	0.322	0.071(7)
C(85B)	0.845	0.540	0.361	0.135(7)
C(86B)	0.808	0.464	0.363	0.039(7)
C(81C)	0.761(4)	0.615(3)	0.394(3)	0.127(7)
C(82C)	0.822	0.642	0.433	0.243(7)
C(83C)	0.908	0.576	0.440	0.153(7)
C(84C)	0.933	0.485	0.407	0.115(7)
C(85C)	0.873	0.459	0.368	0.090(7)
C(86C)	0.786	0.524	0.362	0.225(7)
C(87A)	0.867(4)	0.561(4)	0.419(4)	0.193(7)

TABLE 52

Selected Data for Structurally Characterized Sulfilimine Complexes

Compound	M-N, A	metallic radius, A	diff, A	M-N-S, deg
$F_4W(NSPh_2)_2$	1.807(4)	1.304	0.50	171.7(3)
	1.851(4)		0.55	138.4(3)
$Cl_2VO(NSPh_2)$	1.748(7)	1.224	0.52	134.5(4)
	1.723(7)		0.50	141.9(4)
$[Cl_2Fe(NSPh_2]_2$	1.916(4)	1.165	0.75	138.3(5)
	1.923(7)		0.76	129.6(3)
$Cp^*_2UCl(NSPh_2)$	2.10(1)	1.60	0.50	164.4(9)
$Cp^*_2U(NSPh_2)_2$	2.138(5)	1.60	0.54	151.9(3)
$Cp^*_2UCl_2(HNSPh_2)$	2.44(3)	1.60	0.89	127.6(9)
$Cp^*_2UCl(OH)(HNSPh_2)$	2.41(2)	1.60	0.89	127.6(9)
	2.51(2)	1.60	0.80	130.5(8)
$[Cp^*(Cl)(HNSPh_2)U-$	2.47(1)	1.60	0.87	130.5(9)
$(\mu_3-OH)(\mu_2-O)_2-$	2.50(1)	1.60	0.90	128.5(8)
$U(Cl)(HNSPh_2)_2]_2$	2.57(2)	1.60	0.97	129.8(6)

TABLE 53

N-S Bond Lengths in Sulfilimine Complexes

Complex	N-S Distance, (A)
$F_4W(NSPh_2)_2$	1.589(4)
	1.587(4)
$Cl_2VO(NSPh_2)$	1.609(7)
	1.618(7)
$[Cl_2Fe(NSPh_2]_2$	1.613(4)
$Cp^*_2UCl(NSPh_2)$	1.55(1)
$Cp^*_2U(NSPh_2)_2$	1.556(5)
$Cp^*_2UCl_2(HNSPh_2)$	1.55(2)
$Cp^*_2UCl(OH)(HNSPh_2)$	1.60(2)
	1.54(2)
$[Cp^*(Cl)(HNSPh_2)U-$	1.58(1)
$(\mu_3-OH)(\mu_2-O)_2-$	1.61(2)
$U(Cl)(HNSPh_2)_2]_2$	1.60(2)

TABLE 54

Non-Bonded Distances Between Opposite Cp^* groups in Cp^*_2U-Sulfilimine Complexes

Complex	Interaction	Distance, (A)
$Cp^*_2UCl_2(HNSPh_2)$	C(12M)-C(21M)	3.10
$Cp^*_2UCl(OH)(HNSPh_2)$	C(12M)-C(22M)	3.25
	C(34M)-C(45M)	3.31
$Cp^*_2UCl(NSPh_2)$	C(12M)-C(21M)	3.45
$Cp^*_2U(NSPh_2)_2$	C(34M)-C(34B)	3.47

TABLE 55

Cp^* Methyl Distances from C_5 Mean Planes (A) for $Cp^*_2UCl_2(HNSPh_2)$ and $Cp^*_2UCl(OH)(HNSPh_2)$[a]

	$Cp^*_2UCl_2(HNSPh_2)$	$Cp^*_2UCl(OH)(HNSPh_2)$[b]
C(11)*	-0.0002	0.0000
C(12)*	0.0002	-0.0002
C(13)*	-0.0002	0.0003
C(14)*	0.0002	-0.0003
C(15)*	0.0000	0.0002
C(11M)	0.2900	0.1030
C(12M)	0.3405	0.3193
C(13M)	0.0767	0.0483
C(14M)	0.1094	0.0853
C(15M)	0.3379	0.0301
C(21)*	-0.0001	0.0001
C(22)*	0.0001	-0.0001
C(23)*	-0.0001	0.0001
C(24)*	0.0000	0.0000
C(25)*	0.0001	-0.0001
C(21M)	-0.0810	-0.1252
C(22M)	-0.0789	-0.2723
C(23M)	-0.2907	-0.1138
C(24M)	-0.1222	-0.0168
C(25M)	-0.1207-	0.1171

a) Atoms with an asterisk designate atoms in the plane

b) Distances are shown only for one molecule in the asymmetric unit

TABLE 56

Cp^* Methyl Distances from C_5 Mean Planes (A) for $Cp^*_2UCl(NSPh_2)$[a]

	Distance, (A)
C(11)*	-0.0035
C(12)*	-0.0033
C(13)*	0.0089
C(14)*	-0.0110
C(15)*	0.0089
C(11M)	-0.1293
C(12M)	-0.1615
C(13M)	-0.2405
C(14M)	-0.1329
C(15M)	0.0746
C(21)*	0.0163
C(22)*	-0.0201
C(23)*	0.0149
C(24)*	-0.0049
C(25)*	-0.0061
C(21M)	0.3665
C(22M)	0.1125
C(23M)	0.1225
C(24M)	0.0670
C(25M)	0.2067

a) Atoms with an asterisk designate atoms in the plane

TABLE 57

Cp^* Methyl Distances from C_5 Mean Planes (A) for $Cp^*_2U(NSPh_2)_2$[a]

	Distance, (A)
C(31)*	0.0001
C(32)*	-0.0001
C(33)*	0.0001
C(34)*	-0.0001
C(35)*	0.0000
C(31M)	0.1877
C(32M)	0.1336
C(33M)	0.0491
C(34M)	0.3462
C(35M)	0.0975

a) Atoms with an asterisk designate atoms in the plane

TABLE 58

Cp^* Methyl Distances from C_5 Mean Planes (A)
for $[Cp^*(Cl)(HNSPh_2)U-(\mu_3-OH)(\mu_2-O)_2-U(Cl)(HNSPh_2)_2]_2$

	Distance, (A)
C(1)*	0.0003
C(2)*	-0.0002
C(3)*	0.0000
C(4)*	0.0002
C(5)*	-0.0003
C(1M)	-0.2337
C(2M)	-0.1737
C(3M)	-0.0903
C(4M)	-0.1632
C(5M)	-0.0778

a) Atoms with an asterisk designate atoms in the plane

TABLE 59

Summary of Cp-U Structural Parameters

	Cp^*-U-Cp^*	U-C(Cp^*)[a]	U-Cp^*[b]
$Cp^*_2UCl_2(HNSPh_2)$	130.7	2.77(2)	2.50
$Cp^*_2UCl(OH)(HNSPh_2)$	135.5	2.77(1)	2.50
	136.3	2.75(1)	2.51
$Cp^*_2UCl(NSPh_2)$	133.2	2.73(5)	2.48
$Cp^*_2U(NSPh_2)_2$	130.0	2.804(4)	2.53
$[Cp^*(Cl)(HNSPh_2)U-(\mu_3\text{-}OH)(\mu_2\text{-}O)_2\text{-}U(Cl)(HNSPh_2)_2]_2$		2.80(2)	2.53

a) Average of the U-C(Cp^*) distance

b) Average U-Cp^* (centroid) distance

Chapter 5

SUMMARY

The objective of this study was to synthesize and characterize organouranium complexes of the $RNSR_2$ ligand. This ligand is isoelectronic with the phosphoylide ligand, $[CHPR_3]^-$, whose organoactinide chemistry has been studied in detail.

$Cp^*_2UCl_2$ reacts with $HNSPh_2$ at room temperature to form $Cp^*_2UCl_2(HNSPh_2)$ in high yield as a dark orange material. This compound was characterized by usual chemical and spectroscopic techniques and by single crystal X-ray diffraction. $Cp^*_2UCl_2(HNSPh_2)$ belongs to the bent metallocene family with Cp_2ML_3 coordination type. The sulfilmine ligand enters in the equatorial plane in between the two chlorides. The imino hydrogen of $HNSPh_2$ was not located in the crystal structure. However, there is a signal for this proton in the ^1H-NMR spectrum of $Cp^*_2UCl_2(HNSPh_2)$ at -142 ppm. There is also a signal for the N-H stretch at 3284 cm^{-1} that is 21 cm^{-1} shorter than that of free $HNSPh_2$. The origin of these signals as N-H vibrations was confirmed by deuterium substitution experiments carried out on the imino hydrogen.

The U-Cl distances of $Cp^*_2UCl_2(HNSPh_2)$ are significantly longer than that for a tetravalent uranium complex. The considerable steric crowding on the uranium metal center is probably responsible for this difference. The U-N distance of 2.44(3) A also lies in the upper range of U-N distances as would befit a sterically crowded molecule. The U-N-S angle of 133(1)° indicates that the N is approximately sp^2 hybridized.

If a hydrogen is placed at a calculated position on the nitrogen, it would be in the vicinity of Cl(1). Therefore dehydrochlorination was attempted. However, heating the sample under vacuum or the reflux in toluene over a long period showed no signs of reaction and $Cp^*_2UCl_2(HNSPh_2)$ is stable in the presence of $HNSPh_2$, which is a moderately strong base.

Attempts to synthesize the organouranium derivatives of the $[NSPh_2]^-$ ligand by reaction of $Cp^*_2UCl_2$ with $Me_3SiNSPh_2$ were unsuccessful. On the other hand, $LiNSPh_2$ reacts with $Cp^*_2UCl_2$ to form $Cp^*_2UCl(NSPh_2)$ and $Cp^*_2U(NSPh_2)_2$ depending on the stoichiometry.

The same compounds can be prepared by reacting one or two equivalents of $HNSPh_2$ with $Cp^*_2UCl(CH_2)_2R_2$ which contains a pre-coordinated phosphoylide group. The phosphoylide ylide ligand, which is a strong base,

abstracts the imino-hydrogen of $HNSPh_2$ during the intial step of this reaction. $Cp^*_2U(NSPh_2)_2$ can also be synthesized by direct reaction of $Cp^*_2UCl_2(HNSPh_2)$ with $LiNSPh_2$ in the presence of $HNSPh_2$.

Both $Cp^*_2UCl(NSPh_2)$ and $Cp^*_2U(NSPh_2)_2$ were characterized by the usual chemical and spectroscopic techniques and by single crystal X-ray diffraction. Both these complexes are Cp_2ML_2 bent metallocene complexes.

$Cp^*_2UCl(NSPh_2)$, is considerably less sterically crowded than $Cp^*_2UCl_2(HNSPh_2)$. The U-Cl distance of 2.609(6) A is normal for a tetravalent uranium complex. The U-N distance of 2.10 A, is short as would befit a complex with relatively little steric crowding. The U-N-S angle of 164(1)° of this complex is about 35° wider than that of $Cp^*_2UCl_2(HNSPh_2)$ and indicates that the nitrogen atom is approximately sp hybridized with the U-N-S angle approaching linearity. The U-N distance of $Cp^*_2U(NSPh_2)_2$, 2.138(5) A, is somewhat shorter than that of $Cp^*_2UCl(NSPh_2)$, but lies in the same range. The U-N-S angle of $Cp^*_2U(NSPh_2)_2$ is about 10° narrower than that of $Cp^*_2UCl(NSPh_2)$.

$HNSPh_2$ is available as a hydrate. The synthesis of organouranium-oxo complexes using $Cp^*_2UCl_2$ and $HNSPh_2 \cdot H_2O$ was attempted. $Cp^*_2UCl_2$ reacts with $HNSPh_2 \cdot H_2O$ to form an

intermediate, $Cp^*_2UCl(OH)(HNSPh_2)$, which further reacts with excess $HNSPh_2 \cdot H_2O$ to form a final product which has the formula, $[Cp^*(Cl)(HNSPh_2)U-(\mu_3-OH)(\mu_2-O)_2-U(Cl)(HNSPh_2)_2]_2$. The structure of this complex contains four uranium atoms which are connected by four doubly bridging and two triply bridging oxygens. There are six sulfilimine groups in the molecule. The U-N bond lengths and U-N-S angles suggest that they are free $HNSPh_2$ molecules. The complex is paramagnetic according to ^{1}H-NMR spectra. Based on valancy requirements and the symmetry of the molecule, the four doubly bridging oxygens are identified as O^{2-} groups and the triply bridging oxygens as OH^- groups. The near linear O-U-O angles and extremely short axial U-O distances on U(2) in the structure, Figure 73, resemble a uranyl moiety.

$Cp^*_2UCl(OH)(HNSPh_2)$ and $[Cp^*(Cl)(HNSPh_2)U-(\mu_3-OH)(\mu_2-O)_2-U(Cl)(HNSPh_2)_2]_2$ are the first organo actinide hydroxy complexes to be characterized. These results show that both Cp^* and Cl groups undergo hydrolysis at a comparable rate. Therefore a range of products may form during the hydrolysis of organouranium halides and may explain why it is often difficult to obtain organouranium oxo complexes in a state of high purity and with a good yield.

Chapter 6

SUGGESTIONS FOR FUTURE WORK

Several of the systems studied in this work deserve further investigation. The complexes $Cp^*_2UCl_2(HNSPh_2)$, $Cp^*_2UCl(NSPh_2)$, $Cp^*_2U(NSPh_2)_2$, $Cp^*_2UCl(OH)(HNSPh_2)$ and $[Cp^*(Cl)(HNSPh_2)U-(\mu_3-OH)(\mu_2-O)_2-U(Cl)(HNSPh_2)_2]_2$, are the members of a series of new complexes which contain the sulfilimine ligand, which is isoelectronic to the $[CHPR_3]^-$ ligand. The reaction chemistry of these complexes must be studied in detail, in order to determine if they show analogous reactivity to $[CHPR_3]^-$.

It is also important to study the nature of the U-N bond in these complexes. The U-N distances which range from 2.10(1) A to 2.57(2) A in these complexes indicate that there is an interesting variation of the metal ligand interactions. The U-N distance of 2.10(1)A in $Cp^*_2UCl(NSPh_2)$, falls in the same range as those found among U-N multiple bonds. The $[NSPh_2]^-$ ligand may potentially act as a three electron pair donor according to following resonance forms.

Therefore it is possible that U-N triple bonds exist among these compounds, provided that suitable acceptor orbitals are present on the uranium center. Theoretical calculations should be carried out in order to describe the nature of bonding in these complexes.

According to the results of the reaction of $Cp^*_2UCl_2$ with $HNSPh_2.H_2O$, it is possible that a series of complexes may form during the course of the reaction. Attempts could be made to carry out this reaction under carefully controlled conditions in order to isolate these products in the pure crystalline form. Furthermore, hydrolysis of Cp^*-halide complexes of other f-elements and early transition elements could also be carried out using the same synthetic procedure.

REFERENCES

1 Wittig, G.; Rieber, M. Ann. Chem. 1953, 177, 562.

2 Wittig, G.; Geissler, G. Ann. Chem. 1953, 44, 580.

3 Wittig, G.; Schollkopf, U. Chem. Ber. 1954, 87, 1318.

4 Kaska, W.C. Coord. Chem. Rev. 1983, 48, 62-69.

5 Schmidbaur, H. Acc. Chem. Res. 1975, 8, 2567-2569.

6 Schmidbaur, H. Angew. Chem. Int. Ed. Engl. 1983, 22, 907-927.

7 Manzer, L.E. Inorg. Chem. 1976, 15, 2657-2569.

8 Cramer, R.E.; Maynard, R.B.; Gilje, J.W. J. Am. Chem. Soc. 1978, 100, 5562-5564.

9 Cramer, R.E.; Maynard R.B.; Gilje, J.W. Inorg. Chem. 1980, 19, 2564-2569.

10 Cramer, R.E.; Maynard, R.B.; Gilje, J.W. Inorg. Chem. 1981, 20, 2466-2470.

11 Cramer, R.E.; Maynard, R.B.; Paw, J.C.; Gilje, J.W. Organometallics 1983, 2, 1336-1340.

12 Cramer, R.E.; Maynard, R.B.; Paw, J.C.; Gilje, J.W. J. Am. Chem. Soc. 1981, 103, 3589-3590.

13 Cramer, R.E.; Mori A.L.; Maynard, R.B.; Gilje, J.W.; Tatsumi. K.; Nakamura, A. J. Am. Chem. Soc. 1984, 106, 5920-5926.

14 Perego, G.; Cesari, M; Farina, F.; Lugli, G. Acta. Crystallogra. B **1976**, 32, 3034-3039.

15 Halsted, G.W.; Baker, E.C.; Raymond, K.N. J. Am. Chem. Soc. **1975**, 97, 3049-3055.

16 Atwood, J.L.; Tsutsui, M.; Ely, N.; Gebala, A.E. J. Coord. Chem. **1976**, 5, 209-215.

17 Atwood, J.L.; Hains, C.F.; Tsuitsui, M.; Gebala, A.E. J. of Chem. Soc., Chem. Commun. **1973**, 452-453.

18 Edwards, P.G.; Andersen, R.A.; Zalkin, A. Organometallics **1984**, 3, 293-298.

19 Tatsumi, K.; Nakamura, A. J. Organometal. Chem. **1984**, 272, 141-154.

20 Panchanatheswaren, K.; Ph.D. Thesis, University of Hawaii, 1984.

21 Higa, K.T.; Ph.D. Thesis, University of Hawaii, 1984.

22 Cramer, R.E.; Engelhardt, U.; Higa, K.T.; Gilje J.W. Organometallics **1897**, 6, 41-45.

23 Cramer, R.E.; Maynard, R.B.; Paw J.C.; Gilje, J.W. Organometallics **1982**, 1, 869-871.

24 Cramer, R.E.; Panchanatheswaren, K.; Gilje, J.W. J. Am. Chem. Soc. **1984**, 106, 1853-1854.

25 Cramer, R.E.; Panchanatheswaren, K.; Gilje, J.W. Angew. Chem. Int. Ed. Engl. **1984**, 23, 912-913.

26 Cramer, R.E.; Jeong, J.H.; Gilje, J.W. Organometallics 1987, 5, 2010-2015

27 Jeong, J. H., Ph.D. Thesis, University of Hawaii, 1987.

28 Cramer, R.E.; Higa K.T.; Gilje, J.W. J. Amer. Chem. Soc. 1984, 106, 7245-7247.

29 Cramer, R.E.; Higa, K.T.; Pruskin, S.L.; Gilje, J.W. J. Am. Chem. Soc. 1983, 105, 6749-6752.

30 Cramer, R.E.; Jeong, J.H.; Richmann, P.N.; Gilje, J.W. Organometallics 1990, 9, 1141-1146.

31 Cramer, R.E.; Afzal, D.; Gilje, J.W. unpublished results.

32 Cramer, R.E.; Jeong, J.H.; Gilje, J.W. Organometallics 1987, 6, 2010-2012.

33 Baldwin, J.C.; Keder, N.L.; Strouse, C.E.; Kaska, W.C. Z. Naturforsch. 35b 1980, 1289-1297.

34 Gell, K.I.; Schwartz, J. Inorg. Chem. 1980, 19, 3207-3211.

35 Erker, G.; Czisch, P.; Mynott, R.; Tsay, Y.H.; Kruger C. Organometallics 1985, 4, 1310-1312.

36 De Boer, H.J.R.; Akkermann, O.S.; Bickelhaupt, F.; Erker, G.; Czisch, P.; Mynott, R.; Wallis, J.M.; Kruger, C. Angew. Chem. Int. Ed. Engl. 1986, 25, 639-644.

37 Erker, G.; Czisch, P.; Kruger, C.; Wallis, J.M. Organometallics 1985, 4, 2059-2060.

38 Cardin, D.J.; Lappert, M.F.; Ratson, C.L. "Chemistry of Organo-Zirconium and -Hafnium Compounds" Wllis Horwood Limited, West Sussex, England, 1986, Chapter 10.

39 Schmidbaur, H.; Pichl, R.; Muller, G. Angew. Chem. Int. Ed. Engl. 1986, 25, 574-575.

40 Schmidbaur, H.; Pichl, R. Z.Naturforsch.40b, 1985, 352-356.

41 Schmidbaur, H.; Pichl, R.; Muller, G. Chem. Ber. 1987, 120, 39-44

42 Cramer, R.E.; Roth, S; Edelmann, F.; Bruck, M.A.; Kim, C.C.; Gilje, J.W. Organometallics 1989, 8, 1192-1199.

43 Roth, S. Ph.D. Thesis University of Hawaii, 1988.

44 Wong, W.K.; Chen, H.; Chow, F.L. Polyhedron 1990, 9, 875-879.

45 Cramer, R.E.; Edelmann, F.; Mori, A.L.; Roth S.; Gilje, J.W.; Tatsumi, K.; Nakamura, A. Organometallics 1988, 7, 841-849.

46 Dehnicke, K.; Strahle, J. Polyhedron 1989, 8, 707-726.

47 Zalkin, A.; Brennan, J.G.; Andersen, R.A. Acta Crystallogr. 1988, C44, 1533-1536

48 Burns, C.J.; Smith, W.H.; Huffman, J.C.; Sattelberger, A.P J. Am. Chem. Soc. 1990, 112, 3237-3239.

49 Brennan, J.G.; Andersen, R.A. J. Am. Chem. Soc. 1985, 107, 514-516.

50 Fisher, R.D.; Klaehne, E.; Kopf, J. Z.Naturforsch.33b 1978, 1393-1397.

51 Cramer, R.E.; Gilje, J.W.; Roth S. Organometallics 1989, 8, 2327-2330.

52 Sudhakar, P.V.; Lammertsma, K. J. Am. Chem. Soc. 1991, 113, 1899-1906.

53 Roesky, H.W.; Zimmer, M.; Noltmeyer, M.; Sheldrick, G.M. Chem. Ber. 1988, 121, 1377-1379.

54 Roesky, H.W.; Zimmer, M.; Schmidt, H.G.; Noltemeyer, M. Z.Naturforsch.43b 1988, 1490 -1494.

55 Day, V; Klemperer, W.G.; Maltbie, D. J. Organometal. Chem. 1985, 4, 104-111.

56 Day, V.; Earley, C.W.; Klemperer, W.G.; Maltbie, D.J. J. Am. Chem. Soc. 1985, 107, 8261-8262.

57 Zozulin, A.J.; Moody, D.C.; Ryan, R.R. Inorg. Chem. 1982, 21, 3083-3086.

58 Calderazzero, F.; Dell'Amico, G.; Pasquali, M.; Perego, G. Inorg. Chem. 1978, 17, 474-479.

59 Cotton, F.A.; Marler, D.O.; Schwotzer,W. Inorg. chim. Acta. 1984, 95, 207-209.

60 Evans, W.J.; Sollberger, M.S. J. Am. Chem. Soc. 1986, 581, 6095-6099.

61 Schumann, H.; Kociok-Kohn, G.; Loebel J. Z. Anorg. Allg. Chem. 1990, 581, 69-72.

62 Jin, Z.; Guan, J.; Wei, G.; Hu, J.; Shen, Q. Jiegue Huaxue (J. Struct. Chem.) 1990, 9, 140-142.

63 Evans. W.J.; Grate, J.W.; Bloom. I.; Hunter, W.E.; Atwood, J.L. J. Am. Chem. Soc. 1985, 107, 405-410.

64 Berg, D.J.; Burns, C.J.; Andersen, R.A.; Zalkin, A Organometallics 1989, 8, 1865-1867.

65 Schumann, H.; Palamidis, E.; Loebel, J J. Organometal. Chem. 1990, 384, C49.

66 Evans, W.J.; Hozbor, M.A.; Bott, S.G.; Robinson, G.H.; Atwood, J.L. Inorg. Chem. 1988, 27, 1990-1994.

67 Hitchcock, P.B.; lappert, M.F.; Prashar, S. J. Organometal. Chem. 1991, 413, 79-90.

68 Schumann, H.; Loebel, J.; Pickardt, J. Organometallics 1991, 10, 215-219.

69 Cramer, R.E.; Bruck, M.A.; Gilje, J.W. Organometallics 1988, 7, 1465-1469.

70 Berthet, J.C.; Marechal, J.F.L.; Nierlich, M.; Lance, M.; Vigner, J.; Ephritikhine, M. J. Organometal. Chem. 1991, 408, 335-341.

71 Baumgartner, F.; Fischer, E.O.; Kanellakopulos, B. in Marks, T.J. and Fischer, R.D. (Eds.) Organometallics of the f-Elements Reidel Publ. Co., Dordrecht, The Netherlands, 1979.

72 Appel, R.; Kohnlein, G.; Schollhorn, R Chem. Ber. 1965, 98, 1355-1358.

73 Roesky H.W.; Katti, K.V.; Seske, U.; Scholz, U.; Herbert, R.; Egert, E.; Sheldrich, G.M. Z. Natursorsch 1986, 41b, 1509-1512.

74 Hermann, J.A.; Suttle, J.F. Inorg. Synthesis 1957, 5, 143-146.

75 Fagan, P.J.; Manriquez, J.M.; Maata, E.A.; Seyam, A.M., Marks, T.J. J. Am. Chem. Soc. 1981, 103, 6650-6667.

76 Silverstein, R.M.; Bassler, G.C.; Morril, T.C. Spectrometric Identification of Organic Compounds John Wiley and Sons, New york, 1981, Chapter 3.

77 Nakamoto, K Infrared Spectra of Inorganic Compounds 1963, John Wiley and Sons, Inc., New York. P80.

78 Schrumpf, F; Roesky, H.W.; Noltemeyer, M Z. Naturforsch. **1990**, 45b, 166-1602.

79 Dilworth, J.R.: de Liefde Meijer H.J.; Teuben, J.H. J. Organometal. Chem. **1978**, 159, 47.

80 Roesky, H.W.; Seseke, U.; Noltemeyer, M.; Jones, P.G.; Sheldrick, G.M. J. Chem. Soc., Dalton Trans. **1986**, 1309.

81 Hosler, K.; Weller, F.; Dehnike, K. Z. Naturforsch. **1987**, 42b, 1563.

82 Katti, K.V.; Seseke, U.; Roesky, H.W. Inorg. Chem. **1987**, 26, 814.

83 "XEMP", Empirical Absorption Correction Version 4.2 for MSDOS. Copyright 1990 Siemens.

84 SHELXTL PLUS- Release 4.11/V, Copyright 1990, Siemens Analytical X-ray Instr., Inc.

85 This work.

86 Wong, C.; Yen, T.; Lee,T. Acta Cryst. 1965, 18, 340-342.

87 Bombieri, G.; Bagnall, K.W. J. of Chem. Soc., Chem. Commun. **1975**, 6, 188-192.

88 de Wet, J.F.; Darlow, S.F. Inorg. Nucl. Chem. Lett **1971**, 7, 1041-1043.

89 Bombieri, G.; Brown, D.; Graziani R. J. Chem. Soc., Dalton Trans. 1975, 18, 1873-1076.

90 Greenwood, N.N.; Earnshaw, A. Chemistry of the Elements Pergamon Press Limited, England, P.65.

91 Beckman, W.; Goffart, J.; Rebizant, J.; Spirlet M.R. J. Organometal. Chem. 1986, 307, 23

92 Eigenbrott, C.W; Raymond, K.N. Inorg. Chem. 1982 21, 2650-2660.

93 Lin Z.; LeMarachel, J.F.; Sabat, M; Marks, T.J J. Am. Chem. Soc. 1987, 109, 4127-4129.

94 Smith, G.; Sabat, M.; Marks, T.J. J. Am. Chem. Soc. 1987, 109, 1850-1856.

95 Bruno, J.W.; Smith, G.M.; Marks, T.J.; Schultz, A.; Wiliams, J.M. J. Am. Chem. Soc., 1986, 108, 40-56.

96 Marks, T.J.; Day, V.W. Fundamental and Technological Aspects of Organo-f-Element Chemistry; Marks, T.J., Fragala, I.L., Eds.; Reidel: Dordrecht, 1985, 115-157.

97 Taylor J.C. Coord. Chem.Rev. 1976, 20, 197-273.

98 Cotton, F.A.; Marler, D.O.; Schwotzer, W. Inorg. Chim. Acta 1984, 95, 207-209.

99 Pyykko, P.; Jove, J. New. J. Chem. 1991, 15, 717-720.

100 Wadt, W.R. J. Am. Chem. Soc. 1981, 103, 6053-6057.

101 Mentzen, B.F.; Sautereau, H.; Acta. Cryst. 1980, B.36, 2051-2053.

102 Cattalini, R.; Croatto, U.; Degetto, S.; Tondello, E Inorg. Chim. Acta. Rev. 1971, 5, 19-22.

103 Perry, D.L.; Templeton, D.H.; Zalkin A. Inorg. Chem. 1979, 18, 879-881.

104 Plymale, D.L.; Smith, W.H. J. Inorg. Nucl. Chem. 1968, 30, 2267-2271.

105 Sacconi, L.; Giannoni, G. J. Chem. Soc. 1954, 2368-2370.

106 Yamada, S.; Takeuchi, A. Bull. Chem. Soc. Jpn 1969, 42, 2549-2551.

107 Taylor, J.C.; Ekstrom, A.; Randall, C.H. Inorg. Chem. 1978, 17, 3285-3289.

108 Willis, B.T.M. Proc. Phys. Soc. (London) Ser. A 1963, 274, 122-133.

109 Rundle, R.E.; Baenziger, N.C.; Wilson, A.S.; McDonald, R.A. J. Am. Chem.Soc. 1948, 70, 99-105.

110 Cuy, E.J. J. Am. Chem. Soc. 1927, 49, 201-215.

111 Wells, A.F Structural Inorganic Chemistry Oxford University Press, 1962, 965-969.

112 ibid 362.

113 Nugent, W.A.; Haymore, B.I. Coord. Rev. 1980, 31 123-175.

114 Pauling, L. The Nature of the Chemical Bond 3rd. ed., Cornell University press: Ithaca NY, 1960.

115 Skapski, A.C.; Troughton, P.G.H. Acta. Cryst. Sect.B 1970, 26, 716-720.

116 Corradini, P.; Allegra, G. J. Am. Chem. Soc. 1959, 80, 5510-5515.

117 Thewalt, U.; Schomburg D J. Organometal. Chem. 1977, 127, 169-172.

118 Thewalt, U.; Kebbel, B. J. Organometal Chem. 1978, 150, 59-62.

119 Leichtweis, I.; Roesky, H.W.; Noltemeyer, M.; Schmidt H.G. Chem. Ber. 1991, 124, 253-257.

120 Babcock, L.M.; Day, V.; Klemperer, W.G. Inorg. Chem. 1989, 28, 806-810.